

# **The mechanism of HIV-1 Nef-mediated downregulation of CD4**

**Rittik Chaudhuri**



**University of Cambridge  
Magdalene College**

**A dissertation submitted for the degree of Doctor of Philosophy**

*The Truth shall set you free.*

## **Acknowledgements**

This thesis would not have been possible without the tremendous support provided by my colleagues, friends, and family. I would like to start by thanking my supervisors at the NIH and Cambridge, Juan Bonifacino and Scottie Robinson. Their encouragement, optimism, and patience have been nothing short of remarkable. Next, I must thank my mentor, Wolf Lindwasser. Wolf, more than anyone, taught me how to think critically and promoted my development as a scientist. I am also deeply indebted to Bill Smith, Rafael Mattera, Peter Yang, and Jim Hurley for their contributions to this project. Lin Zhu and Nora Tsai have provided expert technical assistance. The remaining members of the Bonifacino and Robinson Labs (including, but certainly not limited to, Jennifer Hirst, Georg Borner, Daniela Sahlender, Patrycja Kozik, and Katy Janvier) have each left their mark on this thesis through helpful discussions and the generous provision of reagents. I would also like to thank my wonderful friends (particularly Tamara James, India Hook-Barnard, and Travis Barnard) for their companionship. They have become increasingly dear to me over the past five years. I owe special thanks to my girlfriend, Heather Eshleman, for her enduring love and support. Finally, I must thank my family (Prabir Chaudhuri, Bina Chaudhuri, and Rakhi Dimino). They have made sacrifices on my behalf which I am just now beginning to understand. I dedicate this thesis to them.

## Contributors to this work



**Rittik Chaudhuri**

Ph.D. Candidate, NIH-Cambridge Graduate Partnership Program  
Department of Clinical Biochemistry, CIMR, University of Cambridge  
Cell Biology and Metabolism Program, NICHD, NIH



**Juan S. Bonifacino, Ph.D.**

Chief, Cell Biology and Metabolism Program  
National Institute of Child Health and Development  
National Institutes of Health



**Margaret S. Robinson, Ph.D.**

Professor, Department of Clinical Biochemistry  
Cambridge Institute of Medical Research  
University of Cambridge



**James H. Hurley, Ph.D.**

Senior Investigator, Laboratory of Molecular Biology  
National Institute of Diabetes and Digestive and Kidney Diseases  
National Institutes of Health



**O. Wolf Lindwasser, Ph.D.**

Postdoctoral Fellow, Cell Biology and Metabolism Program  
National Institute of Child Health and Development  
National Institutes of Health



**William J. Smith, Ph.D.**

Postdoctoral Fellow, Cell Biology and Metabolism Program  
National Institute of Child Health and Development  
National Institutes of Health



**Rafael Mattera, Ph.D.**

Staff Scientist, Cell Biology and Metabolism Program  
National Institute of Child Health and Development  
National Institutes of Health



**Peter Yang**

Postbaccalaureate Fellow, Cell Biology and Metabolism Program  
National Institute of Child Health and Development  
National Institutes of Health

## **Declaration of work**

This thesis is the result of my own work and includes nothing that is the outcome of work done by others or in collaboration except where specifically indicated in the text or acknowledgements. This work has not been submitted for any degree at this, or any other, university. In addition, this thesis does not exceed the word limit stipulated by the School of Clinical Medicine and Department of Clinical Biochemistry.

Rittik Chaudhuri

13 January, 2010

## Thesis Summary

Nef, an accessory protein of HIV-1, is a critical determinant of viral pathogenicity. The pathogenic effects of Nef are in large part dependent on its ability to decrease the amount of CD4 on the surface of infected cells. Early studies suggested that Nef induces downregulation by linking the cytosolic tail of CD4 to components of the host-cell protein-trafficking machinery. However, the specific sorting pathway that Nef uses to modulate CD4 expression remained uncertain. According to one model, Nef was thought to interfere with the transport of newly synthesized CD4 from the TGN to the cell-surface. Another model claimed that Nef facilitated the removal of CD4 from the plasma membrane.

The primary goal of this thesis was to determine which of these models was correct. To accomplish this objective, a novel Nef-CD4 system was developed in *Drosophila* S2 cells. Nef was not only able to downregulate human CD4 in S2 cells, but it did so in a manner that was phenotypically indistinguishable from its activity in human cells. An RNAi screen targeting protein-trafficking genes in S2 cells revealed a requirement for clathrin and the clathrin-associated, plasma membrane-localized AP-2 complex in the Nef-mediated downregulation of CD4. In contrast, depletion of the related AP-1 and AP-3 complexes, which direct transport from the TGN and endosomes, had no effect. The requirement for AP-2 was subsequently confirmed in a human cell line. Yeast three-hybrid and GST pull-down assays were then used to demonstrate a robust, direct interaction between Nef and AP-2. This interaction was found to depend on a [D/E]xxxL[L/I]-type dileucine motif, located in the C-terminal loop of Nef, that is essential for CD4 downregulation.

While mapping the binding site of AP-2 on Nef, a second determinant of interaction in the C-terminal loop was identified. Mutation of this motif, which conforms to a consensus [D/E]D diacidic sequence, prevented Nef from binding to AP-2 and downregulating CD4. However, the same mutations did not affect the ability of Nef to interact with either AP-1 or AP-3, providing further evidence that these complexes are not required for the modulation of CD4 expression. Additional experiments indicated that the Nef diacidic motif most likely binds to a basic patch on AP-2  $\alpha$ -adaptin that is not present in the homologous AP-1  $\gamma$  and AP-3  $\delta$  subunits. As with the Nef dileucine

and diacidic motifs, the  $\alpha$ -adaptin basic patch was shown to be necessary for CD4 downregulation. Moreover, all three of these motifs were needed for the cooperative assembly of a CD4-Nef-AP-2 tripartite complex, which was observed here for the first time using a yeast four-hybrid system.

The data in this thesis uniformly support an endocytic model of Nef-mediated CD4 downregulation. Indeed, there is now strong evidence that Nef simultaneously binds CD4 and AP-2, thereby connecting the receptor to the cellular endocytic machinery and promoting its rapid internalization from the plasma membrane. In addition, the identification of novel motifs required for this process has provided new insights on endocytosis, and may facilitate the development of pharmacological inhibitors of Nef function.

## ABBREVIATIONS

The abbreviations used in this work are listed below in alphabetical order.

	Abbreviation	Full word or phrase
A	ADH1	alcohol dehydrogenase 1
	AIDS	acquired immune deficiency syndrome
	AP	adaptor protein
	APC	allophycocyanin
B	bp	base pair
	BSA	bovine serum albumin
C	CD	cluster of differentiation
	CCV	clathrin-coated vesicle
	CHC	clathrin heavy chain
	CIMR	Cambridge Institute of Medical Research
	CLC	clathrin light chain
	CMV	cytomegalovirus
	COP	coatamer protein
	CTL	cytotoxic T lymphocyte
D	DBD	DNA-binding domain
	DC-SIGN	dendritic cell-specific intracellular adhesion molecule-3-grabbing non-integrin
	DMEM	Dulbecco's modified Eagle medium
	DMSO	dimethyl sulfoxide
	DNA	deoxyribonucleic acid
	ds	double-stranded
E	ECL	enhanced chemi-luminescence
	EDTA	ethylenediaminetetraacetic acid
	ER	endoplasmic reticulum
	ESCRT	endosomal sorting complex required for transport
F	FBS	fetal bovine serum
	FITC	fluorescein isothiocyanate
G	GAL4AD	GAL4 activation domain
	GAL4BD	GAL4 DNA binding domain
	GFP	green fluorescent protein
	GGA	Golgi-localized, gamma-ear-containing, ARF binding protein(s)
	GST	glutathione <i>S</i> -transferase
H	HBS	HEPES buffered saline
	HEPES	4-(2-hydroxyethyl)-1-piperazinethanesulfonic acid
	HF	high fidelity
	HLA	human leukocyte antigen

	Abbreviation	Full word or phrase
H	His <sub>6</sub>	hexahistidine
	HIV	human immunodeficiency virus
	HIV-1	human immunodeficiency virus type 1
	HIV-2	human immunodeficiency virus type 2
	HRP	horseradish peroxidase
	hr(s)	hour(s)
I	IgG	immunoglobulin G
	Ii	MHC-II-associated invariant chain
	IPTG	isopropyl-β-D-thiogalactopyranoside
	IRES	internal ribosome entry site
	ITAM	immunoreceptor tyrosine-based activation motif
	IVT	in vitro transcription
K	kDa	kilodalton
	kT	kilotesla
L	LAMP1	lysosome associated membrane protein 1
	LATE	lithium acetate, tris, EDTA
	LB	lysogeny broth
	Lck	p56 <sup>Lck</sup>
	LIGHT	lymphotoxin-like, exhibits inducible expression and competes with HSV glycoprotein D for herpes virus entry mediator, a receptor expressed by T lymphocytes
	LTNP	long-term non-progressor
	LTR	long terminal repeat
M	MCS	multiple cloning site
	MHC	major histocompatibility complex
	MHC-I	major histocompatibility complex class I
	MHC-II	major histocompatibility complex class II
	min	minute(s)
	mRNA	messenger RNA
	MVB	multivesicular body
N	NIAID	National Institute of Allergy and Infectious Diseases
	NICHD	National Institute of Child Health and Human Development
	NIH	National Institutes of Health
	NLS	nuclear localizaton sequence
	NMR	nuclear magnetic resonance
	NK	natural killer
	NP-40	nonyl phenoxy polyethoxy ethanol-40
O	OD	optical density
	ORF	open reading frame
P	PACS-1	phosphofurin acidic cluster sorting protein-1

	Abbreviation	Full word or phrase
P	PAGE	polyacrylamide gel electrophoresis
	PBB	protein binding buffer
	PE	phycoerythrin
	PEG	polyethylene glycol
	PCR	polymerase chain reaction
	PIP	phosphatidylinositol phospholipid
	PKC	protein kinase C
R	rfu	relative fluorescence unit
	RNA	ribonucleic acid
	RNAI	RNA-interference
	RPMI	Roswell Park Memorial Institute
	RU	response units
S	SCID	severe combined immunodeficiency
	SCID-hu	severe combined immunodeficiency with human T cells
	SDM	site-directed mutagenesis
	SDS	sodium dodecyl sulphate
	sec	second(s)
	SEM	standard error of the mean
	siRNA	small interfering RNA
	SIV	simian immunodeficiency virus
	SOC	super optimal broth with catabolite repression
SPR	surface plasmon resonance	
T	TBE	tris, boric acid, EDTA
	TBS	tris-buffered saline
	TCR	T cell receptor
	TDN	tris, dithiothreitol, NaCl
	TEV	tabacco etch virus
	TfR	transferrin receptor
	TGN	<i>trans</i> -Golgi network
	TNF	tumor necrosis factor
W	WT	wild-type
Y	YPD	yeast extract, peptone, dextrose
	Y2H	yeast two-hybrid
	Y3H	yeast three-hybrid
	Y4H	yeast four-hybrid
$\alpha$	$\alpha$ R	$\alpha$ -Rescue (an siRNA-resistant version of rat $\alpha$ -adaplin)
3	3AT	3-amino-1,2,4-triazole

## Table of Contents

	<b>Page:</b>
<b>Preface</b>	<b>i</b>
Title page	i
Epigraph	ii
Acknowledgements	iii
Contributors to this work	iv
Declaration of work	v
Thesis summary	vi
Abbreviations	viii
Table of contents	xi
Table of figures	xviii
Table of tables	xxii
<b>Chapter 1: Introduction</b>	<b>1</b>
1.1 Abstract	2
1.2 The human immune system	3
1.2.1 Cells of the myeloid lineage	3
1.2.2 The major histocompatibility complex receptors	8
1.2.3 Cells of the lymphoid lineage	9
1.3 The CD4 receptor	12
1.3.1 Structural features of CD4	12
1.3.2 Intracellular trafficking of CD4	15
1.3.3 Function of CD4	16
1.4 The human immunodeficiency virus	17
1.4.1 Origin and spread of HIV-1	17
1.4.2 The HIV-1 genome	17
1.4.3 The HIV-1 life cycle	18
1.4.4 Progression from HIV-1 infection to AIDS	25
1.5 Nef	27
1.5.1 Nef: a critical determinant of disease progression	27
1.5.2 Structural and biochemical features of Nef	28
1.5.3 Functions of Nef	32

1.6	Intracellular protein transport	38
1.6.1	Clathrin	38
1.6.2	The AP complexes	39
1.6.3	Structural features of AP complexes	39
1.6.4	Cargo recognition by AP complexes	42
1.6.5	Cargo sorting by AP complexes	45
1.6.6	Interactions of Nef with the AP complexes	45
1.7	Nef-mediated MHC-I downregulation	47
1.7.1	Direct interaction between Nef and MHC-I	47
1.7.2	The mechanism of Nef-mediated MHC-I downregulation	47
1.8	Nef-mediated CD4 downregulation	49
1.8.1	Direct interaction between Nef and CD4	50
1.8.2	The mechanism of Nef-mediated CD4 downregulation	51
1.9	Objectives of this thesis	57
<b>Chapter 2: Materials and methods</b>		<b>58</b>
2.1	Abstract	59
2.2	Molecular biology	60
2.2.1	Polymerase chain reactions	60
2.2.2	Restriction endonuclease digests	60
2.2.3	Ligation reactions	60
2.2.4	Site-directed mutagenesis	61
2.2.5	Bacterial transformations	61
2.2.6	DNA purification	61
2.2.7	DNA nucleotide sequencing	62
2.3	Recombinant protein expression, purification, and binding assays	63
2.3.1	Bacterial expression vectors	63
2.3.1.1	pHis	63
2.3.1.2	pGex	63
2.3.1.3	pST	63
2.3.2	Recombinant protein expression and purification	64
2.3.2.1	His <sub>6</sub> -tagged proteins	65
2.3.2.2	GST-tagged proteins	65
2.3.2.3	AP-2 <sup>CORE</sup> complexes	65

2.3.3	Binding assays	66
2.3.3.1	GST pull-down assays	66
2.3.3.2	Surface plasmon resonance assays	67
2.4	Yeast expression vectors, transformations, and hybrid assays	68
2.4.1	Yeast expression vectors	68
2.4.1.1	pBridge	68
2.4.1.2	pGADT7	69
2.4.1.3	pAD	69
2.4.2	HF7c cells and yeast hybrid assays	70
2.4.2.1	Transformation of HF7c cells	70
2.4.2.2	Yeast three-hybrid assays	71
2.4.2.3	Yeast two-hybrid and four-hybrid assays	72
2.5	<i>Drosophila</i> expression vectors, tissue culture, transfections, and knockdowns	73
2.5.1	<i>Drosophila</i> expression vectors	73
2.5.1.1	pAc	73
2.5.1.2	pMt	73
2.5.1.3	pCo-Blast	74
2.5.2	<i>Drosophila</i> S2 cells	74
2.5.2.1	Tissue culture	74
2.5.2.2	Transient DNA transfections	75
2.5.2.3	Generation of a stable CD4-Nef cell line	75
2.5.2.4	RNAi-mediated protein depletion	76
2.6	Human expression vectors, tissue culture, transfections and knockdowns	77
2.6.1	Human expression vectors	77
2.6.1.1	pCMV	77
2.6.1.2	pCI	77
2.6.1.3	pIRES.GFP	77
2.6.2	JM cells	78
2.6.2.1	Tissue culture	78
2.6.2.2	Transient DNA transfections	78
2.6.3	HeLa cells	79
2.6.3.1	Tissue culture	79

2.6.3.2	Transient DNA transfections	79
2.6.3.3	Endocytosis assays	80
2.6.3.4	siRNA-mediated protein depletion of $\mu$ 1, $\mu$ 2, and $\mu$ 3	81
2.6.3.5	$\alpha$ -adaptin knockdown and rescue reagents	81
2.6.3.6	$\alpha$ -adaptin knockdown and rescue transfections	82
2.7	Flow cytometry	83
2.7.1	Antibodies used	83
2.7.2	Harvesting of cells	83
2.7.3	Staining and analysis of cells	83
2.8	Immunofluorescence and confocal microscopy	85
2.8.1	Antibodies used	85
2.8.2	Preparation of cells	85
2.8.3	Staining and imaging of cells	85
2.9	Immunoblotting	86
2.9.1	Antibodies used	86
2.9.2	Lysis, electrophoresis, and protein depletion	86
<b>Chapter 3: Downregulation of CD4 by HIV-1 Nef is dependent on clathrin and involves a direct interaction of Nef with the AP-2 clathrin adaptor</b>		<b>153</b>
3.1	Abstract	154
3.2	Introduction	155
3.3	Results	156
3.3.1	Downregulation of human CD4 by HIV-1 Nef in <i>Drosophila</i> S2 cells	156
3.3.2	Determinants of Nef-induced CD4 downregulation in S2 cells	156
3.3.3	RNAi screen in S2 cells reveals a requirement for clathrin and AP-2 in the Nef-induced downregulation of CD4	166
3.3.4	Requirement of AP-2 for Nef-induced CD4 downregulation in human cells	177
3.3.5	Physical interaction of Nef with AP-2 in the yeast three-hybrid system	180

3.3.6	Direct interaction of Nef and AP-2 in vitro	183
3.4	Discussion	187
3.4.1	Chapter overview	
3.4.2	Role of clathrin and AP-2 in Nef-mediated CD4 downregulation	187
3.4.3	Recognition of dileucine signals by AP-2	189
3.4.4	Do AP-1 and AP-3 participate in Nef-induced CD4 downregulation?	189
3.4.5	Postendocytic fate of internalized CD4	190
3.4.6	Distinct mechanisms for CD4 and MHC-I downregulation	191
<b>Chapter 4: A diacidic motif in HIV-1 Nef is a novel determinant of binding to AP-2</b>		<b>192</b>
4.1	Abstract	193
4.2	Introduction	194
4.3	Results	195
4.3.1	Identification of a diacidic motif required for the interaction of HIV-1 Nef with the AP-2 $\alpha$ - $\sigma$ 2 hemicomplex	196
4.3.2	The diacidic motif is required for direct binding of HIV-1 Nef to AP-2	199
4.3.3	Binding of HIV-1 Nef to AP-2 is dependent on electrostatic interactions	199
4.3.4	The diacidic motif fits a [D/E]D consensus sequence and is not required for the interaction with the AP-1 $\gamma$ - $\sigma$ 1 or AP-3 $\delta$ - $\sigma$ 3 hemicomplexes	202
4.3.5	Correlation between the requirements of the Nef diacidic motif and CD4 downregulation	202
4.3.6	Distinct requirements of different dileucine motifs for the contribution of diacidic motifs	210
4.4	Discussion	213
4.4.1	Chapter overview	213
4.4.2	The Nef diacidic motif is needed for AP-2 binding and CD4 downregulation	213

4.4.3	The AP-1 and AP-3 complexes are largely dispensable for the Nef-mediated downregulation of CD4	214
4.4.4	Analysis of the diacidic motif yields insights on the binding of dileucine signals to AP complexes	216
4.4.5	The diacidic motif: specific to Nef or broadly applicable?	217
<b>Chapter 5: A basic patch on <math>\alpha</math>-adaptin is required for the binding of HIV-1 Nef and cooperative assembly of a CD4-Nef-AP-2 complex</b>		<b>219</b>
5.1	Abstract	220
5.2	Introduction	221
5.3	Results	223
5.3.1	Identification of basic residues on $\alpha$ -adaptin required for the interaction of HIV-1 Nef	223
5.3.2	The $\alpha$ -adaptin K297 and R340 residues form a basic patch that is required for the binding of Nef	228
5.3.3	The AP-2 $\alpha$ K297 and R340 residues are required for direct binding of Nef	231
5.3.4	The $\alpha$ -adaptin K297 and R340 residues are required for Nef-induced CD4 downregulation	232
5.3.5	The CD4 tail, Nef, and the AP-2 $\alpha$ - $\sigma$ 2 hemicomplex assemble cooperatively to form a CD4-Nef-AP-2 tripartite complex	241
5.4	Discussion	245
5.4.1	Chapter overview	245
5.4.2	Characteristics of the $\alpha$ -adaptin basic patch	245
5.4.3	Cooperative assembly of a CD4-Nef-AP-2 tripartite complex	251
<b>Chapter 6: Discussion</b>		<b>254</b>
6.1	Abstract	255
6.2	Summary of results	256
6.3	Ongoing work: identification of the Nef dileucine binding site on AP-2	260
6.4	Future work	282

6.4.1 The effect of Nef-AP-2 binding on surface receptor expression	282
6.4.2 Postendocytic fate of CD4	283
6.5 Concluding remarks	285
<b>References</b>	<b>286</b>
<b>Publications arising from this work</b>	<b>322</b>

## Table of figures

	<b>Page:</b>
<b>Chapter 1: Introduction</b>	<b>1</b>
Fig. 1.1: Hematopoietic lineage of leucocytes	5
Fig. 1.2: Leukocyte function	7
Fig. 1.3: The structure of CD4 and its interaction with MHC-II and gp-120	14
Fig. 1.4: The HIV-1 genome	20
Fig. 1.5: Major functions of HIV-1 proteins	22
Fig. 1.6: The HIV-1 virion	23
Fig. 1.7: Structure and function of HIV-1 Nef	31
Fig. 1.8: Nef targets specific receptors for downregulation	33
Fig. 1.9: Clathrin assembles to form triskelions, lattices, and cages	41
Fig. 1.10: Structure of the adaptor protein complexes	44
Fig. 1.11: Nef-mediated CD4 downregulation	52
Fig. 1.12: Potential mechanisms of Nef-mediated CD4 downregulation	55
<b>Chapter 2: Materials and methods</b>	<b>58</b>
Fig 2.1: pHis plasmid map	89
Fig 2.2: pGEX plasmid map	91
Fig 2.3: pST plasmid map	93
Fig 2.4: pBridge plasmid map	95
Fig 2.5: pGADT7 plasmid map	97
Fig 2.6: pAD plasmid map	99
Fig 2.7: pAc plasmid map	101
Fig 2.8: pMt plasmid map	103
Fig 2.9: pCo-Blast plasmid map	105
Fig 2.10: pCMV plasmid map	107
Fig 2.11: pCI plasmid map	109
Fig 2.12: pIRES.GFP plasmid map	111
<b>Chapter 3: Downregulation of CD4 by HIV-1 Nef is dependent on clathrin and involves a direct interaction of Nef with the AP-2 clathrin adaptor</b>	<b>153</b>

Fig. 3.1:	Downregulation of human CD4 by HIV-1 Nef in <i>Drosophila</i> S2 cells	158
Fig. 3.2:	Comparison of the downregulation of CD4 by Nef from various HIV-1 and SIV variants in <i>Drosophila</i> S2 and human JM CD4 <sup>+</sup> T cells	161
Fig. 3.3:	Determinants of Nef-induced CD4 downregulation in <i>Drosophila</i> S2 and human JM CD4 <sup>+</sup> T cells	163
Fig. 3.4:	Immunofluorescence microscopy of CD4 in S2 cells	165
Fig. 3.5:	Effect of selected RNAi treatments on the Nef-induced downregulation of CD4 in stably transfected S2 cells	168
Fig. 3.6:	Results of the RNAi screen of 68 components of the protein trafficking machinery for their involvement in Nef-induced CD4 downregulation in S2 cells	171
Fig. 3.7:	Analysis of AP-2 knockdown in human cells	179
Fig. 3.8:	Yeast three-hybrid analysis of Nef-AP-2 interactions	182
Fig. 3.9:	Direct interaction of Nef and AP-2 detected in vitro	184
<b>Chapter 4: A diacidic motif in HIV-1 Nef is a novel determinant of binding to AP-2</b>		<b>192</b>
Fig. 4.1:	Identification of residues within the HIV-1 Nef C-terminal flexible loop that contribute to AP-2 binding	198
Fig. 4.2:	In vitro analyses of Nef-AP-2 interaction determinants	201
Fig. 4.3:	Mutational analysis of Nef binding to the AP-1 $\gamma$ - $\sigma$ 1, AP-2 $\alpha$ - $\sigma$ 2, and AP-3 $\delta$ - $\sigma$ 3 hemicomplexes	204
Fig. 4.4:	Immunofluorescence microscopy analysis of CD4 downregulation by wild-type and mutant Nef proteins	207
Fig. 4.5:	Flow cytometric analysis of CD4 downregulation by wild-type and mutant Nef proteins	209
Fig. 4.6:	Y3H analysis reveals qualitative differences among dileucine motifs	211
<b>Chapter 5: A basic patch on <math>\alpha</math>-adaplin is required for the binding of HIV-1 Nef and cooperative assembly of a CD4-Nef-AP-2 complex</b>		<b>219</b>
Fig. 5.1:	Identification of basic residues in the AP-2	225

	$\alpha$ - $\sigma$ 2 hemicomplex that are not conserved in the homologous subunits of AP-1 and AP-3	
Fig. 5.2:	Y3H analysis of the interaction between HIV-1 Nef and AP-2 $\alpha$ - $\sigma$ 2 hemicomplexes containing substitutions for nonconserved basic residues	227
Fig. 5.3:	AP-2 $\alpha$ residues K297 and R340 are required for the interaction of the $\alpha$ - $\sigma$ 2 hemicomplex and HIV-1 Nef	230
Fig. 5.4:	Location of $\alpha$ K297 and R340 on the three-dimensional structure of the AP-2 complex	233
Fig. 5.5:	The $\alpha$ K297 and R340 residues are required for direct binding of AP-2 to HIV-1 Nef	235
Fig. 5.6:	The AP-2 $\alpha$ K297 and R340 residues are necessary for Nef-mediated downregulation of CD4	238
Fig. 5.7:	Cooperative assembly of a tripartite complex consisting of the CD4 cytosolic tail, full-length Nef, and the AP-2 $\alpha$ - $\sigma$ 2 hemicomplex, as demonstrated by yeast hybrid assays	243
Fig. 5.8:	The $\alpha$ K297 and R340 residues are part of a large basic patch on the surface of AP-2	248
Fig. 5.9:	Phylogenetic conservation of $\alpha$ -adaptin basic residues involved in the binding of HIV-1 Nef	250

## **Chapter 6: Discussion**

Fig. 6.1:	Revised model of Nef-mediated CD4 downregulation	258
Fig. 6.2:	Identification of basic residues in the AP-2 $\alpha$ - $\sigma$ 2 hemicomplex that are conserved with the homologous subunits of AP-1 and AP-3	263
Fig. 6.3:	Plasmids used for the Y3H assays shown in this chapter	265
Fig. 6.4:	Y3H analysis of the $\alpha$ mutants: role of the conserved, basic residues in binding the acidic portion of dileucine motifs	267
Fig. 6.5:	Y3H analysis of the $\sigma$ 2 mutants: role of the conserved, basic residues in binding the acidic portion of dileucine motifs	269

Fig. 6.6:	Location of $\alpha$ R21 and adjacent residues on the crystal structure of the AP-2 complex	271
Fig. 6.7:	Sequence conservation of $\alpha$ - $\sigma$ 2 residues potentially involved in binding the hydrophobic portion of dileucine sorting signals	273
Fig. 6.8:	Y3H analysis of the $\alpha$ - $\sigma$ 2 residues potentially involved in binding the hydrophobic portion of dileucine sorting signals	275
Fig. 6.9:	Location of the prospective Nef dileucine binding site on the structure of AP-2	278
Fig. 6.10:	Location of the CD4 dileucine binding site on AP-2	280

## Table of tables

	<b>Page:</b>
<b>Chapter 2: Materials and methods</b>	<b>58</b>
Table 2.1: PCR reagents	112
Table 2.2: PCR thermal cycling conditions	112
Table 2.3: Ligation reagents	113
Table 2.4: SDM reagents	114
Table 2.5: SDM thermal cycling conditions	114
Table 2.6: Combinations of DNA plasmids used to transfect HeLa cells following siRNA-mediated protein depletion of $\mu 1$ , $\mu 2$ , and $\mu 3$	115 116
Table 2.7: Combinations of siRNA duplexes and DNA plasmids used to transfect HeLa cells for the $\alpha$ -adaptin knockdown and rescue assays	
Table 2.8: Plasmids used in this study	117
Table 2.9: Primers used in this study	133
Table 2.10: Antibodies used in this study	149
<b>Chapter 3: Downregulation of CD4 by HIV-1 Nef is dependent on clathrin and involves a direct interaction of Nef with the AP-2 clathrin adaptor</b>	<b>153</b>
Table 3.1: Raw data from the RNAi screen of endogenous proteins involved in the Nef-mediated downregulation of CD4 in S2 cells	172

**Chapter 1:**  
**Introduction**

## **1.1 Abstract**

In this chapter, several topics related to the Nef-mediated downregulation of CD4 will be introduced. The first topic to be covered is the human immune system. Because of the extraordinary complexity of the immune system, this section is not intended to be a comprehensive description of its properties. Instead, the discussion of host-defense mechanisms will simply provide a framework for understanding the critical role that CD4 T cells play in protecting the body from pathogenic organisms. This is followed by a more focused examination of the CD4 molecule itself, which in addition to being the distinguishing feature of CD4 T cells, is a co-receptor for HIV-1. As explained in the next section, the infection and destruction of CD4 T cells by HIV-1 causes AIDS because the integrity of the immune system is slowly degraded. This subject naturally leads to a discussion about Nef, a key regulator of disease progression. In the section devoted to Nef, its contribution to viral pathogenicity and its wide range of functions are described. Of all these functions, the downregulation of CD4 is probably the most important. This process is believed to depend on interactions between Nef and at least some components of the host-cell protein-trafficking machinery. After a brief review of this machinery, two models that potentially explain the mechanism by which Nef downregulates CD4 are presented. The methodology that will be used in this thesis to identify the correct model is described in the final section.

## **1.2 The human immune system**

The human immune system, which is charged with defending the body against attack by foreign organisms, has two major components: the innate immune system and the adaptive immune system (for a detailed description of these systems, see Janeway et al., 2005). The innate immune system is capable of mounting an immediate, but non-specific response against pathogens: in most cases, this response is able to contain and eliminate the infection. However, if the pathogen manages to evade or overwhelm the innate immune system, the adaptive immune system is activated. As its name implies, this system “adapts” to an infection and produces a specific, sustained response to a particular pathogen.

The cells that mediate the innate and adaptive immune responses originate in the bone marrow (see Fig. 1.1). There, pluripotent hematopoietic stem cells give rise to the myeloid and lymphoid progenitors, which are themselves stem cells of a somewhat more limited potential. Myeloid progenitors differentiate into a variety of cell types including, but not limited to, macrophages, neutrophils, and dendritic cells. Lymphoid progenitors, on the other hand, mature into natural killer (NK) cells, B lymphocytes, and T lymphocytes. Each of these cells has a specialized function (Fig. 1.2), and by working in a coordinated fashion, they ensure the proper functioning of the innate and adaptive immune responses.

### **1.2.1 Cells of the myeloid lineage**

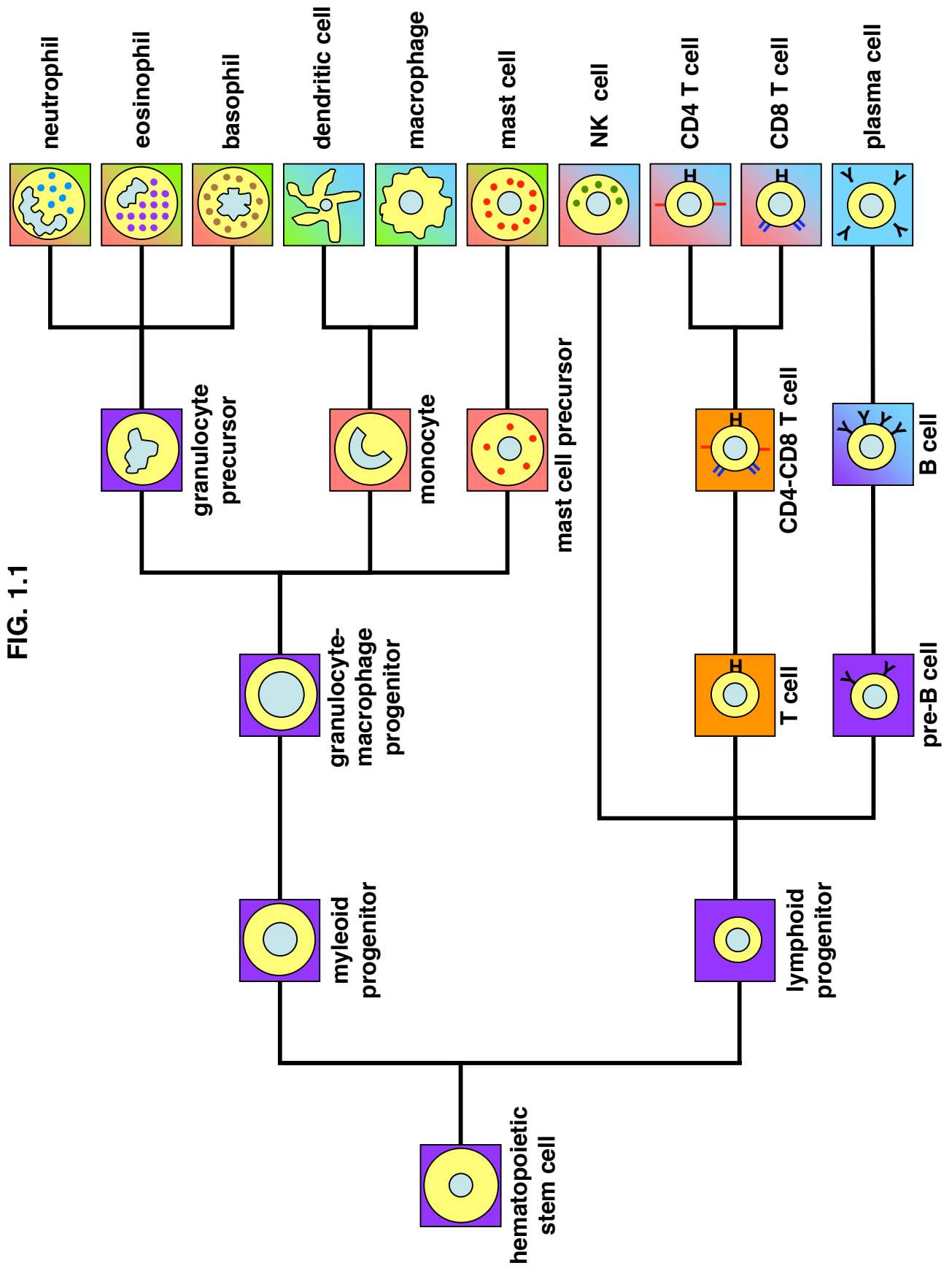
Macrophages, which are present in tissues throughout the body, are generally the first immune cells to appear at the site of an infection. Upon encountering a pathogen, they initiate the innate immune response by engulfing and destroying the foreign organism in a process known as phagocytosis. Activated macrophages also secrete compounds that alert other phagocytes, such as neutrophils and dendritic cells, of the emerging infection. In response to these signals, large numbers of neutrophils migrate from the blood stream to the affected area, where they bolster the innate immune response by rapidly ingesting and neutralizing pathogens. Dendritic cells arrive later, and in fewer numbers, but they act as an important link between the innate and adaptive immune systems. The primary role of these cells is to present peptide fragments, or antigens, derived from phagocytosed pathogens on their surface using a special receptor (which

### FIG. 1.1: Hematopoietic lineage of leukocytes

Leukocytes, which are commonly referred to as white blood cells, mediate the innate and adaptive immune responses. Pluripotent hematopoietic stem cells, located in the bone marrow, develop into myeloid and lymphoid progenitors. The myeloid progenitor gives rise to erythrocytes (red blood cells; not shown) and granulocyte-macrophage progenitors. The granulocyte-macrophage progenitors differentiate to yield granulocytes (neutrophils, eosinophils, and basophils), monocytes (dendritic cells and macrophages), and mast cells. On the other hand, lymphoid progenitors give rise to NK cells, T lymphocytes (CD4 and CD8 T cells), and B lymphocytes (plasma cells). CD4 T cells differentiate further into helper T cells, while CD8 T cells become cytotoxic T lymphocytes (not shown; however, the mechanism of T lymphocyte differentiation is described in Section 1.2.3). In each cell shown below, the **light blue** area represents the nucleus, while the **yellow** area represents the cytoplasm. Granules are colored **blue**, **brown**, **green**, **purple**, and **red**. CD4 is depicted as a single red line [ **I** ] while CD8 $\alpha\beta$  is depicted by two parallel blue lines [ **II** ].

4

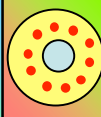
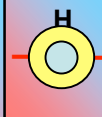
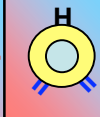
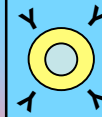
The T cell receptor is shown as a horizontal black [ **H** ] while the B cell receptor and secreted antibodies are depicted as black [ **Y** ]. The square backgrounds for each cell indicates the location that the cell is most likely to be found in. **Purple** represents the bone marrow, **red** represents the blood, **green** represents tissue, **orange** represents the thymus, and **blue** represents the lymph. Cells which circulate between different locations in the body have square backgrounds composed of multiple colors. The functions of each leukocyte listed on the right-hand side is described in Fig. 1.2. It is important to note that, given the complexity of leukocyte differentiation, some intermediate stages have been omitted from this figure for the sake of clarity.



**FIG. 1.2: Leukocyte functions**

The major function of each leukocyte is described below. For each cell-type (neutrophil, eosinophil, basophil, dendritic cell, macrophage, mast cell, NK cell, CD4 T cell, CD8 T cell, and plasma cell), the color conventions introduced in the legend to Fig. 1.1 are maintained.

FIG. 1.2

Cell Type	Function
 Neutrophils	Phagocytes that are primarily involved in the destruction of extracellular pathogens. Granules contain reactive oxygen species and proteolytic enzymes.
 Eosinophils	Attack large antibody-coated parasites by releasing enzymes, normally stored in granules, that degrade proteins and disrupt the integrity of cellular membranes.
 Basophils	Have a poorly defined function, but may be involved in promoting blood flow to the site of an injury or infection. Granules contain histamine and heparin, among other compounds.
 Dendritic cells	Phagocytes that acquire, process, and present antigens on their surface in complex with MHC-II. Mature dendritic cells travel to lymph nodes and activate CD4 T cells.
 Macrophages	Phagocytes that engulf and destroy extracellular pathogens. Like dendritic cells, macrophages can also activate CD4 T cells via the MHC-II antigen-presentation pathway.
 Mast cells	Similar to basophils; promote blood flow by increasing vasodilation and slowing the rate of clotting. Granules contain histamine and heparin.
 NK cells	Kills host-cells that express abnormally low levels of MHC-I on their surface, as this phenotype is often an indication that the cell has been infected by a foreign organism.
 CD4 T cells	Express CD4 and MHC-II-restricted TCRs. Upon activation, differentiate into helper T cells, which secrete cytokines that influence the function of most other immune cells.
 CD8 T cells	Express CD8 and MHC-I-restricted TCRs. Upon activation, differentiate into cytotoxic T cells, which kill host cells that have been infected by foreign organisms.
 Plasma cells	Terminally differentiated B cells; produce and secrete antibodies that neutralize toxins and target extracellular pathogens for destruction.

is described in more detail below). Antigen-presenting dendritic cells then travel from the infection site to a nearby lymph node, where they induce the activation of a subset of lymphocytes and thereby stimulate the adaptive immune response.

### **1.2.2 The major histocompatibility complex receptors**

The receptor that dendritic cells use to display foreign antigens belongs to a family of highly polymorphic genes called the major histocompatibility complex (MHC). There are two kinds of MHC receptors, designated class I (MHC-I) and class II (MHC-II). Both classes of receptor bind peptides at an intracellular location, traffic to the plasma membrane, and present the peptides on the exoplasmic face of the cell to circulating lymphocytes. However, the receptors differ in several important ways, including their cellular expression profiles, the source of their peptide ligands, the organelle where peptide loading takes place, and the specific kind of lymphocyte they activate.

MHC-I molecules (reviewed by Purcell and Elliot, 2008; van Endert, 1999) are found on the surfaces of most cell types, and bind peptides that are obtained from proteins produced within the cell. A randomly chosen fraction of all proteins translated in the cytosol is degraded by the proteasome into short peptide fragments; these peptides are then translocated into the endoplasmic reticulum (ER), where they are loaded onto MHC-I receptors moving through the secretory pathway on their way to the plasma membrane. Because all newly synthesized proteins are potentially subject to this process, many MHC-I antigens are generated from endogenous polypeptides. But if the cell is infected with a pathogen, such as a virus, at least some of the antigens that are displayed on the plasma membrane will be derived from foreign proteins.

Unlike MHC-I receptors, MHC-II molecules (reviewed by Guermonprez et al., 2002; van Niel et al., 2008) are normally expressed only by certain types of phagocytes, like the dendritic cells mentioned above. As the MHC-II receptors pass through the ER, en route to the cell surface, they are prevented from binding the peptides available in this location by the tight association of a transmembrane protein called the invariant chain (Ii). This protein then chaperones MHC-II to the phagolysosome (Dugast et al., 2005; McCormick et al., 2005), an acidic organelle that contains any endogenous or foreign material that the cell may have internalized. Hydrolases in the phagolysosome digest this material, and the resulting peptides are loaded onto MHC-II receptors in place of

ii. Once this process is finished, antigen-bound MHC-II complexes are transported to the plasma membrane for presentation on the exterior of the cell.

### **1.2.3 Cells of the lymphoid lineage**

As described in the preceding section, the MHC-I and MHC-II antigen-presentation pathways play distinct, but complementary, roles in activation of the adaptive immune response: MHC-I receptors are used to alert one set of lymphocytes to the presence of pathogens within the cell, while MHC-II receptors are used to signal to a different set of lymphocytes that there are foreign organisms in the extracellular space. In both cases, the lymphocytes that interact with the antigen-MHC complexes are T cells, so called because they mature in the thymus rather than the bone marrow. These cells express a unique molecule on their surface known as the T cell receptor (TCR).

The function of the TCR is to recognize foreign peptides bound to either MHC-I or MHC-II (for a thorough review of this topic, see Janeway et al., 2005). Because each TCR can recognize only one antigen, the adaptive immune system must have many different TCRs in its repertoire in order to effectively respond to the range of foreign peptides that it is challenged with. Diversity among TCRs is generated by a complex mechanism called somatic recombination, in which the genes that encode the TCR are assembled, in part, by the random joining of highly variable segments of DNA. This process occurs during the early stages of T cell differentiation, and once complete, is irreversible. Thus, each T cell is endowed with a distinct version of the TCR that has unique antigen-recognition properties.

In addition to the TCR, T lymphocytes at this stage of development express several other important surface receptors, including CD4 and CD8. These cells (often referred to as “double-positive” T cells due to the concurrent expression of CD4 and CD8) must undergo two rounds of selection in the thymus before they are allowed to enter the peripheral lymphoid organs. The first round, known as positive selection, ensures that the TCR has at least some inherent affinity for either MHC-I or MHC-II (for a review of this process, see Fowlkes and Schweighoffer, 1995). Positive selection also coordinates expression of CD4 and CD8 with the specificity of the TCR (reviewed by Germain, 2002). From this point onwards, cells with TCRs that preferentially bind MHC-I express only CD8 (and are referred to as CD8 T cells), while those cells that

have MHC-II-restricted TCRs express only CD4 (and are referred to as CD4 T cells). T lymphocytes that harbor versions of the TCR incapable of binding one of the MHC receptors are eliminated. The remaining “single-positive” T cells are then subjected to a round of negative selection, the purpose of which is to delete TCRs that interact too strongly with MHC receptors carrying endogenous peptides (reviewed by Hogquist et al., 2005). Cells with such TCRs are likely to initiate inappropriate immune reactions, and therefore must be purged. CD8 T cells and CD4 T cells that survive both rounds of selection are exported from the thymus to the periphery, where they execute their effector functions.

The primary function of CD8 T cells is to identify and destroy host cells infected by foreign organisms (see Russell and Ley, 2002). As described above, infected cells are able to present peptides derived from foreign proteins on their surface via the MHC-I antigen-presentation pathway, thus signaling that their health has been compromised. Naive CD8 T cells move through the body in search of such cells, using their TCRs to sample many different peptide-MHC-I complexes. TCR-dependent recognition of a foreign antigen causes the CD8 T cell to rapidly proliferate, creating a large number of daughter cells with the same antigen specificity. These clones mature into cytotoxic T lymphocytes (CTLs), which seek out and induce the apoptosis of any cell with the cognate antigen on its surface.

In an attempt to avoid the CTL-mediated killing of their host cells, many viruses have evolved mechanisms to disrupt the MHC-I antigen-presentation pathway (reviewed by Yewdell and Bennink, 1999). Often, this involves the downregulation of MHC-I from the plasma membrane, either by blocking its exit from the ER, or by promoting internalization of the receptor once it reaches the cell surface. Such actions effectively mask the presence of the virus, allowing it to replicate within the cell undetected. To combat this relatively common evasion strategy, the immune system uses NK cells to detect and destroy cells with unusually low levels of MHC-I expression (reviewed by Timonen and Helander, 1997).

CD4 T cells, in contrast to the CTLs and NK cells mentioned above, lack the intrinsic cytotoxic activity needed to kill infected cells directly. Instead, CD4 T cells promote the clearance of pathogens by coordinating the overall immune response (see Janeway et al., 2005). This complex process is normally initiated by dendritic cells, which use

the MHC-II antigen-presentation pathway to inform CD4 T cells of an infection. The TCR-mediated recognition of a foreign peptide induces CD4 T cells to rapidly divide and differentiate into helper T cells (reviewed by Reiner, 2007). These cells produce and secrete a wide variety of molecules, called cytokines, that influence the behavior of target cells. There are two major kinds of helper T cells, known simply as  $T_H1$  and  $T_H2$  cells, that are distinguished largely on the basis of which cytokines they secrete (reviewed by Mosmann and Chapman, 1989).  $T_H1$  cells release cytokines that drive hematopoietic stem cells to mature into macrophages, neutrophils, and dendritic cells; activate existing macrophages, neutrophils and dendritic cells; and stimulate CTLs and NK cells to attack infected cells.  $T_H2$  cells, on the other hand, induce B lymphocytes to secrete antibodies that neutralize toxins and target pathogens for destruction. Thus, CD4 helper T cells play a critical role in regulating the immune system, maximizing its capabilities, and directing its efforts against aggressive foreign organisms.

### 1.3 The CD4 receptor

As described in the previous section, both  $T_{H1}$  and  $T_{H2}$  cells are derived from naive CD4 T cells, and express the CD4 receptor on their surface. In addition, CD4 can be found in small amounts on the plasma membrane of macrophages and dendritic cells; however, the function of the receptor in these cell types is currently unknown. In this section, the structure, intracellular trafficking, and physiological role of CD4 in helper T cells is examined in greater detail.

#### 1.3.1 Structural features of CD4

Human CD4 is a type I transmembrane protein that, in its mature form, has a mass of 55 kDa and is comprised of 433 amino acids (reviewed by Bowers et al., 1997). These amino acids are distributed unevenly among the three major regions of CD4, resulting in a topologically asymmetrical molecule: the N-terminal exoplasmic section contains 371 residues, the transmembrane domain contains 24, and the C-terminal cytoplasmic tail contains 38 (Fig. 1.3). From a structural perspective, the exoplasmic region can be further divided into four smaller domains, all of which have an immunoglobulin-like fold (Bradley et al., 1993; Ryu et al., 1990; Wang et al., 1990). The first two domains (D1 and D2) are located at the N-terminus of the receptor, and are packed together to form a rigid rod. A flexible linker joins this structure to a similar rod, composed of the third and fourth exoplasmic domains (D3 and D4). Immediately following D4 is the  $\alpha$ -helical transmembrane domain, which both anchors the receptor in the membrane and physically connects the exoplasmic region to the cytoplasmic tail. The tail itself is largely unstructured, but under certain conditions, it appears to form an amphipathic  $\alpha$ -helix spanning residues 402-419 (Willbold and Rösch, 1996; Wray et al., 1998). Within this  $\alpha$ -helix lies a pair of leucines (L413 and L414), flanked on either side by serine residues (S408 and S417, respectively). In addition, four cysteine residues are located in the tail, two upstream of the  $\alpha$ -helix (C394 and C397) and two downstream (C420 and C423, as part of a CxCP motif [where x is any amino acid]). These cytoplasmic motifs are important for the post-translational modification of CD4 and the intracellular trafficking of the receptor.

### FIG. 1.3: The structure of CD4 and its interaction with MHC-II and gp120

The CD4 molecule is a type I transmembrane protein with an exoplasmic region, a helical transmembrane domain, and a short cytosolic tail. The exoplasmic region contains four immunoglobulin-like domains (D1, D2, D3, and D4). The D1 domain, colored **green** in this figure, is located at the N-terminus of the receptor. It is tightly linked to D2 (colored **blue**), and together, these two domains form a relatively rigid structure. D1-D2 are connected to the D3-D4 region (colored **orange** and **red**, respectively) by a flexible linker. CD4 functions as a co-receptor for both MHC-II and gp120, as described in the accompanying text and shown below.

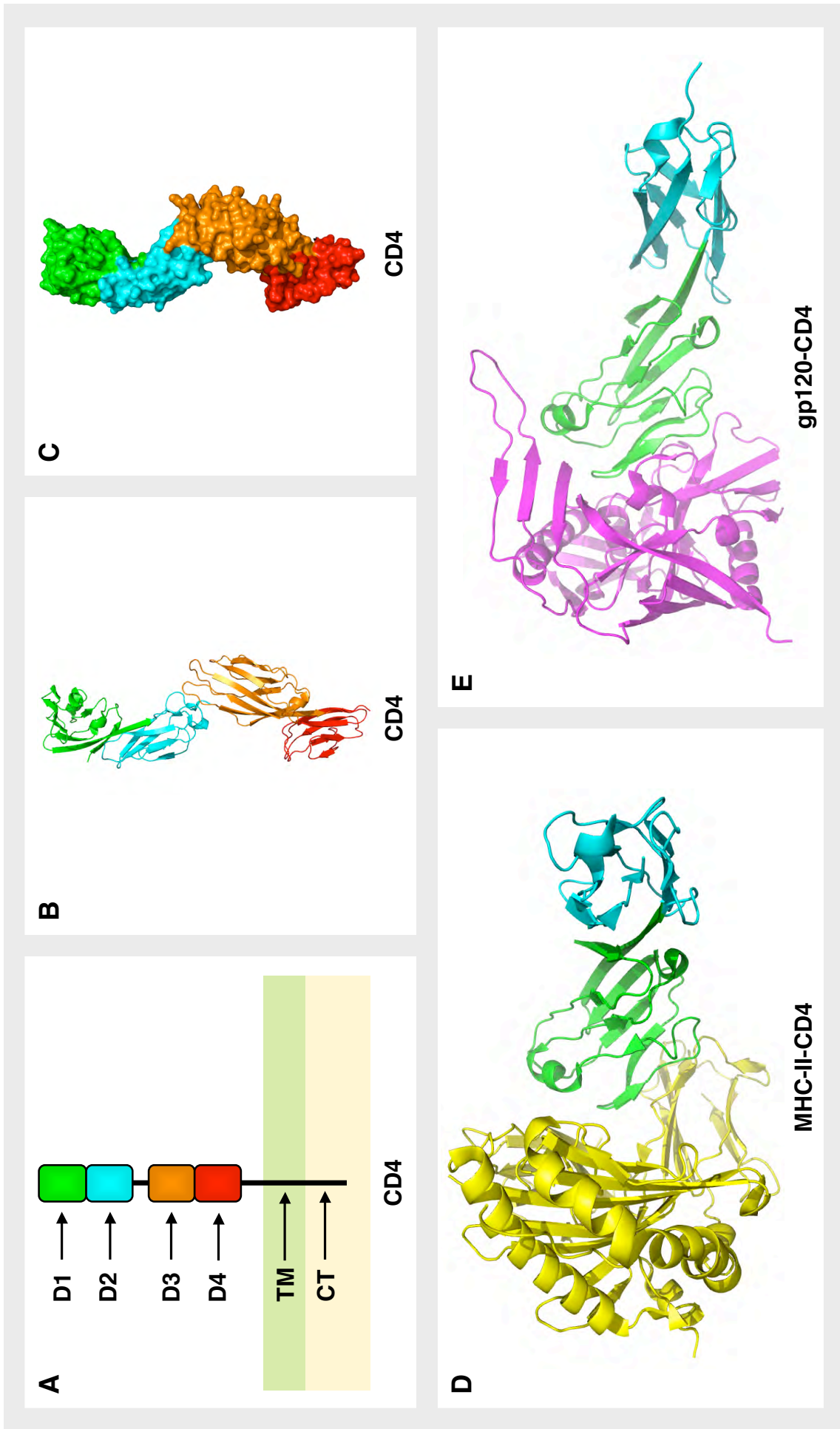
**(A)** Schematic representation of the CD4 structure. The exoplasmic region (composed of D1, D2, D3, and D4), the transmembrane (TM) domain and the cytosolic tail (CT) are shown. In the background, the white area is meant to represent the exoplasmic space, the **light green** area is meant to represent the plasma membrane, and the **light yellow** area is meant to represent the cytoplasm.

**(B-C)** Ribbon diagram and surface representation of the CD4 exoplasmic region (PDB ID numbers 1W10, 1 WIP, and 1W1Q [Wu et al., 1997]).

**(D)** Crystal structure of CD4 bound to the MHC-II receptor (PDB ID number 1JL4 [Wang et al., 2001]). Only the D1 and D2 domains of CD4 are shown. The MHC-II receptor is depicted in **gold**. CD4 interacts with an invariant region of MHC-II, while the TCR binds to a polymorphic area of MHC-II that contains the antigenic peptide (not shown).

**(E)** Crystal structure of CD4 bound to the HIV-1 gp120 envelope protein (PDB ID number 1GC1 [Kwong et al., 1998]). Only the D1 and D2 domains of the CD4 receptor are shown. The gp120 protein is colored **pink**.

FIG. 1.3



Crystal structures from Kwong et al., 1998; Wang et al., 2001; Wu et al., 1997

### 1.3.2 Intracellular trafficking of CD4

CD4, like all transmembrane proteins, is partially inserted into the ER during protein synthesis. As the receptor is translated, its exoplasmic region is drawn into the lumen of the ER, while its tail remains exposed to the cytoplasm. At this stage, carbohydrate moieties are added to two consensus sites on the D3 and D4 domains of CD4 (König et al., 1998). These N-linked oligosaccharides facilitate proper folding of the receptor within the lumen, allowing it to leave the ER and enter the Golgi apparatus (Tiffet et al., 1992). There one of the oligosaccharides is modified in preparation for transport to the cell surface. Meanwhile, on the cytoplasmic side, the C394 and C397 tail residues are acylated by the covalent attachment of palmitate, a saturated fatty acid (Crise and Rose, 1992). The functional significance of palmitoylating the CD4 cytoplasmic tail remains unclear; however, it may stabilize the interactions between CD4 and other proteins by decreasing the lateral mobility of the receptor within the membrane.

One of the proteins that CD4 interacts intimately with is p56<sup>lck</sup> (Lck), a member of the Src family of protein tyrosine kinases (Rudd et al., 1988; Veillette et al., 1988). Lck is expressed by T lymphocytes, and similar to CD4, is palmitoylated at an early stage of the biosynthetic pathway (Bijlmakers and Marsh, 1999). Shortly thereafter, Lck binds to the CD4 cytoplasmic tail, and migrates with the receptor to the plasma membrane (Bijlmakers and Marsh, 1999). This interaction is mediated by a zinc clasp, in which a positively charged zinc ion is coordinated by four cysteines: C20 and C23 on Lck, and C420 and C423 on the CD4 tail (Kim et al., 2003; Turner et al., 1990). Upon reaching the cell surface, Lck retains CD4 at the plasma membrane by significantly decreasing the rate at which the receptor is endocytosed (for further information on endocytosis, see Section 1.6). In the absence of Lck, CD4 is internalized at a rate of 2-5% per min (Pelchen-Matthews et al., 1991). This process requires the CD4 dileucine motif, and is accelerated by the protein kinase C (PKC)-mediated phosphorylation of S408 and S417 on the receptor tail (Shin et al., 1990; Shin et al., 1991). In the presence of Lck, however, the rate of CD4 endocytosis is reduced approximately ten-fold, to 0.2-0.6% per min (Pelchen-Matthews et al., 1992). By trapping CD4 at the plasma membrane, Lck ensures that the receptor-kinase complex is in position to participate in helper T cell signaling events.

### 1.3.3 Function of CD4

In helper T cells, CD4 cooperates with Lck and the TCR complex to initiate a signal transduction pathway that leads to activation of the cell (for a comprehensive review, see Janeway et al., 2005). The first step in this pathway occurs when the TCR binds a peptide-MHC-II complex on the surface of an antigen-presenting cell. CD4 then binds to a non-polymorphic portion of the MHC-II receptor via its D1 domain (see Fig. 1.3; Cammarota et al., 1992; König et al., 1992; Wang et al., 2001). The binding of CD4 and the TCR to the same MHC-II molecule brings Lck into close proximity of several immunoregulatory tyrosine-based activation motifs (ITAMs) located in the cytosolic region of the TCR complex (Xiong et al., 2001). This allows Lck to phosphorylate the ITAMs, which then recruit the kinase ZAP-70 from the cytoplasm (Chan et al., 1992; Iwashima et al., 1994). Lck subsequently phosphorylates ZAP-70, thereby passing the antigen-recognition signal onto another kinase (Yamasaki et al., 1996). The signal is eventually transmitted from the plasma membrane to the nucleus, priming the cell for activation (Zhang et al., 1988). Activation is finally achieved when the cell receives a co-stimulatory signal, usually induced by the interaction of CD28 on the surface of the helper T cell with either CD80 or CD86 on the surface of the antigen-presenting cell (Linsley et al., 1990). The integration of antigen-recognition and co-stimulatory signals causes the helper T cell to proliferate, differentiate, and produce the cytokines that are needed to coordinate the immune response (Harding et al., 1992; Thompson et al., 1989). Although many proteins are involved in the activation of helper T cells, it is clear that CD4 is a critical component of this process. However, CD4 has another, less beneficial function: it also serves as the primary receptor for the human immunodeficiency viruses (HIV).

## **1.4 The human immunodeficiency virus**

The human immunodeficiency viruses, HIV-1 and HIV-2, are the etiological agents of acquired immune deficiency syndrome (AIDS) in humans (please refer to Barin et al., 1985; Barré-Sinoussi et al., 1983; Gallo et al., 1984; Hahn et al., 1984; Popovic et al., 1984a; Sangadarhan et al., 1984; Schüpbach et al., 1984; Vilmer et al., 1984). As its name suggests, AIDS is a condition characterized by failure of the immune system. In nearly all cases, the disease leads to premature death, as opportunistic infections and aggressive cancers eventually overwhelm the body (Gottlieb et al., 1981; Masur et al., 1981; Siegel et al., 1981). Although both viruses can cause AIDS, HIV-1 has had a greater impact on public health because it is more infectious, widespread, and virulent than HIV-2 (reviewed by Rowland-Jones and Whittle, 2007). This thesis, therefore, focuses primarily on HIV-1.

### **1.4.1 Origin and spread of HIV-1**

Sequencing studies performed over several decades have convincingly demonstrated that HIV-1 is closely related to a simian immunodeficiency virus (SIV) found in the chimpanzees of central Africa (reviewed by Holmes, 2001). Phylogenetic analyses of the available sequences later indicated that three strains of this SIV virus were transferred from chimpanzees to humans between 1910 and 1950, giving rise to the three major groups of HIV-1 (Gao et al., 1999; Korber et al., 2000). While it is still unclear how the virus managed to cross the species barrier, among humans HIV-1 is spread by exposure to certain types of contaminated body fluids. This mode of transmission has carried HIV-1 across the globe, creating a pandemic. According to the most recent estimates, 33 million people are currently infected with HIV-1, and another 25 million people have already died of HIV-1-associated AIDS (Cohen et al., 2008; UN Program on HIV/AIDS, 2008). The genome and life cycle of this virus are described below.

### **1.4.2 The HIV-1 genome**

HIV-1 is a retrovirus, meaning that its genome can exist as either a RNA or a DNA molecule depending on the stage of its life cycle (for more detailed information on the HIV-1 life cycle, see Section 1.4.3). Within the virion, the viral genome is encoded by single-stranded RNA. Shortly after the infection of a cell, however, the RNA genome

is converted into double-stranded DNA and inserted into a host chromosome. In this form, the genetic material of HIV-1 is often referred to as a provirus, because it must be transcribed back into RNA before it can be incorporated into another virion.

The HIV-1 provirus contains nine open reading frames (ORFs), flanked on either side by long terminal repeat (LTR) sequences (see Fig. 1.4; Muesing et al., 1985; Ratner et al., 1985; Sanchez-Pescardo et al., 1985; Wain-Hobson et al., 1985). The LTRs do not code for any proteins, but they are required for the integration and transcription of the provirus (Bushman et al., 1990; Rosen et al., 1985; Starich et al., 1985). Of the nine ORFs, three code for large polyproteins, which are cleaved by proteases into several smaller proteins. Thus, HIV-1 can express a total of fifteen proteins (listed in Fig. 1.5; also reviewed by Frankel and Young, 1998; Swanson and Malim, 2008). Although a detailed description of each of these is beyond the limited scope of this thesis, special attention will be paid to the activities of gp120, gp41, reverse transcriptase, integrase, Tat, Rev, and Nef during the viral life cycle.

### **1.4.3 The HIV-1 life cycle**

The surface of the HIV-1 virion (depicted in Fig. 1.6) is coated with heterodimers of gp120 and gp41, which are glycoproteins that regulate fusion of the virus with a host cell (Hu et al., 1986; Robey et al., 1985; Veronese et al., 1985). The gp120 portion of this glycoprotein complex binds to CD4 with high affinity, thereby targeting HIV-1 to macrophages, dendritic cells, immature CD4 T cells, and helper T cells (see Fig. 1.3; Dalglish et al., 1984; Ho et al., 1986; Klatzmann et al., 1984; McDougal et al., 1986; Popovic et al., 1984b). Binding of CD4 by gp120 induces a conformational change in the viral glycoprotein that also allows it to interact with a chemokine receptor on the surface of the host cell, usually either CCR5 or CXCR4 (Alkhatib et al., 1996; Deng et al., 1996; Dragic et al., 1996; Kwong et al., 1998; Oberlin et al., 1996; Trkola et al., 1996). These secondary interactions, in turn, expose a hydrophobic domain on gp41 that triggers fusion of the viral envelope with the cellular membrane (Kowalski et al., 1987; Melkyan et al., 2000). This causes the core of the HIV-1 virion to enter the cell. A short time later, the protective layers of the core disintegrate, and the RNA genome, reverse transcriptase, integrase, and several other viral proteins are released into the cytoplasm (Dvorin and Malim, 2003).

#### FIG. 1.4: The HIV-1 genome

The HIV-1 genome, which takes the form of a single-stranded RNA molecule while in the virion, is inserted into the host-cell cytoplasm shortly after the viral envelope fuses with the plasma membrane. The genome is then converted into double-stranded DNA, transported to the nucleus, and inserted into a chromosome. Regulatory regions, called long terminal repeats (LTR), flank the viral genome and are important for integration and transcription. The HIV-1 genome can be read in three frames, and several of the genes have overlapping reading frames. In addition, some of the genes code for multiple proteins. These features allow HIV-1 to encode many proteins in a relatively small genome. The location of *nef* is highlighted in **red**; all other genes are shown in **gray** boxes.

FIG. 1.4

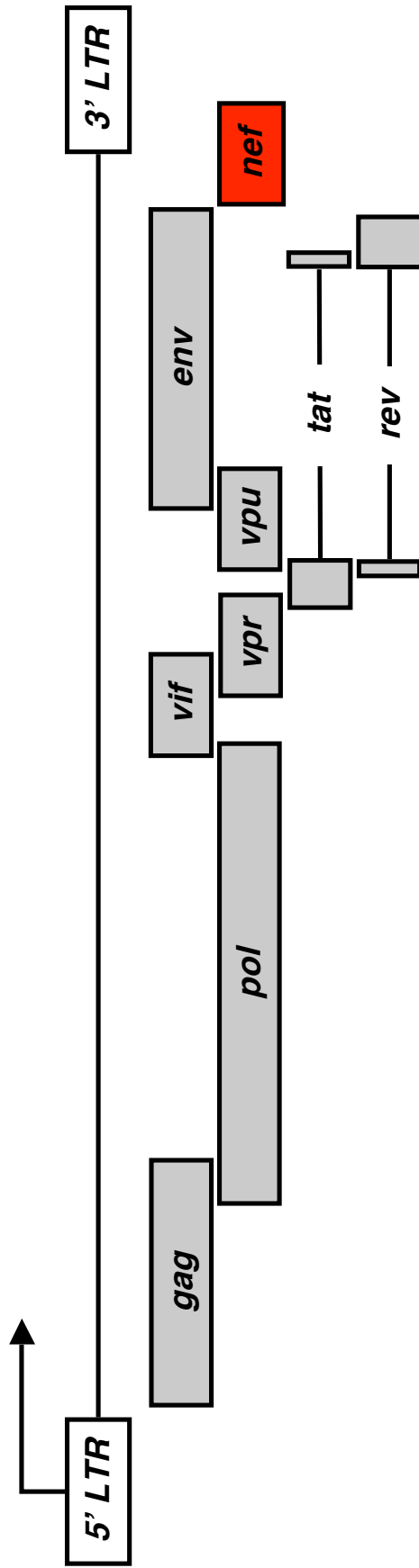


**FIG. 1.5: Major functions of the HIV-1 proteins**

The HIV-1 genome contains nine genes, which together code for at least fifteen proteins. Most of these proteins are pleiotropic; however, their major functions are listed below. Based on their primary function, the HIV-1 proteins are sometimes divided into five groups: structural proteins (p24, p17, p7, and p6), envelope proteins (gp120 and gp41), enzymes (reverse transcriptase, integrase, and protease), transactivators (Tat, Rev, and Vpr), and other regulators (Vif, Vpu, and Nef). Transactivators promote the expression of viral genes, while the other regulators optimize the host-cell environment for viral replication and increase the infectivity of nascent virions.

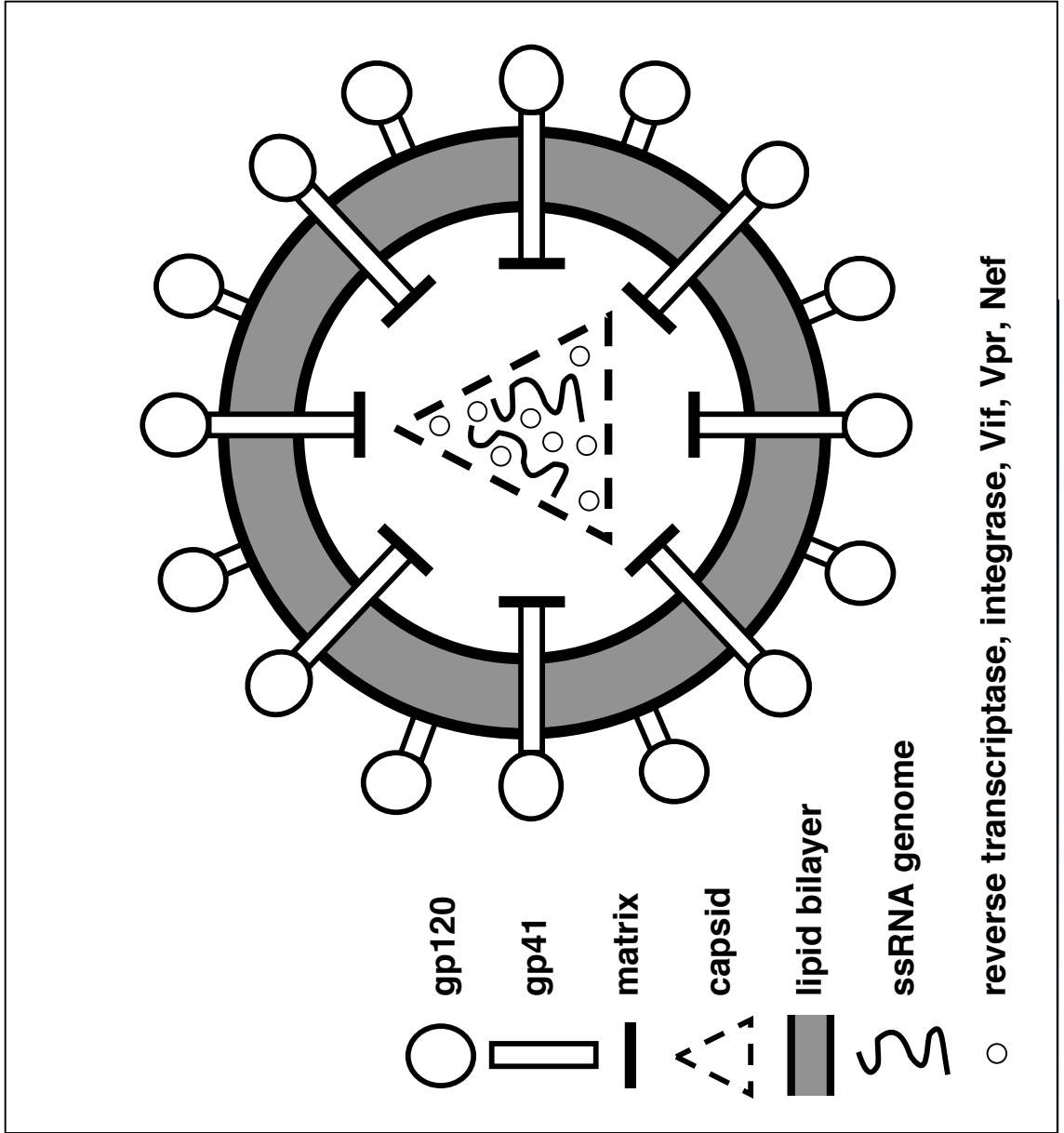
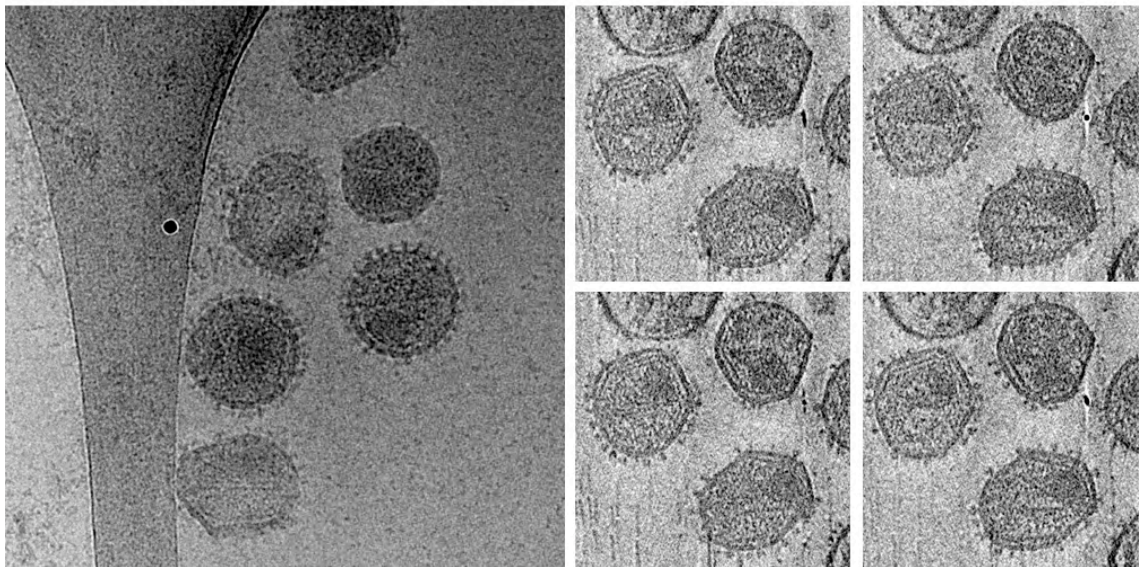
FIG. 1.5

Gene	Protein(s)	Major Function(s)
<i>gag</i>	p24 p17 p7 p6	capsid protein matrix protein capsid protein capsid protein
<i>pol</i>	reverse transcriptase integrase protease	transcribes viral RNA into dsDNA integrates viral dsDNA into host genome cleaves gag and pol precursors
<i>vif</i>	Vif	degradation of host-cell defense protein APOBEC3G
<i>vpr</i>	Vpr	regulates nuclear import of pre-integration complex
<i>tat</i>	Tat	promotes transcription of viral DNA
<i>rev</i>	Rev	allows export of unspliced viral RNA from the nucleus
<i>vpu</i>	Vpu	intracellular degradation of CD4 disrupts function of host-cell defense protein tetherin
<i>env</i>	gp120 gp41	binds CD4, CCR5, and CXCR4 promotes fusion of the virion with the plasma membrane
<i>nef</i>	Nef	downregulation of CD4, MHC-I, and other receptors

**FIG. 1.6: The HIV-1 virion**

Electron micrographs of HIV-1 virions (kindly provided by Rachid Sougrat, NICHD, NIH) are shown on the left, with a schematic drawing of a single virion shown on the right. The surface of HIV-1 virions are studded with gp120-gp41 heterodimers. These heterodimers are embedded in a lipid bilayer and attached to matrix proteins. Within the matrix lies the viral capsid. The capsid contains two copies of the single-stranded RNA genome and various viral proteins, including reverse transcriptase, integrase, Vif, Vpr, and Nef. In the diagram of the virion shown below, some of the structural proteins have been omitted for simplicity.

FIG. 1.6



Reverse transcriptase uses the single-stranded RNA molecule as a template to create a double-stranded DNA genome that, when bound to certain viral proteins, is called the pre-integration complex (Harrich and Hooker, 2002). The pre-integration complex is subsequently transported to the nucleus, where it directs the immediate synthesis of Tat, Rev, and Nef in small but detectable amounts (see Popov et al., 1998; Stevenson et al., 1990; Wu and Marsh, 2001). Integrase then inserts the pre-integration complex into the host cell chromatin via a LTR-dependent mechanism (Bushman et al., 1990; Clavel et al., 1990; Roth et al., 1989). In quiescent cells, the HIV-1 provirus can lay dormant, with little or no transcriptional activity beyond basal levels of Tat, Rev, and Nef production (Chun et al., 1997; Jordan et al., 2001). Activation of the infected cell leads to expression of many endogenous transcription factors, including NF- $\kappa$ B (Sen and Baltimore, 1986a; Sen and Baltimore, 1986b). NF- $\kappa$ B binds to specific sequences in the LTR, and along with Tat, promotes transcription of the viral genes and genome (Berkhout et al., 1990; Liu et al., 1992; Nabel and Baltimore, 1987). Rev then directs the export of unspliced RNA genomes to the cytoplasm, so that they can be packaged into newly-forming virions (Lever, 2002; Malim et al., 1989). The HIV-1 life cycle is completed when these nascent virions bud from the endosomal or plasma membrane to infect surrounding cells (Jouvenet et al., 2008; Neil et al., 2008; Pelchen-Matthews et al., 2003).

#### **1.4.4 Progression from HIV-1 infection to AIDS**

The cycle of HIV-1 replication explained above begins with the infection of a single cell; however, the virus eventually overwhelms the body. Although there are several routes by which an individual may become infected, the cells most likely to make first contact with the virus are macrophages and dendritic cells (reviewed by Martín and Bandrés, 1999). These cells are natural hosts of HIV-1, and they readily transmit the virus to CD4 T lymphocytes (Groot et al., 1998; McDonald et al., 2003). On average, productively infected lymphocytes survive only two to three days (Herz et al., 1996; Perelson et al., 1996). The short life-span of virus-producing cells has been attributed to a variety of factors, the most important of which appear to be the cytopathic effects of HIV-1, CTL-mediated killing of infected cells, and apoptosis (Getchell et al., 1987; Meyaard et al., 1992; Plata et al., 1987; Walker et al., 1987). Repeated rounds of viral replication leads to the near total depletion of CD4 T cells over a period of three to ten

years (Rutherford et al., 1990; Ward et al., 1989). The steady decline of CD4 T cells can be slowed, but not averted, by the application of antiretroviral therapy (Larder et al., 1989; Ledergerber et al., 1999; Mitsuya et al., 1987; Palella et al., 1998). Once the number of CD4 T cells drops below a certain threshold, the body loses its capacity to properly coordinate the immune system (Bonavida et al., 1986; Pinching et al., 1983; Seligmann et al., 1984). This final stage of the disease is marked by a severe immune deficiency, which is the hallmark of AIDS. It is now understood that the progression from HIV-1 infection to AIDS depends not only on the viral proteins described above, but also on the activity of Nef.

## **1.5 Nef**

Sequencing of the proviral genome, performed shortly after the discovery of the virus itself, revealed a 3' ORF of unknown function (Fig. 1.4; Muesing et al., 1985; Ratner et al., 1985; Sanchez-Pescardo et al., 1985; Wain-Hobson et al., 1985). The mRNA transcript and the protein corresponding to this ORF were subsequently identified in samples taken from patients infected with HIV-1 (Allan et al., 1985; Arya and Gallo, 1986; Lee et al., 1986; Franchini et al., 1986; Rabson et al., 1985). Early studies aimed at elucidating the function of this protein found that it was not required for replication of the virus in vitro (Ahmad and Venkatesan, 1988; Fisher et al., 1986; Luciw et al., 1987; Terwilliger et al., 1987). Some of these reports also claimed that expression of the protein actually reduced the rate of viral replication in their tissue culture systems (Ahmad and Venkatesan, 1988; Luciw et al., 1987; Terwilliger et al., 1987). Based on these findings, the protein was called Nef, which is short for "Negative factor" of viral growth (Gallo et al., 1988). Over time, it became clear that the role of Nef had been mischaracterized. Later studies definitively demonstrated that Nef did not have a negative impact on viral replication, and in conditions that more closely resembled the natural setting of HIV-1 infection, viruses with functional Nef proteins were found to grow more rapidly than viruses that lacked Nef (de Ronde et al., 1992; Hammes et al., 1989; Kim et al., 1989a; Miller et al., 1994; Spina et al., 1994). Importantly, Nef has also been shown to be a key determinant of disease progression in vivo. The results of these studies are summarized below.

### **1.5.1 Nef: a critical determinant of disease progression**

A key role for Nef in the development of AIDS is supported by studies on a particular class of patients, known as long-term non-progressors (LTNPs), that remain symptom free for at least ten years after infection without the aid of antiretroviral therapy (see Cao et al., 1995; Learmont et al., 1992; Pantaleo et al., 1995). Analysis of a naturally attenuated virus isolated from an Australian LTNP cohort revealed that it was missing a large portion of the Nef ORF (Deacon et al., 1995). These patients, all of whom had been infected by the same individual, maintained extremely low viral loads and steady CD4 T cell counts for 15-25 years (Birch et al., 2001; Gorry et al., 2007; Learmont et al., 1992; Learmont et al., 1995; Learmont et al., 1997; Rhodes et al., 1999). Similar deletions of the Nef ORF have also been detected among independent LTNP cohorts

located in Asia, Europe, and North America (Kirchhoff et al., 1995; Salvi et al., 1998; Tobiume et al., 2002).

Further evidence for a role of Nef in disease progression is provided by studies of SIV in rhesus macaques. As with humans, deletion of the Nef ORF reduced the pathogenic potential of the virus, and dramatically delayed the onset of AIDS (see Kestler et al., 1991). In fact, the virus appeared to be under strong selective pressure to express Nef. When macaques were infected with engineered SIV strains that contained a premature stop codon or a 12 bp deletion in the Nef ORF, the expression of full-length Nef was quickly and universally restored (Kestler et al., 1991; Whatmore et al., 1995).

Mouse models also indicate that there is a strong correlation between the expression of Nef and the virulence of infection. Upon inoculation with HIV-1, chimeric SCID-hu mice transplanted with human thymic tissue experienced a significant decline of CD4 T cells (Aldrovandi et al., 1993; Bonyhadi et al., 1993; McCune et al., 1988). In this system, viruses that were unable to express Nef had a slower rate of replication, achieved a lower overall titer, and depleted significantly fewer CD4 T cells than their wild-type counterparts (Arora et al., 2002; Jamieson et al., 1994). In another mouse model system, the expression of Nef in CD4-positive cells rapidly induced an AIDS-like disease despite the absence of all other HIV-1 proteins (Hanna et al., 1998; Lindermann et al., 1994; Skowronski et al., 1993).

### **1.5.2 Structural and biochemical features of Nef**

Given the considerable influence of Nef on viral pathogenesis, much work has been done to characterize its structural and biochemical features, which are described here. Translation of the HIV-1 Nef mRNA transcript produces a 27 kDa protein containing 206 amino acids (Allan et al., 1985; Arya and Gallo, 1986; Lee et al., 1986). Because the Nef mRNA molecule is multiply-spliced, it can be exported from the cell nucleus without the help of Rev (see Section 1.4.3). Thus, during the early stages of cellular infection, the Nef mRNA transcript comprises nearly three-quarters of the total viral mRNA load (see Kim et al., 1989b; Klotman et al., 1991; Robert-Guroff et al., 1990). This makes Nef the first HIV-1 protein to be translated in significant quantities (Ranki et al., 1994). During translation, the viral protein is myristoylated by an endogenous enzyme, called N-myristoyltransferase, that cleaves off the initiating methionine and

attaches a saturated fatty acid to the glycine at position two (see Allan et al., 1985; Hill and Skowronski, 2005). Myristoylation of Nef promotes its association with the cytoplasmic leaflet of cellular membranes, and is required for nearly all of its major functions (Aldrovandi et al., 1998; Franchini et al., 1986; Hanna et al., 2004; Mariani and Skowronski, 1993; Yu and Felsted, 1992). In addition, Nef has been reported to be phosphorylated by various kinases on two serine residues (S6 and S9), but unlike myristoylation, the functional consequences of this post-translational modification are not clear (Coats and Harris, 1995; Coats et al., 1997; Li et al., 2004; Luo et al., 1997; Wolf et al., 2008).

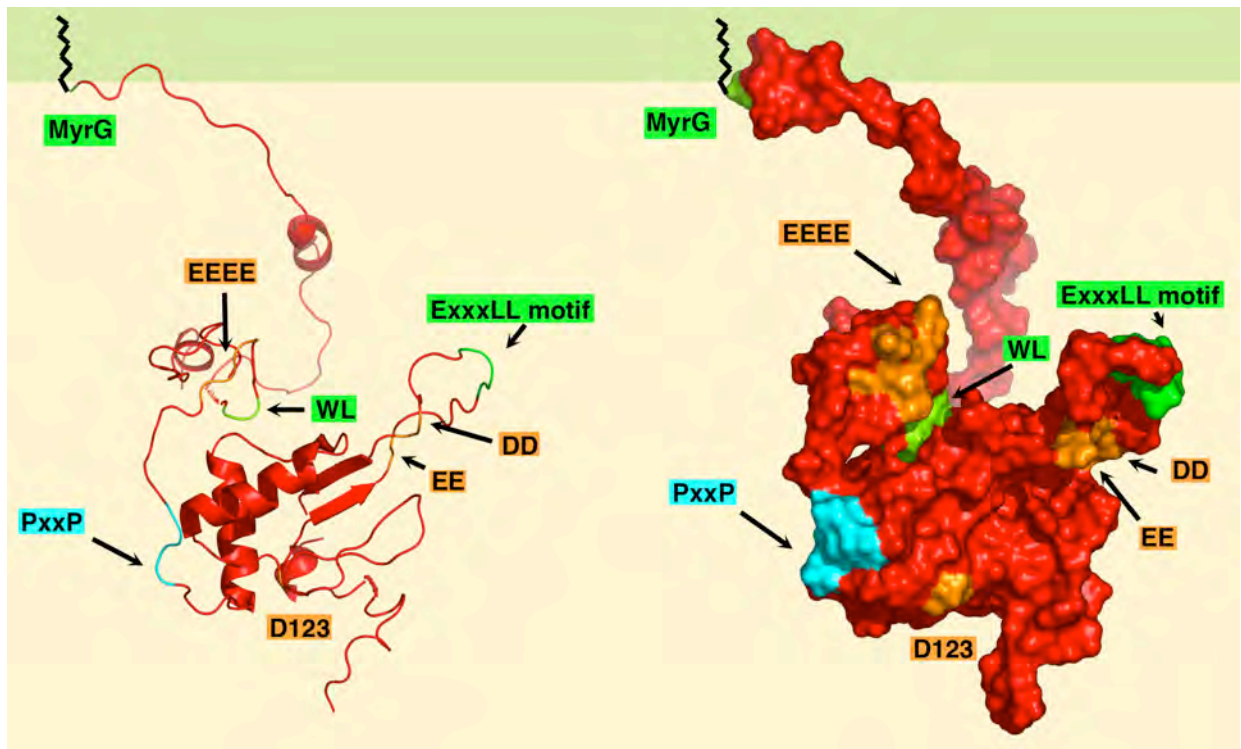
The three-dimensional structure of Nef has largely been solved by a combination of NMR spectroscopy and X-ray crystallography (Fig. 1.7). These studies indicate that Nef can be divided into three domains: a flexible N-terminal region (residues 1-80), a well-folded core (residues 81-147 and 181-206), and a disordered loop (residues 148-180) near the C-terminus of the protein (see Geyer et al., 1999; Grzesiek et al., 1996a; Grzesiek et al., 1997; Lee et al., 1996). Within the flexible N-terminal domain, there are two  $\alpha$ -helices, both of which appear to be stabilized by the addition of myristate. This domain also has four motifs of significance: the aforementioned myristoylation site (G2), a small hydrophobic pocket comprised of tryptophan and leucine residues (WL57,58), an acidic cluster (EEEE62-65), and two prolines (PxxP72,75). The core of Nef contains four  $\alpha$ -helices arranged around a five-stranded antiparallel  $\beta$ -sheet. In this conformation, an aspartate residue (D123) positioned next to the second  $\beta$ -strand is exposed to the solvent. The disordered C-terminal loop connects the fourth and fifth  $\beta$ -strands, and projects outwards from the core. This loop is roughly centered on an acidic dileucine motif (ExxxLL160-165), and is bordered on either end by negatively charged glutamate (EE154,155) and aspartate (DD174,175) pairs.

Myristoylated Nef can adopt a variety of quaternary structures, including monomers, dimers, and trimers (Arold et al., 2000; Dennis et al., 2005; Kienzle et al., 1993). The equilibrium between these states appears to depend on the concentration of Nef, with greater amounts of the viral protein favoring more complex oligomeric arrangements (Arold et al., 2000). Assembly of these oligomers is mediated by the D123 residue in the core domain of Nef (see Fig. 1.8; Arold et al., 2000; Liu et al., 1997). Mutation of this residue prevents the formation of dimers and trimers, and abrogates many of the

### FIG. 1.7: Structure and function of HIV-1 Nef

The structure of HIV-1 Nef is shown in the top panel. In this panel, a ribbon diagram (left) and a surface representation (right) of the protein are depicted. Based on its structure, Nef can be divided into three major domains: an N-terminal arm, a well-folded core, and a flexible C-terminal loop. Important functional motifs within each of these domains is highlighted. The N-terminal arm contains the myristoylation site (MyrG), the CD4 binding site (WL), the acidic cluster (EEEE), and the polyproline motif (PxxP). The core harbors a residue that is critical for the oligomerization of Nef (D123), while the C-terminal loop contains three motifs that have been implicated in CD4 downregulation (EE, ExxxLL, and DD). These motifs have been color-coded for easy recognition: **green** for hydrophobic motifs, **orange** for acidic motifs, and **blue** for the polyproline motif. Myristate is represented as a **black** squiggle embedded in the **light green** membrane bilayer. The cytosol is shown in **light yellow**. The ribbon diagram and surface representation are composites of two structures (PDB ID 1QAF [Geyer et al., 1999] and 2NEF [Grzesiek et al., 1997]) and were drawn using PyMOL (Delano, 2002). Annotations of these images were performed using Microsoft PowerPoint. In the bottom panel, the major functions of each motif are provided, along with their known binding partners.

FIG. 1.7



Motif	Residues	Function	Known Binding Partners
Myristoylation	G2	Membrane association	N-myristate transferase
Hydrophobic pocket	WL57,58	CD4 downregulation	CD4 cytosolic tail
Acidic cluster	EEEE62-65	MHC-I downregulation	AP-1
Polyproline motif	PP72,75	MHC-I downregulation SH3 binding	AP-1 Lck, Src
Aspartic acid residue	D123	Oligomerization	Nef Human thioesterase
Diglutamic acid motif	EE154,155	CD4 downregulation	COP-I
Dileucine motif	ExxxLL160-165	CD4 downregulation	AP-1, AP-2, AP-3
Diaspartic acid motif	DD174,175	CD4 downregulation	V-ATPase

functions of Nef (Liu et al., 1997). Therefore, oligomerization may be necessary for Nef activity in vivo. Oligomerization reduces the amount of solvent-exposed surface area for each Nef molecule; however, for a protein of its size, Nef remains extremely accessible. Calculations indicate that the total exposed surface area of monomeric Nef is 17,600 Å<sup>2</sup> (Geyer et al., 2001). By comparison, the compact nuclear import protein Ran, which also contains 206 residues, has a total accessible surface area of 9,950 Å<sup>2</sup> (Geyer et al., 2001). Crystallographic models of Nef dimers and trimers suggest that oligomerization of the viral protein occludes only a minor fraction of the surface area, because in both cases the contact interfaces are predicted to be relatively small (Arold et al., 2000). The combination of flexible domains and highly exposed surface areas may account for the numerous protein interactions and functions attributed to Nef.

### **1.5.3 Functions of Nef**

Despite initial reports that suggested Nef was a GTPase, the viral protein is not known to have any inherent catalytic activities (Backer et al., 1991; Guy et al., 1987; Harris et al., 1992; Samuel et al., 1987). Instead, Nef is believed to exert itself by binding to endogenous proteins and physically modulating their functions. Nef has in fact been reported to interact with several dozen proteins, although it is not clear how many of these interactions are biologically significant (for a list of Nef binding partners, please see Fu et al., 2009). Nevertheless, by all accounts Nef is a pleiotropic protein, capable of executing a variety of intracellular functions that increase the overall pathogenicity of the virus (reviewed by Greenway et al., 2000). These include the enhancement of virion infectivity, disruption of T cell signaling, regulation of apoptotic pathways, and perhaps most importantly, alteration of cell-surface receptor expression (Fig. 1.7). In this latter regard, Nef does not appear to affect the expression of all plasma membrane receptors indiscriminately; rather, it targets specific receptors for either upregulation or downregulation (Fig. 1.8). Nef increases the surface levels of Ii, LIGHT, and TNF, while decreasing the levels of CD1, CD4, CD8, CD28, CD71, CD80, CD86, CCR5, CXCR4, MHC-I, and mature MHC-II (Aiken et al., 1994; Chadhury et al., 2005; Cho et al., 2006; Coleman et al., 2006; Fleis et al., 2002; Greenberg et al., 1998; Guy et al., 1987; Hrecka et al., 2005; Lama and Ware, 2000; Madrid et al., 2005; Michel et al., 2005; Piguet et al., 2000; Roeth et al., 2004; Schindler et al., 2003; Schwartz et al., 1996; Shinya et al., 2004; Sol-Foloun et al., 2002; Stumptner-Cuvelette et al., 2002;

### **FIG. 1.8: Nef targets specific receptors for downregulation**

To test whether Nef affects the expression of a large number of cell-surface receptors, or targets only a few for downregulation, CD4-CD8 double-positive thymocytes were transfected with vectors coding for Nef and stained with a variety of antibodies. These cells were compared to similar thymocytes that had been transfected at the same time with empty vectors. All cells were analyzed by flow cytometry (see Section 2.7), and representative histograms are shown. A total of 54 cell-surface receptors were tested; however, these particular thymocytes (JM cells, see Section 2.6.2) expressed only 31. Two isotype controls (IgG1 and IgG2a) were also included in the experiment. Each condition was repeated a minimum of three times. Background fluorescence (i.e., the appropriate isotype control for the given antibody) is shaded **gray**, while the surface-expression of receptors is shown in **green** for cells transfected with the empty vector and **orange** for cells transfected with the Nef vector. Of the 31 receptors found to be expressed on the surface of these cells, Nef downregulates only 7. Thus, Nef does not appear to disrupt general trafficking pathways; instead, it targets specific receptors for downregulation. These receptors are highlighted in **red**. Following the histograms, a chart lists the function of each receptor expressed on the JM cell-surface and tested in the assay. This experiment was performed by the author.

FIG. 1.8

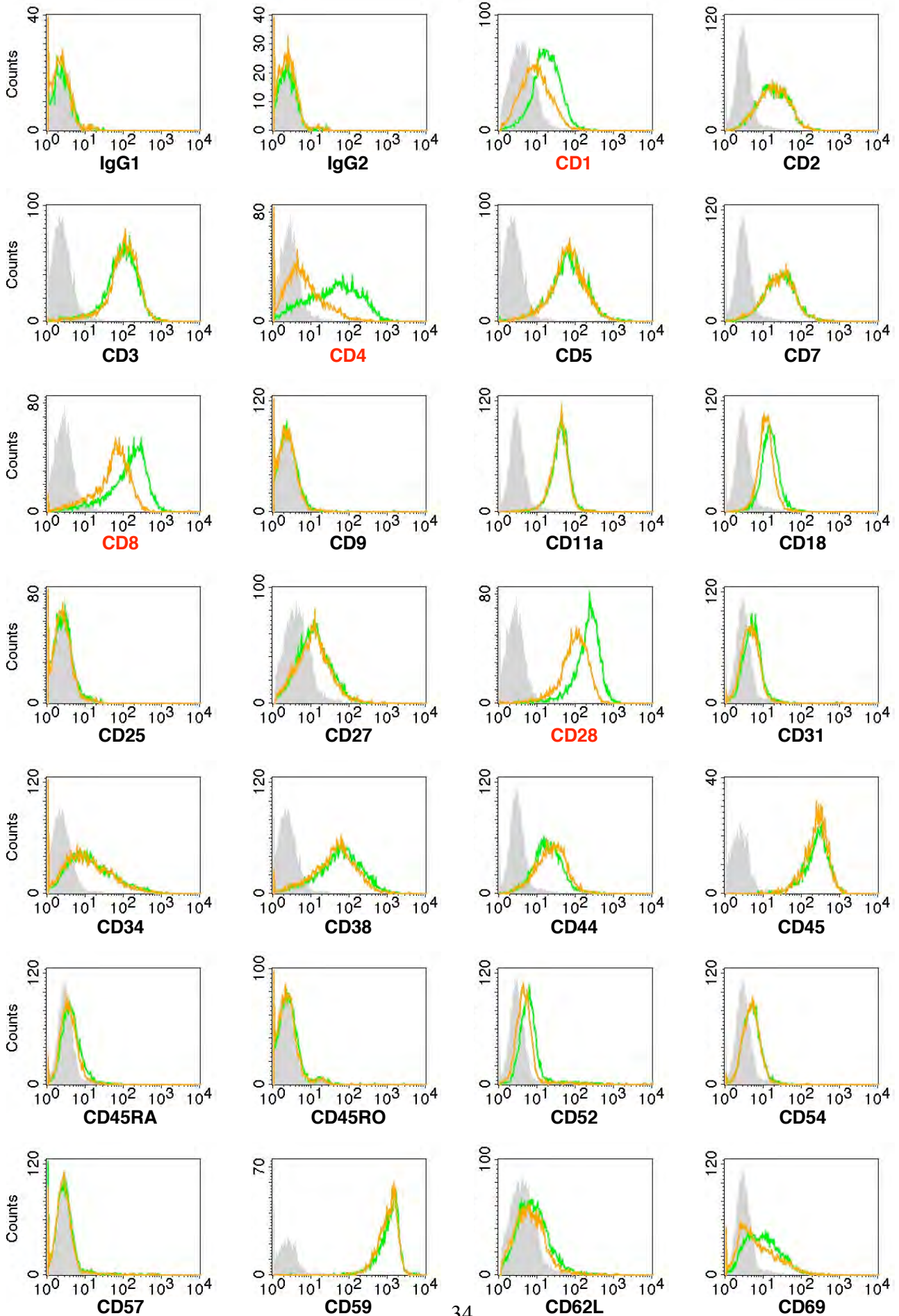


**FIG. 1.8, continued**

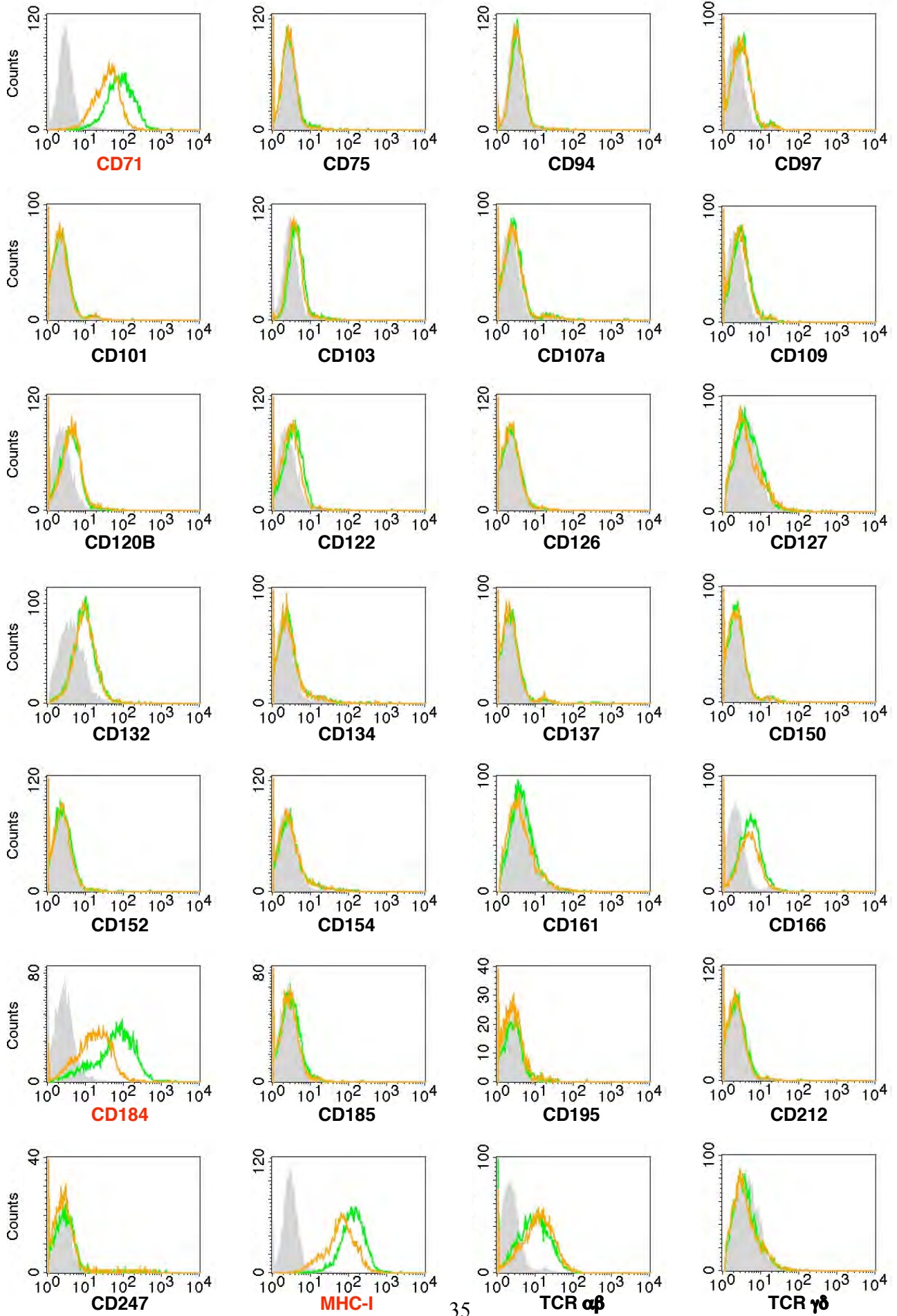


**FIG. 1.8, continued**

#	Antigen	Other Names	Function(s)
1	IgG1	Immunoglobulin G1	Isotype control
2	IgG2a	Immunoglobulin G2	Isotype control
3	CD1	N/A	Presentation of lipid antigens
4	CD2	SRBC	Adhesion molecule; binds Lck
5	CD3	N/A	Associated with the TCR; signal transduction
6	CD4	N/A	Co-receptor for MHC-II; binds Lck; binds HIV-1 gp120
7	CD5	LEU-1	Involved in activation and adhesion
8	CD7	LEU-9	Unknown; binds phosphoinositide 3 kinase
9	CD8	N/A	Co-receptor for MHC-I; binds Lck
10	CD11a	LFA-1	Adhesion molecule; binds CD18 and CD54
11	CD18	N/A	Adhesion molecule; binds CD11a and CD54
12	CD27	N/A	Involved in the stimulation of B cells
13	CD28	N/A	Co-stimulatory molecule; binds CD80 and CD86
14	CD31	PECAM-1	Adhesion molecule
15	CD34	N/A	Adhesion molecule; binds CD62L
16	CD38	N/A	Involved in activation; NAD glycohydrolase
17	CD44	Hermes antigen	Adhesion molecule
18	CD45	LCA	Protein tyrosine phosphatase involved in signaling
19	CD45RA	N/A	Short isoform of CD45; also a tyrosine phosphatase
20	CD52	CAMPATH-1	Unknown
21	CD54	ICAM-1	Adhesion molecule; binds CD11a and CD18
22	CD59	Protectin	Inhibits initiation of complement cascade on membrane
23	CD62L	L-selectin	Adhesion molecule; binds CD34
24	CD69	N/A	Involved in activation
25	CD71	Transferrin receptor	Uptake of iron
26	CD120b	TNFR2	Cytokine receptor for tumor necrosis factor
27	CD122	IL-2Rb	Cytokine receptor for interleukin-2b
28	CD132	N/A	Cytokine receptor for various interleukins
29	CD166	ALCAM	Adhesion molecule
30	CD184	CXCR4	Chemokine receptor; binds gp120 of some HIV-1 strains
31	CD185	CXCR5	Chemokine receptor
32	MHC-I	HLA-A, B, C, etc.	Presentation of peptide antigens
33	TCR ab	T cell receptor	T cell activation; binds antigen-loaded MHC-I or MHC-II

Swan et al., 2001; Swigut et al., 2002). The mechanisms that Nef uses to upregulate and downregulate these receptors are poorly understood. In most cases, however, Nef seems to alter the expression of surface receptors by interacting with the intracellular protein-trafficking machinery. The major components of this machinery are described in the next section.

## **1.6 Intracellular protein transport**

Within eukaryotic cells, macromolecules are transported between organelles by small, membrane-enclosed structures known as vesicles (Palade, 1975). These vesicles bud from a donor compartment, travel along the cytoskeleton, and fuse with an acceptor compartment (see Bonifacino and Glick, 2004; Hehly and Stammes, 2007). Central to this process are coat proteins, which are distinguished by the polyhedral cages they form around nascent vesicles. There are several kinds of coat proteins, but they are all either directly or indirectly involved in cargo selection, donor membrane deformation, and the recruitment of additional proteins required for vesicle scission, transport, and fusion (reviewed by Bonifacino and Lippincott-Schwartz, 2003; Kirchhausen, 2000; Schekman and Orci, 1996). The three most well-characterized coat proteins are COPI, COPII, and clathrin. Each of these appears to regulate one or more distinct trafficking pathways: COPI-coated vesicles traffic primarily from the Golgi complex to the ER, although they have also been suggested to have a role in endosomal transport; COPII-coated vesicles move from the ER to the Golgi; and clathrin-coated vesicles (CCVs) shuttle between multiple post-Golgi organelles (Anderson et al., 1977a; Barlowe et al., 1994; Letourneur et al., 1994; Orci et al., 1986; Pearse, 1975; Roth and Porter, 1964; Waters et al., 1991; Whitney et al., 1995). Previous work has demonstrated that Nef co-localizes with some clathrin-coated structures (Foti et al., 1997; Greenberg et al., 1997). Therefore, the remainder of this section focuses on clathrin, clathrin-associated proteins, and the interactions between Nef and these proteins.

### **1.6.1 Clathrin**

The first observation of coated vesicles was made during studies on mosquito oocytes that were actively taking up yolk (Roth and Porter, 1964). These vesicles were found to bud from the plasma membrane, covered in bristle-like projections that were lost as the vesicle moved towards the cell center. Similar coated vesicles were subsequently described around the Golgi area of the cell (Friend and Farquhar, 1967). Purification and characterization of these vesicles revealed that the coats were composed of two major proteins: a 180 kDa polypeptide named clathrin heavy chain, and a 33-36 kDa polypeptide called clathrin light chain (Kanaseki and Kadota, 1969; Keen et al., 1979; Pearse, 1975). Additional studies showed that the basic unit of clathrin cages was the triskelion, comprised of three heavy and three light chains (Kirchhausen and Harrison,

1981; Ungewickell and Branton, 1981). Electron micrographs have since confirmed that these triskelions assemble into the lattice of pentagons and hexagons commonly seen on the surface of CCVs (Fig. 1.9; Crowther and Pearse, 1981; Fotin et al., 2004; Heuser, 1980).

The incorporation of transmembrane cargo proteins into CCVs was initially believed to occur through a direct interaction with clathrin (Anderson et al., 1977b; Brown and Goldstein, 1979). However, careful biochemical and ultrastructural analyses of CCVs indicated that, in addition to clathrin, the coats contained two 100 kDa polypeptides situated between the lattice and the membrane (Keen et al., 1979; Unanue et al., 1981; Vigers et al., 1986). These non-clathrin proteins were found to facilitate the assembly of CCVs *in vitro*, and were thus called “assembly polypeptides” (Keen et al., 1979). It later became evident that the principal role of the assembly polypeptides was to bind cargo molecules and link them to the clathrin lattice (Glickman et al., 1989; Ohno et al., 1995; Sorkin and Carpenter, 1993). Their name was therefore changed to “adaptor proteins” (APs) to more accurately reflect this function (Pearse and Bretscher, 1981).

### **1.6.2 The AP complexes**

Detailed studies of the APs revealed that they were part of separate heterotetrameric complexes (Keen, 1987; Pearse and Robinson, 1984). These distinct complexes were designated AP-1 [which is composed of  $\gamma$ ,  $\beta 1$ ,  $\mu 1$ , and  $\sigma 1$  subunits] and AP-2 [ $\alpha$ ,  $\beta 2$ ,  $\mu 2$ ,  $\sigma 2$ ]. Two more adaptor complexes, AP-3 [ $\delta$ ,  $\beta 3$ ,  $\mu 3$ ,  $\sigma 3$ ] and AP-4 [ $\epsilon$ ,  $\beta 4$ ,  $\mu 4$ ,  $\sigma 4$ ], have since been identified by searching sequence databases for homologs of AP-1 and AP-2 subunits (see Dell’Angelica et al., 1997; Dell’Angelica et al., 1999; Hirst et al., 1999; Simpson et al., 1996; Simpson et al., 1997). Phylogenetic analyses indicate that the AP complexes appeared during the early stages of eukaryotic evolution; however, some lineages have lost AP-4 (see Section 3.3.3; Boehm and Bonifacino, 2001; Hirst et al., 1999).

### **1.6.3 Structural features of AP complexes**

The AP complexes share many basic features, including the size of their subunits and their three-dimensional structure. In each AP complex, the two largest subunits [ $\gamma$ ,  $\alpha$ ,  $\delta$ ,  $\epsilon$  and  $\beta 1-4$ ] are 100-130 kDa, the medium subunit [ $\mu 1-4$ ] is approximately 50 kDa

### FIG. 1.9: Clathrin assembles to form triskelions, lattices, and cages

Clathrin-coated vesicles constitute a major transport intermediary in several post-Golgi sorting pathways. The outermost layer of these vesicles is comprised of clathrin heavy and light chains, both of which are electron dense. These two proteins assemble to form triskelions, lattices, and cages, as shown in the images below.

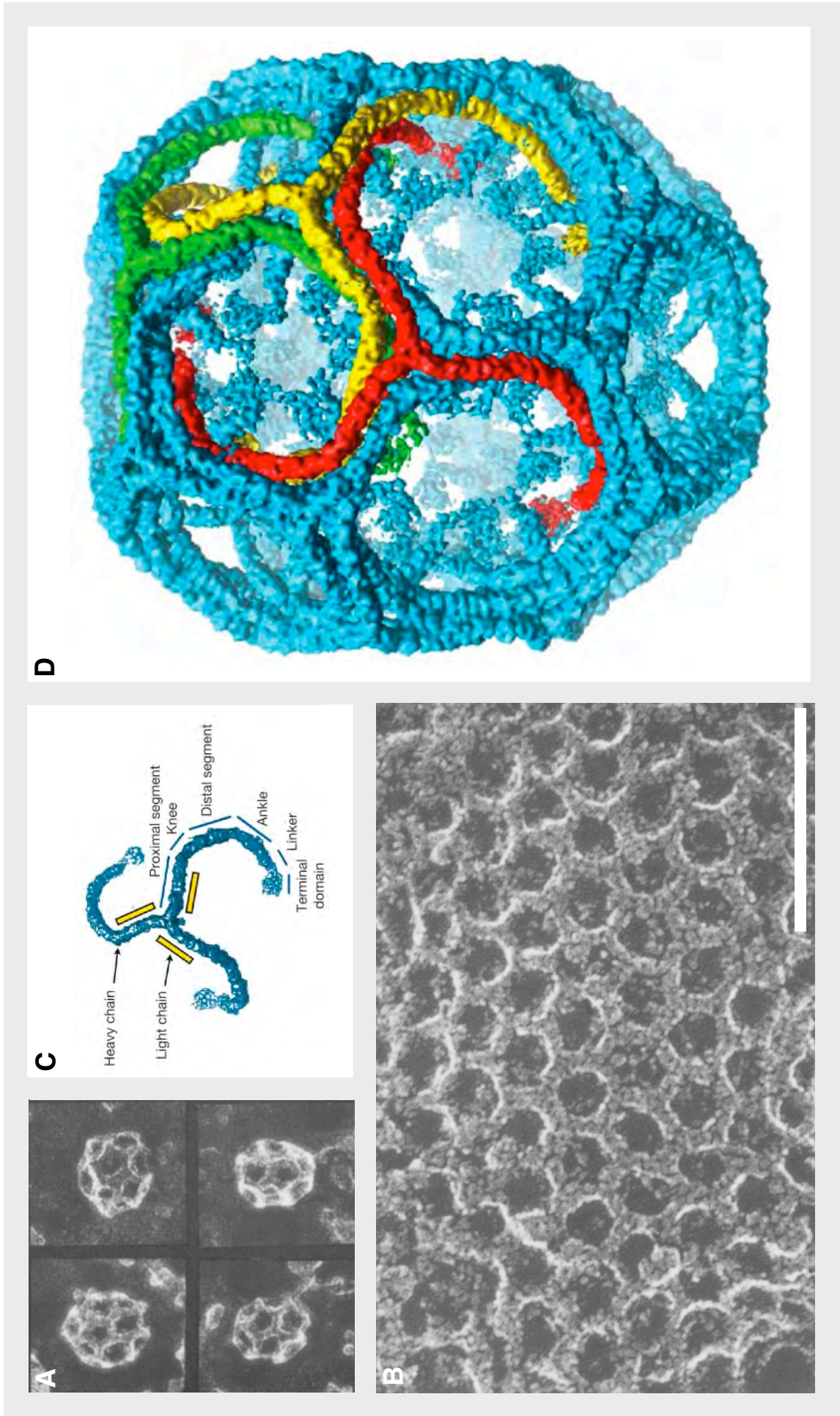
**(A)** Polyhedral clathrin cages (Heuser, 1980). These cages were viewed in freeze-fractured fibroblasts using deep-etch electron microscopy. The cages shown here have a high degree of curvature and are composed mostly of pentagons.

**(B)** Large clathrin lattice imaged using the same method described in part A (Heuser, 1980). Unlike the sharply-curved cages, the clathrin lattice is nearly flat and is composed primarily of hexagons. The reorganization of clathrin chains to form pentagons would increase the curvature of the lattice and could yield clathrin cages. Bar, 0.1  $\mu\text{m}$ .

**(C)** Structure of a single clathrin triskelion, as determined by cryo-electron microscopy (Fotin et al., 2004). Each triskelion is comprised of three heavy chains (colored in **blue**) and up to three light chains (colored in **yellow**). Positions of the light chains are shown schematically. The heavy chains are the major structural elements of the triskelion, while the light chains may play a regulatory role. The exact function of the light chains has not been determined, although they have been implicated in uncoating (Ybe et al., 1998).

**(D)** Structure of a clathrin cage (Fotin et al., 2004), similar to those shown in part A. The positions of three triskelions (colored **red**, **yellow**, and **green**) are highlighted; the remaining triskelions have been left **blue**. Only clathrin heavy chains are depicted in this image, which was obtained using cryo-electron microscopy.

**FIG. 1.9**



Images from Heuser, 1980 and Fotin et al., 2004

and the smallest subunit [ $\sigma$ 1-4] is 15-20 kDa (Keen, 1987; Dell'Angelica et al., 1997; Dell'Angelica et al., 1999; Hirst et al., 1999; Simpson et al., 1996). Proteolytic assays and electron micrographs have revealed that the N-terminal domains of the two large subunits combine with the small subunits to form a well-folded core (see Fig. 1.10; Heuser and Keen, 1988; Schröder and Ungewickell, 1991; Zaremba and Keen, 1985). A flexible linker extends from each of the large subunits to connect the core to folded appendages, called “ears” (Heuser and Keen, 1988; Kirchhausen et al., 1989). X-ray crystallography studies have provided more detailed information on the structure of the core and ear domains (Fig. 1.10; reviewed by Owen et al., 2004). Within the core, the large subunits fold into solenoids, while the medium and small subunits form  $\beta$ -sheets that are flanked by  $\alpha$ -helices (Collins et al., 2002; Heldwein et al., 2004). Both ears have similar bi-lobal structures and contain platform-like subdomains (see Brett et al., 2002; Owen et al., 1999; Owen et al., 2000; Traub et al., 1999).

#### **1.6.4 Cargo recognition by AP complexes**

In addition to having a similar structure, all of the AP complexes are able to recognize linear peptide motifs (reviewed by Bonifacino and Traub, 2003). These motifs, which are present in the cytosolic domains of transmembrane proteins, generally conform to one of two consensus sequences: Yxx $\emptyset$  (where  $\emptyset$  is a bulky hydrophobic residue) or [D/E]xxxL[L/I] (Canfield et al., 1991; Johnson and Kornfeld, 1992; Lazavorits and Roth, 1988; Letourneur and Klausner, 1992). A variety of assays have convincingly demonstrated that Yxx $\emptyset$ -type motifs, often referred to as tyrosine signals, bind to the C-terminal region of all four  $\mu$  subunits (Boll et al., 1996; Dell'Angelica et al., 1997; Hirst et al., 1999; Ohno et al., 1995; Ohno et al., 1998; Owen and Evans, 1998). The recognition site for [D/E]xxxL[L/I]-type dileucine signals is less certain, as different experimental approaches have yielded conflicting results. Phage display screens and yeast two-hybrid assays initially suggested that, like tyrosine signals, dileucine motifs bound to the  $\mu$  subunits of AP complexes (Bremens et al., 1998; Craig et al., 2000; Rodionov and Bakke, 1998). These findings were contested by photoaffinity labeling experiments, which implicated the  $\beta$  subunits (Rapoport et al., 1998). More recently, yeast three-hybrid assays have indicated that dileucine signals interact with the AP-1  $\gamma$ - $\sigma$ 1 and AP-3  $\delta$ - $\sigma$ 3 hemicomplexes (Janvier et al., 2003). Thus, the specific binding site for dileucine motifs on AP complexes remains controversial.

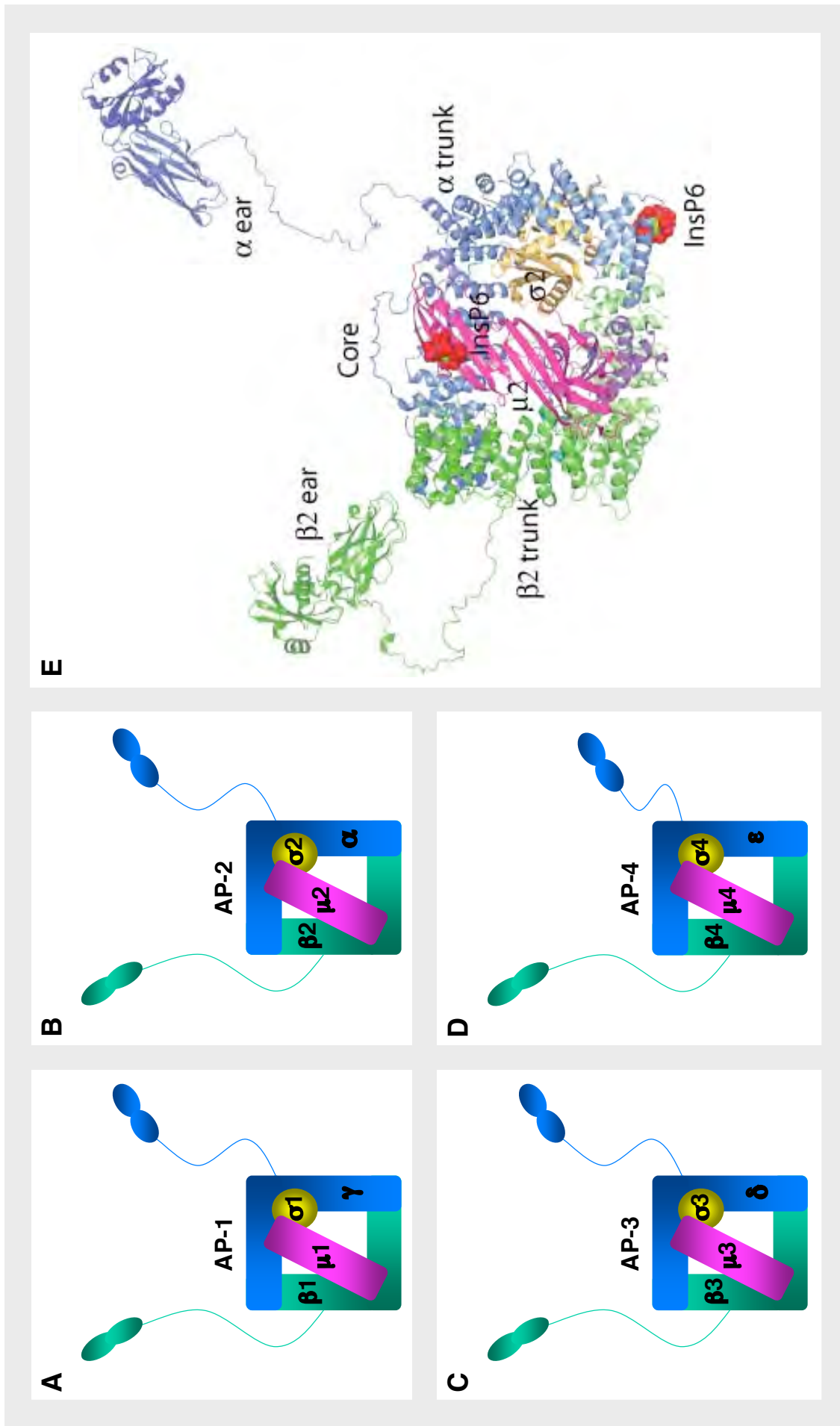
### FIG. 1.10: Structure of the adaptor protein complexes

The adaptor protein (AP) complexes are a related set of proteins (known as AP-1, AP-2, AP-3, and AP-4) that participate in the sorting of cargo molecules. Each of these heterotetrameric AP complexes binds protein and lipid molecules on a donor membrane and facilitates their delivery to an acceptor membrane. However, the AP complexes control different sorting pathways within the cell. AP-1 and AP-2, which utilize clathrin as a scaffold protein, operate at the TGN and the plasma membrane, respectively. AP-3 and AP-4, which may be able to function independently of clathrin, mediate the transport of cargo to lysosomes and the basolateral membrane of polarized cells. The structure of all four AP complexes is shown below.

**(A-D)** Subunit organization of AP-1, AP-2, AP-3, and AP-4. For each complex, the most divergent subunit ( $\gamma$ ,  $\alpha$ ,  $\delta$ , and  $\epsilon$ ) is colored **dark blue**, the  $\beta$  subunit ( $\beta 1$ ,  $\beta 2$ ,  $\beta 3$ , and  $\beta 4$ ) is colored **green**, the  $\mu$  subunit ( $\mu 1$ ,  $\mu 2$ ,  $\mu 3$ , and  $\mu 4$ ) is colored **pink**, and the  $\sigma$  subunit ( $\sigma 1$ ,  $\sigma 2$ ,  $\sigma 3$ , and  $\sigma 4$ ) is colored **gold**.

**(E)** Structure of the AP-2 complex. This image is a composite of three crystal structures: the  $\alpha$ -appendage (Owen et al., 1999), the  $\beta 2$ -appendage (Owen et al., 2000), and the AP-2 core (Collins et al., 2002). The color conventions are the same as those indicated in parts A-D. InsP6 (D-myo-inositol-1,2,3,4,5,6-hexakisphosphate), colored in **red**, is an analog for polyphosphatidylinositol phosphate (PIP) headgroups, which recruit AP-2 to the plasma membrane. In this structure, InsP6 is shown to bind to both the  $\alpha$  and  $\mu 2$  subunits; however, only the  $\alpha$  binding site appears to be important for AP-2 function (Motley et al., 2006). Clathrin binds to the flexible linker that connects the  $\beta 2$  trunk and appendage domains (otherwise known as the  $\beta 2$  hinge domain). Cargo proteins bind to the core region, while accessory proteins bind to platform-like subdomains on the  $\alpha$  and  $\beta 2$  appendages. The structures of the other three AP complexes probably resemble AP-2 (Heldwein et al., 2004).

FIG. 1.10



Crystal structure from Collins et al., 2002

### 1.6.5 Cargo sorting by AP complexes

The primary function of AP complexes is to bind transmembrane proteins that contain either tyrosine or dileucine signals, and mediate their transport from one organelle to another (reviewed by Robinson, 2004). Each AP complex, however, directs a distinct sorting pathway. AP-1 is involved in the trafficking of cargo between the *trans*-Golgi network (TGN) and endosomes, although the directionality of this movement is still under debate (Doray et al., 2002; Meyer et al., 2000; Puertollano et al., 2003; Reusch et al., 2002; Robinson, 1987). AP-2 controls an endocytic pathway, and is responsible for transporting a large number of proteins from the plasma membrane to endosomes, including CD4 (Ahle et al., 1988; Motley et al., 2003; Nesterov et al., 1999; Pelchen-Matthews et al., 1993; Pitcher et al., 1999). Both AP-1 and AP-2 interact directly with clathrin via a small motif in the flexible linker of their  $\beta$  subunits, and depend on this interaction to execute their respective functions (Dell'Angelica et al., 1998; Galluser and Kirchhausen, 1993; Shih et al., 1995; ter Harr et al., 2000). In contrast, AP-3 may be able to operate independently of clathrin, even though it contains a similar clathrin-binding motif (Dell'Angelica et al., 1998; Newman et al., 1995; Peden et al., 2002). While its relationship to clathrin is poorly defined, there is widespread agreement that AP-3 promotes delivery of cargo from the TGN and endosomes to lysosomes (Cowles et al., 1997; Le Borgne et al., 1998; Rous et al., 2002). AP-4 is devoid of a canonical clathrin-binding motif, and it does not appear to associate with clathrin (Borner et al., 2006; Hirst et al., 1999). Thus, like AP-3, the AP-4 complex may utilize another coat protein. The sorting function of AP-4 is not yet established, but it has been implicated in the trafficking of proteins from the TGN to the basolateral membrane of polarized epithelial cells (Simmen et al., 2002).

### 1.6.6 Interactions of Nef with the AP complexes

Because Nef contains a well-conserved dileucine motif, it has long been considered a candidate to interact with the AP complexes (Greenberg et al., 1997; Bresnahan et al., 1998). Indeed, various assays have suggested that the viral protein binds AP-1, AP-2, and AP-3 in a dileucine-dependent manner, although an interaction with AP-4 has not yet been reported. As with other dileucine ligands, the location of the Nef binding site on AP complexes is disputed. Nef has been shown to interact with  $\mu 1$  and  $\mu 3$  by yeast two-hybrid experiments, and  $\beta 1$  and  $\beta 2$  by photoaffinity labeling analyses; however,

the affinity of Nef for these adaptin subunits appeared to be relatively weak (Craig et al., 2000; Greenberg et al., 1998a; Rose et al., 2005). Yeast three-hybrid assays later demonstrated that Nef binds far more robustly to the  $\gamma$ - $\sigma$ 1 and  $\delta$ - $\sigma$ 3 hemicomplexes of AP-1 and AP-3, but a similar interaction between Nef and the  $\alpha$ - $\sigma$ 2 hemicomplex of AP-2 was not detected (Janvier et al., 2003). While the manner in which Nef binds the AP complexes must still be resolved, the viral protein most likely relies on these interactions to downregulate cell-surface receptors. The mechanisms used by Nef to affect the expression of the two such receptors, MHC-I and CD4, are examined more closely in the following sections.

## **1.7 Nef-mediated MHC-I downregulation**

As mentioned earlier, many viruses interfere with the expression of MHC-I in order to escape detection and destruction by the adaptive immune system (Section 1.2.3; also see Yewdell and Bennink, 1999). HIV-1 is among these viruses, as it reduces the level of MHC-I on the surface of infected cells (Scheppeler et al., 1989). The HIV-1 protein primarily responsible for this activity is Nef, which is capable of downregulating two of the three major MHC-I alleles: HLA-A and HLA-B (Cohen et al., 1999; Le Gall et al., 1998; Schwartz et al., 1996). Nef does not alter the expression of HLA-C, the other major MHC-I allele (Cohen et al., 1999; Le Gall et al., 1998). HLA-A and HLA-B are known to present antigens to CTLs, while HLA-C interacts with inhibitory receptors on NK cells (Lanier, 1998; Littau et al., 1991; Yokoyama, 1998). The ability of Nef to selectively downregulate MHC-I molecules, therefore, protects infected cells from the cytopathic effects of both CTLs and NK cells (Section 1.2.3; Cohen et al., 1999; Collins et al., 1998; Le Gall et al., 1998).

### **1.7.1 Direct interaction between Nef and MHC-I**

Although multiple mechanisms for the Nef-mediated downregulation of MHC-I have been proposed, the most convincing model involves a direct interaction between the viral protein and the endogenous receptor (Blagoveshchenskaya et al., 2002; Le Gall et al., 1998; Schwartz et al., 1996). Co-immunoprecipitation experiments indicate that Nef binds to the cytoplasmic tail of some MHC-I alleles (Williams et al., 2002). GST pull-down assays have subsequently demonstrated that this interaction depends on an  $\alpha$ -helix in the N-terminal domain of Nef, and a YSQAA motif in the tails of HLA-A and HLA-B (Cohen et al., 1999; LeGall et al., 2000; Williams et al., 2002; Williams et al., 2005). HLA-C lacks the YSQAA motif, which may explain why it is not downregulated by Nef (Cohen et al., 1999; LeGall et al., 1998; Williams et al., 2002).

### **1.7.2 The mechanism of Nef-mediated MHC-I downregulation**

In addition to the N-terminal  $\alpha$ -helix, mutational analyses have identified three other motifs on Nef that are required for the downregulation of MHC-I: the myristoylation site, the acidic cluster, and the polyproline motif (Fig. 1.7 and 1.8; Mangasarian et al., 1999; Peng and Robert-Guroff, 2001). According to the prevailing model of MHC-I

downregulation, these regions of Nef work together to connect HLA-A and HLA-B to the host-cell protein-trafficking machinery (Kasper and Collins, 2003; Kasper et al., 2005; Lubben et al., 2007; Noviello et al., 2008; Roeth et al., 2004; Williams et al., 2005; Wonderlich et al., 2007). The myristoylation of Nef allows it to associate with the cytosolic leaflet of most intracellular membranes, including that of the TGN (Yu and Felsted, 1992). While located at the TGN, Nef simultaneously binds to the tail of an MHC-I receptor, via its  $\alpha$ -helix, and the AP-1  $\mu$ 1 subunit, via its acidic cluster and its polyproline motif (Kasper et al., 2005; Noviello et al., 2008; Williams et al., 2005). Although HLA-A and HLA-B do not normally interact with AP-1, Nef increases the affinity of these molecules for each other by permitting the YSQAA motif to function as a canonical tyrosine-based sorting signal (Noviello et al., 2008; Wonderlich et al., 2007). As ligands for AP-1, HLA-A and HLA-B are no longer transported to the cell-surface (Kasper and Collins, 2003). Instead, the MHC-I receptors are directed towards lysosomes, where Nef ensures that they are degraded (Roeth et al., 2004; Schaefer et al., 2008). Like HLA-A and HLA-B, the degradation of CD4 by Nef may also depend on interactions with the clathrin adaptor protein complexes. However, the mechanism of CD4 downregulation remains uncertain, as described below.

## 1.8 Nef-mediated CD4 downregulation

Similar to other viruses, HIV-1 reduces the expression of its own receptors soon after it enters the host-cell (Dalgleish et al., 1984; Hrecka et al., 2005; Michel et al., 2004; Salman et al., 1988). In particular, the downregulation of CD4 appears to be a critical step in the HIV-1 life cycle, because viral strains that lack this function have difficulty spreading both *in vitro* and *in vivo* (Lundquist et al., 2002; Stoddart et al., 2003). This diminished level of infectivity is generally attributed to a profound inhibition of viral budding. Indeed, the presence of CD4 on the surface of infected cells has been shown to trap newly-formed virions as they attempt to bud from the plasma membrane (Bour et al., 2001; Marshall et al., 1991; Ross et al., 1999). CD4 surface-expression has also been found to decrease the rate of viral replication by making host-cells susceptible to superinfection (Pauza et al., 1990; Robinson and Zinkus, 1990). Superinfection occurs when multiple virions infect the same cell, and it often results in the accumulation of a large amount of unintegrated viral DNA (Bergeron and Sodroski, 1992). This causes the host-cell to undergo apoptosis, prematurely ending the production of new virions (Daniel et al., 1999).

Given the deleterious effects of CD4 expression on viral replication, it is perhaps not surprising that HIV-1 uses three proteins to ensure that the receptor is downregulated efficiently (Chen et al., 1996). Nef, Env (the uncleaved precursor of gp41 and gp120), and Vpu have all been implicated in this process (Garcia and Miller, 1991; Stevenson et al., 1988; Willey et al., 1992; Wildum et al., 2006). Nef is the first of these proteins to be expressed during the viral life cycle, as its mRNA transcript is multiply-spliced and does not need the aid of Rev to be exported from the nucleus (see Section 1.4.3). Although the mechanism that Nef utilizes to downregulate CD4 is still under debate, it clearly directs the receptor from a post-Golgi compartment to lysosomes (Rhee and Marsh, 1994). Env and Vpu, in contrast, are expressed later in the viral life cycle with the help of Rev, and intercept CD4 in the ER (reviewed by Lama, 2003). Env binds to CD4 in the ER lumen, forming aggregates that block transport of the receptor to the cell-surface. Vpu then induces the degradation of CD4 molecules retained in the ER via a proteasomal pathway.

Of the three HIV-1 proteins involved in CD4 downregulation, Nef appears to have the most significant role. Indeed, experiments measuring the relative contribution of each

protein to this process have demonstrated that Nef accounts for the largest fraction of total CD4 downregulation activity (Chen et al., 1996; Wildum et al., 2006). While all three viral proteins are required to completely eliminate expression of the receptor on the plasma membrane, Nef-mediated CD4 downregulation is capable of enhancing the release of nascent virions and protecting host-cells from superinfection (Lundquist et al., 2002; Ross et al., 1996; Wildum et al., 2006). Thus, the ability of Nef to modulate CD4 surface-levels is a key aspect of viral replication (Lundquist et al., 2004; Ross et al., 1996; Miller et al., 2004).

There is evidence to suggest that CD4 downregulation is, in fact, the most important Nef function. Of all the activities that have been attributed to the viral protein, it is the one that best correlates with faster replication and overall disease progression (Cortes et al., 2002; Glushakova et al., 2001; Mariani et al., 1996; Stoddart et al., 2003). In the SCID-hu model system described earlier, the depletion of thymocytes was dependent on the ability of Nef to downregulate CD4, and not on its ability to modulate MHC-I expression (see Section 1.5.1; Stoddart et al., 2003). Similarly, HIV-1 strains isolated from some LTNP have been found to code for Nef proteins that cannot downregulate CD4, but are fully functional in all other respects, including MHC-I degradation (Carl et al., 2000; Mariani et al., 1996; Tobiume et al., 2002). Conversely, Nef proteins that are derived from virulent HIV-1 strains are known to downregulate CD4 aggressively (Argañaraz et al., 2003). In order for Nef to execute this critical function, it must bind directly to CD4. Details of this interaction are described below.

### **1.8.1 Direct interaction between Nef and CD4**

The binding of Nef to CD4 was first demonstrated in heterologous expression systems (Harris and Neil, 1994; Rossi et al., 1996). These initial experiments, which involved yeast two-hybrid assays and GST pull-downs, revealed that the CD4 cytoplasmic tail was both necessary and sufficient for the interaction with full-length Nef. Subsequent NMR studies managed to identify the specific binding site on each protein (Grzesiek et al., 1996; Preusser et al., 2001; Wray et al., 1998). According to the NMR data, an  $\alpha$ -helical region of the CD4 tail containing LL413,414 binds to a hydrophobic pocket on Nef composed of WL57,58 (see Sections 1.3.1 and 1.5.2 for more information on these motifs). The dissociation constant of this interaction was calculated to be in the low micromolar range. A CD4-Nef complex has since been detected in human cells

using a variety of methods, including chemical cross-linking, co-immunoprecipitation under native conditions, and bioluminescence resonance energy transfer (Bentham et al., 2003; Cluet et al., 2005). Sensitive techniques are needed to observe this complex in situ because the interaction between CD4 and Nef is relatively weak and probably short-lived (Grzesiek et al., 1996; Cluet et al., 2005; Rossi et al., 1996). After binding CD4, Nef rapidly downregulates the receptor and promotes its degradation (Aiken et al., 1994; Rhee and Marsh, 1994; Piguet et al., 1999). The mechanism that Nef uses to eliminate CD4 expression, however, remains highly controversial. In the next section, the intracellular trafficking pathways that Nef might exploit to downregulate CD4 are presented.

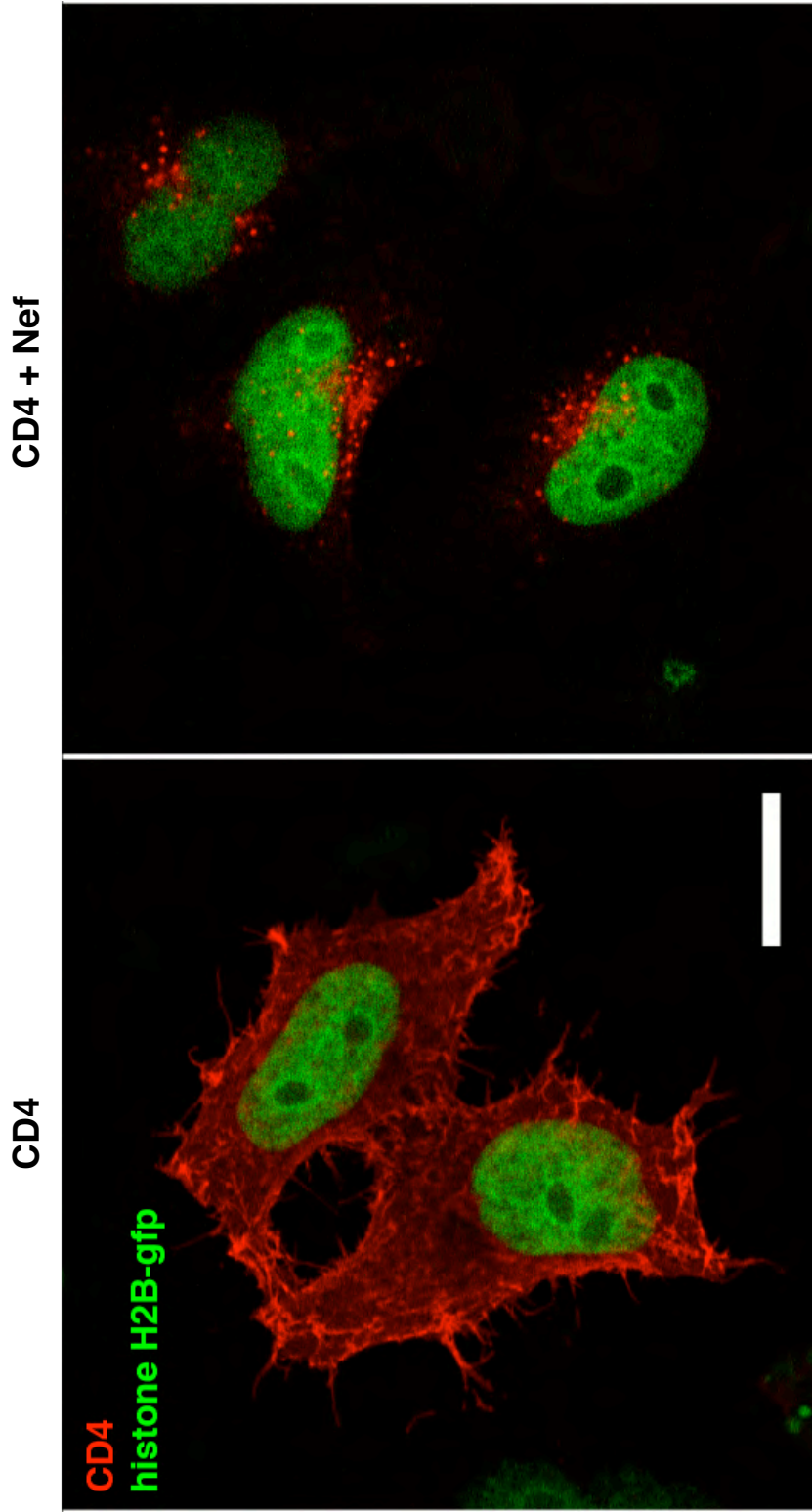
### **1.8.2 The mechanism of Nef-mediated CD4 downregulation**

Two competing models have emerged that attempt to explain the mechanism of Nef-mediated CD4 downregulation. Both models agree that Nef binds to the CD4 tail on a post-Golgi membrane, and then directs the receptor to perinuclear endosomes en route to lysosomes (see Fig. 1.11; Piguet et al., 1999). The post-Golgi nature of this process strongly suggests that clathrin and a clathrin adaptor protein are involved, and several groups have speculated that a CD4-Nef-AP complex forms during the initial stages of downregulation (see Section 1.5; Blagoveshchenskaya et al., 2002; Craig et al., 2000; Foti et al., 1997; Greenberg et al., 1997; Janvier et al., 2003; Rose et al., 2005). In this respect, CD4 downregulation may superficially resemble the effect of Nef on MHC-I; however, the manner in which Nef connects CD4 to the AP complex must be entirely different than that used for HLA-A and HLA-B (Mangasarian et al., 1999). While the Nef acidic cluster and polyproline domains are thought to link HLA-A and HLA-B to AP-1, neither motif is required for CD4 downregulation (Stove et al., 2005). Instead, Nef uses the leucine-tryptophan hydrophobic pocket in its N-terminal region to bind CD4 and the dileucine motif in its C-terminal loop to interact with the AP complexes (Craig et al., 2000; Grzesiek et al., 1996). The two models mentioned above differ in the particular AP complex deemed most important for CD4 downregulation (see Fig. 1.12). According to the traditional model, Nef relies on AP-2 to accelerate the rate of CD4 endocytosis from the plasma membrane. More recent data, though, has tended to favor a model in which Nef utilizes one of the other AP complexes to prevent newly-synthesized CD4 molecules from reaching the cell-surface.

**FIG. 1.11: Nef-mediated CD4 downregulation**

Confocal micrographs of HeLa cells transiently transfected with human CD4 and HIV-1 Nef expression vectors are shown here. The fluorescent protein histone H2B-gfp marks the nuclei of transfected cells and appears **green**. CD4 was detected 24 hrs post-transfection by indirect immunofluorescence and appears **red**. In the left panel are control cells that were cotransfected with CD4 and an empty vector. CD4 is visible primarily on the plasma membrane. The right panel contains cells that were cotransfected with CD4 and Nef. In these cells, most of the CD4 appears to be located in endosomal vesicles near the nucleus. Bar, 10  $\mu\text{m}$ . These images were kindly provided by Wolf Lindwasser.

FIG. 1.11

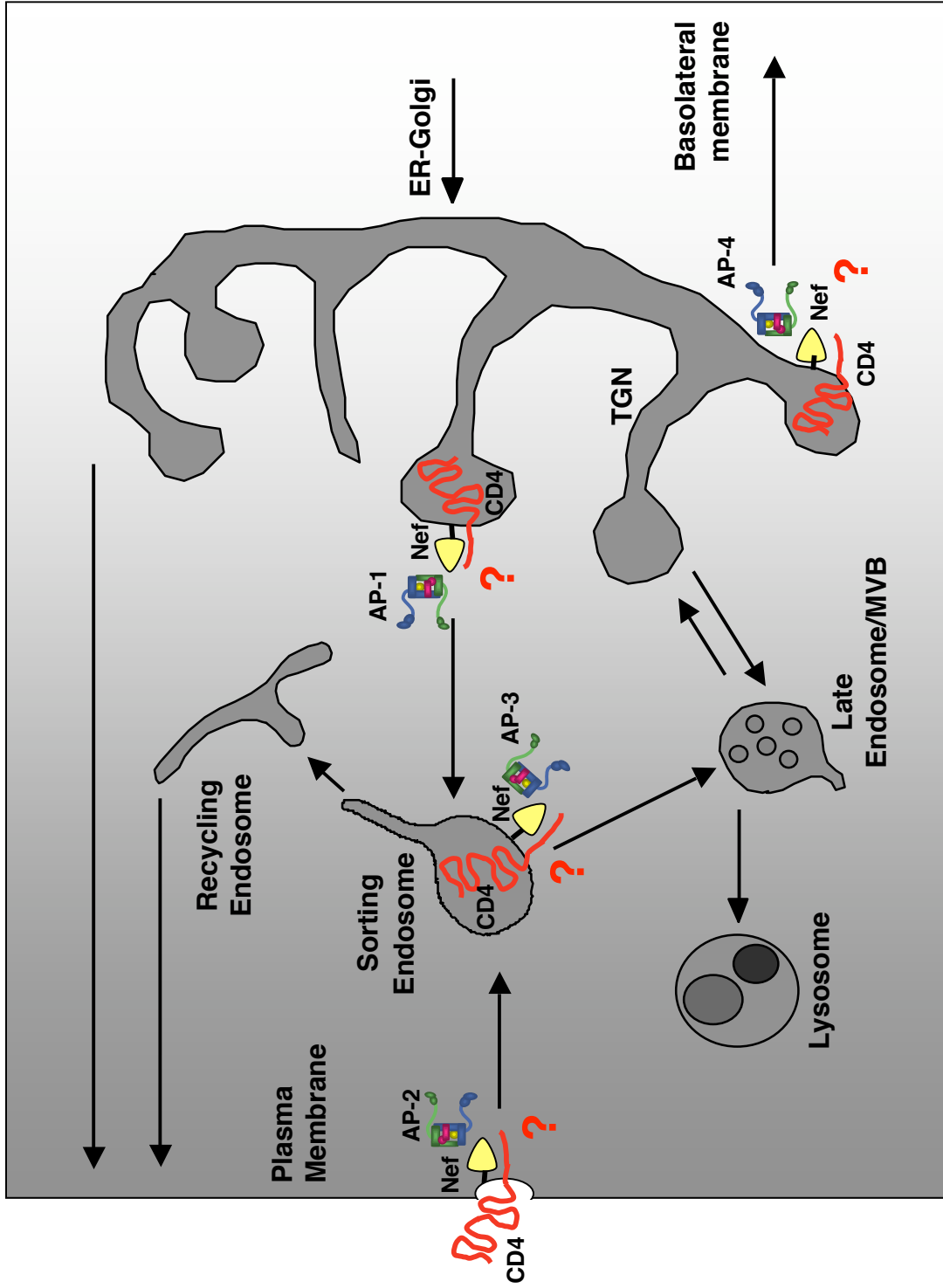


Wolf Lindwasser

**FIG. 1.12: Potential mechanisms of Nef-mediated CD4 downregulation**

This figure depicts four distinct pathways Nef might use to downregulate CD4. Each of these hypothetical pathways begins on a unique organelle, and involves the interaction of Nef with one or more of the clathrin adaptor proteins. This interaction may allow Nef to link CD4 to the cellular protein trafficking machinery, and drive the receptor towards lysosomes. CD4 is shown as a **red** squiggle, Nef is represented by a **yellow** triangle attached to a **black** myristate lipid anchor, and the four AP complexes are depicted with the same color conventions introduced in Fig. 1.10. **Red** question marks are included along each pathway to highlight the uncertainty surrounding the mechanism of Nef-mediated CD4 downregulation.

FIG. 1.12



Preliminary studies on the mechanism of Nef-mediated CD4 downregulation reported that the expression of Nef did not interfere with the movement of CD4 from the ER to the Golgi complex, as determined by resistance of the receptor to endoglycosidase H degradation (Craig et al., 1998; Rhee and Marsh, 1994). One of these studies further claimed, on the basis of biotinylation studies, that CD4 was transported to the plasma membrane with normal kinetics in the presence of Nef, although this finding has since been contested by others (Rhee and Marsh, 1994; Rose et al., 2005). Antibody uptake experiments, performed in conjunction with the endoglycosidase H and biotinylation assays, showed that Nef accelerated the endocytosis of CD4 (Aiken et al., 1994; Rhee and Marsh, 1994). Thus, Nef was proposed to act on CD4 only after the receptor had reached the cell-surface. In support of this model, Nef was later observed to promote the formation of clathrin coated pits at the plasma membrane, and Nef-GFP chimeras were found to partially colocalize with AP-2 (Foti et al., 1997; Greenberg et al., 1997; Mangasarian et al., 1997).

While these studies provide compelling evidence that Nef uses AP-2 to downregulate CD4 via an endocytic mechanism, this model has been undermined by more recently acquired data. In particular, the RNAi-mediated depletion of AP-2 by itself does not appear to have a substantial effect on the ability of Nef to reduce CD4 expression (Jin et al., 2005; Rose et al., 2005). Moreover, a robust interaction between Nef and AP-2 has not yet been observed. Some reports indicate that Nef binds weakly to AP-2, but it is not clear whether this low level of affinity is sufficient to alter the dynamics of CD4 trafficking (see Section 1.6). Much stronger interactions have been reported between Nef and the AP-1 and AP-3 complexes, leading some to argue that these adaptors are more likely to be utilized by Nef than AP-2 (Craig et al., 2000; Janvier et al., 2003b; Rose et al., 2005). Nef has in fact been shown to stabilize the association of AP-1 and AP-3 with intracellular membranes (Janvier et al., 2003a). These results prompted one group to reassess the effect of Nef expression on CD4 transport, and their data sharply disagreed with earlier reports. Instead of finding that Nef accelerated the endocytosis of CD4, they observed that Nef slowed the rate at which CD4 molecules moved from the Golgi complex to the plasma membrane (Rose et al., 2005). This group therefore suggested that Nef acts on CD4 not at the cell-surface, but in the vicinity of the TGN, where it directs the receptor towards lysosomes with the aid of AP-1 or AP-3 (Rose et al., 2005).

## **1.9 Objectives of this thesis**

The primary goal of this thesis is to determine which model – accelerated endocytosis or intracellular retention – most accurately describes the mechanism of Nef-mediated CD4 downregulation. This will be accomplished using a variety of techniques drawn from the cell biology tool kit, including RNAi knockdowns, yeast three-hybrid assays, and GST pull-down experiments. RNAi knockdowns will be used to confirm that the ability of Nef to alter CD4 expression depends on clathrin, and to identify the clathrin adaptor protein that is most critical for this process. Yeast three-hybrid and GST pull-down assays will then be used to ascertain whether Nef binds to this AP complex, and if so, whether the interaction is direct. If the interaction is found to be direct, then the surfaces of both Nef and the AP complex will be closely examined to identify novel motifs that are required for binding and CD4 downregulation. Finally, an attempt will be made to demonstrate the formation of a CD4-Nef-AP tripartite complex, which has long been predicted, but never observed. The results obtained from these experiments should provide new insights on the mechanism used by Nef to downregulate CD4, an important component of HIV-1 replication and disease progression.

**Chapter 2:**  
**Materials and Methods**

## 2.1 Abstract

This chapter is divided into eight major sections (2.2 - 2.9). The first of these sections (2.2) describes molecular biology techniques, which were used to generate most of the plasmids required for this study. The next four sections (2.3 - 2.6) describe the materials and methods used for experiments with bacterial, yeast, *Drosophila*, and human cell lines, respectively. Expression vectors, reagents, and assays particular to one cell type are described in the section devoted to that system. Assays performed on multiple cell types, such as flow cytometry, immunofluorescence, and immunoblotting, are described in the final three sections (2.7 - 2.9). Comprehensive tables listing all plasmids, primers, and antibodies used in this work can be found at the end of the chapter.

## **2.2 Molecular biology**

### **2.2.1 Polymerase chain reactions**

Polymerase chain reactions (PCRs) were carried out using the Phusion High Fidelity (HF) PCR Kit (Finnzymes, Woburn, MA, USA) and appropriate primers purchased from a commercial vendor (Eurofins MWG Operon, Hunstville, AL, USA or Sigma-Genosys, Haverhill, Suffolk, UK). The reagents and thermal cycling conditions used for the PCRs are listed in Table 2.1, Table 2.2, and Table 2.9. Upon completion of each reaction, the PCR product was subjected to agarose gel electrophoresis in Tris-boric acid-EDTA (TBE) buffer [89 mM Tris, 89 mM boric acid, 2 mM EDTA (pH 8.0)], and its size was determined by comparison against a 100 bp - 12,000 bp DNA ladder (Invitrogen, Carlsbad, CA, USA). The PCR product was then purified using the QIAquick PCR Purification Kit (Qiagen, Valencia, CA, USA) and eluted in sterile water.

### **2.2.2 Restriction endonuclease digests**

PCR products and plasmids were digested with restriction endonucleases (purchased from New England BioLabs, Ipswich, MA, USA) according to the manufacturer's instructions. For each digest, 1 µg of DNA was used, and the reactions were carried out at 37°C for 3 hr. In some cases, digested vectors were incubated with a small amount of Calf Intestinal Phosphatase (New England BioLabs) at 37°C for 1 hr to prevent re-circularization of the vector during a subsequent ligation reaction. In all cases, the digested DNA was analyzed by agarose gel electrophoresis. The desired DNA fragments were then purified from the gel using the QIAquick Gel Extraction Kit (Qiagen) and eluted in sterile water. Subsequent ligation reactions were carried out as described in Section 2.2.3.

### **2.2.3 Ligation reactions**

DNA ligation reactions were performed using the T4 DNA Ligase Kit (New England BioLabs) according to the manufacturer's instructions. The reagents for each reaction are listed in Table 2.3. The ligation reaction was incubated at 25.0°C for 1 hr and then the temperature was reduced to 15.0°C for 15 hrs. After completion of the reaction, ligated plasmids were used to transform bacteria as described in Section 2.2.5.

#### **2.2.4 Site-directed mutagenesis**

Site-directed mutagenesis (SDM) reactions were used to introduce point mutations into the open reading frames (ORFs) of selected genes. For each mutagenesis reaction, complimentary primers were designed such that they annealed to opposite strands of the ORF and coded for the desired mutation (please see Table 2.9 for further information on the individual primers). The primers (purchased from Eurofins MWG Operon or Sigma-Genosys) were combined with template DNA, containing the ORF to be mutated, and reagents from the QuikChange II Kit (Stratagene, La Jolla, CA, USA) as described in Table 2.4. The thermal cycling conditions used for the mutagenesis reactions are listed in Table 2.5. Upon completion of each reaction, the methylated template DNA was digested by incubation with 1.0  $\mu$ L of DpnI enzyme at 37°C for 1 hr. The unmethylated, newly synthesized DNA, containing the mutated ORF, was then used to transform bacteria as described in Section 2.2.5.

#### **2.2.5 Bacterial transformations**

Competent XL-10 Blue DH-5 $\alpha$  *Echeveria coli* (purchased from Stratagene) were transformed with plasmids containing antibiotic resistance markers using the standard heat-shock protocol. For each transformation, a small aliquot of bacteria was thawed, incubated with the plasmid for 30 min on ice, and then heat shocked at 42°C for 45 sec. The transformed bacteria were chilled for 2 min on ice, supplemented with room temperature SOC medium [2% tryptone (wt/vol), 0.5% yeast extract (wt/vol), 10 mM NaCl, 2.5 mM KCl, 10 mM MgCl<sub>2</sub>, 10 mM MgSO<sub>4</sub>, 20 mM glucose], and incubated at 37°C for 1 hr with shaking. The bacteria were finally transferred to LB-Agar plates containing the appropriate antibiotic [1.0% tryptone (wt/vol), 0.5% yeast extract (wt/vol), 1.0% NaCl (wt/vol), 1.5% agar (wt/vol) with either 100  $\mu$ g/mL ampicillin or 50  $\mu$ g/mL kanamycin], and incubated at 37°C overnight to allow selection and colony growth to occur. Purification of DNA from selected colonies was performed as described in Section 2.2.6.

#### **2.2.6 DNA purification**

All plasmids described here were initially purified from transformed bacteria using

the QIAprep Spin Miniprep Kit (Qiagen) according to the manufacturer's instructions. Some of the more frequently used plasmids were subsequently purified in greater quantities using the HiSpeed Plasmid Maxiprep Kit (Qiagen). The concentration of purified plasmid DNA was measured using a NanoDrop spectrophotometer (Thermo Fisher Scientific, Waltham, MA, USA).

### **2.2.7 DNA nucleotide sequencing**

The ORFs of all plasmids described in this work were verified by nucleotide sequence analysis (sequencing runs performed by Nora Tsai, *Eunice Kennedy Shriver* National Institute of Child Health and Human Development [NICHD], National Institutes of Health [NIH], Bethesda, MD, USA and Geneservice Limited, Cambridge, UK).

## **2.3 Recombinant protein expression, purification, and binding assays**

### **2.3.1 Bacterial expression vectors**

The pHis (Section 2.3.1.1), pGEX (Section 2.3.1.2), and pST (Section 2.3.1.3) vectors were used to express recombinant fusion proteins in bacteria cells; these proteins were subsequently purified and used in various in vitro binding assays. A description of these expression vectors, along with information on how the protein coding sequences were inserted into the plasmids, is provided below.

#### **2.3.1.1 pHis**

The pHis-Parallel2 vector (Sheffield et al. 1999) allows for the expression of an N-terminal hexahistidine (His<sub>6</sub>) fusion protein in bacteria under the control of the T7 promoter. The wild-type NL4-3 Nef coding sequence was amplified from pCI.Nef<sub>NL4-3</sub> (described in Section 2.6.1.2) by PCR using 5' BamHI and 3' EcoRI primers, digested with the appropriate enzymes, and subcloned into pHis-Parallel2 to create pHis.Nef (Fig. 2.1) SDM reactions on this construct resulted in the pHis.Nef LL164,165AA and pHis.Nef DD174,175AA plasmids.

#### **2.3.1.2 pGEX**

The pGEX-5X-1 plasmid (GE Healthcare, Piscataway, NJ, USA) allows for inducible expression of a N-terminal glutathione *S*-transferase (GST) fusion protein. Expression of the fusion protein is controlled by the tac promoter, which is a hybrid of the trp and lac promoters; its activity is repressed by the LacI protein, which in turn is inactivated by isopropyl- $\beta$ -D-thiogalactopyranoside (IPTG). Therefore, the addition of IPTG to the growth medium drives expression of the GST fusion protein from pGEX. The ear domains of AP-2  $\alpha$ C-adaptin, AP-3  $\beta$ 3-adaptin, and AP-4  $\epsilon$ -adaptin were subcloned into the EcoRI-XhoI restriction sites of pGEX (by Rafael Mattera and William Smith) to create pGEX.GST- $\alpha$ C ear, pGEX.GST- $\beta$ 3 ear, and pGEX.GST- $\epsilon$  ear, respectively (Fig. 2.2).

#### **2.3.1.3 pST**

pST39 (Tan, 2001) is a polycistronic expression vector that allows for the independent

translation of four genes from a single mRNA transcript. The plasmid contains a T7 promoter upstream of four expression cassettes; each cassette has its own ribosome binding site and multiple cloning site (MCS). Portions of the four subunits of AP-2 were subcloned into pST39 (by William Smith and Bridgette Beach of the Jim Hurley Laboratory, National Institute of Diabetes and Digestive and Kidney Diseases, NIH) to generate pST.AP-2<sup>CORE</sup>. The coding sequence for residues 1-141 of rat  $\mu$ 2-adaptin ( $\mu$ 2-N) was subcloned into the XbaI-BamHI restriction sites of cassette 1; the coding sequence for residues 1-621 of rat  $\alpha$ C-adaptin ( $\alpha$ C trunk) with a C-terminal fusion to GST was subcloned into the EcoRI-HindIII restriction sites of cassette 2; the coding sequence for residues 1-143 of rat  $\sigma$ 2-adaptin (full-length  $\sigma$ 2) was subcloned into the SacI-KpnI restriction sites of cassette 3; and the coding sequence for residues 1-591 of rat  $\beta$ 2-adaptin ( $\beta$ 2 trunk) with a N-terminal His<sub>6</sub> tag was subcloned into the BspEI-MluI restriction sites of cassette 4 (Fig. 2.3). Tobacco etch virus (TEV) protease cleavage sites were inserted between  $\alpha$ C and the GST tag, and between the His<sub>6</sub> tag and  $\beta$ 2, so that those epitopes could be removed from the AP-2<sup>CORE</sup> construct as desired. SDM reactions on pST.AP-2<sup>CORE</sup> (also referred to as pST.AP-2<sup>CORE</sup>  $\alpha$  wild-type [WT]) yielded pST.AP-2<sup>CORE</sup>  $\alpha$  KR297,340EE.

### 2.3.2 Recombinant protein expression and purification

The bacterial expression vectors described in Section 2.3.1 were transformed into *Escherichia coli* Rosetta2 BL21 (DE3) cells (Novagen, San Diego, CA, USA) using the standard heat shock protocol. These cells contain a chromosomal copy of the T7 bacteriophage RNA polymerase under the control of the lac operator; the addition of IPTG to the growth medium allows for expression of the T7 RNA polymerase and subsequent transcription of genes downstream of a T7 promoter. The Rosetta2 BL21 (DE3) cells also contain several tRNAs that utilize codons more commonly found in eukaryotic systems, thus facilitating the translation of eukaryotic proteins. Methods used to purify the His<sub>6</sub>-tagged, GST-tagged, and AP-2<sup>CORE</sup> recombinant proteins are described in separate sections below. All protein purification steps were carried out by either William Smith or Rafael Mattera.

### 2.3.2.1 His<sub>6</sub>-tagged proteins

Bacteria transformed with pHis.Nef, pHis.Nef LL164,165AA, or pHis.Nef DD174, 175AA were grown overnight at 18°C in LB medium supplemented with 0.5 mM IPTG. The bacteria were then harvested and lysed in Tris-Buffered Saline (TBS) [50 mM Tris-HCl with 500 mM NaCl (pH 8.0)], and the supernatants were applied to HisTrap Fast Flow columns (GE Healthcare). The His<sub>6</sub>-tagged Nef proteins were eluted in TBS containing 0.25 M imidazole, concentrated, and then purified by gel filtration on Superdex 200 columns (GE Healthcare) in Tris-dithiothreitol-NaCl (TDN) buffer [50 mM Tris-HCl with 5 mM dithiothreitol and 150 mM NaCl (pH 8.0)].

### 2.3.2.2 GST-tagged proteins

Bacteria that had been transformed with empty pGEX.GST, pGEX.GST- $\alpha$ C ear, pGEX.GST- $\beta$ 3 ear, or pGEX.GST- $\epsilon$  ear were likewise grown overnight at 18°C in LB medium supplemented with 0.5 mM IPTG. The bacteria were harvested and lysed as described above, and the supernatants applied to glutathione-Sepharose affinity columns (GE Healthcare). After extensive washing with TBS, unfused GST, GST- $\alpha$ C ear, GST- $\beta$ 3 ear, and GST- $\epsilon$  ear were eluted with 10 mM glutathione, concentrated, and purified in TDN using Superdex 200 columns.

### 2.3.2.3 AP-2<sup>CORE</sup> complexes

The AP-2<sup>CORE</sup> constructs were designed to have both a His<sub>6</sub>-tag (fused to the N-terminus of the  $\beta$ 2 trunk) and a GST-tag (fused to the C-terminus of the  $\alpha$ C trunk); therefore, a combination of the two protein purification strategies described above was used to isolate AP-2<sup>CORE</sup> complexes. Bacteria that had been transformed with pST.AP-2<sup>CORE</sup> or pST.AP-2<sup>CORE</sup>  $\alpha$  KR297,340EE were grown in LB medium at 37°C to an optical density (OD) of 0.8 at 600 nm. The temperature was then lowered to 18°C and expression of the AP-2<sup>CORE</sup> complexes was induced by the addition of IPTG to a final concentration of 0.5 mM. The bacteria were allowed to grow under these conditions for 12 hrs, after which the cells were harvested and lysed in TBS. Insoluble material was cleared from the lysates by centrifugation, and the supernatants were applied to HisTrap Fast Flow columns. After the columns were washed extensively

with TBS to remove contaminants, the AP-2<sup>CORE</sup> complexes were eluted in TBS containing 0.25 M imidazole. The complexes were then transferred to glutathione-Sepharose affinity columns, washed again with TBS, and eluted in TBS containing 10 mM glutathione. AP-2<sup>CORE</sup> and AP-2<sup>CORE</sup>  $\alpha$  KR297,340EE were finally purified in TDN using Superdex 200 columns. For surface plasmon resonance (SPR) assays (see Section 2.3.3.2), purified AP-2<sup>CORE</sup> was treated with a His<sub>6</sub>-tagged TEV protease to cleave the His<sub>6</sub>-tag from the  $\beta$ 2 trunk and the GST-tag from the  $\alpha$ C trunk. The complex was then isolated from the protease using a HisTrap Fast Flow column; the untagged AP-2<sup>CORE</sup> complex passed through the column and was collected in the filtrate, while the His<sub>6</sub>-tagged TEV protease remained bound to the column.

### **2.3.3 Binding assays**

The ability of wild-type or mutant Nef proteins to bind wild-type or mutant AP-2<sup>CORE</sup> complexes were assayed by GST pull-down experiments (performed by William Smith and Rafael Mattera and described in Section 2.3.3.1) and surface plasmon resonance experiments (performed by William Smith and described in Section 2.3.3.2).

#### **2.3.3.1 GST pull-down assays**

Saturating amounts (5  $\mu$ g) of the purified GST-tagged proteins (including AP-2<sup>CORE</sup>, AP-2<sup>CORE</sup>  $\alpha$  KR297,340EE, GST- $\alpha$ C ear, GST- $\beta$ 3 ear, GST- $\epsilon$  ear, and unfused GST) were immobilized onto 30  $\mu$ L of glutathione-Sepharose beads at 4°C in TBS. The beads were then washed with TBS and incubated with 3  $\mu$ g of a His<sub>6</sub>-tagged Nef protein (either His<sub>6</sub>-Nef, His<sub>6</sub>-Nef LL164,165AA, or His<sub>6</sub>-Nef DD174,175AA) at 4°C for 2 hrs in a final volume of 1 mL of Protein Binding Buffer (PBB) [15 mM HEPES (pH 7.0), 75 mM NaCl, 0.25% (vol/vol) Triton-X-100, 0.15% (wt/vol) bovine serum albumin (BSA), and supplemented with a protease inhibitor cocktail (Roche Applied Science, Basel, Switzerland)]. Following the incubation, the beads were washed with PBB lacking BSA, and then centrifuged at 2000 g for 2 min at 4°C. Proteins bound to the beads were eluted by resuspension in 50  $\mu$ L of NuPAGE Laemmli sodium dodecyl sulphate (SDS) sample buffer (Invitrogen) and incubated at 90°C for 10 min. The samples were then centrifuged at 16,000 g for 2 min at room temperature, and equal volumes of the supernatants were subjected to SDS-PAGE and immunoblotting (please see Section 2.9 for further information). To determine whether the interaction

between Nef and AP-2 was salt-sensitive, identical aliquots of immobilized AP-2<sup>CORE</sup> were incubated with His<sub>6</sub>-Nef in the presence of varying concentrations of NaCl (from 0 M to 1.0 M). The beads were prepared for analysis as described above.

### 2.3.3.2 Surface plasmon resonance assays

Surface plasmon resonance (SPR) was used to measure the binding of untagged AP-2<sup>CORE</sup> complex to His<sub>6</sub>-tagged wild-type and DD174,175AA Nef proteins. All SPR experiments were performed using a Biacore T100 instrument (Biacore, Uppsala, Sweden) at room temperature with HEPES-Buffered Saline (HBS) [10 mM sodium HEPES with 150 mM NaCl (pH 7.4)]. The assay was begun by activating a CM5 sensor chip (Biacore) using N-hydroxysuccinimide-1-ethyl-3-(3-dimethylaminopropyl) carbodiimide at a flow rate of 5  $\mu$ L/min for 400 sec. Equivalent amounts of GST-tagged  $\epsilon$  ear domain of AP-4 (used as a negative control) and His<sub>6</sub>-tagged wild-type and DD174,175AA Nef in 10 mM acetate buffer (pH 5.0) were then covalently attached to separate surfaces of the CM5 chip by passing the recombinant proteins over individual flow cells at a rate of 20  $\mu$ L/min. With the sensitivity of the Biacore T100 set to 10,000 response units (RU), the binding of recombinant untagged AP-2<sup>CORE</sup> to wild-type and DD174,175AA Nef was simultaneously measured by passing AP-2<sup>CORE</sup> over consecutive flow cells with association and dissociation times of 120 sec and 400 sec, respectively. Between subsequent injections of AP-2<sup>CORE</sup> proteins, the chip surfaces were regenerated with an injection of HBS supplemented with 500 mM NaCl for 15 sec at 100  $\mu$ L/min. Sensorgram RU data was normalized by subtracting the values obtained from the portion of the CM5 chip containing the AP-4  $\epsilon$  ear domain negative control. Steady-state binding data of AP-2<sup>CORE</sup> for Nef were fitted using Bia-evaluation software (Biacore) with globally floating  $K_D$  (equilibrium dissociation constant),  $R_{max}$ , and refractive index values.

## 2.4 Yeast expression vectors, transformations, and hybrid assays

### 2.4.1 Yeast expression vectors

The pBridge (Section 2.4.1.1), pGADT7 (Section 2.4.1.2), and pAD (Section 2.4.1.3) vectors were used to express heterologous proteins in *Saccharomyces cerevisiae* HF7c cells for yeast hybrid assays. A description of these expression vectors, along with information on how the protein coding sequences were inserted into the plasmids, is provided below.

#### 2.4.1.1 pBridge

The pBridge vector (Clontech, Mountain View, CA, USA; Fig. 2.4) has two MCS and a TRP1 nutritional marker that allows yeast auxotrophs transformed with pBridge to grow on drop-out medium lacking tryptophan. The first MCS (MCS1) of pBridge is downstream of a constitutively active yeast alcohol dehydrogenase (ADH1) promoter and the coding sequence for the GAL4 DNA Binding Domain (BD). Genes inserted into MCS1 are expressed as GAL4BD fusion proteins. These fusion proteins are targeted to the yeast nucleus by virtue of a nuclear localization sequence (NLS) that is an intrinsic component of the GAL4BD. The second MCS (MCS2) is downstream of a conditional MET25 promoter; this promoter induces expression of the gene cloned into MCS2 when methionine is absent from the growth medium. An exogenous SV40 NLS positioned just upstream of MCS2 ensures that gene products expressed from this region of pBridge are directed to the yeast nucleus. The pBridge.Tyr.σ1, pBridge.Tyr.σ2, and pBridge.Tyr.σ3 plasmids, in which the coding sequence for the cytosolic tail of mouse tyrosinase had been subcloned into the EcoRI-PstI sites of MCS1, and the ORFs of rat σ1A, rat σ2A, and rat σ3A had been subcloned into the NotI-BglII sites of MCS2, have been previously described (Theos et al., 2005). SDM reactions on pBridge.Tyr.σ2 yielded the various mutants of this plasmid (listed in Table 2.8). The coding sequence for NL4-3 Nef was subcloned from pCI.Nef<sub>NL4-3</sub> (described in Section 2.6.1.2) and inserted into the EcoRI-SalI restriction sites of pBridge MCS1 to generate pBridge.Nef. The rat σ1A, σ2A, and σ3A ORFs were subcloned from the pBridge.Tyr.σ1, pBridge.Tyr.σ2, and pBridge.Tyr.σ3 plasmids and inserted into MCS2 of pBridge.Nef to make pBridge.Nef.σ1, pBridge.Nef.σ2, and pBridge.Nef.σ3. SDM reactions on these plasmids generated a large number of mutants used in this

study (for a complete list, please refer to Table 2.8).

#### **2.4.1.2 pGADT7**

The pGADT7 expression vector (Clontech; Fig. 2.5) has a LEU2 nutritional marker that allows yeast auxotrophs carrying the plasmid to grow on limiting medium lacking leucine, and a single MCS. The MCS is downstream of the constitutively active yeast ADH1 promoter and the coding sequence for the GAL4 Activation Domain (AD). Genes inserted into the MCS of pGADT7 are expressed as GAL4AD fusion proteins. These proteins are targeted to the yeast nucleus by a SV40 NLS located at the N-terminus of the GAL4AD. The pGADT7. $\gamma$ , pGADT7. $\alpha$ , and pGADT7. $\delta$  plasmids, in which the coding sequences for mouse  $\gamma$ 1-adaptin, rat  $\alpha$ C-adaptin, and human  $\delta$ -adaptin were inserted into the SmaI-XhoI restriction sites of the pGADT7 MCS, have been previously described (Janvier et al., 2003b). Resequencing of the original rat  $\alpha$ C-adaptin cDNA insert revealed the presence of a point mutation that changed an alanine at position 131 to threonine. This codon was reverted back to alanine by SDM, resulting in the pGADT7. $\alpha$  plasmid used in this study. SDM was also used to generate a large number of desired mutations in pGADT7. $\alpha$  (all of which are listed in Table 2.8).

#### **2.4.1.3 pAD**

To create the pAD series of expression vectors (Fig. 2.6), the pMET25-MCS2-tPGK cassette was excised from pBridge (Section 2.4.1.1) by ApaI digestion, polished with DNA polymerase I, and inserted into the PvuII site of pGAD424 (Clontech) by blunt-end ligation. This process generated a new vector, hereafter referred to as pAD, which has two MCS: one downstream of the ADH1 promoter and the GAL4AD sequence (MCS1), and one downstream of the MET25 promoter (MCS2). Genes inserted into MCS1 are expressed as GAL4AD fusion proteins, and are targeted to the nucleus by a SV40 NLS located on the GAL4AD. Genes inserted into the MCS2 of pAD are expressed as unfused proteins, but are also targeted to the nucleus by the presence of a NLS. The coding sequence for the cytosolic tail of human CD4 was amplified from pCMV.CD4 (Section 2.6.1.1) by PCR and subcloned into the EcoRI-SalI restriction sites of pAD MCS1 to create pAD.CD4. To generate pAD.CD4. $\alpha$ , the  $\alpha$ C ORF was amplified from pGADT7. $\alpha$  (Section 2.4.1.2) by PCR using primers containing NotI

and BamHI restriction sites, digested with the appropriate enzymes, and ligated into the compatible NotI-BglIII site of pAD.CD4 MCS2. The pAD.CD4.α-KR297,340EE plasmid was prepared by a similar procedure, using pGADT7.α-KR297,340EE as the PCR template.

#### **2.4.2 HF7c cells and yeast hybrid assays**

The haploid *Saccharomyces cerevisiae* strain HF7c (Feilotter et al., 1994), which is commonly used in yeast hybrid experiments (Fields and Song, 1989; Aguilar et al., 1997; Janvier et al., 2003b; Theos et al., 2005), lacks the TRP1 and LEU2 genes. HF7c cells, therefore, are unable to grow on medium lacking leucine and tryptophan unless transformed with plasmids (such as pBridge, pGADT7, and pAD) that carry the TRP1 and LEU2 genes. In addition, HF7c cells are engineered so that the single copy of the HIS3 gene is substituted for the GAL4 transcription factor downstream of the GAL4 promoter. This prevents HF7c cells from growing on medium lacking histidine unless the expression of HIS3 is induced by the presence of an artificial GAL4 transcription factor. This transcription factor can be reconstituted in the nucleus of yeast cells by the physical interaction of proteins fused to the GAL4BD (expressed from pBridge MCS1) and GAL4AD (expressed from pGADT7 or pAD MCS1). Additional nuclear-localized proteins (expressed from MCS2 of pBridge or pAD) may be required for the fusion proteins to bind and bring the separate GAL4BD and GAL4AD domains into close proximity of each other. Thus, the growth of HF7c cells co-transformed with plasmids that express GAL4BD and GAL4AD fusion proteins on medium lacking histidine is indicative of an interaction between these two proteins.

##### **2.4.2.1 Transformation of HF7c cells**

HF7c cells were transformed with pairs of pBridge and pGADT7 (or pAD) plasmids as previously described (Schiestl and Gietz, 1989; Gietz and Schiestl, 1991; Gietz et al., 1995). Briefly, the yeast were grown in YPD Broth [1% (wt/vol) yeast extract, 2% (wt/vol) peptone, 2% (wt/vol) dextrose (Sunrise Science Products, San Diego, CA, USA)] at 30°C overnight, after which the culture was diluted in YPD to an OD of 0.35 and grown at 30°C for 3 additional hrs to an OD of approximately 0.80. The culture was then centrifuged at 1000 g for 5 min, resuspended in sterile H<sub>2</sub>O, and centrifuged again at 1000 g for 5 min to collect the yeast. For each transformation,

0.80 OD units of HF7c cells were resuspended in 100  $\mu$ L of LATE solution [0.1 M Lithium Acetate, 0.1 M Tris, and 0.5 M EDTA (pH 8.0)] containing 1  $\mu$ g of single-stranded salmon sperm carrier DNA (Sigma). The cells were then combined with 1  $\mu$ g of each vector (pBridge and either pGADT7 or pAD), mixed with 600  $\mu$ L of LATE solution that had been supplemented with 40% (wt/vol) polyethylene glycol (PEG), and incubated at 30°C for 1 hr with shaking. At the end of this incubation period, 60  $\mu$ L of dimethyl sulfoxide (DMSO) was added to the mixture, and the yeast were transformed by heat shock at 42°C for 15 min. The HF7c cells were then cooled on ice for 30 sec, pelleted, resuspended in 30  $\mu$ L of H<sub>2</sub>O, and transferred to drop-out agar plates lacking leucine, tryptophan, and methionine. Yeast that had been successfully transformed with both plasmids produced visible colonies on the plates after 4 days.

#### **2.4.2.2 Yeast three-hybrid assays**

For the yeast three-hybrid (Y3H) assay, three heterologous proteins were expressed in yeast cells and targeted to the nucleus. Wild-type and mutant versions of NL4-3 Nef or the cytosolic tail of mouse tyrosinase were expressed as GAL4BD fusion proteins from the pBridge vector, along with rat  $\sigma$ 1A, rat  $\sigma$ 2A, or rat  $\sigma$ 3A (Section 2.4.1.1). Mouse  $\gamma$ 1, wild-type and mutant versions of rat  $\alpha$ C, and human  $\delta$  were also expressed as GAL4AD fusion proteins from the pGADT7 plasmid (Section 2.4.1.2). HF7c cells were transformed with pairs of pBridge and pGADT7 plasmids, and co-transformants were selected on drop-out agar plates containing all necessary amino acids except leucine, tryptophan, and methionine (Section 2.4.2.1). For each sample, colonies were allowed to grow on these plates for 4 days, after which they were pooled, normalized to 0.1 OD units (at 600 nm) in H<sub>2</sub>O, and transferred to three sets of drop-out plates: those lacking leucine, tryptophan, and methionine (i.e., +His); those lacking histidine, leucine, tryptophan, and methionine (-His); and those lacking histidine, leucine, tryptophan, and methionine, and supplemented with 1-3 mM 3-amino-1,2,4-triazole, an inhibitor of histidine biosynthesis (-His+3AT). Colony growth on the three sets of plates was analyzed 4 days later. The growth of transformed yeast on the -His plates is indicative of an interaction between the GAL4BD and GAL4AD fusion proteins (see Section 2.4.2), while growth on the -His+3AT plates is indicative of stronger interactions.

### 2.4.2.3 Yeast two-hybrid and four-hybrid assays

For the yeast two-hybrid (Y2H) and yeast four-hybrid (Y4H) assays, two and four heterologous proteins were expressed in yeast cells, respectively. In the Y2H assay, a GAL4BD-Nef fusion protein was expressed from pBridge MCS1 (Section 2.4.1.1), while a GAL4AD-CD4 cytosolic tail fusion protein was expressed from pAD MCS1 (Section 2.4.1.3). In the Y4H assay, a GAL4BD-Nef fusion protein was expressed from pBridge MCS1, rat  $\sigma$ 2A was expressed from pBridge MCS2 (Section 2.4.1.1), the GAL4AD-CD4 fusion protein was expressed from pAD MCS1, and rat  $\alpha$ C was expressed from pAD MCS2 (Section 2.4.1.2). Y2H, Y3H, and Y4H assays using the pBridge and pAD plasmids were carried out according to the procedure described above with only one modification: following the selection of positive transformants, the densities of the corresponding yeast suspensions were normalized to 1.6 OD units (at 600 nm), and the suspensions were serially diluted to 0.1 OD units before transfer to the +His and –His drop-out agar plates.

## 2.5 *Drosophila* expression vectors, tissue culture, transfections, and knockdowns

### 2.5.1 *Drosophila* expression vectors

The pAc (Section 2.5.1.1) and pMt (Section 2.5.1.2) vectors were used to express heterologous proteins in *Drosophila melanogaster* S2 cells for various cell biological assays. The pCo-Blast (Section 2.5.1.3) vector was used in the generation of stable cell lines. A description of these expression vectors, along with information on how protein coding sequences were inserted into the pAc and pMt plasmids, is given below.

#### 2.5.1.1 pAc-V5

The pAc-V5 vector (Invitrogen; Fig. 2.7) contains a constitutive *Drosophila* actin 5C promoter upstream of a MCS and a sequence coding for a V5 epitope tag. Human CD4 cDNA was amplified by PCR from pCMV.CD4 (Section 2.6.1.1) and subcloned into the EcoRI and XhoI restriction sites of pAc-V5 to create pAc.CD4. A stop codon at the end of the CD4 gene prevented the attachment of a C-terminal V5 tag during translation. SDM on pAc.CD4 was used to generate pAc.CD4 LL413,414AA. *Drosophila* cDNAs for AP-1  $\mu$ 1 (CG9388); AP-2  $\mu$ 2 (CG7057); AP-3  $\mu$ 3 (CG3035); and Golgi-localized, gamma-ear-containing, ARF-binding protein (GGA, CG3002) were obtained from the *Drosophila* Genomics Resource Center (Bloomington, IN, USA), while the cDNA for *Drosophila* clathrin light chain (CLC, CG6948) was kindly provided by Henry Chang (Purdue University, West Lafayette, IN, USA). Each cDNA was amplified by PCR without a stop codon and inserted into the EcoRI and ApaI restriction sites of pAc-V5 such that they would be expressed with C-terminal V5 epitope tags; this process was used to generate pAc. $\mu$ 1-V5, pAc. $\mu$ 2-V5, pAc. $\mu$ 3-V5, pAc.GGA-V5, and pAc.CLC-V5.

#### 2.5.1.2 pMt

The pMt vector (Invitrogen; Fig. 2.8) contains an inducible metallothionein promoter upstream of a MCS. The metallothionein promoter is normally inactive; however, it drives high levels of expression of downstream genes in response to some divalent metal cations, such as  $\text{Cu}^{2+}$ . The coding sequence for NL4-3 Nef was amplified by

PCR from the pIRES.Nef<sub>NL4-3</sub>.IRES.GFP (described in Section 2.6.1.3) and subcloned into the EcoRI-XhoI restriction sites of pMt to create pMt.Nef<sub>NL4-3</sub>. A similar method was used to subclone four other HIV-1 and SIV Nef alleles in pMt, using pIRES.GFP based plasmids as a template (all described in Section 2.6.1.3); this process generated pMt.Nef<sub>NA7</sub>, pMt.Nef<sub>DH12-3</sub>, pMt.Nef<sub>248</sub>, and pMt.Nef<sub>SIVmac239</sub>. SDM on pMt.Nef<sub>NL4-3</sub> created pMt.Nef<sub>NL4-3</sub>G<sub>2</sub>A, pMt.Nef<sub>NL4-3</sub>WL57,58AA, pMt.Nef<sub>NL4-3</sub>EEEE62-65AAAA, pMt.Nef<sub>NL4-3</sub>PP72,75AA, and pMt.Nef<sub>NL4-3</sub>LL164,165AA.

### 2.5.1.3 pCo-Blast

The pCo-Blast vector (Invitrogen; Fig. 2.9) contains a strong, constitutively active *Drosophila* promoter upstream of a blasticidin resistance gene. Blasticidin is a nucleoside antibiotic that inhibits protein synthesis in eukaryotic cells. The blasticidin resistance gene expressed from pCo-Blast is a deaminase that converts blasticidin into a non-toxic compound. The pCo-Blast plasmid is therefore a useful selection marker when generating stable clones; *Drosophila* S2 cells co-transfected with pCo-Blast and other plasmids (such as pAc and pMt) can be selected from untransfected cells by the addition of blasticidin to the growth medium (see Section 2.5.2.3).

### 2.5.2 *Drosophila* S2 cells

*Drosophila melanogaster* Schneider 2 (S2) cells, originally derived from a late-stage *Drosophila* embryo and having phagocyte-like properties (Schneider, 1972), were kindly provided by Mary Lilly (*Eunice Kennedy Shriver* NICHD, NIH).

#### 2.5.2.1 Tissue culture

S2 cells were cultured in complete Schneider's medium [Schneider's *Drosophila* medium (Invitrogen) supplemented with 10% (vol/vol) fetal bovine serum (FBS), 100 U/mL of penicillin, 0.1 mg/mL of streptomycin, and 2 mM L-glutamine] at 24°C in humidified air containing ambient levels of carbon dioxide (CO<sub>2</sub>). The S2 cells were grown on standard tissue culture plates and passaged every 2 to 3 days.

### **2.5.2.2 Transient DNA transfections**

S2 cells were transfected with plasmids using the Amaxa Nucleofector (Amaxa, Walkersville, MD, USA). Prior to the transfection, S2 cells were harvested from a tissue culture plate and counted using a hemocytometer and trypan blue.  $1 \times 10^6$  live cells were centrifuged at 1000 g for 5 min, washed once with room temperature Phosphate Buffered Saline (PBS) [0.8% (wt/vol) NaCl, 0.115% (wt/vol)  $\text{Na}_2\text{HPO}_4$ , 0.02% (wt/vol) KCl, 0.02% (wt/vol)  $\text{KH}_2\text{PO}_4$  (pH 7.4)], and centrifuged again at 1000 g for 5 min. The S2 cells were then resuspended in 100  $\mu\text{L}$  of room temperature V-solution (Amaxa), to which 1  $\mu\text{g}$  of each plasmid to be transfected had already been added. The cells and transfection solution were mixed gently, transferred to a metal-plated cuvette, and electroporated using the Nucleofector set to program O-20. Immediately following the electric shock, the cuvette was withdrawn from the Nucleofector, and 1.9 mL of complete Schneider's medium pre-warmed to  $24^\circ\text{C}$  was added. The transfected cells were then divided equally between two wells in a 12-well plate, each well having a total volume of 1.0 mL. The next day, one of the wells in the pair was treated with 5  $\mu\text{L}$  of 100 mM  $\text{CuSO}_4$  (for a final concentration of 0.5 mM) to activate the metallothionein promoter of the pMt plasmid and induce Nef expression. The cells were incubated at  $24^\circ\text{C}$  for another day, at which time various assays were performed (48 hrs post-transfection and 24 hrs post Nef-induction).

### **2.5.2.3 Generation of a stable CD4-Nef cell line**

To generate a stable CD4-Nef cell line, in which CD4 was constitutively expressed and Nef was expressed upon the addition of  $\text{CuSO}_4$ ,  $1 \times 10^7$  S2 cells were transfected with 4  $\mu\text{g}$  of pAc.CD4, 4  $\mu\text{g}$  of pMt.Nef<sub>NL4-3</sub>, and 1  $\mu\text{g}$  of pCo-Blast using the Amaxa Nucleofector as described in Section 2.5.1.2. The cells were initially plated on a 15  $\text{cm}^2$  tissue culture dish and grown for 1 week in complete Schneider's medium; after this period, stable clones were selected and maintained by supplementing the medium with 25  $\mu\text{g}/\text{mL}$  of blasticidin. After several weeks, surviving clones were transferred to individual wells of a 96-well plate, and then to a 12-well plate, as cell growth permitted. At this stage, the clones were assayed by flow cytometry for CD4 surface levels before and after induction of Nef expression. Of the clones assayed, the D6 cell line was chosen for its uniform CD4 surface expression and consistent, inducible

downregulation of CD4 by Nef.

#### **2.5.2.4 RNAi-mediated protein depletion**

The Expression Arrest *Drosophila* RNA-interference (RNAi) Library, a collection of double-stranded (ds) DNA templates representing most of the ORFs in the *Drosophila* genome, was obtained from Open Biosystems (Huntsville, AL, USA). Each template contained 200-800 bp of cDNA sequence from a particular gene, and was flanked by T7 RNA polymerase initiation sites. Sixty-six genes, the homologues of which had previously been implicated in protein trafficking processes in yeast and animals, were selected from the library for use in this study. Similar dsDNA sequences for another five genes (*Drosophila* CLC, *Drosophila* Tsg101, human CD4, HIV-1 NL4-3 Nef, and Green Fluorescent Protein [the latter three used as controls]) were made by PCR using primers containing T7 promoters and the appropriate cDNA sequences (see Table 2.9 for further information). In vitro transcription (IVT) reactions were carried out on the dsDNA templates of the selected genes using the MEGAscript T7 Kit (Ambion, Austin, TX, USA) at 37°C for 16 hrs to produce the desired dsRNAs. Each dsRNA was analyzed by agarose gel electrophoresis to determine that a product of expected size was obtained, after which the yield of the IVT reaction was quantified using a NanoDrop spectrophotometer. To deplete target proteins, S2 cells were treated with dsRNAs according to a five day protocol. On day 1, the cells were incubated for 1 hr in serum-free growth medium containing 30 ng/mL of dsRNA, after which FBS was added to a final concentration of 10% (vol/vol). On day 3, cells receiving a particular dsRNA treatment were split into two equivalent wells in a tissue culture dish. On day 4, the expression of Nef was induced in one of the wells by the addition of CuSO<sub>4</sub> (to a final concentration of 0.5 mM), while the other well was left uninduced. On day 5, the S2 cells were prepared for flow cytometric analysis (96 hrs post dsRNA-treatment and 24 hrs post Nef-induction; see Section 2.7 for further information).

## **2.6 Human expression vectors, tissue culture, transfections, and knockdowns**

### **2.6.1 Human expression vectors**

The pCMV (Section 2.6.1.1), pCI (Section 2.6.1.2), and pIRES.GFP (Section 2.6.1.3) vectors were used to express proteins in JM and HeLa cells for various cell biological and biochemical assays. A description of these expression vectors, along with detailed information on how protein coding sequences were inserted into these plasmids, is provided below.

#### **2.6.1.1 pCMV**

The pCMV expression vector (Clontech) contains a human cytomegalovirus (CMV) immediate-early enhancer-promoter upstream of a single MCS. The CMV promoter is constitutively active and induces high levels of expression of downstream genes in many human cell lines, including JM and HeLa cells. The pCMV.CD4 plasmid, in which the coding sequence for human CD4 was inserted between the BamHI and EcoRI restriction sites of pCMV, was kindly provided by Klaus Strebel (National Institute of Allergy and Infectious Diseases [NIAID], NIH; see Fig. 2.10).

#### **2.6.1.2 pCI**

Like pCMV, the pCI expression vector (Promega, Madison, WI, USA) has a CMV immediate-early enhancer-promoter upstream of a single MCS. Several pCI-based plasmids containing different HIV and SIV Nef alleles, including pCI.Nef<sub>NL4-3</sub>, pCI.Nef<sub>DH12-3</sub>, pCI.Nef<sub>248</sub>, and pCI.Nef<sub>SIVmac239</sub>, were kindly provided by Sundararajan Venkatesan (NIAID, NIH; see Fig. 2.11). In all cases, the Nef coding sequence had been inserted between the EcoRI and Sall restriction sites of pCI. SDM reactions on pCI.Nef<sub>NL4-3</sub> yielded pCI.Nef<sub>NL4-3</sub>LL164,165AA, pCI.Nef<sub>NL4-3</sub>D174E, pCI.Nef<sub>NL4-3</sub>D175E, and pCI.Nef<sub>NL4-3</sub>DD174,175AA.

#### **2.6.1.3 pIRES.GFP**

The pIRES2.eGFP expression vector (Clontech; hereafter referred to as pIRES.GFP) contains a CMV immediate-early enhancer-promoter upstream of a MCS, an internal ribosome entry site (IRES), and the coding sequence for enhanced Green Fluorescent

Protein (GFP). Thus, this plasmid allows for the independent translation of a gene of interest (cloned into the MCS) and GFP from a single bicistronic mRNA transcript (see Fig. 2.12). GFP fluorescence can then be used to identify cells that have been transfected with the plasmid and that express the gene of interest. The coding sequences of NL4-3 Nef, DH12-3 Nef, 248 Nef, and SIVmac239 Nef were subcloned from pCI-based vectors (described in Section 2.6.1.2) into the EcoRI-SalI restriction sites of the pIRES.GFP MCS to generate pNef<sub>NL4-3</sub>.IRES.GFP, pNef<sub>DH12-3</sub>.IRES.GFP, pNef<sub>248</sub>.IRES.GFP, and pNef<sub>SIVmac239</sub>.IRES.GFP. The NA7 Nef ORF from pCDNA.Nef<sub>NA7</sub> (kindly provided by Jacek Skowronski, Cold Spring Harbor Laboratory, Cold Spring Harbor, NY, USA) was amplified by PCR and also inserted into the EcoRI-SalI restriction sites of pIRES.GFP to create pNef<sub>NA7</sub>.IRES.GFP. SDM of pNef<sub>NL4-3</sub>.IRES.GFP yielded all permutations of this plasmid (for a complete listing, see Table 2.8). The p $\alpha$ R-V5.IRES.GFP and p $\alpha$ R-KR297,340EE-V5.IRES.GFP plasmids, used in the  $\alpha$ -adaptin knockdown and rescue assays, are described in Section 2.6.3.4.

## **2.6.2 JM cells**

JM cells are immature CD4<sup>+</sup>/CD8<sup>+</sup> human T cells that were originally isolated from an adolescent male lymphoblastoid leukemia patient prior to the thymic selection process (Schneider, 1977). The JM cells were obtained from the NIH AIDS Research and Reference Reagent Program (NIAID, NIH, Germantown, MD, USA).

### **2.6.2.1 Tissue culture**

JM cells were cultured in complete RPMI-1640 [Roswell Park Memorial Institute-1640 medium (Invitrogen) supplemented with 10% (vol/vol) FBS, 100 U/mL of penicillin, 0.1 mg/mL of streptomycin and 2 mM L-glutamine] at 37°C in humidified air containing 5% CO<sub>2</sub>. The JM cells were grown in standard tissue culture flasks and passaged every 2 to 3 days; a cell density of 1x10<sup>5</sup> to 8x10<sup>5</sup> cells/mL was maintained at all times.

### **2.6.2.2 Transient DNA transfections**

JM cells were transiently transfected with plasmids using the Amaxa Nucleofector in a manner similar to that described in Section 2.5.2.2. For each transfection, 1x10<sup>6</sup> live

JM cells were harvested by centrifugation at 1000 g for 5 min, washed once with room temperature PBS, and pelleted again by centrifugation at 1000 g for 5 min. The cells were then resuspended in 100  $\mu$ L of room-temperature V-solution, to which 1  $\mu$ g of DNA had already been added. The cells and transfection reagents were mixed gently, placed in a cuvette supplied by the manufacturer, and electroporated using the Nucleofector set to program O-17. After the electric shock, the cuvette was withdrawn from the Nucleofector, and 500  $\mu$ L of complete RPMI-1640 pre-warmed to 37°C was added. The transfected cells were then transferred from the cuvette to a T-25 tissue culture flask containing 9.5 mL of complete RPMI-1640 and incubated overnight at 37°C. Assays were performed on the JM cells the following day (24 hrs post-transfection).

### **2.6.3 HeLa cells**

HeLa cells are human cervical cancer cells originally isolated from an adult female patient. The HeLa cells used in this study were purchased from the American Type Culture Collection (Manassas, VA, USA).

#### **2.6.3.1 Tissue Culture**

HeLa cells were cultured in complete DMEM [Dulbecco's modified Eagle medium (Invitrogen) supplemented with 10% (vol/vol) FBS, 100 U/mL of penicillin, 0.1 mg/mL of streptomycin, and 2 mM L-glutamine] at 37°C in humidified air containing 5% CO<sub>2</sub>. The HeLa cells were grown on standard tissue culture plates and passaged every 3 to 4 days.

#### **2.6.3.2 Transient DNA transfections**

HeLa cells were transiently transfected with expression vectors using Lipofectamine 2000 (Invitrogen) according to instructions provided by the manufacturer. For each transfection, two 100  $\mu$ L aliquots of Opti-MEM I (Invitrogen) were brought to room temperature. To one aliquot, 1.0  $\mu$ g of DNA was added; to the other aliquot of Opti-MEM I, 3  $\mu$ L of Lipofectamine 2000 was added. The two solutions were incubated at room temperature for 5 min, mixed, and then incubated at room temperature for a further 20-25 min. During the second incubation step, HeLa cells growing on a 6-well

tissue culture dish at 30-50% confluency were removed from the incubator and washed once with room temperature Opti-MEM I; each well was then seeded with 800  $\mu$ L of serum-free DMEM supplemented with 100 U of penicillin/mL, 0.1 mg of streptomycin/mL, and 2 mM L-glutamine. The transfection mixture was then applied drop-wise to the well (for a total volume of 1000  $\mu$ L), and the tissue culture dish was swirled gently before being placed back in the incubator. Three hrs later, 500  $\mu$ L of DMEM supplemented with 30% FBS (vol/vol), 100 U of penicillin/mL, 0.1 mg of streptomycin/mL, and 2 mM L-glutamine was added to each well, and the cells were incubated for another 24 hrs at 37°C. Various assays were performed on the cells the following day (24 hrs post-transfection) as described below and in Sections 2.7, 2.8, and 2.9.

### **2.6.3.3 Endocytosis assays**

Endocytosis assays were used to measure the rate at which CD4 was internalized from the plasma membrane in the absence and presence of Nef. HeLa cells growing on 9-cm-diameter tissue culture plates at approximately 70% confluency were transfected with the appropriate plasmids as described in Section 2.6.3.2. The following day, the plates were washed with PBS pre-warmed to 37°C, incubated in detachment buffer [PBS supplemented with 2mM EDTA] for 30 min at 37°C, and harvested. The harvested cells were washed twice with ice-cold PBS and then incubated on ice for 30 min in Endocytosis Binding Buffer (EBB) [Opti-MEM I with 2% (wt/vol) BSA] containing a 1:100 dilution of mouse anti-human CD4 antibody. An aliquot of cells was incubated without the primary antibody as a control. The cells were then washed twice with ice-cold PBS, resuspended in EBB pre-warmed to 37°C, and incubated at 37°C. An aliquot of cells that remained on ice was reserved for the 0-min time point. At the indicated time intervals, equal aliquots of cells were transferred from the incubation tubes to ice-cold PBS. At the end of the time course, the samples were subjected to two additional washes with ice-cold PBS and incubated in PBA [PBS with 1% (wt/vol) BSA and 0.1% (vol/vol) sodium azide] containing a 1:100 dilution of goat anti-mouse antibody conjugated to allophycocyanin (APC) for 1 hr on ice. The cells were finally washed three times with ice-cold PBS, fixed in PBA-F [PBA with 1% (vol/vol) paraformaldehyde], and analyzed by flow cytometry as described in Section 2.7.3.

#### **2.6.3.4 siRNA-mediated protein depletion of $\mu$ 1, $\mu$ 2, and $\mu$ 3**

The expression of  $\mu$ 1-adaptin,  $\mu$ 2-adaptin, and  $\mu$ 3-adaptin was depleted in HeLa cells by using small interfering RNA (siRNA) duplexes. For each gene to be silenced, siRNA duplexes were designed ( $\mu$ 1 sense sequence: 5'-AAGGCAUCAAGUAUCGG AAGA-3',  $\mu$ 2: 5'-AAGUGGAUGCCUUUCGGGUCA-3',  $\mu$ 3: 5'-AAGGAGAACA GUUCUUGCGGC-3') and purchased, along with a non-targeting oligonucleotide duplex called siCONTROL 1, from Dharmacon (Lafayette, CO, USA). For each transfection reaction, two aliquots of Opti-MEM I were brought to room temperature. The first aliquot of Opti-MEM I (8  $\mu$ L) was combined with 2  $\mu$ L of Lipofectamine 2000, while the second aliquot of Opti-MEM I (185  $\mu$ L) was combined with 5  $\mu$ L of an siRNA duplex at a stock concentration of 20  $\mu$ M. The two solutions were allowed to incubate at room temperature for 5 min, after which they were mixed and incubated at room temperature for another 25 min. At the end of the second incubation period, HeLa cells growing on a 6-well tissue culture dish (at ~30% confluence) were washed with Opti-MEM I, and each well was seeded with 800  $\mu$ L of fresh Opti-MEM I. The siRNA transfection solution was then added drop-wise to the well (for a total volume of 1000  $\mu$ L and a final siRNA duplex concentration of 100 nM). The dish was swirled gently and placed back in the tissue culture incubator; the following day, 500  $\mu$ L of DMEM supplemented with 30% FBS (vol/vol), 300 U of penicillin/mL, 0.3 mg of streptomycin/mL, and 6 mM L-glutamine was added to each well. For each siRNA-mediated protein depletion experiment, HeLa cells were transfected twice with the targeting and non-targeting siRNA duplexes over 6 days according to the protocol described above. On day 1, HeLa cells received the first siRNA treatment. On day 3, the cells were split onto fresh six-well dishes in a 1:3 ratio. On day 4, the HeLa cells received the second siRNA treatment. On day 5, the cells were transfected with DNA plasmids as detailed in Section 2.6.3.2 and Table 2.6. On day 6, the cells were harvested and prepared for flow cytometric analysis (as described in Section 2.7) and immunoblot analysis (as described in Section 2.9).

#### **2.6.3.5 $\alpha$ -adaptin knockdown and rescue reagents**

HeLa cells express two isoforms of  $\alpha$ -adaptin,  $\alpha$ A and  $\alpha$ C. To simultaneously silence

the expression of both isoforms, a single siRNA duplex was designed (sense sequence 5'-GAGCAUGUGCACGCUGGCCATT-3'; Qiagen) that targeted nucleotides 1053 to 1072 of the human  $\alpha A$  and  $\alpha C$  ORFs. An siRNA-resistant version of  $\alpha C$ -adaplin (hereafter referred to as  $\alpha R$ ) was generated by introducing three silent substitutions into the rat  $\alpha C$  cDNA (C→T, C→T, and G→C at nucleotides 1053, 1059, and 1065, respectively, of the rat  $\alpha C$  sequence). These substitutions resulted in a total of four mismatches between  $\alpha R$  and the siRNA-sensitive human  $\alpha A/\alpha C$  sequences (the rat  $\alpha C$  cDNA contains an additional A→G substitution at position 1062 compared to the human  $\alpha A/\alpha C$  sequences). The sequence for a V5 epitope tag was fused to the 3' end of the  $\alpha R$  ORF by PCR, and the  $\alpha R$ -V5 cassette was subcloned into the BamHI-Sall restriction sites of pIRES.GFP to generate p $\alpha R$ -V5.IRES.GFP. SDM on this plasmid yielded p $\alpha R$ -KR297,340EE-V5.IRES.GFP (also referred to as p $\alpha R$ -KREE-V5.IRES.GFP; see Section 2.6.1.3 for more information on the pIRES.GFP expression vector).

#### **2.6.3.6 $\alpha$ -adaplin knockdown and rescue transfections**

In HeLa cells, the expression of endogenous  $\alpha$ -adaplin was silenced by transfection with siRNA and replaced with  $\alpha R$  according to a seven day protocol. On day 1, HeLa cells growing on six-well plates (at ~15% confluence) were either left untreated or transfected with the  $\alpha A/\alpha C$  siRNA duplex (100 nM) using Lipofectamine 2000 and Opti-MEM I as described in Section 2.6.3.4. On day 3, the cells were split at a 1:3 ratio onto fresh 6-well plates. On day 4, the cells (at ~50% confluence) were transfected with a second round of siRNA and/or a unique combination of DNA plasmids (pCMV.CD4; pCI or pCI.Nef<sub>NL4-3</sub>; and pIRES.GFP, p $\alpha R$ -V5.IRES.GFP, or p $\alpha R$ -KR297,340EE-V5.IRES.GFP; see Table 2.7) using Lipofectamine 2000 and Opti-MEM I. On day 6, the cells were split again onto fresh 6-well plates in a 1:2 ratio. On day 7, the cells were harvested and prepared for flow cytometric analysis (as described in Section 2.7) and immunoblot analysis (Section 2.9).

## **2.7 Flow Cytometry**

Flow cytometry was used to quantify the amount of CD4 and other proteins on the surface of S2, JM, and HeLa cells in the absence and presence of Nef. Regardless of the type, the cells were analyzed by flow cytometry in the same manner, with the exception of the method in which they were harvested.

### **2.7.1 Antibodies used**

The following primary and secondary antibodies were used to stain harvested cells for flow cytometry: unconjugated mouse immunoglobulin G (IgG [used as an isotype control]) (Jackson ImmunoResearch, West Grove, PA, USA), unconjugated mouse anti-human CD4 (Caltag, Burlingame, CA, USA), unconjugated mouse anti-human transferrin receptor (TfR) CD71 (Sigma-Aldrich), unconjugated mouse anti-human lysosomal associated membrane protein 1 (LAMP1) CD107a (Abcam, Cambridge, MA, USA), APC-conjugated mouse anti-human CD4 (Caltag), APC-conjugated goat anti-mouse IgG (Jackson ImmunoResearch), phycoerythrin (PE)-conjugated mouse anti-human CD71 (Sigma-Aldrich), and PE-conjugated goat anti-mouse IgG (Jackson ImmunoResearch).

### **2.7.2 Harvesting of cells**

S2 cells, which are only loosely adherent to the surfaces on which they grow, were harvested from tissue culture plates by gentle pipetting. JM cells, which grow in suspension, were collected by centrifugation. HeLa cells, which adhere strongly to the surface of tissue culture plates, were washed once in PBS pre-warmed to 37°C, and then incubated in detachment buffer for 30 min at 37°C. The HeLa cells were then harvested from the tissue culture plates by gentle pipetting.

### **2.7.3 Staining and analysis of cells**

For each sample, the harvested cells were washed three times with 1 mL of ice-cold PBS, and then resuspended in 100  $\mu$ L of PBA containing a primary antibody diluted to the appropriate concentration (please refer to Section 2.7.1 and Table 2.10 for further information on the antibodies used). The cells were then incubated for 1 hr on ice, with gentle mixing every 20 min. For those samples in which the primary

antibody used was conjugated to a fluorophore, the cells were then washed three times with 1 mL of ice-cold PBS, and fixed in 100  $\mu$ L of PBA-F. For those samples in which the primary antibody was not directly conjugated to a fluorophore, the cells were washed three times with 1 mL of ice-cold PBS, and then resuspended in 100  $\mu$ L of PBA containing a fluorescently-conjugated secondary antibody diluted to the appropriate concentration. These cells were incubated for an additional 1 hr on ice with gentle mixing every 20 min, and then washed three times with 1 mL of ice-cold PBS and fixed in 100  $\mu$ L of PBA-F. The amount of fluorescence associated with intact cells for each sample was measured using a FACSCalibur multicolor flow cytometer (Becton Dickinson, Franklin Lakes, NJ, USA). For JM and HeLa cells transfected with a pIRES.GFP construct, GFP fluorescence was used as a marker to identify and gate around transfected cells. In each case, the data were analyzed using CellQuest software (Becton Dickinson).

## **2.8 Immunofluorescence and confocal microscopy**

Immunofluorescence and confocal microscopy were used to visualize the distribution of CD4 in S2 and HeLa cells either lacking or expressing Nef. The methods used to prepare the S2 and HeLa cells for immunofluorescent analysis differed slightly; however, all cells were fixed, stained, and imaged in a similar manner.

### **2.8.1 Antibodies used**

Unconjugated mouse anti-human CD4 (Caltag) and Alexa 594-conjugated donkey anti-mouse IgG (Invitrogen) antibodies were used for immunofluorescence staining and confocal microscopy imaging.

### **2.8.2 Preparation of cells**

S2 cells were transfected (as described in Section 2.5.2.2) and then seeded onto glass coverslips coated with poly-L-lysine (Sigma-Aldrich), while HeLa cells were initially seeded onto uncoated glass coverslips and then transfected (as described in Section 2.6.3.2) with the appropriate plasmids.

### **2.8.3 Staining and imaging of cells**

S2 cells (24 hrs post Nef-induction) and HeLa cells (24 hrs post-transfection) were fixed for 10 min in PBS-F [PBS with 4% (vol/vol) paraformaldehyde], permeabilized for 10 min in PBS-T [PBS with 0.1% (wt/vol) Triton-X-100], and incubated for 1 hr in blocking buffer [PBS with 4% (vol/vol) FBS]. The cells were then incubated for 1 hr in blocking buffer containing mouse anti-human CD4 antibody (1:100 dilution), washed three times with PBS, incubated for 1 hr in blocking buffer containing donkey anti-mouse antibody conjugated to the Alexa 594 fluorophore (1:100 dilution), washed three more times with PBS, and mounted on slides. The cells were imaged on a Zeiss LSM510 laser scanning confocal microscope (Carl Zeiss, Thornwood, NY, USA) with a 63X plan apochromat 1.4 numerical-aperture objective using the 543 nm line of the He-Ne laser. Emission data were collected over the range of 560 to 660 nm with appropriate filter sets.

## **2.9 Immunoblotting**

Immunoblotting was used to detect the expression of various proteins in S2 and HeLa cell lysates following transfection of live cells with DNA plasmids and/or treatment with RNAi reagents. Immunoblotting was also used to check for protein interactions after GST pull-down experiments (see Section 2.3.3.1 for information on how these samples were prepared for electrophoresis and protein detection).

### **2.9.1 Antibodies used**

The following antibodies were used for immunoblotting: unconjugated mouse anti-V5 epitope (Invitrogen), unconjugated mouse anti-His<sub>6</sub> epitope (Abcam), unconjugated mouse anti-human CD4 (Caltag), unconjugated mouse anti-human  $\alpha$ -tubulin (Sigma-Aldrich), unconjugated mouse anti-human  $\alpha$ -adaptin clone numbers “100/2” (Sigma-Aldrich) and “8/Adaptin  $\alpha$ ” (Becton Dickinson), unconjugated rabbit anti-human  $\mu$ 1A-adaptin (Juan Bonifacino, NICHD, NIH), unconjugated rabbit anti-human  $\mu$ 2-adaptin (Juan Bonifacino), unconjugated rabbit anti- $\mu$ 3A-adaptin (Juan Bonifacino), unconjugated rabbit anti-HIV-1 Nef (NIH AIDS Research and Reference Reagent Program, originally deposited by Ronald Swanstrom; see Shugars et al., 1993), horseradish peroxidase (HRP)-conjugated sheep anti-mouse IgG (GE Healthcare), and HRP-conjugated donkey anti-rabbit IgG (GE Healthcare).

### **2.9.2 Lysis, electrophoresis, and protein detection**

S2 and HeLa cells were lysed at 4°C for 20-30 min in lysis buffer [PBS supplemented with 1% (vol/vol) NP-40 and a protease inhibitor cocktail (Roche Applied Science)]. The lysates were then centrifuged to remove insoluble material, and NuPAGE Laemmli SDS sample buffer was added to the supernatants. The samples were boiled for 3 min and then subjected to electrophoresis on 4-12% NuPAGE Novex Bis-Tris gradient gels (Invitrogen) using a constant voltage of 150 V for 1 hr. The separated proteins were then transferred from the gels to nitrocellulose membranes using a constant current of 350 mA for 1.5 hrs. Membranes were blocked in PBS-T-DM [PBS with 0.01% (vol/vol) Tween 20 and 5% (wt/vol) dry milk] for 1 hr at room temperature or overnight at 4°C. Primary antibodies were added to the PBS-T-DM mixture and incubated with the membranes for 1 hr at room temperature or overnight

at 4°C. The membranes were washed three times with PBS-T [PBS with 0.01% (vol/vol) Tween 20], incubated with HRP-conjugated secondary antibodies in PBS-T-DM for 1 hr at room temperature, and washed three more times with PBS-T. Proteins were detected using the Enhanced Chemi-Luminescence (ECL) Plus Kit (GE Healthcare) according to the instructions provided by the manufacturer.

### FIG. 2.1: pHis plasmid map

The pHis expression vector contains a T7 promoter (**pT7**) upstream of a hexahistidine (**His<sub>6</sub>**) epitope tag and a multiple cloning site (**MCS**). The coding sequence for wild-type or mutant HIV-1 NL4-3 Nef was subcloned into the BamHI and EcoRI restriction sites (marked by asterisks) to generate pHis.Nef. Bacteria transformed with pHis.Nef expressed a N-terminal His<sub>6</sub>-tagged Nef protein. The plasmid has the ampicillin-resistance (**Amp<sup>R</sup>**) gene  $\beta$ -lactamase to allow for selection and propagation in bacteria. Not shown: bacterial origin of replication, transcriptional termination signals, and the promoter for  $\beta$ -lactamase. See Section 2.3.1.1 and Table 2.8 for further details on the pHis plasmids used in this study. All plasmid backbones shown in this work were drawn with the aid of PlasMapper, a web-based software program (Dong et al., 2004). The backbones were annotated using PowerPoint (Microsoft, Seattle, WA, USA). In these representations, regulatory elements and genes outside of the grey circle are on the forward strand, while those inside of the grey circle are on the reverse strand. The following color conventions are used for all plasmid maps: **promoter**, **epitope tag**, **MCS**, and **selectable marker**. Additional colors are used to represent plasmid-specific features and are described in the legend for those plasmid maps.

FIG. 2.1

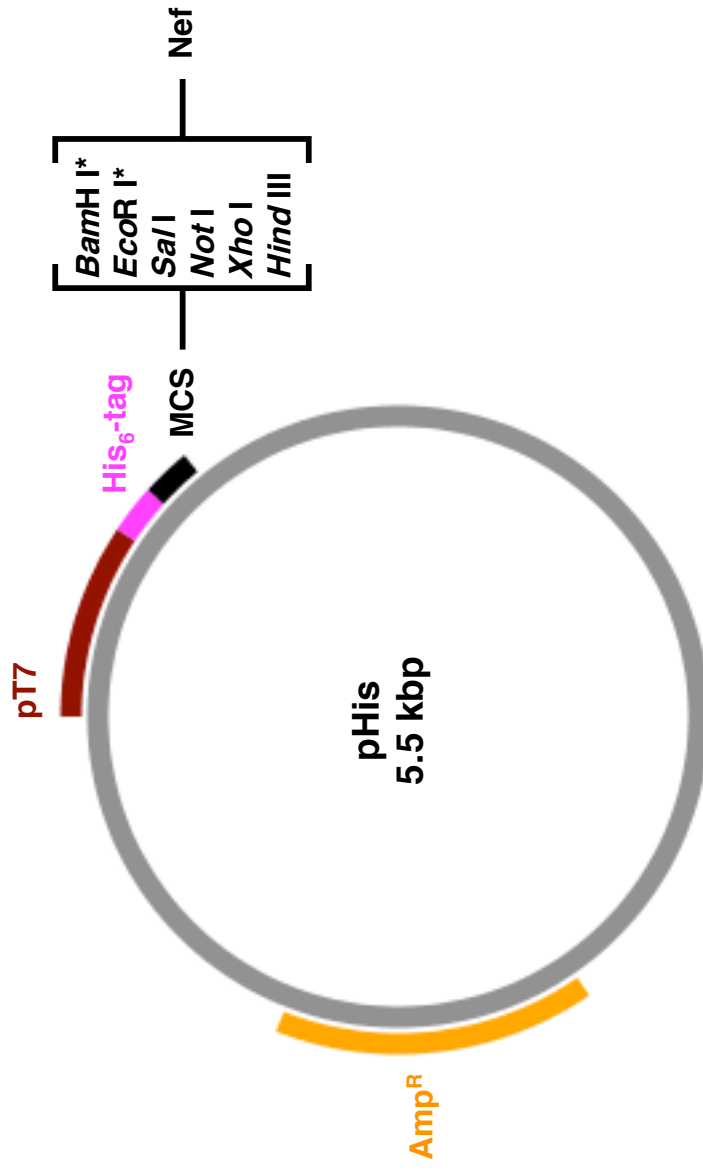


### FIG. 2.2: pGEX plasmid map

The pGEX expression vector contains a Tac promoter (**pTac**) upstream of a glutathione *S*-transferase (**GST**) epitope tag and a multiple cloning site (**MCS**). The open reading frames of  $\alpha$ C-adaptin ear,  $\beta$ 3-adaptin ear, and  $\epsilon$ -adaptin ear were inserted between the EcoRI and XhoI restriction sites (marked by asterisks) to generate pGEX.GST- $\alpha$ C-ear, pGEX.GST- $\beta$ 3-ear, and pGEX.GST- $\epsilon$ -ear. Bacteria transformed with these plasmids expressed GST- $\alpha$ C-ear, GST- $\beta$ 3-ear, and GST- $\epsilon$ -ear proteins, respectively, while bacteria transformed with the pGEX empty vector expressed unfused GST. The pGEX plasmid contains the ampicillin-resistance (**Amp<sup>R</sup>**) gene  $\beta$ -lactamase for selection and propagation in bacteria. Not shown: bacterial origin of replication, transcriptional termination signals, and the promoter for  $\beta$ -lactamase. See Section 2.3.1.2 and Table 2.8 for more information on the pGEX plasmids used in this study.

FIG. 2.2

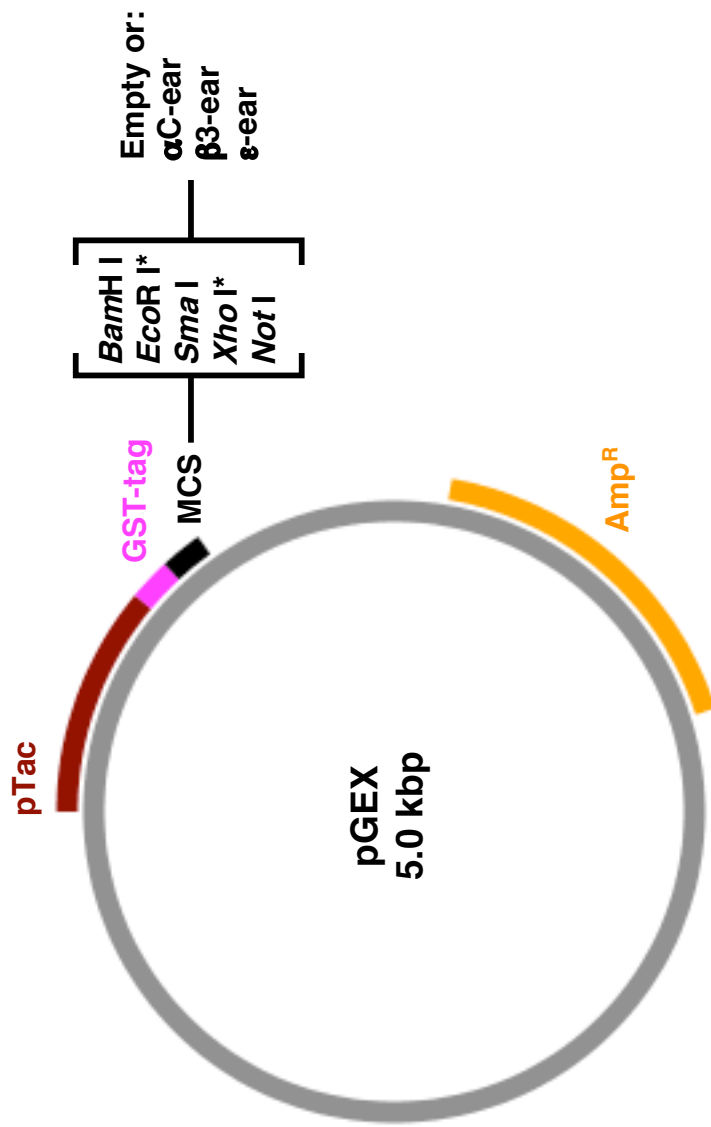


### FIG. 2.3: pST plasmid map

The pST expression vector contains a T7 promoter (**pT7**) upstream of four multiple cloning sites (**MCS**), each of which has its own ribosome binding site (not shown). Thus, up to four genes can be independently translated from the same mRNA transcript. Coding sequences corresponding to portions of the four AP-2 subunits (residues 1-141 of  $\mu$ 2-adaptin [ **$\mu$ 2-N**], residues 1-621 of wild-type or mutant  $\alpha$ C-adaptin with a C-terminal glutathione *S*-transferase-tag [ **$\alpha$ C-trunk-GST**], residues 1-143 of  $\sigma$ 2-adaptin [full-length  **$\sigma$ 2**], and residues 1-591 of  $\beta$ 2-adaptin with a N-terminal hexahistidine-tag [**His<sub>6</sub>- $\beta$ 2-trunk**]) were subcloned into pST using the restriction sites marked by asterisks to generate pST.AP-2<sup>CORE</sup>. Bacteria transformed with this plasmid expressed the AP-2<sup>CORE</sup> complex, the purification of which was facilitated by the presence of the GST and His<sub>6</sub> epitope tags. The plasmid also contains the ampicillin-resistance (**Amp<sup>R</sup>**) gene  $\beta$ -lactamase for selection and propagation in bacteria. Additional features of the pST plasmid that are not shown: bacterial origin of replication, transcriptional termination signals, and the promoter for  $\beta$ -lactamase. See Section 2.3.1.3 and Table 2.8 for further information on the pST plasmids used in this study.

FIG. 2.3

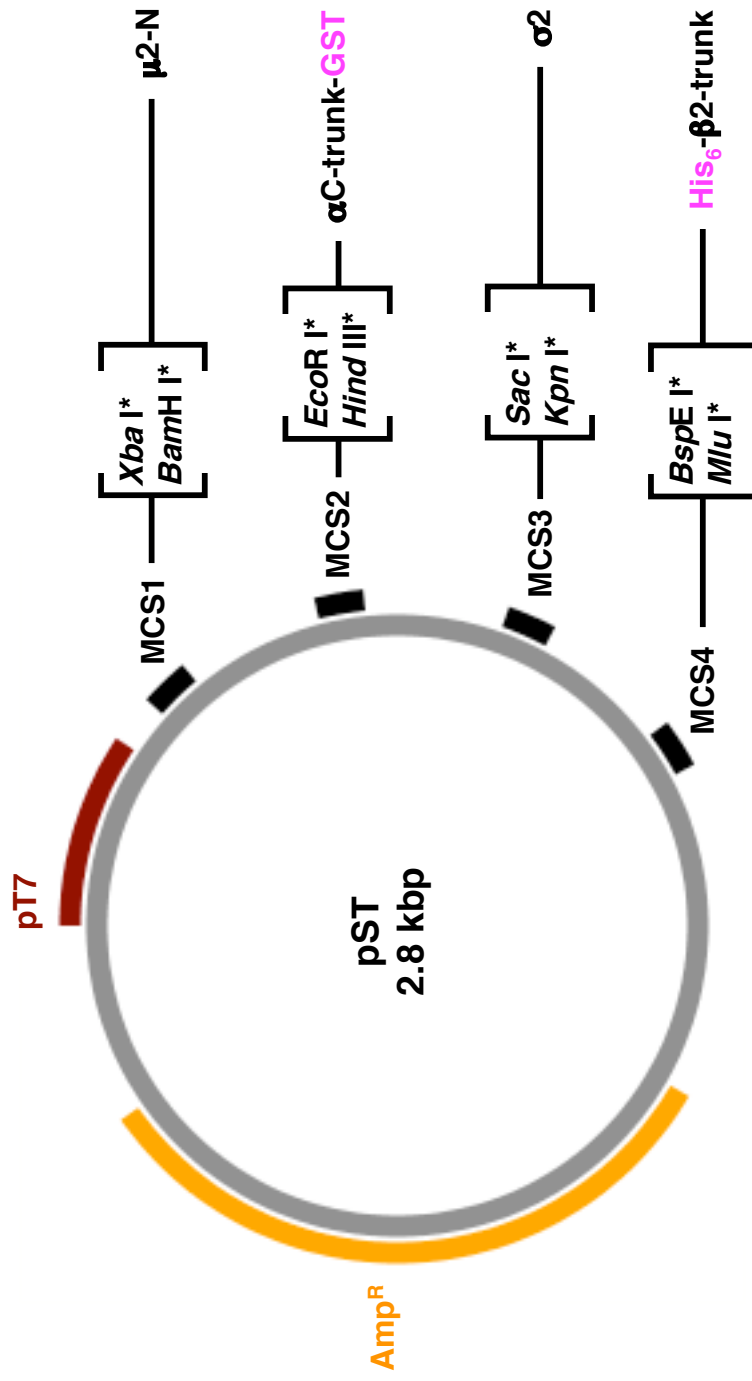


#### FIG. 2.4: pBridge plasmid map

The pBridge expression vector has two independent promoters, each of which has its own multiple cloning site (MCS). In the first expression cassette, the constitutive alcohol dehydrogenase 1 promoter (**pADH1**) is upstream of the coding sequence for the GAL4 DNA Binding Domain (**GAL4BD**) and **MCS1**. The open reading frames (ORFs) of full-length HIV-1 NL4-3 **Nef** and the cytoplasmic tail (**ct**) of mouse **tyrosinase** were subcloned into the EcoRI-SalI and EcoRI-PstI restriction sites (marked by asterisks) of **MCS1**, and expressed in yeast cells as GAL4BD-Nef and GAL4BD-tyrosinase ct fusion proteins, respectively. In the second expression cassette, the methionine-sensitive MET25 promoter (**pMET25**) is positioned upstream of **MCS2**. This MCS was either left **empty** or had the coding sequence of a  **$\sigma$ -adaptin** subunit (either rat  $\sigma$ 1A, rat  $\sigma$ 2, or rat  $\sigma$ 3) inserted into it, using the NotI-BglIII restriction sites. The  $\sigma$ -adaptin subunits were expressed in yeast cells as unfused proteins. The pBridge plasmid also contains the tryptophan 1 (**TRP1**) gene for selection in yeast and the ampicillin-resistance (**Amp<sup>R</sup>**) gene  $\beta$ -lactamase for selection in bacteria. Not shown: mutant ORFs of Nef, tyrosinase ct, and  $\sigma$ 2 subcloned into this plasmid; nuclear localization signals upstream of the GAL4BD and **MCS2**; transcriptional termination signals; yeast and bacterial origins of replication; yeast-specific promoter for **TRP1**; and the bacterial promoter for  $\beta$ -lactamase. See Section 2.4.1.1 and Table 2.8 for more information on the pBridge plasmids used in this study.

FIG. 2.4

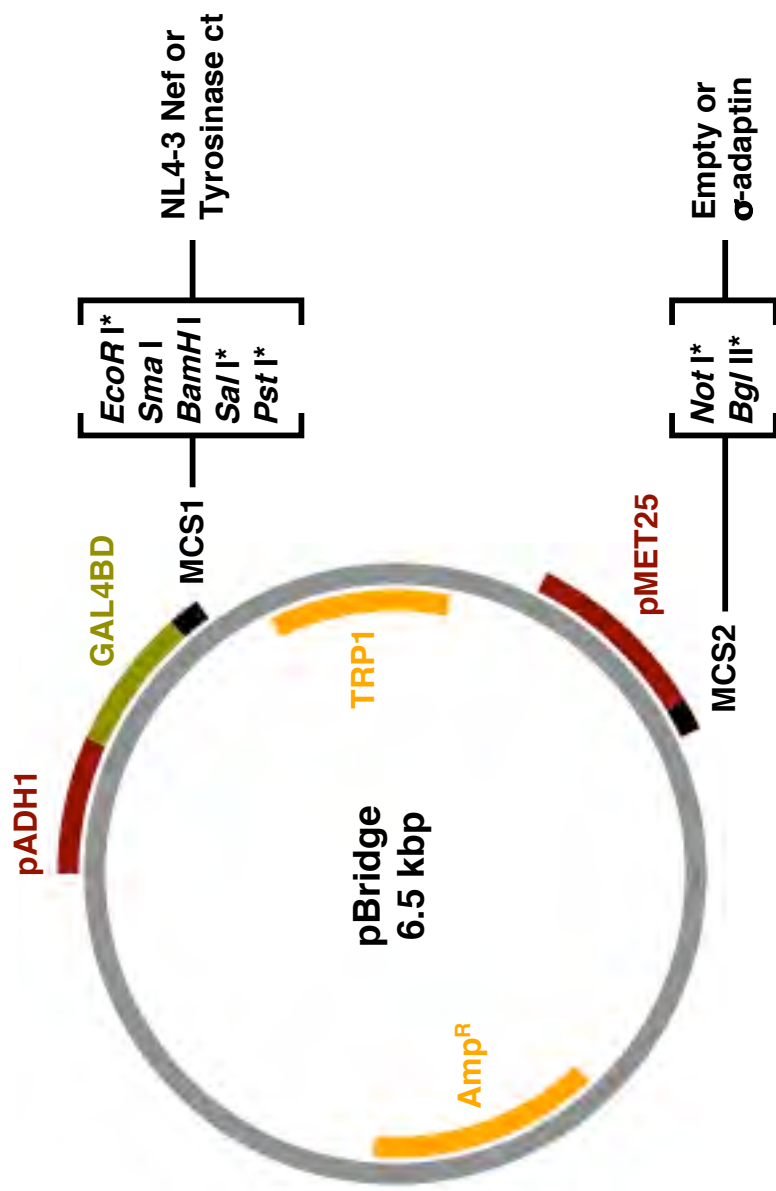


### FIG. 2.5: pGADT7 plasmid map

The pGADT7 expression vector has a constitutive alcohol dehydrogenase 1 promoter (**pADH1**) upstream of the GAL4 Activation Domain (**GAL4AD**) and a multiple cloning site (**MCS**). The coding sequences for mouse  $\gamma$ 1-adaptin ( **$\gamma$** ), wild-type or mutant rat  $\alpha$ C-adaptin ( **$\alpha$** ), and human  $\delta$ -adaptin ( **$\delta$** ) were subcloned into the SmaI-XhoI restriction sites (marked by asterisks) and expressed in yeast cells as GAL4AD fusion proteins. The pGADT7 plasmid also contains the leucine 2 (**LEU2**) gene for selection in yeast and the ampicillin-resistance (**Amp<sup>R</sup>**) gene  $\beta$ -lactamase for selection in bacteria. Not shown: nuclear localization signal upstream of the GAL4AD, transcriptional termination signals, yeast and bacterial origins of replication, yeast-specific promoter for LEU2, and the bacterial promoter for  $\beta$ -lactamase. See Section 2.4.1.2 and Table 2.8 for further details on the pGADT7 plasmids used in this study.

FIG. 2.5

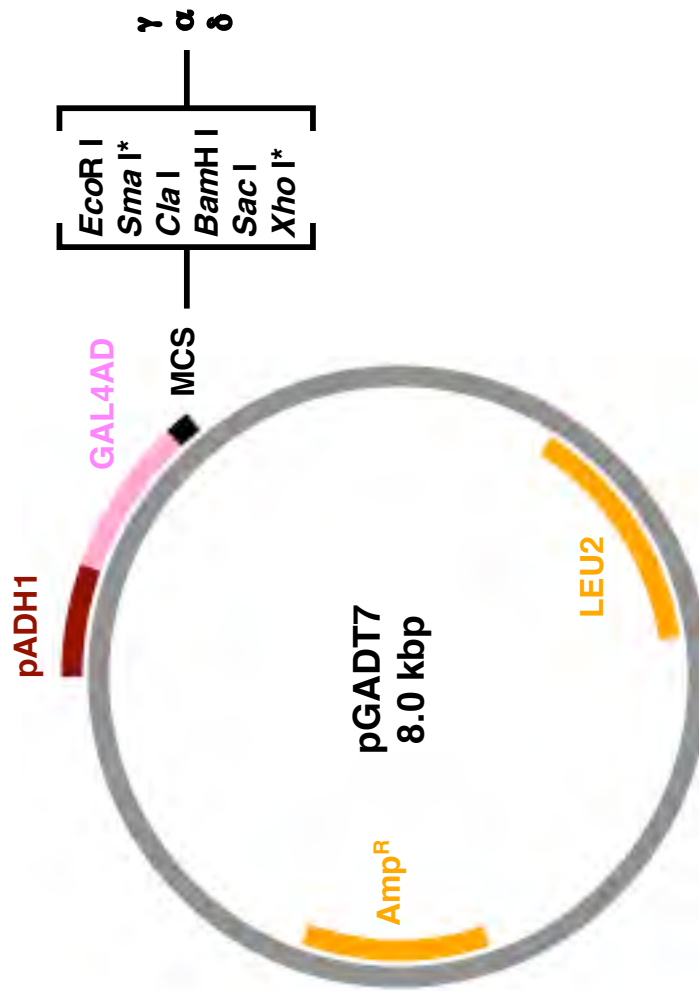


### FIG. 2.6: pAD plasmid map

The pAD expression vector has two independent promoters, each of which has its own multiple cloning site (MCS). In the first expression cassette, the constitutive alcohol dehydrogenase 1 promoter (**pADH1**) is upstream of the coding sequence for the GAL4 Activation Domain (**GAL4AD**) and **MCS1**. The open reading frame of the human **CD4** cytoplasmic tail (**ct**) was subcloned into the EcoRI-Sall restriction sites (marked by asterisks) of MCS1, and expressed in yeast cells as the GAL4AD-CD4 ct fusion protein. In the second expression cassette, the methionine-sensitive MET25 promoter (**pMET25**) is upstream of MCS2. This MCS was either left **empty** or had the coding sequence for wild-type or mutant rat  $\alpha$ C-adaptin ( **$\alpha$ -adaptin**) inserted into it, using the NotI-BglII restriction sites. The  $\alpha$ -adaptin subunit was expressed in yeast cells as an unfused protein. The pAD plasmid also contains the leucine 2 (**LEU2**) gene for selection in yeast and the ampicillin-resistance (**Amp<sup>R</sup>**) gene  $\beta$ -lactamase for selection in bacteria. Not shown: nuclear localization signals upstream of the GAL4AD and MCS2, transcriptional termination signals, yeast and bacterial origins of replication, yeast-specific promoter for LEU2, and bacterial promoter for  $\beta$ -lactamase. See Section 2.4.1.3 and Table 2.8 for more information on the pAD plasmids used in this study.

FIG. 2.6

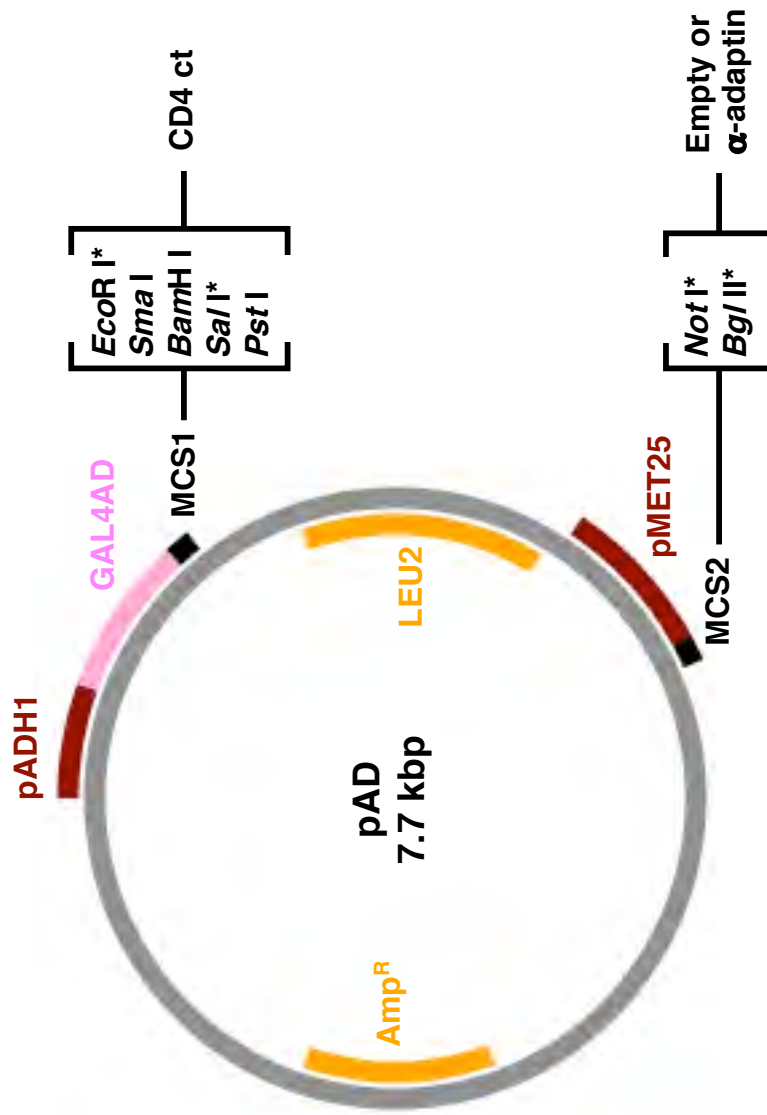


### FIG. 2.7: pAc plasmid map

The pAc expression vector contains a constitutive *Drosophila* actin-5C promoter (**pAc-5C**) upstream of a multiple cloning site (**MCS**) and a **V5** epitope tag. The coding sequence for full-length human **CD4** was subcloned into the EcoRI-XhoI restriction sites (marked by asterisks) with a stop codon, so that CD4 was expressed as an untagged protein in *Drosophila* cells. Open reading frames for *Drosophila*  $\mu$ 1-adaptin ( **$\mu$ 1**);  $\mu$ 2-adaptin ( **$\mu$ 2**);  $\mu$ 3-adaptin ( **$\mu$ 3**); Golgi-localized, gamma-ear-containing, ARF-binding protein (**GGA**); and clathrin light chain (**CLC**) were inserted between the EcoRI-ApaI restriction sites without stop codons, so that those proteins were expressed in *Drosophila* cells with C-terminal V5 tags. The pAc plasmid also has the ampicillin-resistance (**Amp<sup>R</sup>**) gene  $\beta$ -lactamase for selection and propagation in bacteria. Not shown: transcriptional termination signals, bacterial origin of replication, and the bacterial promoter for  $\beta$ -lactamase. See Section 2.5.1.1 and Table 2.8 for further details on the pAc plasmids used in this study.

FIG. 2.7

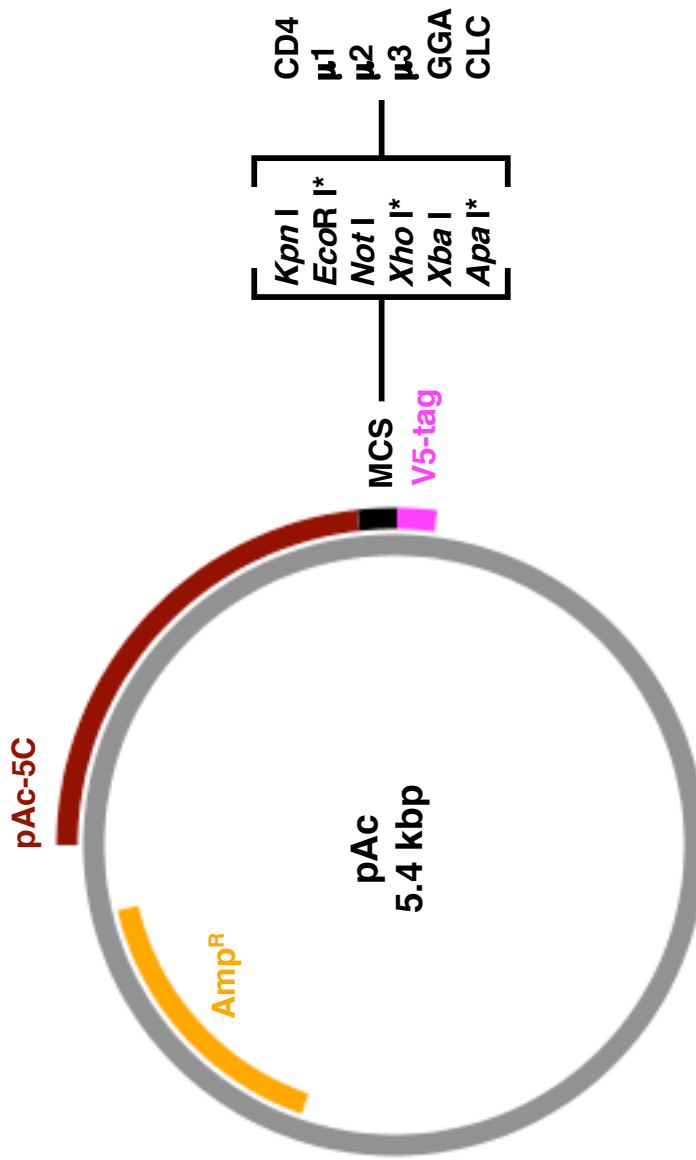


### FIG. 2.8: pMt plasmid map

The pMt expression vector contains an inducible *Drosophila* metallothionein promoter (**pMt**) upstream of a multiple cloning site (**MCS**). The coding sequences for wild-type and mutant HIV-1 and SIV Nef proteins were subcloned into the EcoRI-XhoI restriction sites (marked by asterisks). These proteins were expressed in *Drosophila* cells upon the addition of divalent copper cations (in the form of CuSO<sub>4</sub>) to the tissue culture media. The pMt plasmid also contains the ampicillin-resistance (**Amp<sup>R</sup>**) gene β-lactamase for selection and propagation in bacteria. Not shown: transcriptional termination signals, bacterial origin of replication, and the bacterial promoter for β-lactamase. See Section 2.5.1.2 and Table 2.8 for more information on the pMt plasmids used in this study.

FIG. 2.8

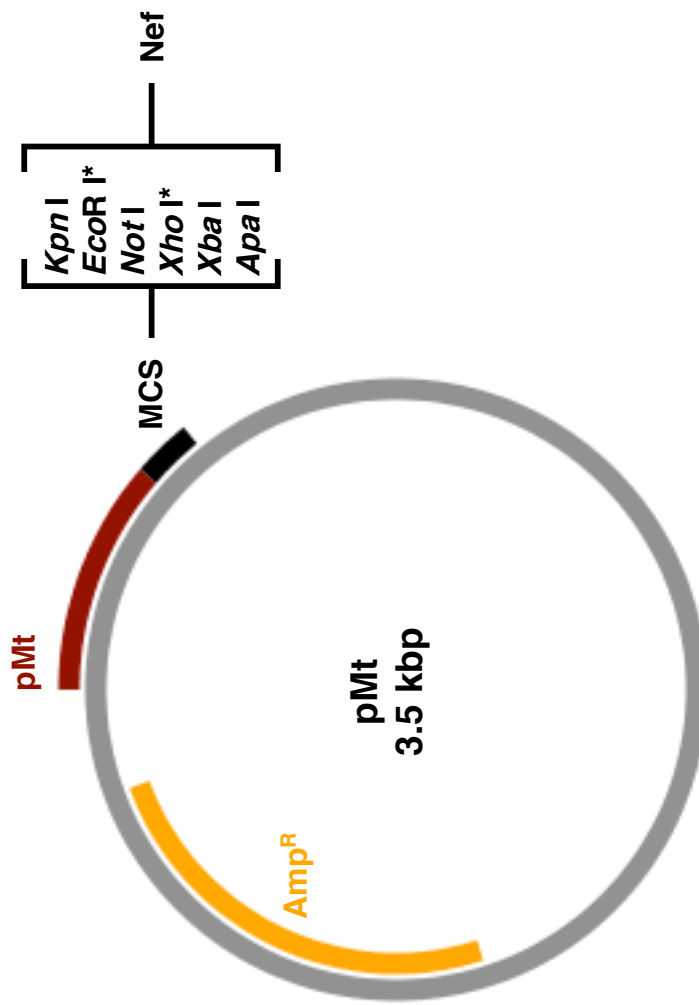


### FIG. 2.9: pCo-Blast plasmid map

The pCo-Blast plasmid has a constitutive *Drosophila* copia promoter (**pCo**) upstream of the blastocidin-resistance (**Blast<sup>R</sup>**) gene *bsr*. The *bsr* protein converts blastocidin, a nucleoside antibiotic that inhibits protein synthesis in eukaryotic cells, into a non-toxic compound. The pCo-Blast vector also contains the ampicillin-resistance (**Amp<sup>R</sup>**) gene  $\beta$ -lactamase for selection and propagation in bacteria. Not shown: transcriptional termination signals, bacterial origin of replication, and the bacterial promoter for  $\beta$ -lactamase. See Sections 2.5.1.3 and 2.5.2.3 for more information on how pCo-Blast was used in this study.

**FIG. 2.9**

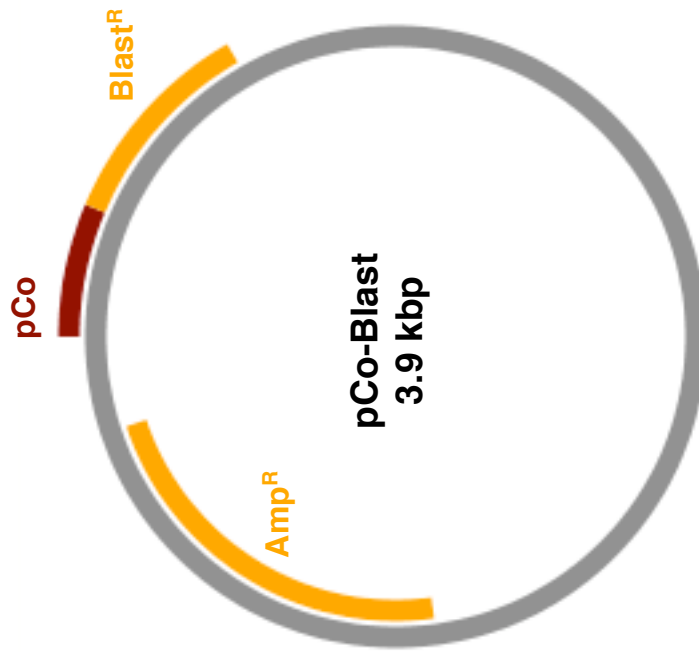


### FIG. 2.10: pCMV plasmid map

The pCMV expression vector has a constitutive human cytomegalovirus immediate-early enhancer-promoter (**pCMV**) upstream of a multiple cloning site (**MCS**). The coding sequence for human **CD4** was subcloned (by others) into the BamHI-EcoRI restriction sites (marked by asterisks) to generate pCMV.CD4 (kindly provided by Klaus Strebel).  $\beta$ -lactamase, an ampicillin-resistance (**Amp<sup>R</sup>**) gene, allows for selection and propagation of the pCMV vector in bacteria. Not shown: transcriptional termination signals, bacterial origin of replication, and the bacterial promoter for  $\beta$ -lactamase. See Section 2.6.1.1 for more information on the pCMV plasmid.

FIG. 2.10

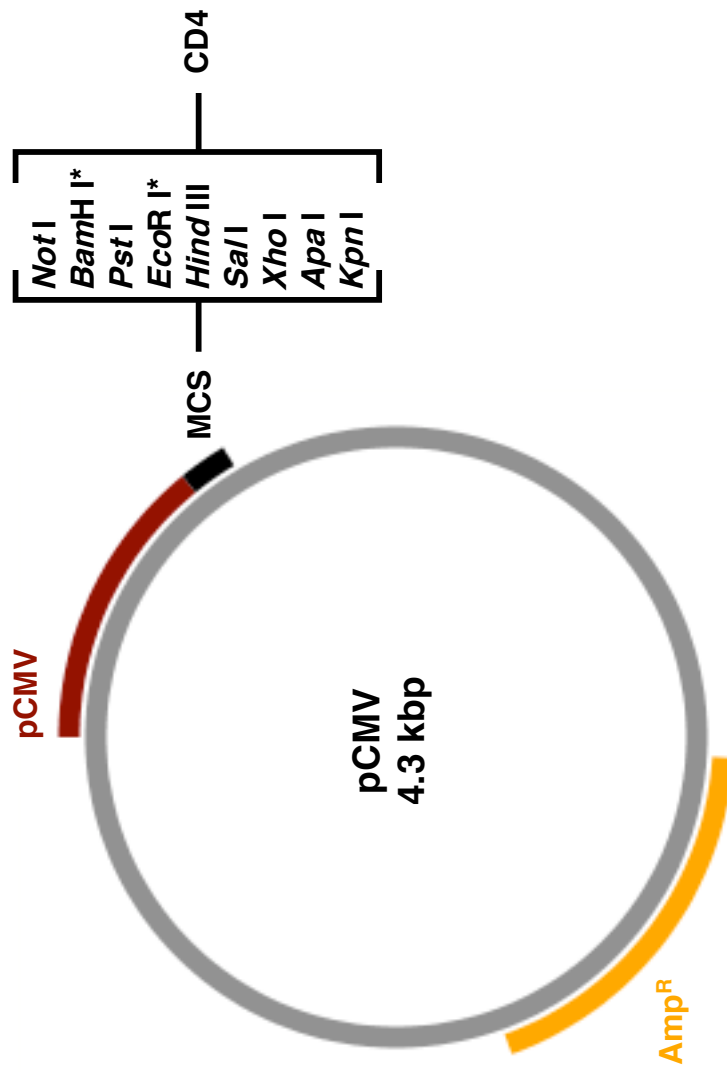


### FIG. 2.11: pCI plasmid map

The pCI expression vector contains a constitutive human cytomegalovirus immediate-early enhancer-promoter (**pCMV**) upstream of a multiple cloning site (**MCS**). Coding sequences for wild-type HIV-1 and SIV Nef proteins were subcloned (by others) into the EcoRI-SalI restriction sites (marked by asterisks) to create pCI.Nef<sub>NL4-3</sub>, pCI.Nef<sub>DH12-3</sub>, pCI.Nef<sub>248</sub>, and pCI.Nef<sub>SIVmac239</sub> (all kindly provided by Sundararajan Venkatesan). Mutant versions of pCI.Nef<sub>NL4-3</sub> were generated by the author. The ampicillin-resistance (**Amp<sup>R</sup>**) gene  $\beta$ -lactamase allows for selection of the pCI plasmids in bacteria. Not shown: transcriptional termination signals, bacterial origin of replication, and the bacterial promoter for  $\beta$ -lactamase. See Section 2.6.1.2 and Table 2.8 for further details on the pCI plasmids used in this study.

FIG. 2.11

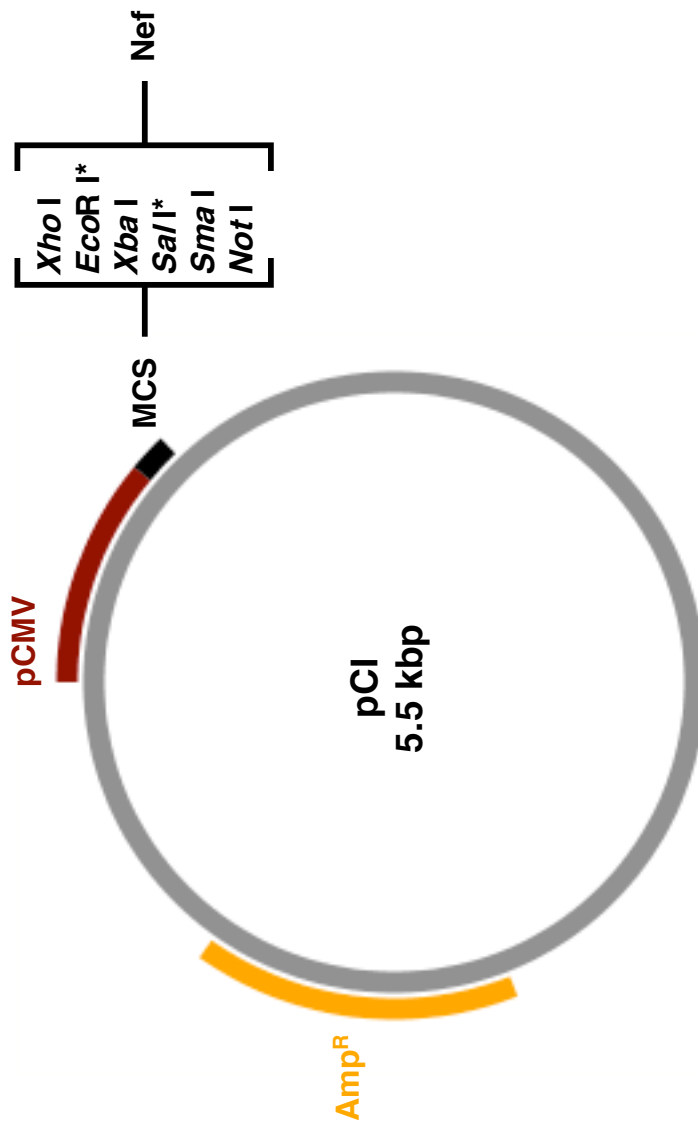


### FIG. 2.12: pIRES.GFP plasmid map

The pIRES.GFP expression vector contains a constitutive human cytomegalovirus immediate-early enhancer-promoter (**pCMV**) upstream of a multiple cloning site (**MCS**), an encephalomyocarditis internal ribosome entry site (**IRES**), and the coding sequence for enhanced Green Fluorescent Protein (**GFP**). The presence of the IRES sequence allows for the independent translation of a particular gene (cloned into the MCS) and GFP from the same bicistronic mRNA transcript. The open reading frames (ORFs) of wild-type and mutant versions of HIV-1 and SIV **Nef** proteins were subcloned into the EcoRI-SalI restriction sites (marked by asterisks), while the ORFs of wild-type and mutant versions  **$\alpha$ R-V5** (an siRNA-resistant version of  $\alpha$ C-adaptin with a C-terminal V5 epitope tag) were subcloned into the SalI-BamHI restriction sites (also marked by asterisks). The pIRES.GFP plasmid also contains the kanamycin-resistance (**Kan<sup>R</sup>**) gene nptII for selection and propagation in bacteria. Not shown: transcriptional termination signals, bacterial origin of replication, and the bacterial promoter for nptII. See Section 2.6.1.3, Section 2.6.3.5, and Table 2.8 for more information on the pIRES.GFP plasmids used in this study.

FIG. 2.12

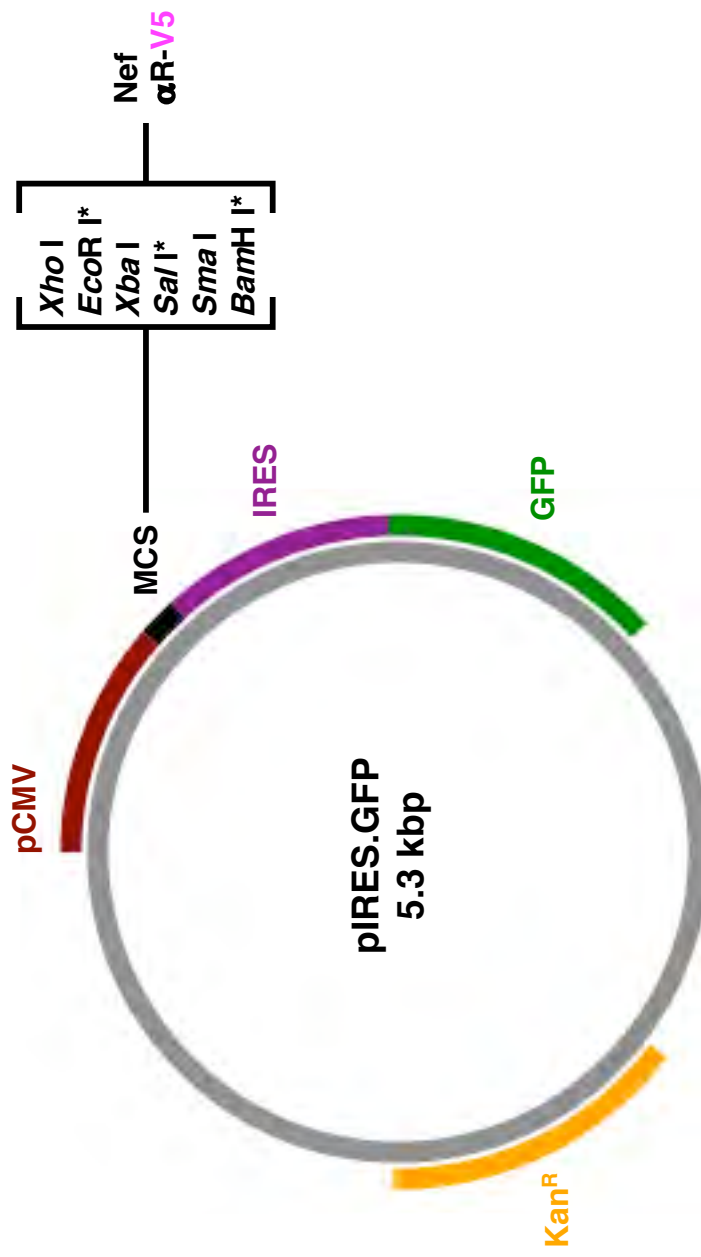


**Table 2.1: PCR reagents.** For each reaction, the following reagents were combined to yield a total volume of 50  $\mu\text{L}$ . See Table 2.9 for more further information on the individual forward and reverse primers.

Reagent	Initial Conc.	Volume	Final Conc.
H <sub>2</sub> O	N/A	32.5 $\mu\text{L}$	N/A
HF PCR Buffer	5X	10.0 $\mu\text{L}$	1X
dNTPs	10 mM	1.0 $\mu\text{L}$	200 $\mu\text{M}$
Forward Primer	10 $\mu\text{M}$	2.5 $\mu\text{L}$	0.5 $\mu\text{M}$
Reverse Primer	10 $\mu\text{M}$	2.5 $\mu\text{L}$	0.5 $\mu\text{M}$
DNA Template	100 ng/ $\mu\text{L}$	1.0 $\mu\text{L}$	2 ng/ $\mu\text{L}$
Phusion DNA Polymerase	2 U/ $\mu\text{L}$	0.5 $\mu\text{L}$	0.02 U/ $\mu\text{L}$

**Table 2.2: PCR thermal cycling conditions.** The temperature for the annealing step was generally set to 2°C below the calculated primer melting temperature ( $T_m$ ), and the duration of the extension step was set to 1.0 min per 1.0 kbp of PCR product. The remaining temperatures and times remained constant for all reactions.

Cycle step	Temperature	Time	Cycles
Initial denaturation	95°C	1.0 min	1
Denaturation	95°C	0.5 min	30
Annealing	55-64°C	0.5 min	
Extension	72°C	1.0 min per kbp	
Final Extension	72°C	10.0 min	1

**Table 2.3: Ligation reagents.** For each ligation reaction, the following reagents were combined to yield a total volume of 20  $\mu\text{L}$ .

Reagent	Initial Conc.	Volume	Final Conc.
H <sub>2</sub> O	N/A	13.0 $\mu\text{L}$	N/A
T4 DNA Ligase Buffer	10X	2.0 $\mu\text{L}$	1X
DNA insert	20 ng/ $\mu\text{L}$	3.0 $\mu\text{L}$	3 ng/ $\mu\text{L}$
DNA vector	20 ng/ $\mu\text{L}$	1.0 $\mu\text{L}$	1 ng/ $\mu\text{L}$
T4 DNA Ligase	400 U/ $\mu\text{L}$	1.0 $\mu\text{L}$	20 U/ $\mu\text{L}$

**Table 2.4: SDM reagents.** For each mutagenesis reaction, the following reagents were combined to yield a total volume of 50  $\mu\text{L}$ . See Table 2.9 for more information on the individual forward and reverse primers.

Reagent	Initial Conc.	Volume	Final Conc.
H <sub>2</sub> O	N/A	37.0 $\mu\text{L}$	N/A
SDM Buffer	10X	5.0 $\mu\text{L}$	1X
dNTPs	10 mM	1.0 $\mu\text{L}$	200 $\mu\text{M}$
Forward Primer	10 $\mu\text{M}$	2.5 $\mu\text{L}$	0.5 $\mu\text{M}$
Reverse Primer	10 $\mu\text{M}$	2.5 $\mu\text{L}$	0.5 $\mu\text{M}$
DNA Template	100 ng/ $\mu\text{L}$	1.0 $\mu\text{L}$	2 ng/ $\mu\text{L}$
Pfu Ultra DNA Polymerase	2.5 U/ $\mu\text{L}$	1.0 $\mu\text{L}$	0.05 U/ $\mu\text{L}$

**Table 2.5: SDM thermal cycling conditions.** The following temperatures, times, and cycles were used for each mutagenesis reaction.

Cycle step	Temperature	Time	Cycles
Initial denaturation	95°C	1.0 min	1
Denaturation	95°C	0.5 min	18
Annealing	55°C	0.5 min	
Extension	68°C	12.0 min	
Final Extension	68°C	12.0 min	1

**Table 2.6: Combinations of DNA plasmids used to transfect HeLa cells following siRNA-mediated protein depletion of  $\mu$ 1,  $\mu$ 2, and  $\mu$ 3.** HeLa cells were treated with 100 nM of the siRNA duplex shown below on days 1 and 4 of the knockdown assay. On day 5, the cells were transfected with 0.3  $\mu$ g of DNA plasmid 1 and 0.3  $\mu$ g of DNA plasmid 2 (if applicable). On day 6, the siRNA-treated and DNA-transfected cells were prepared for flow cytometric and immunoblot analysis. See Section 2.5.3.4 for further detail.

Row	siRNA	DNA 1	DNA 2
1	siCONTROL 1	pIRES.GFP	None
2	siCONTROL 1	pNef <sub>NL4-3</sub> .IRES.GFP	pCMV.CD4
3	siCONTROL 1	pNef <sub>NL4-3</sub> LL164,165AA.IRES.GFP	pCMV.CD4
4	$\mu$ 1A-adaptin	pIRES.GFP	None
5	$\mu$ 1A-adaptin	pNef <sub>NL4-3</sub> .IRES.GFP	pCMV.CD4
6	$\mu$ 1A-adaptin	pNef <sub>NL4-3</sub> LL164,165AA.IRES.GFP	pCMV.CD4
7	$\mu$ 2-adaptin	pIRES.GFP	None
8	$\mu$ 2-adaptin	pNef <sub>NL4-3</sub> .IRES.GFP	pCMV.CD4
9	$\mu$ 2-adaptin	pNef <sub>NL4-3</sub> LL164,165AA.IRES.GFP	pCMV.CD4
10	$\mu$ 3A-adaptin	pIRES.GFP	None
11	$\mu$ 3A-adaptin	pNef <sub>NL4-3</sub> .IRES.GFP	pCMV.CD4
12	$\mu$ 3A-adaptin	pNef <sub>NL4-3</sub> LL164,165AA.IRES.GFP	pCMV.CD4

**Table 2.7: Combinations of siRNA duplexes and DNA plasmids used to transfect HeLa cells for the  $\alpha$ -adaptin knockdown and rescue assays.** On day 1 of the assay, HeLa cells were either left untreated or treated with 100 nM of the  $\alpha$ -adaptin siRNA duplex. On day 4, the cells were again either left untreated or treated with 100 nM of the  $\alpha$ -adaptin siRNA, and also transfected with 0.4  $\mu$ g of DNA plasmid 1, 0.3  $\mu$ g of DNA plasmid 2, and 0.3  $\mu$ g of DNA plasmid 3. On day 7, the transfected HeLa cells were prepared for flow cytometric and immunoblot analysis. See Sections 2.5.3.5 and 2.5.3.6 for further detail.

Row	siRNA	DNA 1	DNA 2	DNA 3
1	None	pIRES.GFP	pCI	pCMV.CD4
2	None	pIRES.GFP	pCI.Nef <sub>NL4-3</sub>	pCMV.CD4
3	$\alpha$ -adaptin	pIRES.GFP	pCI	pCMV.CD4
4	$\alpha$ -adaptin	pIRES.GFP	pCI.Nef <sub>NL4-3</sub>	pCMV.CD4
5	$\alpha$ -adaptin	p $\alpha$ R-V5.IRES.GFP	pCI	pCMV.CD4
6	$\alpha$ -adaptin	p $\alpha$ R-V5.IRES.GFP	pCI.Nef <sub>NL4-3</sub>	pCMV.CD4
7	$\alpha$ -adaptin	p $\alpha$ R-KREE-V5.IRES.GFP	pCI	pCMV.CD4
8	$\alpha$ -adaptin	p $\alpha$ R-KREE-V5.IRES.GFP	pCI.Nef <sub>NL4-3</sub>	pCMV.CD4

**Table 2.8: Plasmids used in this study.**

The following table provides a list of all plasmids used in this study, along with pertinent information as to how they were subcloned. From left to right, the columns in the Table indicate the plasmid number, the name of the plasmid, the proteins expressed from the plasmid, the restriction sites used to insert the protein coding sequences, the parental vectors from which the plasmid was subcloned, the primers used in the subcloning reaction (the numbers in this column correspond to the PCR and SDM primers described in Table 2.9). The plasmids are grouped according to their vector backbone (BB), given in the far right-hand column. The BBs are, in turn, listed in the same order as they appear in the text of the Materials and Methods, for ease of reference. Please refer to Figs. 2.1 - 2.12 for diagrams of the plasmids listed below.

Of the 217 plasmids used in this study, 191 were generated by the author, 9 were purchased from commercial vendors, and 17 were subcloned by others and kindly donated. Purchased vectors include: pGEX (GE Healthcare); pBridge, pGADT7, and pCMV (Clontech); pAc, pMt, pCo. Blast, and pIRES.GFP (Invitrogen); and pCI (Promega). Donated vectors include: pHis (Zygmunt Derewenda); pGEX. $\alpha$ C-ear and pGEX. $\beta$ 3-ear (Rafael Mattera); pGEX. $\epsilon$ -ear (William Smith); pST (Song Tan); pST.AP-2<sup>CORE</sup> (Jim Hurely); pBridge.Tyrosinase. $\sigma$ 1, pBridge.Tyrosinase. $\sigma$ 2, pBridge.Tyrosinase. $\sigma$ 3, pGADT7. $\alpha$  A131T, pGADT7. $\gamma$ , and pGADT7. $\delta$  (Katy Janvier); pCMV.CD4 (Klaus Strebel); pCI.Nef<sub>248</sub>, pCI.Nef<sub>HI12-3</sub>, pCI.Nef<sub>NI4-3</sub>, and pCI.Nef<sub>SIVmac239</sub> (Sundararajan Venkatesan).

**Table 2.8: Plasmids used in this study.**

#	Plasmid Name	Proteins Expressed	Restriction Sites	Subcloned From	Primers	BB
1	pHis	N/A	N/A	N/A	N/A	pHis
2	pHis.Nef	His <sub>6</sub> -Nef	BamHI-EcoRI	1, 192	11, 13	pHis
3	pHis.Nef.LL164,165AA	His <sub>6</sub> -Nef.LL164,165AA	BamHI-EcoRI	2	88, 89	
4	pHis.Nef.DD174,175AA	His <sub>6</sub> -Nef.DD174,175AA	BamHI-EcoRI	2	114, 115	
5	pGEX	GST	N/A	N/A	N/A	
6	pGEX.αC-ear	GST-αC-ear	EcoRI-XhoI	5	29, 30	pGEX
7	pGEX.β3-ear	GST-β3-ear	EcoRI-XhoI	5	38, 39	
8	pGEX.ε-ear	GST-ε-ear	EcoRI-XhoI	6	40, 41	
9	pST	N/A	N/A	N/A	N/A	
10	pST.AP-2 <sup>CORE</sup>	μ2-N	XbaI-BamHI	9	42, 43	pST
		αC-trunk-GST	EcoRI-HindIII		31, 32	
		σ2	SacI-KpnI		47, 49	
		His <sub>6</sub> -β2-trunk	BspEI-MluI		36, 37	
11	pST.AP-2 <sup>CORE</sup> α KR297,340EE	μ2-N	XbaI-BamHI	10	220, 221 232, 233	pBridge
		αC-trunk-KR297,340EE-GST	EcoRI-HindIII			
		σ2	SacI-KpnI			
		His <sub>6</sub> -β2-trunk	BspEI-MluI			
12	pBridge	GAL4BD	N/A	N/A	N/A	pBridge
13	pBridge.Nef	GAL4BD-Nef	EcoRI-SalI	12, 192	N/A	
14	pBridge.Nef.σ1	GAL4BD-Nef	EcoRI-SalI	13	44, 45	
		σ1	NotI-BglIII			
15	pBridge.Nef.σ2	GAL4BD-Nef	EcoRI-SalI	13	46, 48	
		σ2	NotI-BglIII			

**Table 2.8: Plasmids used in this study, continued.**

#	Plasmid Name	Proteins Expressed	Restriction Sites	Subcloned From	Primers	BB
16	pBridge.Nef.σ3	GAL4BD-Nef σ3	EcoRI-Sall NotI-BglIII	13	50, 51	pBridge
17	pBridge.Nef G2A.σ2	GAL4BD-Nef G2A σ2	EcoRI-Sall NotI-BglIII	15	54, 55	
18	pBridge.Nef WL57,58AA.σ2	GAL4BD-Nef WL57,58AA σ2	EcoRI-Sall NotI-BglIII	15	56, 57	
19	pBridge.Nef EEEEE62-65AAAA.σ2	GAL4BD-Nef EEEEE62-65AAAA σ2	EcoRI-Sall NotI-BglIII	15	58, 59	
20	pBridge.Nef PP72,75AA.σ2	GAL4BD-Nef PP72,75AA σ2	EcoRI-Sall NotI-BglIII	15	60, 61	
21	pBridge.Nef E154A.σ2	GAL4BD-Nef E154A σ2	EcoRI-Sall NotI-BglIII	15	62, 63	
22	pBridge.Nef E155A.σ2	GAL4BD-Nef E155A σ2	EcoRI-Sall NotI-BglIII	15	64, 65	
23	pBridge.Nef N157A.σ2	GAL4BD-Nef N157A σ2	EcoRI-Sall NotI-BglIII	15	66, 67	
24	pBridge.Nef K158A.σ2	GAL4BD-Nef K158A σ2	EcoRI-Sall NotI-BglIII	15	68, 69	
25	pBridge.Nef G159A.σ2	GAL4BD-Nef G159A σ2	EcoRI-Sall NotI-BglIII	15	70, 71	
26	pBridge.Nef E160A.σ2	GAL4BD-Nef E160A σ2	EcoRI-Sall NotI-BglIII	15	72, 73	

**Table 2.8: Plasmids used in this study, continued.**

#	Plasmid Name	Proteins Expressed	Restriction Sites	Subcloned From	Primers	BB
27	pBridge.Nef E160D.σ1	GAL4BD-Nef E160D σ1	EcoRI-Sall NotI-BglIII	14	74, 75	pBridge
28	pBridge.Nef E160D.σ2	GAL4BD-Nef E160D σ2	EcoRI-Sall NotI-BglIII	15	74, 75	
29	pBridge.Nef E160D.σ3	GAL4BD-Nef E160D σ3	EcoRI-Sall NotI-BglIII	16	74, 75	
30	pBridge.Nef E160K.σ2	GAL4BD-Nef E160K σ2	EcoRI-Sall NotI-BglIII	15	76, 77	
31	pBridge.Nef N161A.σ2	GAL4BD-Nef N161A σ2	EcoRI-Sall NotI-BglIII	15	78, 79	
32	pBridge.Nef NTS161-163RQP.σ2	GAL4BD-Nef NTS161-163RQP σ2	EcoRI-Sall NotI-BglIII	15	80, 81	
33	pBridge.Nef NTS161-163/DD174,175AA.σ2	GAL4BD-Nef NTS161-163RQP/DD174,175AA σ2	EcoRI-Sall NotI-BglIII	32	114, 115	
34	pBridge.Nef T162A.σ2	GAL4BD-Nef T162A σ2	EcoRI-Sall NotI-BglIII	15	82, 83	
35	pBridge.Nef S163A.σ2	GAL4BD-Nef S163A σ2	EcoRI-Sall NotI-BglIII	15	84, 85	
36	pBridge.Nef L164A.σ2	GAL4BD-Nef L164A σ2	EcoRI-Sall NotI-BglIII	15	86, 87	
37	pBridge.Nef LL164,165AA.σ1	GAL4BD-Nef LL164,165AA σ1	EcoRI-Sall NotI-BglIII	14	88, 89	

**Table 2.8: Plasmids used in this study, continued.**

#	Plasmid Name	Proteins Expressed	Restriction Sites	Subcloned From	Primers	BB
38	pBridge.Nef LL164,165AA.σ2	GAL4BD-Nef LL164,165AA σ2	EcoRI-Sall NotI-BgIII	15	88, 89	pBridge
39	pBridge.Nef LL164,165AA.σ3	GAL4BD-Nef LL164,165AA σ3	EcoRI-Sall NotI-BgIII	16	88, 89	
40	pBridge.Nef L165A.σ2	GAL4BD-Nef L165A σ2	EcoRI-Sall NotI-BgIII	15	90, 91	
41	pBridge.Nef H166A.σ2	GAL4BD-Nef H166A σ2	EcoRI-Sall NotI-BgIII	15	92, 93	
42	pBridge.Nef P167A.σ2	GAL4BD-Nef P167A σ2	EcoRI-Sall NotI-BgIII	15	94, 95	
43	pBridge.Nef V168A.σ2	GAL4BD-Nef V168A σ2	EcoRI-Sall NotI-BgIII	15	96, 97	
44	pBridge.Nef S169A.σ2	GAL4BD-Nef S169A σ2	EcoRI-Sall NotI-BgIII	15	98, 99	
45	pBridge.Nef L170A.σ2	GAL4BD-Nef L170A σ2	EcoRI-Sall NotI-BgIII	15	100, 101	
46	pBridge.Nef H171A.σ2	GAL4BD-Nef H171A σ2	EcoRI-Sall NotI-BgIII	15	102, 103	
47	pBridge.Nef G172A.σ2	GAL4BD-Nef G172A σ2	EcoRI-Sall NotI-BgIII	15	104, 105	
48	pBridge.Nef M173A.σ2	GAL4BD-Nef M173A σ2	EcoRI-Sall NotI-BgIII	15	106, 107	

**Table 2.8: Plasmids used in this study, continued.**

#	Plasmid Name	Proteins Expressed	Restriction Sites	Subcloned From	Primers	BB
49	pBridge.Nef D174A.σ1	GAL4BD-Nef D174A σ1	EcoRI-Sall NotI-BglIII	14	108, 109	pBridge
50	pBridge.Nef D174A.σ2	GAL4BD-Nef D174A σ2	EcoRI-Sall NotI-BglIII	15	108, 109	
51	pBridge.Nef D174A.σ3	GAL4BD-Nef D174A σ3	EcoRI-Sall NotI-BglIII	16	108, 109	
52	pBridge.Nef D174E.σ1	GAL4BD-Nef D174E σ1	EcoRI-Sall NotI-BglIII	14	110, 111	
53	pBridge.Nef D174E.σ2	GAL4BD-Nef D174E σ2	EcoRI-Sall NotI-BglIII	15	110, 111	
54	pBridge.Nef D174E.σ3	GAL4BD-Nef D174E σ3	EcoRI-Sall NotI-BglIII	16	110, 111	
55	pBridge.Nef D174N.σ1	GAL4BD-Nef D174N σ1	EcoRI-Sall NotI-BglIII	14	112, 113	
56	pBridge.Nef D174N.σ2	GAL4BD-Nef D174N σ2	EcoRI-Sall NotI-BglIII	15	112, 113	
57	pBridge.Nef D174N.σ3	GAL4BD-Nef D174N σ3	EcoRI-Sall NotI-BglIII	16	112, 113	
58	pBridge.Nef DD174,175AA.σ1	GAL4BD-Nef DD174,175AA σ1	EcoRI-Sall NotI-BglIII	14	114, 115	
59	pBridge.Nef DD174,175AA.σ2	GAL4BD-Nef DD174,175AA σ2	EcoRI-Sall NotI-BglIII	15	114, 115	

**Table 2.8: Plasmids used in this study, continued.**

#	Plasmid Name	Proteins Expressed	Restriction Sites	Subcloned From	Primers	BB
60	pBridge.Nef DD174,175AA.σ3	GAL4BD-Nef DD174,175AA σ3	EcoRI-Sall NotI-BglIII	16	114, 115	pBridge
61	pBridge.Nef D175A.σ1	GAL4BD-Nef D175A σ1	EcoRI-Sall NotI-BglIII	14	116, 117	
62	pBridge.Nef D175A.σ2	GAL4BD-Nef D175A σ2	EcoRI-Sall NotI-BglIII	15	116, 117	
63	pBridge.Nef D175A.σ3	GAL4BD-Nef D175A σ3	EcoRI-Sall NotI-BglIII	16	116, 117	
64	pBridge.Nef D175E.σ1	GAL4BD-Nef D175E σ1	EcoRI-Sall NotI-BglIII	14	118, 119	
65	pBridge.Nef D175E.σ2	GAL4BD-Nef D175E σ2	EcoRI-Sall NotI-BglIII	15	118, 119	
66	pBridge.Nef D175E.σ3	GAL4BD-Nef D175E σ3	EcoRI-Sall NotI-BglIII	16	118, 119	
67	pBridge.Nef D175N.σ1	GAL4BD-Nef D175N σ1	EcoRI-Sall NotI-BglIII	14	120, 121	
68	pBridge.Nef D175N.σ2	GAL4BD-Nef D175N σ2	EcoRI-Sall NotI-BglIII	15	120, 121	
69	pBridge.Nef D175N.σ3	GAL4BD-Nef D175N σ3	EcoRI-Sall NotI-BglIII	16	120, 121	
70	pBridge.Nef P176A.σ2	GAL4BD-Nef P176A σ2	EcoRI-Sall NotI-BglIII	15	122, 123	

**Table 2.8: Plasmids used in this study, continued.**

#	Plasmid Name	Proteins Expressed	Restriction Sites	Subcloned From	Primers	BB
71	pBridge.Nef E177A.σ2	GAL4BD-Nef E177A σ2	EcoRI-Sall NotI-BgIII	15	124, 125	pBridge
72	pBridge.Nef R178A.σ2	GAL4BD-Nef R178A σ2	EcoRI-Sall NotI-BgIII	15	126, 127	
73	pBridge.Nef E179A.σ2	GAL4BD-Nef E179A σ2	EcoRI-Sall NotI-BgIII	15	128, 129	
74	pBridge.Nef V180A.σ2	GAL4BD-Nef V180A σ2	EcoRI-Sall NotI-BgIII	15	130, 131	
75	pBridge.Nef.σ2 R3D	GAL4BD-Nef σ2 R3D	EcoRI-Sall NotI-BgIII	15	246, 247	
76	pBridge.Nef.σ2 K13E	GAL4BD-Nef σ2 K13E	EcoRI-Sall NotI-BgIII	15	248, 249	
77	pBridge.Nef.σ2 R15D	GAL4BD-Nef σ2 R15D	EcoRI-Sall NotI-BgIII	15	250, 251	
78	pBridge.Nef.σ2 K18E	GAL4BD-Nef σ2 K18E	EcoRI-Sall NotI-BgIII	15	252, 253	
79	pBridge.Nef.σ2 R53E	GAL4BD-Nef σ2 R53E	EcoRI-Sall NotI-BgIII	15	254, 255	
80	pBridge.Nef.σ2 K56E	GAL4BD-Nef σ2 K56E	EcoRI-Sall NotI-BgIII	15	256, 257	
81	pBridge.Nef.σ2 R60E	GAL4BD-Nef σ2 R60E	EcoRI-Sall NotI-BgIII	15	258, 259	

**Table 2.8: Plasmids used in this study, continued.**

#	Plasmid Name	Proteins Expressed	Restriction Sites	Subcloned From	Primers	BB
82	pBridge.Nef.σ2 R61D	GAL4BD-Nef σ2 R61D	EcoRI-Sall NotI-BgIII	15	260, 261	pBridge
83	pBridge.Nef.σ2 A63D	GAL4BD-Nef σ2 A63D	EcoRI-Sall NotI-BgIII	15	262, 263	
84	pBridge.Nef.σ2 V88D	GAL4BD-Nef σ2 V88D	EcoRI-Sall NotI-BgIII	15	264, 265	
85	pBridge.Nef.σ2 E89A	GAL4BD-Nef σ2 E89A	EcoRI-Sall NotI-BgIII	15	266, 267	
86	pBridge.Nef.σ2 N92A	GAL4BD-Nef σ2 N92A	EcoRI-Sall NotI-BgIII	15	268, 269	
87	pBridge.Nef.σ2 E100A	GAL4BD-Nef σ2 E100A	EcoRI-Sall NotI-BgIII	15	270, 271	
88	pBridge.Nef.σ2 L101A	GAL4BD-Nef σ2 L101A	EcoRI-Sall NotI-BgIII	15	272, 273	
89	pBridge.Nef.σ2 D102A	GAL4BD-Nef σ2 D102A	EcoRI-Sall NotI-BgIII	15	274, 275	
90	pBridge.Nef.σ2 L103S	GAL4BD-Nef σ2 L103S	EcoRI-Sall NotI-BgIII	15	276, 277	
91	pBridge.Nef.σ2 F105A	GAL4BD-Nef σ2 F105A	EcoRI-Sall NotI-BgIII	15	278, 279	
92	pBridge.Nef.σ2 N106A	GAL4BD-Nef σ2 N106A	EcoRI-Sall NotI-BgIII	15	280, 281	

**Table 2.8: Plasmids used in this study, continued.**

#	Plasmid Name	Proteins Expressed	Restriction Sites	Subcloned From	Primers	BB
93	pBridge.Nef.σ2 RK124,130EE	GAL4BD-Nef σ2 RK124,130EE	EcoRI-Sall NotI-BgIII	15	282, 283	pBridge
94	pBridge.Tyrosinase.σ1	GAL4BD-Tyrosinase σ1	EcoRI-PstI NotI-BgIII	12	N/A	
95	pBridge.Tyrosinase.σ2	GAL4BD-Tyrosinase σ2	EcoRI-PstI NotI-BgIII	12	N/A	
96	pBridge.Tyrosinase.σ3	GAL4BD-Tyrosinase σ3	EcoRI-PstI NotI-BgIII	12	N/A	
97	pBridge.Tyrosinase E513K.σ2	GAL4BD-Tyrosinase E513K ct σ2	EcoRI-PstI NotI-BgIII	95	132, 133	
98	pBridge.Tyrosinase RQP514-516NTS.σ2	GAL4BD-Tyrosinase RQP514-515NTS ct σ2	EcoRI-PstI NotI-BgIII	95	134, 135	
99	pBridge.Tyrosinase LL517,518AA.σ2	GAL4BD-Tyrosinase LL517,518AA ct σ2	EcoRI-PstI NotI-BgIII	95	136, 137	
100	pBridge.Tyrosinase DD522,523AA.σ2	GAL4BD-Tyrosinase DD522,523AA ct σ2	EcoRI-PstI NotI-BgIII	95	138, 139	
101	pBridge.Tyrosinase.σ2 RK124,130EE	GAL4BD-Tyrosinase σ2 RK124,130EE	EcoRI-PstI NotI-BgIII	95	282, 283	
102	pGADT7	GAL4AD	N/A	N/A	N/A	
103	pGADT7.α	GAL4AD-α	SmaI-XhoI	125	182, 183	
104	pGADT7.α K6E	GAL4AD-α K6E	SmaI-XhoI	105	140, 141	
105	pGADT7.α GG7,9GG	GAL4AD-α GG7,9GG	SmaI-XhoI	103	142, 143	
106	pGADT7.α R11E	GAL4AD-α R11E	SmaI-XhoI	103	144, 145	

**Table 2.8: Plasmids used in this study, continued.**

#	Plasmid Name	Proteins Expressed	Restriction Sites	Subcloned From	Primers	BB
107	pGADT7.α L13A	GAL4AD-α L13A	SmaI-XhoI	103	146, 147	pGADT7
108	pGADT7.α R21D	GAL4AD-α R21D	SmaI-XhoI	103	148, 149	
109	pGADT7.α K24E	GAL4AD-α K24E	SmaI-XhoI	103	150, 151	
110	pGADT7.α K26E	GAL4AD-α K26E	SmaI-XhoI	103	152, 153	
111	pGADT7.α K31E	GAL4AD-α K31E	SmaI-XhoI	103	154, 155	
112	pGADT7.α R32E	GAL4AD-α R32E	SmaI-XhoI	103	156, 157	
113	pGADT7.α R41E	GAL4AD-α R41E	SmaI-XhoI	103	158, 159	
114	pGADT7.α K43E	GAL4AD-α K43E	SmaI-XhoI	103	160, 161	
115	pGADT7.α K45E	GAL4AD-α K45E	SmaI-XhoI	103	162, 163	
116	pGADT7.α K48E	GAL4AD-α K48E	SmaI-XhoI	103	164, 165	
117	pGADT7.α K55E	GAL4AD-α K55E	SmaI-XhoI	103	166, 167	
118	pGADT7.α K56E	GAL4AD-α K56E	SmaI-XhoI	103	168, 169	
119	pGADT7.α K61E	GAL4AD-α K61E	SmaI-XhoI	103	170, 171	
120	pGADT7.α R87E	GAL4AD-α R87E	SmaI-XhoI	103	172, 173	
121	pGADT7.α K91E	GAL4AD-α K91E	SmaI-XhoI	103	174, 175	
122	pGADT7.α R110E	GAL4AD-α R110E	SmaI-XhoI	103	176, 177	
123	pGADT7.α K117E	GAL4AD-α K117E	SmaI-XhoI	103	178, 179	
124	pGADT7.α R123D	GAL4AD-α R123D	SmaI-XhoI	103	180, 181	
125	pGADT7.α A131T	GAL4AD-α A131T	SmaI-XhoI	102	N/A	
126	pGADT7.α R141D	GAL4AD-α R141D	SmaI-XhoI	103	184, 185	
127	pGADT7.α K165E	GAL4AD-α K165E	SmaI-XhoI	103	186, 187	
128	pGADT7.α R174D	GAL4AD-α R174D	SmaI-XhoI	103	188, 189	
129	pGADT7.α R177E	GAL4AD-α R177E	SmaI-XhoI	103	190, 191	

**Table 2.8: Plasmids used in this study, continued.**

#	Plasmid Name	Proteins Expressed	Restriction Sites	Subcloned From	Primers	BB
130	pGADT7.α R191D	GAL4AD-α R191D	SmaI-XhoI	103	192, 193	pGADT7
131	pGADT7.α K217E	GAL4AD-α K217E	SmaI-XhoI	103	194, 195	
132	pGADT7.α K223E	GAL4AD-α K223E	SmaI-XhoI	103	196, 197	
133	pGADT7.α R232E	GAL4AD-α R232E	SmaI-XhoI	103	198, 199	
134	pGADT7.α K235E	GAL4AD-α K235E	SmaI-XhoI	103	200, 201	
135	pGADT7.α K260E	GAL4AD-α K260E	SmaI-XhoI	103	202, 203	
136	pGADT7.α R263E	GAL4AD-α R263E	SmaI-XhoI	103	204, 205	
137	pGADT7.α R276E	GAL4AD-α R276E	SmaI-XhoI	103	206, 207	
138	pGADT7.α K289E	GAL4AD-α K289E	SmaI-XhoI	103	208, 209	
139	pGADT7.α K295A	GAL4AD-α K295A	SmaI-XhoI	103	210, 211	
140	pGADT7.α K295E	GAL4AD-α K295E	SmaI-XhoI	103	212, 213	
141	pGADT7.α KKK295,297,298AAA	GAL4AD-α KKK295,297,298AAA	SmaI-XhoI	142	214, 215	
142	pGADT7.α KKK295,297,298EEE	GAL4AD-α KKK295,297,298EEE	SmaI-XhoI	103	216, 217	
143	pGADT7.α KKKR295,297,298,340AAAA	GAL4AD-α KKKR295,297,298,340AAAA	SmaI-XhoI	153	214, 215	
144	pGADT7.α KKKR295,297,298,340EEEEE	GAL4AD-α KKKR295,297,298,340EEEEE	SmaI-XhoI	154	216, 217	
145	pGADT7.α K297A	GAL4AD-α K297A	SmaI-XhoI	103	218, 219	
146	pGADT7.α K297E	GAL4AD-α K297E	SmaI-XhoI	103	220, 221	
147	pGADT7.α KR297,340AA	GAL4AD-α KR297,340AA	SmaI-XhoI	153	218, 219	
148	pGADT7.α KR297,340EE	GAL4AD-α KR297,340EE	SmaI-XhoI	154	220, 221	
149	pGADT7.α K298A	GAL4AD-α K298A	SmaI-XhoI	103	222, 223	
150	pGADT7.α K298E	GAL4AD-α K298E	SmaI-XhoI	103	224, 225	
151	pGADT7.α K305E	GAL4AD-α K305E	SmaI-XhoI	103	226, 227	
152	pGADT7.α R328D	GAL4AD-α R328D	SmaI-XhoI	103	228, 229	

**Table 2.8: Plasmids used in this study, continued.**

#	Plasmid Name	Proteins Expressed	Restriction Sites	Subcloned From	Primers	BB
153	pGADT7.α R340A	GAL4AD-α R340A	SmaI-XhoI	103	230, 231	pGADT7
154	pGADT7.α R340E	GAL4AD-α R340E	SmaI-XhoI	103	232, 233	
155	pGADT7.α R345D	GAL4AD-α R345D	SmaI-XhoI	103	234, 235	
156	pGADT7.α K366E	GAL4AD-α K366E	SmaI-XhoI	103	236, 237	
157	pGADT7.α R385E	GAL4AD-α R385E	SmaI-XhoI	103	238, 239	
158	pGADT7.α R387E	GAL4AD-α R387D	SmaI-XhoI	103	240, 241	
159	pGADT7.α R420E	GAL4AD-α R420E	SmaI-XhoI	103	242, 243	
160	pGADT7.αR	GAL4AD-αR	SmaI-XhoI	103	244, 245	
161	pGADT7.γ	GAL4AD-γ	SmaI-XhoI	102	N/A	
162	pGADT7.δ	GAL4AD-δ	SmaI-XhoI	102	N/A	
163	pAD	GAL4AD	N/A	pGAD424, 12	N/A	
164	pAD.CD4	GAL4AD-CD4 ct	EcoRI-Sall	163	3, 4	
165	pAD.CD4.α	GAL4AD-CD4 ct α	EcoRI-Sall NotI-BglIII	103, 164	27, 28	
166	pAD.CD4.α KR297,340EE	GAL4AD-CD4 ct α KR297,340EE	EcoRI-Sall NotI-BglIII	148, 164	27, 28	pAc
167	pAc	N/A	N/A	N/A	N/A	
168	pAc.CD4	CD4	EcoRI-XhoI	167, 187	1, 2	
169	pAc.CD4 LL413,414AA	CD4 LL413,414AA	EcoRI-XhoI	168	52, 53	
170	pAc.μ1-V5	μ1-V5	EcoRI-Apal	167	17, 18	
171	pAc.μ2-V5	μ2-V5	EcoRI-Apal	167	19, 20	
172	pAc.μ3-V5	μ3-V5	EcoRI-Apal	167	21, 22	
173	pAc.CLC-V5	CLC-V5	EcoRI-Apal	167	23, 24	

**Table 2.8: Plasmids used in this study, continued.**

#	Plasmid Name	Proteins Expressed	Restriction Sites	Subcloned From	Primers	BB	
174	pAc.GGA-V5	GGA-V5	EcoRI-ApaI	167	25, 26	pAc	
175	pMt	N/A	N/A	N/A	N/A	pMt	
176	pMt.Nef <sub>248</sub>	248 Nef	EcoRI-XhoI	175, 200	5, 6		
177	pMt.Nef <sub>DH12-3</sub>	DH12-3 Nef	EcoRI-XhoI	175, 201	7, 8		
178	pMt.Nef <sub>NA7</sub>	NA7 Nef	EcoRI-XhoI	175, 202	9, 10		
179	pMt.Nef <sub>NL4-3</sub>	NL4-3 Nef	EcoRI-XhoI	175, 203	12, 14		
180	pMt.Nef <sub>NL4-3</sub> G2A	NL4-3 Nef G2A	EcoRI-XhoI	179	54, 55		
181	pMt.Nef <sub>NL4-3</sub> WL57,58AA	NL4-3 Nef WL57,58AA	EcoRI-XhoI	179	56, 57		
182	pMt.Nef <sub>NL4-3</sub> EEEE62-65AAAA	NL4-3 Nef EEEE62-65AAAA	EcoRI-XhoI	179	58, 59		
183	pMt.Nef <sub>NL4-3</sub> PP72,75AA	NL4-3 Nef PP72,75AA	EcoRI-XhoI	179	60, 61		
184	pMt.Nef <sub>NL4-3</sub> LL164,165AA	NL4-3 Nef LL164,165AA	EcoRI-XhoI	179	88, 89		
185	pMt.Nef <sub>SIVmac239</sub>	SIVmac239 Nef	EcoRI-XhoI	175, 215	15, 16		
186	pCo.Blast	bsr (blasticidin-resistance protein)	N/A	N/A	N/A		pCo
187	pCMV	N/A	N/A	N/A	N/A		pCMV
188	pCMV.CD4	CD4	BamHI-EcoRI	187	N/A		
189	pCI	N/A	N/A	N/A	N/A		pCI
190	pCI.Nef <sub>248</sub>	248 Nef	EcoRI-SalI	189	N/A		
191	pCI.Nef <sub>DH12-3</sub>	DH12-3 Nef	EcoRI-SalI	189	N/A		
192	pCI.Nef <sub>NL4-3</sub>	NL4-3 Nef	EcoRI-SalI	189	N/A		
193	pCI.Nef <sub>NL4-3</sub> E160D	NL4-3 Nef E160D	EcoRI-SalI	192	74, 75		
194	pCI.Nef <sub>NL4-3</sub> LL164,165AA	NL4-3 Nef LL164,165AA	EcoRI-SalI	192	88, 89		
195	pCI.Nef <sub>NL4-3</sub> D174E	NL4-3 Nef D174E	EcoRI-SalI	192	110, 111		
196	pCI.Nef <sub>NL4-3</sub> DD174,175AA	NL4-3 Nef DD174,175AA	EcoRI-SalI	192	114, 115		

**Table 2.8: Plasmids used in this study, continued.**

#	Plasmid Name	Proteins Expressed	Restriction Sites	Subcloned From	Primers	BB
197	pCI.Nef <sub>NL4-3</sub> D175E	NL4-3 Nef D175E	EcoRI-Sall	192	118, 119	pCI
198	pCI.Nef <sub>SIVmac239</sub>	SIVmac239 Nef	EcoRI-Sall	189	N/A	
199	pIRES.GFP	GFP	BstXI-NotI	N/A	N/A	
200	pNef <sub>248</sub> .IRES.GFP	248 Nef GFP	EcoRI-Sall BstXI-NotI	190, 199	N/A	
201	pNef <sub>DH12-3</sub> .IRES.GFP	DH12-3 Nef GFP	EcoRI-Sall BstXI-NotI	191, 199	N/A	
202	pNef <sub>NA7</sub> .IRES.GFP	NA7 Nef GFP	EcoRI-Sall BstXI-NotI	pCDNA.Nef <sub>NA7</sub> 199	N/A	
203	pNef <sub>NL4-3</sub> .IRES.GFP	NL4-3 Nef GFP	EcoRI-Sall BstXI-NotI	192, 199	N/A	
204	pNef <sub>NL4-3</sub> G2A.IRES.GFP	NL4-3 Nef G2A GFP	EcoRI-Sall BstXI-NotI	203	54, 55	
205	pNef <sub>NL4-3</sub> WL57,58AA.IRES.GFP	NL4-3 Nef WL57,58AA GFP	EcoRI-Sall BstXI-NotI	203	56, 57	
206	pNef <sub>NL4-3</sub> EEEE62-65AAAA.IRES.GFP	NL4-3 Nef EEEE62-65AAAA GFP	EcoRI-Sall BstXI-NotI	203	58, 59	
207	pNef <sub>NL4-3</sub> PP72,75AA.IRES.GFP	NL4-3 Nef PP72,75AA GFP	EcoRI-Sall BstXI-NotI	203	60, 61	
208	pNef <sub>NL4-3</sub> E160D.IRES.GFP	NL4-3 Nef E160D GFP	EcoRI-Sall BstXI-NotI	203	74, 75	
209	pNef <sub>NL4-3</sub> LL164,165AA.IRES.GFP	NL4-3 Nef LL164,165AA GFP	EcoRI-Sall BstXI-NotI	203	88, 89	

**Table 2.8: Plasmids used in this study, continued.**

#	Plasmid Name	Proteins Expressed	Restriction Sites	Subcloned From	Primers	BB
210	pNef <sub>NL4-3</sub> D174A.IRES.GFP	NL4-3 Nef D174A GFP	EcoRI-Sall BstXI-NotI	203	108, 109	pIRES.GFP
211	pNef <sub>NL4-3</sub> D174E.IRES.GFP	NL4-3 Nef D174E GFP	EcoRI-Sall BstXI-NotI	203	110, 111	
212	pNef <sub>NL4-3</sub> DD174,175AA.IRES.GFP	NL4-3 Nef DD174,175AA GFP	EcoRI-Sall BstXI-NotI	203	114, 115	
213	pNef <sub>NL4-3</sub> D175A.IRES.GFP	NL4-3 Nef D175A GFP	EcoRI-Sall BstXI-NotI	203	116, 117	
214	pNef <sub>NL4-3</sub> D175E.IRES.GFP	NL4-3 Nef D175E GFP	EcoRI-Sall BstXI-NotI	203	118, 119	
215	pNef <sub>SIVmac239</sub> .IRES.GFP	SIVmac239 Nef GFP	EcoRI-Sall BstXI-NotI	198, 199	N/A	
216	p $\alpha$ R-V5.IRES.GFP	$\alpha$ R-V5 GFP	BamHI-Sall BstXI-NotI	160, 199	33, 34	
217	p $\alpha$ R-KR297,340EE-V5.IRES.GFP	$\alpha$ R-KR297,340EE-V5 GFP	BamHI-Sall BstXI-NotI	216	220, 221 232, 233	

**Table 2.9: DNA primers used in this study.**

The following table provides a list of all DNA primers used in this study, along with their sequence (in the 5' → 3' direction), their melting temperature ( $T_m$ ), and their application (either PCR, SDM, or sequencing). For the PCR and sequencing primers, the melting temperature was calculated using the basic formula  $T_m = 2(\text{the number of adenines [A] and thymines [T]} + 4(\text{the number of guanines [G] and cytosines [C]})$ , while the melting temperature for the SDM primers was calculated according to the algorithm recommended by Stratagene and available on its website (<http://www.stratagene.com/QPCR/tmCalc.aspx>). Abbreviations (in alphabetical order): Dm (*Drosophila melanogaster*), Fwd (forward), IVT (in vitro transcription), Rev (reverse), Tyr (tyrosinase).

**Table 2.9: DNA Primers used in this study.**

#	Primer Name	Sequence (5' → 3')	T <sub>m</sub> (°C)	Type
1	CD4 5' EcoRI Fwd	GCGAATTCATGAACCGGGGAGTCCCTTTTAG	70.0	PCR Primers
2	CD4 3' XhoI Rev	GTCCTCGAGTCAAATGGGGCTACATGCTCTCTG	70.0	
3	CD4-ct 5' EcoRI Fwd	GCGAATTCCTGTGTCAAGGTGCCGGCACC	64.0	
4	CD4-ct 3' SalI Rev	GCTAGTCGACTCAAATGGGGCTACATGTCTTC	64.0	
5	Nef <sub>248</sub> 5' EcoRI Fwd	GCGAATTCATGGGTGGCAAGTGGTCAAAAC	66.0	
6	Nef <sub>248</sub> 3' XhoI Rev	GTCCTCGAGTCAAGTTTTTGTAGTACTCCGGATG	68.0	
7	Nef <sub>DH12-3</sub> 5' EcoRI Fwd	GCGAATTCATGGGTGGCAAGTTGTCAAAG	62.0	
8	Nef <sub>DH12-3</sub> 3' XhoI Rev	GTCCTCGAGTCAGCAGTCTTGTAGTACTC	60.0	
9	Nef <sub>NA7</sub> 5' EcoRI Fwd	GCGAATTCATGGGTGGCAAGTGGTCAAAAC	66.0	
10	Nef <sub>NA7</sub> 3' XhoI Rev	GTCCTCGAGTCAGCAGTCTTGTAGTACTCCG	68.0	
11	Nef <sub>NL4-3</sub> 5' BamHI Fwd	GCGGATCCATGGGTGGCAAGTGGTCAAAAG	68.0	
12	Nef <sub>NL4-3</sub> 5' EcoRI Fwd	GCGAATTCATGGGTGGCAAGTGGTCAAAAG	68.0	
13	Nef <sub>NL4-3</sub> 3' EcoRI Rev	GCGAATTCAGCAGTCTTGAAGTACTCCG	68.0	
14	Nef <sub>NL4-3</sub> 3' XhoI Rev	GTCCTCGAGTCAGCAGTCTTGAAGTACTCCG	68.0	
15	Nef <sub>SIVmac239</sub> 5' EcoRI Fwd	GCGAATTCATGGGTGGAGCTAATTTCCATG	62.0	
16	Nef <sub>SIVmac239</sub> 3' XhoI Rev	GTCCTCGAGTCAGCGAGTTTCCCTTCTTGTGTC	62.0	
17	Dm $\mu$ 1 5' EcoRI Fwd	GCGAATTCATGTCTTCGTCCGGCCATTTTC	62.0	
18	Dm $\mu$ 1 3' ApaI Rev	CTGGGCCCATTTGGTGCCTAGCTGATAGTC	62.0	
19	Dm $\mu$ 2 5' EcoRI Fwd	GCGAATTCATGATTTGGCGGCTGTTCGTC	66.0	
20	Dm $\mu$ 2 3' ApaI Rev	CTGGGCCCGCAGCGGCTCATAACAAGC	64.0	
21	Dm $\mu$ 3 5' EcoRI Fwd	GCGAATTCATGATACACAGTCTGTTATTGTAAC	70.0	
22	Dm $\mu$ 3 3' ApaI Rev	CTGGGCCCATCCGCACCTGGAACTTGCC	68.0	
23	Dm CLC 5' EcoRI Fwd	GCGAATTCATGGACTTCGGGAGACGATTTCGC	70.0	

**Table 2.9: DNA Primers used in this study, *continued*.**

#	Primer Name	Sequence (5' → 3')	T <sub>m</sub> (°C)	Type
24	Dm CLC 3' ApaI Rev	CTGGGCCCGGTGCTCTTCTGCACCTGGATG	70.0	PCR Primers
25	Dm GGA 5' EcoRI Fwd	GCGAATTCATGACACACCGACGAGAGCATAATG	70.0	
26	Dm GGA 3' ApaI Rev	CTGGGCCCGTCCACATAGTCAATGCCTTTGG	68.0	
27	α 5' NotI Fwd	CAGCGGCCGCTATGCCGGCCGTATCCAAGG	62.0	
28	α 3' BamHI Rev	GCGGATCCCTTAGAACTGTTCCGACAGCAATTC	68.0	
29	α-ear 5' EcoRI Fwd	GCGAATTCCTCTGAAGACAACCTTTGCCAGG	62.0	
30	α-ear 3' XhoI Rev	GTCTCGAGTTAGAACTGTTCCGACAGCAATTC	68.0	
31	α-trunk-GST 5' EcoRI Fwd	GCGAATTCATGCCGGCCGTATCCAAGG	62.0	
32	α-trunk-GST 3' HindIII Rev	GATCAAGCTTTCATTTTGGAGGATGGTCGCC	64.0	
33	αR-V5 5' BamHI Fwd	CGGATCCTGATGCCGGCCGTATCCAAG	64.0	
34	αR-V5 3' SalI Rev	GCTAGTCGACCGTAGAATCGAGACCGAGAGGGTTAGGGATAGGCTTACCGAACTGT	62.0	
35		TCCGACAGCAATTC		
36	His <sub>6</sub> -β2-trunk 5' BspEI Fwd	GCTATCCGGACATCACCCATCACCGATTAC	70.0	
37	His <sub>6</sub> -β2-trunk 3' MluI Rev	GAACGGGTCTATTTGCCGATGAATGCCATGGC	68.0	
38	β3-ear 5' EcoRI Fwd	GCGAATTCGTCAATCAGTGTCACTACTCCTG	66.0	
39	β3-ear 3' XhoI Rev	GTCTCGAGTTACTGCTGTAGGGAAGAAGATTTC	70.0	
40	ε-ear 5' EcoRI Fwd	GCGAATTCGAGTCACTCACAGAACTGCC	62.0	
41	ε-ear 3' XhoI Rev	GTCTCGAGTTAGCTTAGGTCACCTTTTGAG	62.0	
42	μ2-N 5' XbaI Fwd	GCTCTAGAATGATCGGAGGCTTATTCATC	60.0	
43	μ2-N 3' BamHI Rev	GCGGATCCCTAGCAGCGGGTTTCATAAATG	64.0	
44	σ1 5' NotI Fwd	CAGCGGCCGCATGATGCGGTTCAATGCTATTATTC	66.0	
45	σ1 3' BglII Rev	GTCAGATCTCTATGCCAAACCCCATCTCCCTC	64.0	
46	σ2 5' NotI Fwd	CAGCGGCCGCATGATCCGCTTATCCTCATCC	64.0	

**Table 2.9: DNA Primers used in this study, *continued*.**

#	Primer Name	Sequence (5' → 3')	T <sub>m</sub> (°C)	Type
47	σ2 5' SacI Fwd	CAGAGCTCATGATCCGATTTCATTTCTCATCCAG	68.0	PCR Primers
48	σ2 3' BglII Rev	GTCAGATCTTCACACTCCAGGGACTGTAGCATC	68.0	
49	σ2 3' KpnI Rev	CAGGTACCCTCACTCCAGCGACTGCAGCATC	70.0	
50	σ3 5' NotI Fwd	CAGCGCCGCATGATCAAGCGGATCCTAATCTTC	68.0	
51	σ3 3' BamHI Rev	GCGGATCCCTTATTAAAGAGGGCAGGTTTGGC	70.0	
52	CD4 LL413,414AA Fwd	GCGGATGTCTCAGATCAAGAGAGCCCGCAGTGAGAAGAAGACCTGCCAG	79.6	SDM Primers
53	CD4 LL413,414AA Rev	CTGGCAGGTCTTCTTCTCCTACTGGCGGCTCTCTTGATCTGAGACATCCCGC	79.6	
54	Nef <sub>NL4-3</sub> G2A Fwd	GCTCAAGCTTCGAAATTCATGGCTGGCAAGTGGTCAAAAAG	80.6	
55	Nef <sub>NL4-3</sub> G2A Rev	CTTTTGGACCACCTTGCCAGCCATGAATTCGAAGCTTGAGC	80.6	
56	Nef <sub>NL4-3</sub> WL57,58AA Fwd	GCTAAACAATGCTGTGTTGTGCCGGCAGAGAAGCAAGAGGAGGAAGAG	78.8	
57	Nef <sub>NL4-3</sub> WL57,58AA Rev	CTCTTCCCTCCTTGTGTCTTCTGCCCGGCACAAGCAGCATTTGTTAGC	78.8	
58	Nef <sub>NL4-3</sub> EEEE62-65AAAA Fwd	GCCTGGCTAGAAAGCACAAGCGGGCGGAGCGGTGGGTTTCCAGTC	80.4	
59	Nef <sub>NL4-3</sub> EEEE62-65AAAA Rev	GACTGGAAAAACCCACCCGCTGCCCGCCGCTTGTGCTTCTAGCCAGGC	80.4	
60	Nef <sub>NL4-3</sub> PP72,75AA Fwd	GTGGGTTTTCCAGTCCACAGCTCAGGTGAGCTTTAAGACCAATGACTTAC	79.5	
61	Nef <sub>NL4-3</sub> PP72,75AA Rev	GTAAGTCATTTGGTCTTAAAGCTACCTGAGCTGTGACTGGAAAACCCAC	79.5	
62	Nef <sub>NL4-3</sub> E154A Fwd	GAGCCAGATAAGGTAGCAGAGGCCAATAAAGGAG	79.2	
63	Nef <sub>NL4-3</sub> E154A Rev	CTCCTTTAATTGGCCCTCTGCTACCTTATCTGGCTC	79.2	
64	Nef <sub>NL4-3</sub> E155A Fwd	GCCAGATAAGGTAGAAGCGGCCAATAAAGGAGAG	79.2	
65	Nef <sub>NL4-3</sub> E155A Rev	CTCTCCTTTATTTGGCCGCTTCTACCTTATCTGGC	79.2	
66	Nef <sub>NL4-3</sub> NI157A Fwd	GCCAGATAAGGTAGAAGAGGCCGCTAAAGGAGAGAACACCAG	82.1	
67	Nef <sub>NL4-3</sub> NI157A Rev	CTGGTGTCTCTCCTTTAGCGGCCCTCTTACCTTATCTGGC	82.1	
68	Nef <sub>NL4-3</sub> K158A Fwd	GATAAGGTAGAAGAGGCCAATGCAAGGAGAGAACACCAGC	80.1	
69	Nef <sub>NL4-3</sub> K158A Rev	GCTGGTGTCTCTCCTGCAATTGGCCCTTCTACCTTATC	80.1	

**Table 2.9: DNA Primers used in this study, *continued*.**

#	Primer Name	Sequence (5' → 3')	T <sub>m</sub> (°C)	Type
70	Nef <sub>NL4.3</sub> G159A Fwd	GTAGAAGAGGCCAATAAAGCAGAGAACACCCAGCTTGTAC	80.6	SDM Primers
71	Nef <sub>NL4.3</sub> G159A Rev	GTAACAAGCTGGTGTCTCTGCTTTATTGGCCCTCTTCTAC	80.6	
72	Nef <sub>NL4.3</sub> E160A Fwd	GAAGAGGCCAATAAAGGAAAGCGAACACCCAGCTTGTACACCCCTG	82.5	
73	Nef <sub>NL4.3</sub> E160A Rev	CAGGGTGTAAACAAGCTGGTGTTCGCTTCCCTTATTGGCCCTCTTC	82.5	
74	Nef <sub>NL4.3</sub> E160D Fwd	GAAGAGGCCAATAAAGGAGAcAACACCAGCTTGTACACCCCTG	82.5	
75	Nef <sub>NL4.3</sub> E160D Rev	CAGGGTGTAAACAAGCTGGTGTTCCTCCCTTATTGGCCCTCTTC	82.5	
76	Nef <sub>NL4.3</sub> E160K Fwd	GAAGAGGCCAATAAAGGAAAGAACACCAGCTTGTACACCCCTG	82.5	
77	Nef <sub>NL4.3</sub> E160K Rev	CAGGGTGTAAACAAGCTGGTGTCTTTCCTTATTGGCCCTCTTC	82.5	
78	Nef <sub>NL4.3</sub> NI61A Fwd	GAGGCCAATAAAGGAGAGGCCACCAGCTTGTACACCCCTG	80.6	
79	Nef <sub>NL4.3</sub> NI61A Rev	CAGGGTGTAAACAAGCTGGTGGCCCTCTCCTTATTGGCCCTC	80.6	
80	Nef <sub>NL4.3</sub> NTS161-163RQP Fwd	GATAAGGTAGAAGAGGCCAATAAAGGAGAGGCCAGCCCTTGTACACCCCTGTGAGCCTGCATGGAATG	80.0	
81	Nef <sub>NL4.3</sub> NTS161-163RQP Rev	CATTCCATGCAGGCTCACAGGGTGTAAACAAGGGCTGGCGCTCTCCTTTATTGGCCCTCTTC TACCTTATC	80.0	
82	Nef <sub>NL4.3</sub> T162A Fwd	GCCAATAAAGGAGAGAAACGCCAGCTTGTACACCCCTGTGAG	83.6	
83	Nef <sub>NL4.3</sub> T162A Rev	CTCACAGGGTGTAAACAAGCTGGCGTTCTCTCCTTTATTGGC	83.6	
84	Nef <sub>NL4.3</sub> S163A Fwd	CAATAAAGGAGAGAAACACCCCTTGTACACCCCTGTGAGC	80.1	
85	Nef <sub>NL4.3</sub> S163A Rev	GCTCACAGGGTGTAAACAAGGGGTGTCTCTCCTTTATTG	80.1	
86	Nef <sub>NL4.3</sub> L164A Fwd	GAGAGAACCAGCCGTTACACCCCTGTGAGCCCTGC	82.3	
87	Nef <sub>NL4.3</sub> L164A Rev	GCAGGCTCACAGGGTGTAAACCGCGCTGGTGTCTCTC	82.3	
88	Nef <sub>NL4.3</sub> LL164,165AA Fwd	GCCAATAAAGGAGAGAAACACCAGCCGGCACACCCCTGTGAGCCCTG	78.6	
89	Nef <sub>NL4.3</sub> LL164,165AA Rev	CAGGCTCACAGGGTGTGCCCGCTGGTGTCTCTCCTTTATTGGC	78.6	
90	Nef <sub>NL4.3</sub> L165A Fwd	GAGAGAACCAGCTTGGCACACCCCTGTGAGCCCTGC	80.0	

**Table 2.9: DNA Primers used in this study, *continued*.**

#	Primer Name	Sequence (5' → 3')	T <sub>m</sub> (°C)	Type
91	Nef <sub>NL4-3</sub> L165A Rev	GCAGGCTCACAGGGTGTGCCAAGCTGGTGTCTCTC	80.0	SDM Primers
92	Nef <sub>NL4-3</sub> H166A Fwd	GAGAGAACCACAGCTTGTAGCCCCCTGTGAGCCTGCATG	80.1	
93	Nef <sub>NL4-3</sub> H166A Rev	CATGCAGGCTCACAGGGGCTAACAAAGCTGGTGTCTCTC	80.1	
94	Nef <sub>NL4-3</sub> P167A Fwd	GAACACCAGCTTGTACACGCTGTGAGCCTGCATGGAATG	82.6	
95	Nef <sub>NL4-3</sub> P167A Rev	CATCCATGCAGGCTCACAGCGTGTAAACAAGCTGGTGTTC	82.6	
96	Nef <sub>NL4-3</sub> V168A Fwd	CAGCTTGTACACCCCTCCGAGCCTGCATGGAATGGATG	82.7	
97	Nef <sub>NL4-3</sub> V168A Rev	CATCCATTCCATGCAGGCTCCGAGGGTGTAAACAAGCTG	82.7	
98	Nef <sub>NL4-3</sub> S169A Fwd	CAGCTTGTACACCCCTGTGGCCCTGCATGGAATGGATGAC	79.1	
99	Nef <sub>NL4-3</sub> S169A Rev	GTCATCCATTCCATGCAGGGCCACAGGGTGTAAACAAGCTG	79.1	
100	Nef <sub>NL4-3</sub> L170A Fwd	GCTTGTACACCCCTGTGAGCGCGCATGGAATGGATGACCCCTG	81.2	
101	Nef <sub>NL4-3</sub> L170A Rev	CAGGGTCAATCCATTCCATGCAGCGCTCACAGGGTGTAAACAAGC	81.2	
102	Nef <sub>NL4-3</sub> H171A Fwd	GTTACACCCCTGTGAGCCTGGCTGGAAATGGATGACCCCTGAG	81.2	
103	Nef <sub>NL4-3</sub> H171A Rev	CTCAGGGTCATCCATTCCAGCCAGGCTCACAGGGTGTAAAC	81.2	
104	Nef <sub>NL4-3</sub> G172A Fwd	CACCCCTGTGAGCCTGCATGCAATGGATGACCCCTGAGAG	82.7	
105	Nef <sub>NL4-3</sub> G172A Rev	CTCTCAGGGTCATCCATTGCATGCAGGCTCACAGGGTG	82.7	
106	Nef <sub>NL4-3</sub> M173A Fwd	CACCCCTGTGAGCCTGCATGGAGCGGATGACCCCTGAGAGAG	83.2	
107	Nef <sub>NL4-3</sub> M173A Rev	CTCTCTCAGGGTCATCCGCTCCATGCAGGCTCACAGGGTG	83.2	
108	Nef <sub>NL4-3</sub> D174A Fwd	CACCCCTGTGAGCCTGCATGGAATGGCTGACCCCTGAGAGAGAAGTGTAG	87.4	
109	Nef <sub>NL4-3</sub> D174A Rev	CTAACACTTCTCTCTCAGGGTCAGCCATTCCATGCAGGCTCACAGGGTG	87.4	
110	Nef <sub>NL4-3</sub> D174E Fwd	CACCCCTGTGAGCCTGCATGGAATGGAGACCCCTGAGAGAGAAGTGTAG	87.4	
111	Nef <sub>NL4-3</sub> D174E Rev	CTAACACTTCTCTCTCAGGGTCCCTCCATCCATGCAGGCTCACAGGGTG	87.4	
112	Nef <sub>NL4-3</sub> D174N Fwd	CACCCCTGTGAGCCTGCATGGAATGAACGACCCCTGAGAGAGAAGTGTAG	85.4	
113	Nef <sub>NL4-3</sub> D174N Rev	CACCCCTGTGAGCCTGCATGGAATGAACGACCCCTGAGAGAGAAGTGTAG	85.4	

**Table 2.9: DNA Primers used in this study, *continued*.**

#	Primer Name	Sequence (5' → 3')	T <sub>m</sub> (°C)	Type
114	Nef <sub>NL4-3</sub> DD174,175AA Fwd	CACCCGTGTGAGCCTGCATGGAATGGCTGCTCCTGAGAGAGAAGTGTAG	83.4	SDM Primers
115	Nef <sub>NL4-3</sub> DD174,175AA Rev	CTAACACTTCTCTCAGGAGCAGCCATTCCATGCAGGGCTCACAGGGTG	83.4	
116	Nef <sub>NL4-3</sub> DI75A Fwd	CACCCGTGTGAGCCTGCATGGAATGGATGCCCTGAGAGAGAAGTGTAG	87.4	
117	Nef <sub>NL4-3</sub> DI75A Rev	CTAACACTTCTCTCAGGGGCATCCATCCATCCATGCAGGCTCACAGGGTG	87.4	
118	Nef <sub>NL4-3</sub> DI75E Fwd	CACCCGTGTGAGCCTGCATGGAATGGATGAGCCTGAGAGAGAAGTGTAG	87.4	
119	Nef <sub>NL4-3</sub> DI75E Rev	CTAACACTTCTCTCAGGCTCATCCATCCATCCATGCAGGCTCACAGGGTG	87.4	
120	Nef <sub>NL4-3</sub> DI75N Fwd	CACCCGTGTGAGCCTGCATGGAATGGATAACCCCTGAGAGAGAAGTGTAG	88.3	
121	Nef <sub>NL4-3</sub> DI75N Rev	CTAACACTTCTCTCAGGGTTATCCATTCATCCATGCAGGCTCACAGGGTG	88.3	
122	Nef <sub>NL4-3</sub> P176A Fwd	CTGCATGGAATGGATGACCGCTGAGAGAGAAGTGTAGAGTG	81.6	
123	Nef <sub>NL4-3</sub> P176A Rev	CACTCTAACACTTCTCTCAGCGTCAATCCATCCATCCATGCAG	81.6	
124	Nef <sub>NL4-3</sub> E177A Fwd	CATGGAATGGATGACCCCTGCGAGAGAGAAGTGTAGAGTG	81.6	
125	Nef <sub>NL4-3</sub> E177A Rev	CACCTCTAACACTTCTCTCGCAGGGTCAATCCATCCATGCAG	81.6	
126	Nef <sub>NL4-3</sub> R178A Fwd	CATGGAATGGATGACCCCTGAGAGGGCAAGTGTAGAGTGGAGGTTTG	81.2	
127	Nef <sub>NL4-3</sub> R178A Rev	CAAACCTCCACTCTAACACTTGCCTCTCAGGGTCAATCCATCCATGCAG	81.2	
128	Nef <sub>NL4-3</sub> E179A Fwd	GAATGGATGACCCCTGAGAGAGCAGTGTAGAGTGGAGGTTTGACACAG	81.2	
129	Nef <sub>NL4-3</sub> E179A Rev	CTGTCAAACCTCCACTCTAACACTGCTCTCTCAGGGTCAATCCATCCATGCAG	81.2	
130	Nef <sub>NL4-3</sub> V180A Fwd	GATGACCCCTGAGAGAGAAAGCGTTAGAGTGGAGGTTTGACACAG	82.6	
131	Nef <sub>NL4-3</sub> V180A Rev	CTGTCAAACCTCCACTCTAACCGTTCTCTCTCAGGGTCAATCCATCCATGCAG	82.6	
132	Tyr E513K Fwd	GCAACCCAGGAGAAAGGCAGCCACTCCCTC	81.6	
133	Tyr E513K Rev	GAGGAGTGGTGCCTTTTCTCCTGGGGTTGC	81.6	
134	Tyr RQP514-516NTS Fwd	GAAGAAGCAACCCAGGAGGAAACACAGAGTCTCCTCATGGACAAAGACGACTACCACAGCTTGC	79.4	

**Table 2.9: DNA Primers used in this study, *continued*.**

#	Primer Name	Sequence (5' → 3')	T <sub>m</sub> (°C)	Type
135	Tyr RQP514-516NTS Rev	GCAAGCTGTGGTAGTCGTCTTTGTCCATGAGGAGACTCGTGTTTTCCTCCTGGGGTTGCTTCTTC	79.4	SDM Primers
136	Tyr LL517,518AA Fwd	CCCAGGAGGAAAGGCAGCCAGCCGCCATGGACAAAGACGACTACCAC	80.4	
137	Tyr LL517,518AA Rev	GTGGTAGTCGTCTTTGTCCATGGCGGTGGCTGCCCTTTCCTCCTGGG	80.4	
138	Tyr DD522,523AA Fwd	CTCCTCATGGACAAAGCCGCCCTACCACAGCTTGTGTATCAG	81.2	
139	Tyr DD522,523AA Rev	CTGATACAGCAAGCTGTGGTAGGCGGCTTTGTCCATGAGGAG	81.2	
140	α K6E Fwd	GCCACCATGCCGGCCGTATCCGAGGGTGAGGGTATGCGGAG	81.6	
141	α K6E Rev	CTCGCATACCCCTCACCCCTCGGATACGGCCGGCATGGTGGC	81.6	
142	α GG7,9GG Fwd	CGTATCCAAGGGTGAGGGTATGCGAGGCCCTAGC	88.8	
143	α GG7,9GG Rev	GCTAGGCCCTCGCATCCCTCACCCCTTGGATACG	88.8	
144	α R11E Fwd	GTATCCAAGGGTGAGGGTATGGAAGGCCCTAGCGGTCTTC	81.1	
145	α R11E Rev	GAAGACCGCTAGGCCCTCCATACCCCTCACCCCTTGGATAC	81.1	
146	α L13A Fwd	GAGGGTATGCGAGGGCGCAGCGGTCTTCATCTCCG	79.9	
147	α L13A Rev	CGGAGATGAAAGACCCGCTGCGCCCTCGCATACCCCTC	79.9	
148	α R21D Fwd	GCGGTCTTCATCTCCGATATCGATAACTGTAAAAGTAAAGAAGCTG	78.5	
149	α R21D Rev	CAGCTTCTTTACTTTTACAGTTATCGATATCGAGATGAAGACCCG	78.5	
150	α K24E Fwd	CATCTCCGATATCCGTAACCTGTGAAAGTAAAGAAAGCTGAAATAAAG	78.9	
151	α K24E Rev	CTTTATTTTCAGCTTCTTTACTTTTCACAGTTACGGATATCGGAGATG	78.9	
152	α K26E Fwd	CTCCGATATCCGTAACCTGTAAAAGTGAAGAAGCTGAAATAAAGAG	79.8	
153	α K26E Rev	CTCTTTATTTTCAGCTTCTTCACTTTTACAGTTACGGATATCGGAG	79.8	
154	α K31E Fwd	CTGTAAAAGTAAAGAAAGCTGAAATAAGAGAGGATAAATAAGGAGCTGGC	79.9	
155	α K31E Rev	GCCAGCTCCTTATTTATCCCTCTCTATTTTCAGCTTCTTTACTTTTACAG	79.9	
156	α R32E Fwd	CTGTAAAAGTAAAGAAAGCTGAAATAAAGGAGATAAATAAGGAGCTGGCAAATATTAG	78.4	

**Table 2.9: DNA Primers used in this study, *continued*.**

#	Primer Name	Sequence (5' → 3')	T <sub>m</sub> (°C)	Type
157	α R32E Rev	CTAATATTTGCCAGCTCCTTATTTATCTCCTTTATTTTCAGCTTCTTTACTTTTACAG	78.4	SDM Primers
158	α R41E Fwd	GAGCTGGCAAATATTTGAATCAAAAATTTAAAGGTGACAAAGGCTCTTTGATGG	78.7	
159	α R41E Rev	CCATCAAGAGCCTTGTCAACCTTTAAATTTTGAATTCATATTTGCCAGCTC	78.7	
160	α K43E Fwd	GAGCTGGCAAATATTTAGATCAGAAATTTAAAGGTGACAAAGGCTC	78.7	
161	α K43E Rev	GAGCCTTGTCAACCTTTAAATTTCTGATCTAATATTTGCCAGCTC	78.7	
162	α K45E Fwd	GCTGGCAAATATTTAGATCAAAAATTTGAAAGGTGACAAAGGCTCTTG	78.8	
163	α K45E Rev	CAAGAGCCTTGTCAACCTTCAAAATTTTGAATCTAATATTTGCCAGC	78.8	
164	α K48E Fwd	GATCAAAAATTTAAAGGTGACGAGGCTCTTGTATGGCTACAG	78.5	
165	α K48E Rev	CTGTAGCCATCAAGAGCCTCGTCACCTTTAAATTTTGATC	78.5	
166	α K55E Fwd	CTCTTGTATGGCTACAGTGAGAAAGAAAGTATGTCTGCAAGTTAC	79.6	
167	α K55E Rev	GTAACCTTGACAGACATACTTCTCTCACTGTAGCCATCAAGAG	79.6	
168	α K56E Fwd	CTCTTGTATGGCTACAGTAAAGGAGAAAGTATGTCTGCAAG	78.4	
169	α K56E Rev	CTTGCAGACATACTTCTCCTTACTGTAGCCATCAAGAG	78.4	
170	α K61E Fwd	GTAAGAAGAAGTATGTCTGCGAGTTACTCTTCAICTTCTCCTTGGTC	81.6	
171	α K61E Rev	GACCAAGGAGAAAGATGAAGAGTAACTCGCAGACATACTTCTTCTTAC	81.6	
172	α R87E Fwd	GTGAATCTTCTGAGCTCAAACGAAATACACGGAAAGCAGATCGGC	81.2	
173	α R87E Rev	GCCGATCTGCTTTTCCGTGTATTCGTTTGAGCTCAGAAGATTAC	81.2	
174	α K91E Fwd	CAAACAGATACACGGAAAGAGCAGATCGGGTACCTTTTC	79.4	
175	α K91E Rev	GAAAAGGTAGCCGATCTGCTCTTCCGTGTATCTGTTT	79.4	
176	α R110E Fwd	GGTGAATTCAAATAGTGAACCTGATCGAGTTGATTAACAATGCCATCAAG	77.9	
177	α R110E Rev	CTTGATGGCATTGTTAATCAACTCGATCAGTTCACTAATTTGAATTCACC	77.9	
178	α K117E Fwd	GATTAAACAATGCCATCGAAGATGACCTGGCCAGCCG	80.5	
179	α K117E Rev	CGGCTGGCCAGGTCATCTCGATGGCAATGTTAATC	80.5	

**Table 2.9: DNA Primers used in this study, *continued*.**

#	Primer Name	Sequence (5' → 3')	T <sub>m</sub> (°C)	Type
180	α R123D Fwd	CAAGAATGACCTGGCCAGCGACAATCCTACATTTATGGGTC	79.2	SDM Primers
181	α R123D Rev	GACCCATAAATGTAGGATTGTCGGTGGCCAGGTCATCTTG	79.2	
182	α T131A Fwd	CTACATTTATGGTCTGGCGCTGCACTGCATCGCCAATG	82.7	
183	α T131A Rev	CATTGGCGATGCAGTGCAGCGCCAGACCCATAAAATGTAG	82.7	
184	α R141D Fwd	CGCCAATGTGGGTAGCGGATGAGATGGCAGAGGGC	78.6	
185	α R141D Rev	GCCTCTGCCATCTCATCGCTACCCACATTGGCG	78.6	
186	α K165E Fwd	GATACCATGGACAGTGTGGAGCAGAGCGGCAGCCCTG	83.9	
187	α K165E Rev	CAGGGCTGCGCTCTGCTCCACACTGTCCATGGTATC	83.9	
188	α R174D Fwd	GCCCTGTGCTTGTGGACCTGTACAGGACGTCAACCTG	81.1	
189	α R174D Rev	CAGGTGACGTCCTGTACAGGTCCAACAAGCACAGGGC	81.1	
190	α R177E Fwd	GCTTGTGGCGCTGTACGAGACGTCACTGACCTAG	80.0	
191	α R177E Rev	CTAGGTCAGGTGACGTCTCGTACAGGCGCAACAAGC	80.0	
192	α R191D Fwd	CTATGGCGGACTGGACATCCGATGTGGTACACCTCCTC	81.1	
193	α R191D Rev	GAGGAGGTGTACCACATCGGATGTCCAGTCGCCCATAG	81.1	
194	α K217E Fwd	CACCACACTGGCCCAGGAGAGATCCTGAGGAGTTC	81.6	
195	α K217E Rev	GAACTCCTCAGGATTCTCCTGGGCCAGTGTGGTG	81.6	
196	α K223E Fwd	GATCCTGAGGAGTTCGAGACCTCTGTCTCTCTAG	79.3	
197	α K223E Rev	CTAGAGAGACAGAGGTCTCGAACTCCTCAGGATTC	79.3	
198	α R232E Fwd	GTCTCTAGCTGTCTCTGAACCTGAGCAGAAATGTGACG	78.0	
199	α R232E Rev	CGTCACAAATCTGCTCAGTTCAGATCAGAGACAGTAGAGAC	78.0	
200	α K235E Fwd	GCTGTCTCTCGACTGAGCGAAATTTGTGACGTCCCGCTC	81.1	
201	α K235E Rev	GACGCGGACGTCAACAATTCGCTCAGTCGAGAGACAGC	81.1	
202	α K260E Fwd	CTCCTTGGCTGTCAGTCCGAACTTCTGAGACTGCTG	80.4	

**Table 2.9: DNA Primers used in this study, *continued*.**

#	Primer Name	Sequence (5' → 3')	T <sub>m</sub> (°C)	Type
203	α K260E Rev	CAGCAGTCTCAGAAGTTCGACTGACAGCCAAAGGAG	80.4	SDM Primers
204	α R263E Fwd	CTCCTTGGCTGTCAAGTCAAACTTCTGAACTGCTGCAGTGTCTAC	82.1	
205	α R263E Rev	GTAGCACTGCAGCAGTTCACAGAAGTTTGACTGACAGCCAAAGGAG	82.1	
206	α R276E Fwd	GACCCTGCGGTGGATGGCCGCCCTGACTG	78.1	
207	α R276E Rev	CAGTCAGCGCGCCATCCACCCGACGGGTC	78.1	
208	α K289E Fwd	CTTGGAGACCATCCTGATGAGGCCACAGGAGC	81.6	
209	α K289E Rev	GCTCCTGGGCCCTCATTCAAGGATGGTCTCCAAAG	81.6	
210	α K295A Fwd	GCCCAGGAGCCTCCCCGCTCCAAGAAAGTCCAGCATTCAAAATG	80.8	
211	α K295A Rev	CATTTGAATGCTGGACTTCTTGGACCGGGAGGCTCCTGGGC	80.8	
212	α K295E Fwd	GCCCAGGAGCCTCCCCGAGTCCAAGAAAGTCCAGCATTCAAAATG	83.1	
213	α K295E Rev	CATTTGAATGCTGGACTTCTTGGACTCGGGAGGCTCCTGGGC	83.1	
214	α KKK295,297,298AAA Fwd	GCCCAGGAGCCTCCCCGCTCCCGGGCAGTCCAGCATTCAAAATG	83.6	
215	α KKK295,297,298AAA Rev	CATTTGAATGCTGGACTGCCCGGGACCGGGGAGGCTCCTGGGC	83.6	
216	α KKK295,297,298EEE Fwd	GCCCAGGAGCCTCCCCGAGTCCGAGGAAGTCCAGCATTCAAAATG	78.4	
217	α KKK295,297,298EEE Rev	CATTTGAATGCTGGACTTCTCCTCGGACTCGGGAGGCTCCTGGGC	78.4	
218	α K297A Fwd	GCCCAGGAGCCTCCCCAAGTCCCGGAAAGTCCAGCATTCAAAATG	80.8	
219	α K297A Rev	CATTTGAATGCTGGACTTTCGGGGACTTGGGAGGCTCCTGGGC	80.8	
220	α K297E Fwd	GCCCAGGAGCCTCCCCAAGTCCGAGAAAGTCCAGCATTCAAAATG	83.1	
221	α K297E Rev	CATTTGAATGCTGGACTTCTCCTGGACTTGGGAGGCTCCTGGGC	83.1	
222	α K298A Fwd	GCCCAGGAGCCTCCCCAAGTCCAAGGCAGTCCAGCATTCAAAATG	80.8	
223	α K298A Rev	CATTTGAATGCTGGACTGCCCTTGGACTTGGGAGGCTCCTGGGC	80.8	
224	α K298E Fwd	GCCCAGGAGCCTCCCCAAGTCCAAGGAAGTCCAGCATTCAAAATG	83.1	
225	α K298E Rev	CATTTGAATGCTGGACTTCTCCTTGGACTTGGGAGGCTCCTGGGC	83.1	

**Table 2.9: DNA Primers used in this study, *continued*.**

#	Primer Name	Sequence (5' → 3')	T <sub>m</sub> (°C)	Type
226	α K305E Fwd	CAGCATTCAAATGCCGAGAACGCTGTGCTGTTTG	78.0	SDM Primers
227	α K305E Rev	CAAAACAGCACAGCGTTCTCGGCATTTGAATGCTG	78.0	
228	α R328D Fwd	GCCAAACCTCCTGGTCGATGCCGTGCAACCAGC	79.8	
229	α R328D Rev	GCTGGTTGCAGGCATCGACCAGGAGGTTGGGC	79.8	
230	α R340A Fwd	CCAGTTCCTGCAGCATGCCGAGACAAACCTGGCG	82.8	
231	α R340A Rev	GCGCAGGTTTGTCTCCGCATGCTGCAGGAACTGG	82.8	
232	α R340E Fwd	CCAGTTCCTGCAGCATGAGGAGACAAACCTGGCG	78.7	
233	α R340E Rev	GCGCAGGTTTGTCTCCTCATGCTGCAGGAACTGG	78.7	
234	α R345D Fwd	CATCGGAGACAAACCTGGACTACCTGGCTCTGGAGAG	81.1	
235	α R345D Rev	CTCTCCAGAGCCAGGTAGTCCAGGTTTGTCTCCCGATG	81.1	
236	α K366E Fwd	CTCACGAGGCTGTCGAGACCCACATCGAG	78.8	
237	α K366E Rev	CTCGATGTGGGTCTCGACAGCCTCGTGAG	78.8	
238	α R385E Fwd	CGAGATGTGAGTGTGGAGCAGCGGGCAGTGGACCTG	82.3	
239	α R385E Rev	CAGGTCCACTGCCCGCTGCTCCACACTCACATCTCG	82.3	
240	α R387E Fwd	GATGTAGTGTGCGGCAGGAGGCAGTGGACCTGCTCTAC	80.1	
241	α R387E Rev	GTAGAGCAGGTCCACTGCCCTCCTGCCGCACACTCACATC	80.1	
242	α R420E Fwd	GAAACAGCTGACTACTCCATCCATCGAGGAGGAAATTGTGCTGAAG	79.2	
243	α R420E Rev	CTTCAGCACAAATTTCTCCTCGATGGAGTAGTCAGCTGTTTC	79.2	
244	αR SCL351,353,355SCL Fwd	GCGCTACCTGGCTCTGGAGAGTATGTACACTCGCCAGCTCTGAGTTCTCTCACC	86.7	
245	αR SCL351,353,355SCL Rev	CGTGAGAGAACTCAGAGCTGGCGAGTGTACATACTCTCCAGAGCCAGGTAGCGC	86.7	
246	σ2 R3D Fwd	GTGGCGCCGCCATGATCGACTTTATCCTCATCCAGAAC	80.1	
247	σ2 R3D Rev	GTTCTGGATGAGGATAAAGTCGATCATGGCGGCCGCCAC	80.1	
248	σ2 K13E Fwd	CAGAACCGGGCAGGGCAGACACGCCTGGCCAAAG	85.3	

**Table 2.9: DNA Primers used in this study, *continued*.**

#	Primer Name	Sequence (5' → 3')	T <sub>m</sub> (°C)	Type
249	σ2 K13E Rev	CTTGGCCAGGGGTGTCTCGCCTGCCCGGTTCTG	85.3	SDM Primers
250	σ2 R15D Fwd	CGGGCAGGCAAGACAGACAGACCTGGCCAAAGTGGTATATG	80.0	
251	σ2 R15D Rev	CATATACCACACTTGGCCAGGTCTGTCTTGCCTGCCCCG	80.0	
252	σ2 K18E Fwd	CAAGACACGCCCTGGCCGAGTGGTATATATGCAGTTC	80.4	
253	σ2 K18E Rev	GAACGTGCATATACCACTCGGCCAGGCCGTGTCTTG	80.4	
254	σ2 R53E Fwd	CACACCAACTTTGTGGAGTTCGAGAACTTCAAGATCATCTACCG	79.3	
255	σ2 R53E Rev	CGGTAGATGATCTTGAAGTTCCTCGAACTCCACAAAAGTTGGTGTG	79.3	
256	σ2 K56E Fwd	GTGGAGTCCGGAACTTCGAGATCATCTACCCGGC	80.4	
257	σ2 K56E Rev	GCCGGTAGATGATCTCGAAGTTCCTCCGGAACCTCCAC	80.4	
258	σ2 R60E Fwd	GAAC TTCAAGATCATCTACGAGCGCTACCGCTGGCCCTC	78.9	
259	σ2 R60E Rev	GAGGCCAGGTAGCGCTCGTAGATGATCTTGAAGTTC	78.9	
260	σ2 R61D Fwd	GAAC TTCAAGATCATCTACCGGGACTACCGCTGGCCCTCTAC	80.1	
261	σ2 R61D Rev	GTAGAGGCCA GCGTAGTCCCGGTAGATGATCTTGAAGTTC	80.1	
262	σ2 A63D Fwd	GATCATCTACCGCGCTACGATGGCCCTACTTCTGCATC	84.7	
263	σ2 A63D Rev	GATGCAGAAAGTAGAGGCCATCGTAGCGCCGGTAGATGATC	84.7	
264	σ2 V88D Fwd	CTTGAGGCCATCCACAACCTTCGACGAAAGTGTAAATGAATACTCCAC	81.2	
265	σ2 V88D Rev	GTGGAAAGTATTCATTTAACACTTCGTCGAAAGTTGTGGATGGCCCTCAAG	81.2	
266	σ2 E89A Fwd	GAGGCCATCCACAACCTTCGTAGCAGTGTAAATGAATACTTCCAC	80.7	
267	σ2 E89A Rev	GTGGAAAGTATTCATTTAACACTGCTACCGAAAGTTGTGGATGGCCCTC	80.7	
268	σ2 N92A Fwd	GCCATCCACAACCTTCGTAGAAAGTGTAGCTGAATACTCCACAATGTCTGTG	81.2	
269	σ2 N92A Rev	CACAGACATTTGTGGAAGTATTCAGCTAACACTTCTACGAAAGTTGTGGATGGC	81.2	
270	σ2 E100A Fwd	GAATACTCCACAATGTCTGTGCACCTGGACCTGGTGTCAACTTCTACAAG	84.0	
271	σ2 E100A Rev	CTTGTAGAAAGTTGACACCCAGGTCCAGTGCACAGACATTTGTGGAAAGTATTC	84.0	

**Table 2.9: DNA Primers used in this study, *continued*.**

#	Primer Name	Sequence (5' → 3')	T <sub>m</sub> (°C)	Type	
272	σ2 L101A Fwd	GAATACTTCCACAATGTCTGTGAAGGGACCCTGGTGTCAAACCTTCTACAAG	81.2	SDM Primers	
273	σ2 L101A Rev	CTTGTAAGAAGTTGAACACCAGGTCCGGCTTACACAGACATTTGTGGAAGTATTC	81.2		
274	σ2 D102A Fwd	CTTCCACAATGTCTGTGAACCTGGCCCTGGTGTCAAACCTTCTAC	81.6		
275	σ2 D102A Rev	GTAGAAGTTGAACACCAGGGCCAGTTCACAGACATTTGTGGAAG	81.6		
276	σ2 L103S Fwd	CTTCCACAATGTCTGTGAACCTGGACAGTGTGTCAAACCTTCTACAAGGTTTACAC	80.9		
277	σ2 L103S Rev	GTGTAAACCTTGTAGAAAGTTGAACACACACTGTCCAGTTCACAGACATTTGTGGAAG	80.9		
278	σ2 F105A Fwd	GTCTGTGAACCTGGACCTGGTGGCCAACTTCTACAAGGTTTACACG	81.2		
279	σ2 F105A Rev	CGTGTAAACCTTGTAGAAAGTTGGCCACCAGGTCCAGTTCACAGAC	81.2		
280	σ2 N106A Fwd	GTCTGTGAACCTGGACCTGGTGTTCGCCCTTCTACAAGGTTTACACG	81.2		
281	σ2 N106A Rev	CGTGTAAACCTTGTAGAAAGGGCAACACCAGGTCCAGTTCACAGAC	81.2		
282	σ2 RK124,130EE Fwd	GCAGGAGAGATCGAAGAGACGAGCCAGACGGAGGTGCTGAAGCAG	82.6		
283	σ2 RK124,130EE Rev	CTGCTTCAGCACCTCCGTCCTGGTCTCGTCTCTTCGATCTCTCCCTGC	82.6		
284	CD4 5' T7 Fwd	TAATACGACTCACTATAGGGAGACCACGGGGGGTGCATCGTGGTGTAGCTTTCCAG	70.0		IVT Primers
285	CD4 3' T7 Rev	TAATACGACTCACTATAGGGAGACCACGGGGGGTGGATTCCAGCAGGACCTG	64.0		
286	GFP 5' T7 Fwd	TAATACGACTCACTATAGGGAGACCACGGGGGGTATGTGAGCAAGGGCGAGGAG	68.0		
287	GFP 3' T7 Rev	TAATACGACTCACTATAGGGAGACCACGGGGGGTGTCTCGTCCATGCCGAGAG	66.0		
288	Nef 5' T7 Fwd	TAATACGACTCACTATAGGGAGACCACGGGGGGTGGGAGCAGTATCTCGAG	64.0		
289	Nef 3' T7 Rev	TAATACGACTCACTATAGGGAGACCACGGGGGGTGCAGCTCTCGGGCCACG	60.0		
290	Dm CLC 5' T7 Fwd	TAATACGACTCACTATAGGGAGACCACGGGGGGTGTACGGGTGGATCTGCATCAG	64.0		
291	Dm CLC 3' T7 Rev	TAATACGACTCACTATAGGGAGACCACGGGGGGTAAACCAGTCCAGCTCCCTTC	66.0		
292	Dm Tsg101 5' T7 Fwd	TAATACGACTCACTATAGGGAGACCACGGGGGGTGTAGCAACTTTCCACCCTATCCCAC	72.0		
293	Dm Tsg101 3' T7 Rev	TAATACGACTCACTATAGGGAGACCACGGGGGGTGCATATCAATAATGTTCCGGCTC	64.0		
294	pHis Fwd	GATCTTCCCCATCGGTGATG	62.0		

**Table 2.9: DNA Primers used in this study, *continued*.**

#	Primer Name	Sequence (5' → 3')	T <sub>m</sub> (°C)	Type
295	pHis Rev	GTATGCTAGTTATTGCTCAGC	62.0	Sequencing Primers
296	pGEX Fwd	GTTGTATGACCGCTCTTGATGTTG	66.0	
297	pGEX Rev	CGTCTTCAAGAATTATACAC	66.0	
298	pST MCS1 Fwd	TAATACGACTCACTATAGGG	56.0	
299	pST MCS1 Rev	ACTGGCCGTCGTTTTACA	54.0	
300	pST MCS2 Fwd	TGTAAAACGACGGCCAGT	54.0	
301	pST MCS2 Rev	GACTGGGAAAACCCCTGGCG	62.0	
302	pST MCS3 Fwd	CGCCAGGGTTTCCCAGTC	62.0	
303	pST MCS3 Rev	TGTGAAATGTTATCCGCT	52.0	
304	pST MCS4 Fwd	AGCGATAACAATTCACA	52.0	
305	pST MCS4 Rev	GCTAGTTATTGCTCAGCGG	58.0	
306	pBridge MCS1 Fwd	CACATCTGACAGAAAGTGGAAATC	64.0	
307	pBridge MCS1 Rev	GTGCACCTGCCGGGCATGC	60.0	
308	pBridge MCS2 Fwd	CGTGTAAATACAGGGTCGTCAG	64.0	
309	pBridge MCS2 Rev	CGCTGAACCCGAACATAG	56.0	
310	pGADT7 Fwd	CAATTGCCCTCCTCTAACGTTT	62.0	
311	pGADT7 Rev	GCTTCTGAATAAGCCCTCG	68.0	
312	pAD MCS1 Fwd	CTTCATGAATAATGAAATCACGGC	66.0	
313	pAD MCS1 Rev	GTCCAAAGCTTCTGAATAAGC	60.0	
314	pAD MCS2 Fwd	CAGTTGGGATCTCGACTCTAG	68.0	
315	pAD MCS2 Rev	GCTGGCCTTTTGCTCACATG	62.0	
316	pAc Fwd	GAACGGACTTGAGAGCG	58.0	
317	pAc Rev	CTTATCATGTCTGGATCCTC	58.0	

**Table 2.9: DNA Primers used in this study, *continued*.**

#	Primer Name	Sequence (5' → 3')	T <sub>m</sub> (°C)	Type
318	pMt Fwd	GCTTCTGCACACGCTCCAC	64.0	Sequencing Primers
319	pMt Rev	ATTGCAGCTTATAATGGTTAC	56.0	
320	pCMV Fwd	CATTGACGTC AATGGGAGTTTG	64.0	
321	pCMV Rev	GCTGATTATGATCATGACAGAC	64.0	
322	pCI Fwd	GTAGCCTTGCAGAAAGTTGGTC	64.0	
323	pCI Rev	CGCCAGCCCCGGATCGATC	62.0	
324	pIRES.GFP Fwd	GCAGTACATCAATGGGGC	66.0	
325	pIRES.GFP Rev	GAAGCTTCCAGAGGAACTGC	62.0	
326	α 11 Fwd	GAGGCC TAGGGTCTTCATC	64.0	
327	α 159 Fwd	GACAGTGTGAGCAGAGCGC	64.0	
328	α 330 Fwd	GCAACCAGCTGGGCCAGTTC	66.0	
329	α 500 Fwd	CTACATCCTGGGCGAGTTTG	62.0	
330	α 676 Fwd	CACCTCTGGCGGTGGGTAC	66.0	

**Table 2.10: Antibodies used in this study**

The following table provides a list of all antibodies used in this study, along with their application, dilution, and the source from which they were obtained. Abbreviations (in alphabetical order): 1° (primary antibody), 2° (secondary antibody), APC (allophycocyanin), FACS (fluorescence activated cell sorting), CD (cluster of differentiation), FITC (fluorescein isothiocyanate), HIV (human immunodeficiency virus), HRP (horseradish peroxidase), IB (immunoblot), IF (immunofluorescence), IgG (immunoglobulin G), LAMP1 (lysosome-associated membrane protein 1), MHC-I (major histocompatibility complex class I), TCR (T cell receptor), TfR (transferrin receptor), PE (phycoerythrin).

**Table 2.10: Antibodies used in this study.**

#	Antibody name	1° or 2°	Application(s)	Dilution	Source
1	Unconjugated mouse IgG [Isotype control]	1°	FACS	1:100	Jackson ImmunoResearch
2	Unconjugated mouse anti-His <sub>6</sub> epitope	1°	IB	1:1000	Abcam
3	Unconjugated mouse anti-V5 epitope	1°	IB	1:2500	Invitrogen
4	Unconjugated mouse anti-human CD4	1°	FACS, IB, IF	1:100	Caltag
5	Unconjugated mouse anti-human CD71 [TfR]	1°	FACS	1:50	Sigma-Aldrich
6	Unconjugated mouse anti-human CD107a [LAMP1]	1°	FACS	1:50	Abcam
7	Unconjugated mouse anti-human $\alpha$ -adaptin clone 100/2	1°	IB	1:500	Sigma-Aldrich
8	Unconjugated mouse anti-human $\alpha$ -adaptin clone 8/Adaptin $\alpha$	1°	IB	1:1000	Becton Dickinson
9	Unconjugated mouse anti-human $\alpha$ -tubulin	1°	IB	1:1000	Sigma-Aldrich
10	Unconjugated rabbit anti-human $\mu$ 1A-adaptin	1°	IB	1:1000	Juan Bonifacino
11	Unconjugated rabbit anti-human $\mu$ 2-adaptin	1°	IB	1:1000	Juan Bonifacino
12	Unconjugated rabbit anti-human $\mu$ 3A-adaptin	1°	IB	1:1000	Juan Bonifacino
13	Unconjugated rabbit anti-HIV-1 Nef	1°	IB	1:1000	Ronald Swanstrom
14	Alexa 594-conjugated donkey anti-mouse IgG	2°	IF	1:100	Invitrogen
15	APC-conjugated mouse anti-human CD4	2°	FACS	1:100	Caltag
16	APC-conjugated goat anti-mouse IgG	1°	FACS	1:100	Jackson ImmunoResearch
17	FITC-conjugated mouse anti-human CD2	1°	FACS	1:100	Invitrogen
18	FITC-conjugated mouse anti-human CD7	1°	FACS	1:100	Serotec
19	FITC-conjugated mouse anti-human CD11a	1°	FACS	1:100	Invitrogen
20	FITC-conjugated mouse anti-human CD18	1°	FACS	1:100	Becton Dickinson
21	FITC-conjugated mouse anti-human CD31	1°	FACS	1:100	Becton Dickinson
22	FITC-conjugated mouse anti-human CD44	1°	FACS	1:100	Invitrogen
23	FITC-conjugated mouse anti-human CD45RA	1°	FACS	1:100	Invitrogen
24	FITC-conjugated mouse anti-human CD52	1°	FACS	1:100	Abcam
25	FITC-conjugated mouse anti-human CD54	1°	FACS	1:100	Invitrogen

**Table 2.10: Antibodies used in this study, continued.**

#	Antibody name	1° or 2°	Application(s)	Dilution	Source
26	FITC-conjugated mouse anti-human CD57	1°	FACS	1:100	Becton Dickinson
27	FITC-conjugated mouse anti-human CD69	1°	FACS	1:100	Becton Dickinson
28	FITC-conjugated mouse anti-human CD71 [TfR]	1°	FACS	1:100	Sigma-Aldrich
29	FITC-conjugated mouse anti-human CD75	1°	FACS	1:100	Becton Dickinson
30	FITC-conjugated mouse anti-human CD94	1°	FACS	1:100	Becton Dickinson
31	FITC-conjugated mouse anti-human CD103	1°	FACS	1:100	Invitrogen
32	FITC-conjugated mouse anti-human CD107a [LAMP1]	1°	FACS	1:50	Abcam
33	FITC-conjugated mouse anti-human MHC-I	1°	FACS	1:100	Invitrogen
34	HRP-conjugated sheep anti-mouse IgG	2°	IB	1:7500	GE Healthcare
35	HRP-conjugated donkey anti-rabbit IgG	2°	IB	1:8500	GE Healthcare
36	PE-conjugated mouse IgG1 [Isotype control]	1°	FACS	1:100	Abcam
37	PE-conjugated mouse IgG2a [Isotype control]	1°	FACS	1:100	Abcam
38	PE-conjugated mouse anti-human CD1	1°	FACS	1:100	US Biological
39	PE-conjugated mouse anti-human CD3	1°	FACS	1:100	Becton Dickinson
40	PE-conjugated mouse anti-human CD4	1°	FACS	1:100	Caltag
41	PE-conjugated mouse anti-human CD5	1°	FACS	1:100	Invitrogen
42	PE-conjugated mouse anti-human CD8	1°	FACS	1:100	Caltag
43	PE-conjugated mouse anti-human CD9	1°	FACS	1:100	Becton Dickinson
44	PE-conjugated mouse anti-human CD25	1°	FACS	1:100	Invitrogen
45	PE-conjugated mouse anti-human CD27	1°	FACS	1:100	Abcam
46	PE-conjugated mouse anti-human CD28	1°	FACS	1:100	Abcam
47	PE-conjugated mouse anti-human CD34	1°	FACS	1:100	Becton Dickinson
48	PE-conjugated mouse anti-human CD38	1°	FACS	1:100	Abcam
49	PE-conjugated mouse anti-human CD45	1°	FACS	1:100	Invitrogen
50	PE-conjugated mouse anti-human CD45RO	1°	FACS	1:100	Invitrogen
51	PE-conjugated mouse anti-human CD59	1°	FACS	1:100	Becton Dickinson

**Table 2.10: Antibodies used in this study, continued.**

#	Antibody name	1° or 2°	Application(s)	Dilution	Source
52	PE-conjugated mouse anti-human CD62L	1°	FACS	1:100	Invitrogen
53	PE-conjugated mouse anti-human CD71 [TfR]	1°	FACS	1:50	Sigma-Aldrich
54	PE-conjugated mouse anti-human CD97	1°	FACS	1:100	Becton Dickinson
55	PE-conjugated mouse anti-human CD101	1°	FACS	1:100	Abcam
56	PE-conjugated mouse anti-human CD109	1°	FACS	1:100	Becton Dickinson
57	PE-conjugated mouse anti-human CD120b	1°	FACS	1:100	Invitrogen
58	PE-conjugated mouse anti-human CD122	1°	FACS	1:100	Becton Dickinson
59	PE-conjugated mouse anti-human CD126	1°	FACS	1:100	Becton Dickinson
60	PE-conjugated mouse anti-human CD127	1°	FACS	1:100	Becton Dickinson
61	PE-conjugated mouse anti-human CD132	1°	FACS	1:100	Becton Dickinson
62	PE-conjugated mouse anti-human CD134	1°	FACS	1:100	Invitrogen
63	PE-conjugated mouse anti-human CD137	1°	FACS	1:100	Becton Dickinson
64	PE-conjugated mouse anti-human CD150	1°	FACS	1:100	Abcam
65	PE-conjugated mouse anti-human CD152	1°	FACS	1:100	Becton Dickinson
66	PE-conjugated mouse anti-human CD154	1°	FACS	1:100	Becton Dickinson
67	PE-conjugated mouse anti-human CD161	1°	FACS	1:100	Abcam
68	PE-conjugated mouse anti-human CD166	1°	FACS	1:100	Becton Dickinson
69	PE-conjugated mouse anti-human CD184	1°	FACS	1:100	Caltag
70	PE-conjugated mouse anti-human CD185	1°	FACS	1:100	Becton Dickinson
71	PE-conjugated mouse anti-human CD195	1°	FACS	1:100	Becton Dickinson
72	PE-conjugated mouse anti-human CD212	1°	FACS	1:100	Becton Dickinson
73	PE-conjugated mouse anti-human CD247	1°	FACS	1:100	Abcam
74	PE-conjugated mouse anti-human TCR $\alpha\beta$	1°	FACS	1:100	Abcam
75	PE-conjugated mouse anti-human TCR $\gamma\delta$	1°	FACS	1:100	Abcam
76	PE-conjugated goat anti-mouse IgG1	2°	FACS	1:100	Jackson ImmunoResearch

**Chapter 3:**  
**Downregulation of CD4 by HIV-1 Nef is dependent on clathrin and involves a  
direct interaction of Nef with the AP-2 clathrin adaptor**

### 3.1 Abstract

Nef, an accessory protein of human and simian immunodeficiency viruses, is a critical determinant of pathogenesis that promotes progression of the disease from infection to AIDS. The pathogenic effects of Nef are in large part dependent on its ability to downregulate the macrophage and T cell co-receptor, CD4. It has been proposed that Nef induces downregulation by linking the cytosolic tail of CD4 to components of the host-cell protein trafficking machinery. To identify these components, a novel Nef-CD4 downregulation system was developed in *Drosophila melanogaster* S2 cells. It was found that human immunodeficiency virus type 1 (HIV-1) Nef downregulates human CD4 in S2 cells, and that this process is subject to the same sequence requirements as in human cells. An RNA interference screen targeting protein trafficking genes in S2 cells revealed a requirement for clathrin and the clathrin-associated, plasma membrane-localized AP-2 complex in the downregulation of CD4. The requirement for AP-2 was confirmed in the human HeLa cell line. Yeast three-hybrid and glutathione *S*-transferase pull down assays were also used to demonstrate a robust, direct interaction between HIV-1 Nef and AP-2. This interaction requires a dileucine motif in Nef that is also essential for downregulation of CD4. Together, these results support a model in which HIV-1 Nef downregulates CD4 by promoting its accelerated endocytosis via a clathrin/AP-2 pathway.

### 3.2 Introduction

As mentioned earlier, the primary goal of this thesis is to determine the mechanism of Nef-mediated CD4 downregulation (see Section 1.9). Previous studies have revealed that several regions of Nef are essential for this process, including the myristoylation site, the hydrophobic pocket, and the dileucine motif (see Fig. 1.7; Stove et al., 2005). Myristoylation allows Nef to associate with intracellular membranes, where it binds to the cytosolic tail of CD4 via the hydrophobic pocket (Grzesiek et al., 1996; Harris and Neil, 1994; Peng and Robert-Guroff, 2001; Yu and Felsted, 1992). The role of the dileucine motif is less certain, although it has been suggested to connect Nef to some components of the host-cell protein trafficking machinery, such as the clathrin adaptor protein complexes (Bresnahan et al., 1998; Craig et al., 1998; Greenberg et al., 1998; Mangasarian et al., 1997; Janvier et al., 2003b). However, each AP complex controls protein sorting at a different location within the cell, leaving in doubt the pathway that Nef might use to downregulate CD4 (see Section 1.6).

Prior attempts to clarify this pathway by depleting human cells of the AP complexes have produced conflicting results, probably due to low RNAi transfection efficiencies and incomplete knockdowns (Jin et al., 2005; Rose et al., 2005). In the next section, a similar RNAi-based approach will be utilized to determine which AP complex is most important for the downregulation of CD4, and to screen for other endogenous proteins that might participate in this process. However, the initial RNAi experiments will be performed on *Drosophila melanogaster* S2 cells expressing Nef and CD4; compared to human cells, S2 cells are easier to transfect and are therefore more suitable for use in RNAi screens (see Agaisse et al., 2005; Derré et al., 2007; Elwell and Engel, 2005; Philips et al., 2005; Ramet et al., 2002). Once the RNAi screen is finished, homologs of the most promising candidates will be knocked down in HeLa cells. Although these human cells are less amenable to RNAi treatment than the *Drosophila* S2 cells, they provide a more physiologically relevant setting in which to evaluate the contribution of endogenous proteins to the Nef-mediated downregulation of CD4. In vitro binding assays will then be used to determine whether one of these proteins interacts directly with Nef, and if so, whether this interaction depends on the dileucine motif described above. When taken together, the data from the RNAi and in vitro binding experiments should yield a clearer understanding of how Nef modulates CD4 expression.

### 3.3 Results

#### 3.3.1 Downregulation of human CD4 by HIV-1 in *Drosophila* S2 cells

To identify host cell factors that are required for the downregulation of CD4 by Nef, an RNAi screen was performed using the *Drosophila melanogaster* S2 cell line. This system was chosen because the efficiency of RNAi and DNA transfections is nearly 100%, RNAi treatment is carried out by the simple addition of dsRNA to the tissue culture medium, and an RNAi library targeting most of the *Drosophila* genome was available at a reasonable price. This approach was predicated on the assumption that HIV-1 Nef would be able to downregulate human CD4 in the *Drosophila* cells. To determine whether this was indeed the case, S2 cells were transiently co-transfected with a plasmid driving constitutive expression of human CD4 (pAc.CD4; see Section 2.5.1.1) and another plasmid driving Cu<sup>2+</sup>-inducible expression of the NL4-3 variant of HIV-1 Nef (pMt.Nef<sub>NL4-3</sub>; see Section 2.5.1.2). Immunoblot analysis revealed that both CD4 and Nef were expressed in the transfected S2 cells; as expected, Nef was apparent only in cells incubated with Cu<sup>2+</sup> (Fig. 3.1A). Importantly, in the absence of Nef expression, CD4 was detected on the plasma membrane of S2 cells by flow cytometry (Fig. 3.1B) and immunofluorescence microscopy (Fig 3.1C). The induction of Nef expression by the addition of Cu<sup>2+</sup> (in the form of CuSO<sub>4</sub>) caused an approximately 3-fold reduction in the surface level of CD4 (Fig 3.1B) and its redistribution to intracellular vesicles (Fig. 3.1C). These effects of Nef expression on CD4 distribution were similar to those previously demonstrated in human cells by others (Fig. 1.11; Aiken et al., 1994; Garcia and Miller, 1991; Rose et al., 2005).

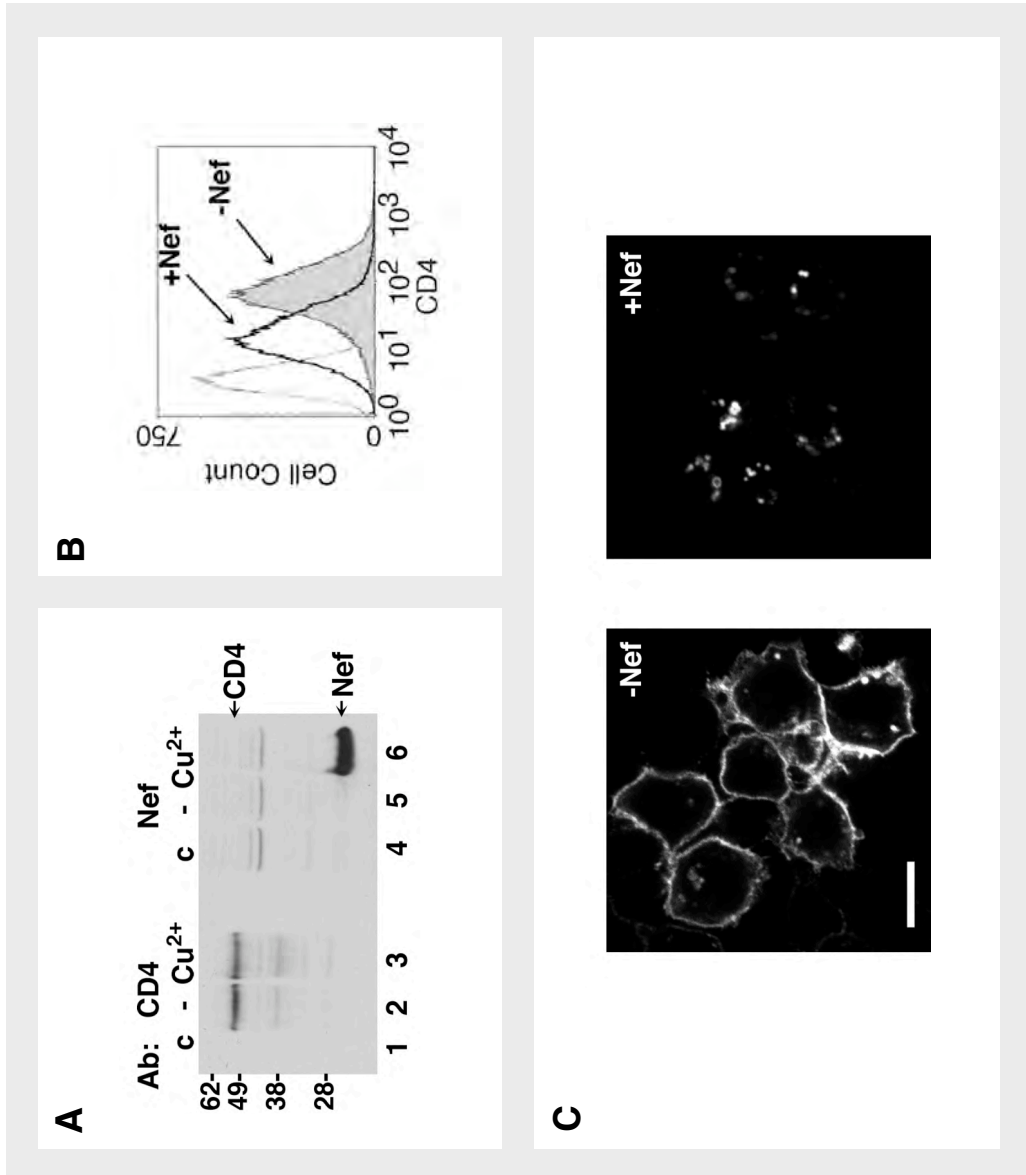
#### 3.3.2 Determinants of Nef-induced CD4 downregulation in S2 cells

Next, the ability of several Nef alleles to downregulate CD4 in *Drosophila* S2 and human JM CD4<sup>+</sup> T cells was tested. Despite high primary sequence variability among different HIV-1 and SIV clades, the ability to downregulate CD4 in human cells is a strongly conserved feature of Nef proteins (Benson et al., 1993; Hua et al., 1997; Janvier et al., 2003b; Mariani and Skowronski, 1993). S2 cells were co-transfected with pAc.CD4 and pMt.Nef plasmids (see Section 2.5.1.2), while CD4<sup>+</sup> JM cells were transfected with pNef.IRES.GFP plasmids (see Section 2.6.1.3). CD4 surface levels were measured by flow cytometry. The data showed that all four HIV-1 Nef variants

**FIG. 3.1: Downregulation of human CD4 by HIV-1 Nef in *Drosophila* S2 cells**

- (A)** Immunoblot analysis of S2 cells 48 hours after transfection with the pAc.CD4 and pMt.Nef<sub>NL4-3</sub> plasmids, and 24 hours after induction of Nef expression with CuSO<sub>4</sub>. Lysates from untransfected control (lanes 1 and 4) and doubly transfected cells either without (lanes 2 and 5) or with (lanes 3 and 6) Cu<sup>2+</sup> induction were analyzed by immunoblotting with antibodies (Ab) to CD4 and Nef. The positions of molecular mass markers (in kilodaltons [kDa]) are shown on the left.
- (B)** S2 cells transfected with pAc.CD4 and pMt.Nef<sub>NL4-3</sub>, incubated without (shaded gray) or with (bold line) CuSO<sub>4</sub>, and stained with mouse monoclonal antibody to human CD4 and PE-conjugated goat antibody to mouse IgG. Untransfected cells were also stained as a negative control (light gray line) in order to demonstrate specificity of the antibody. After staining, the cells were analyzed by flow cytometry. The *x* axis represents CD4 fluorescence on a logarithmic scale, and the *y* axis represents the number of cells on a linear scale.
- (C)** Immunofluorescence microscopy of CD4 in S2 cells. Cells were transfected with pAc.CD4 and pMt.Nef<sub>NL4-3</sub>, incubated for 24 hours, and either left untreated (i.e., -Nef) or treated with CuSO<sub>4</sub> (i.e., +Nef) for another 24 hours, fixed, permeabilized, and stained with mouse monoclonal antibody to human CD4 and AlexaFluor 594-conjugated donkey antibody to mouse IgG. Stained cells were examined by confocal microscopy. Bar, 5  $\mu$ m.

**FIG. 3.1**



tested (from the NL4-3, NA7, DH12-3, and 248 strains), as well as an SIV Nef variant (mac239), significantly reduced CD4 surface levels in both S2 and JM cells (Fig. 3.2).

Further evidence for the suitability of a CD4-Nef expression system in S2 cells was obtained by pairwise comparisons of various NL4-3 Nef mutants in S2 and JM cells (see Roeth and Collins, 2006 for a review of Nef functional domains). S2 cells were co-transfected with pAc.CD4 and wild-type or mutant pMt.NL4-3 Nef plasmids (see Section 2.5.1.2), while the CD4<sup>+</sup> JM cells were transfected with wild-type or mutant pNef<sub>NL4-3</sub>.IRES.GFP plasmids (see Section 2.6.1.3). As before, CD4 surface levels were measured by flow cytometry (Fig. 3.3). For both S2 and JM cells, mutation of the Nef myristoylation site (G2A), CD4-binding site (WL57,58AA), and dileucine motif (LL164,165AA) abrogated the ability of the viral protein to downregulate CD4. On the other hand, mutation of the acidic cluster (EEEE62-65AAAA) and the polyproline motif (PP72,75AA), which are required for downregulation of the major histocompatibility complex class I (MHC-I) receptor (Janvier et al., 2001; Piguet et al., 2000), had no effect on the ability of Nef to modulate CD4 surface levels in both S2 and JM cells. Immunofluorescence assays confirmed that the Nef WL57,58AA and LL164,165AA mutant proteins did not alter the plasma membrane-localization of CD4 in S2 cells, while the Nef EEEE62-65AAAA and PP72,75AA mutants redirected CD4 from the surface to intracellular vesicles (Fig. 3.4). Thus, identical motifs on Nef are required for the downregulation of CD4 in S2 and JM cells. Another hallmark of Nef-mediated CD4 downregulation in human cells is the requirement of a pair of leucines in the CD4 cytosolic tail (Aiken et al., 1994; Anderson et al., 1994). In a similar fashion, mutation of the CD4 dileucine motif (LL413,414AA) also prevented downregulation of the receptor in S2 cells (Fig. 3.3A).

Taken together, these data provide strong evidence that the downregulation of CD4 by HIV-1 Nef occurs via a similar mechanism in S2 and JM cells, and likely involves homologous host-cell trafficking proteins. S2 cells were therefore considered to be a suitable system for an RNAi screen aimed at identifying host-cell proteins involved in Nef-induced CD4 downregulation.

**FIG. 3.2: Comparison of the downregulation of CD4 by Nef from various HIV-1 and SIV variants in *Drosophila* S2 and human JM CD4<sup>+</sup> T cells**

(A) Flow cytometric histograms of *Drosophila* S2 cells that were co-transfected with pAc.CD4 and pMt vectors encoding a variety of HIV-1 (NL4-3, NA7, DH12-3, and 248) and SIV (mac239) Nef alleles, incubated without (shaded gray) or with CuSO<sub>4</sub> (bold line), and then stained with a mouse monoclonal antibody to human CD4 and a PE-conjugated goat antibody to mouse IgG. Uninduced control cells were also stained with a non-specific mouse monoclonal IgG (as an isotype antibody control) and the aforementioned PE-conjugated goat antibody to mouse IgG (light gray line) in order to demonstrate the level of background fluorescence.

(B) Bar graph depicting the levels of cell surface CD4 in *Drosophila* S2 cells co-transfected with pAc.CD4 and pMt.Nef encoding various HIV-1 and SIV alleles (dark gray) and in human JM CD4<sup>+</sup> T cells transfected with pNef.IRES.GFP encoding the same HIV-1 and SIV alleles (light gray). S2 cells were stained with appropriate antibodies 24 hours after Nef induction with CuSO<sub>4</sub>, and the JM cells were stained 24 hours after transfection, as described in the Materials and Methods (Sections 2.4.2.2 and 2.5.2.2). For S2 cells, the control represents the amount of CD4 on the surface of cells transfected with NL4-3 Nef, but left uninduced. For JM cells, the control represents the amount of CD4 on the surface of cells transfected with the empty vector, pIRES.GFP. In order to compare between different cell types, CD4 surface levels are shown as a percentage of the control condition. Numerical values depicted in the bar graph are the mean relative CD4 surface level percentage  $\pm$  the standard error of the mean (SEM) from three independent experiments.

**FIG. 3.2**

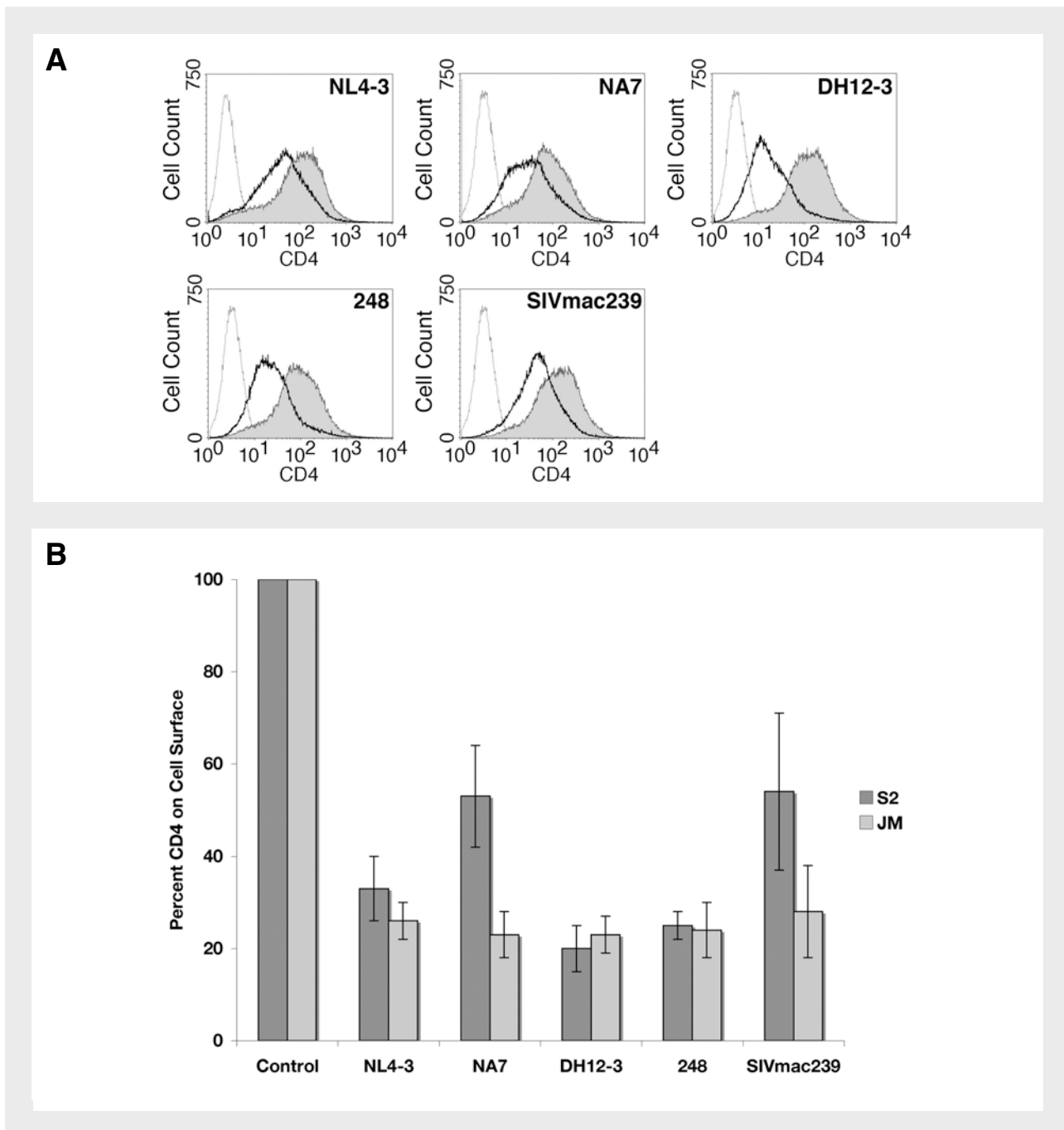


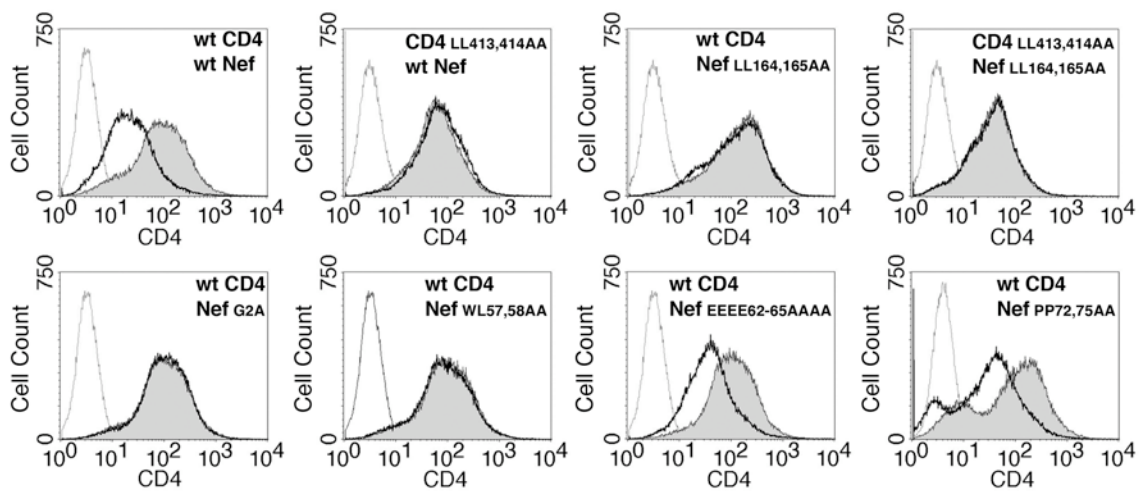
**FIG. 3.3: Determinants of Nef-induced CD4 downregulation in *Drosophila* S2 and human JM CD4<sup>+</sup> T cells**

(A) Flow cytometric histograms of *Drosophila* S2 cells co-transfected with pairs of pAc.CD4 and pMt.Nef<sub>NL4-3</sub> plasmids, encoding wild-type or mutant versions of CD4 and NL4-3 Nef, respectively. Following transfection, the cells were either left untreated (shaded gray) or treated with CuSO<sub>4</sub> to induce Nef expression (bold line). The cells were then stained with mouse monoclonal antibody to human CD4 and PE-conjugated goat antibody to mouse IgG. Uninduced control cells were also stained with an isotype antibody control and PE-conjugated goat antibody to mouse IgG (light gray line).

(B) Bar graph depicting the level of CD4 on the plasma membrane of *Drosophila* S2 cells co-transfected with pAc.CD4 and wild-type or mutant versions of pMt.Nef<sub>NL4-3</sub> (dark gray) and human JM CD4<sup>+</sup> T cells transfected with wild-type or mutant versions of pNef<sub>NL4-3</sub>.IRES.GFP (light gray). S2 cells were stained with antibodies 24 hours after induction of Nef expression with CuSO<sub>4</sub>, while JM cells were stained 24 hours after transfection. The controls are the same as those described in Fig. 3.2B: for S2 cells, the control represents the amount of CD4 on the surface of cells transfected with wild-type Nef and left uninduced, while for JM cells, the control represents the amount of CD4 on the surface of cells transfected with the empty vector, pIRES.GFP. To compare between different cell types, CD4 surface levels in cells transfected with the various Nef mutants are shown as a percentage of the control condition. Values are the mean relative CD4 surface level percentage  $\pm$  SEM from three independent experiments.

**FIG. 3.3**

**A**



**B**

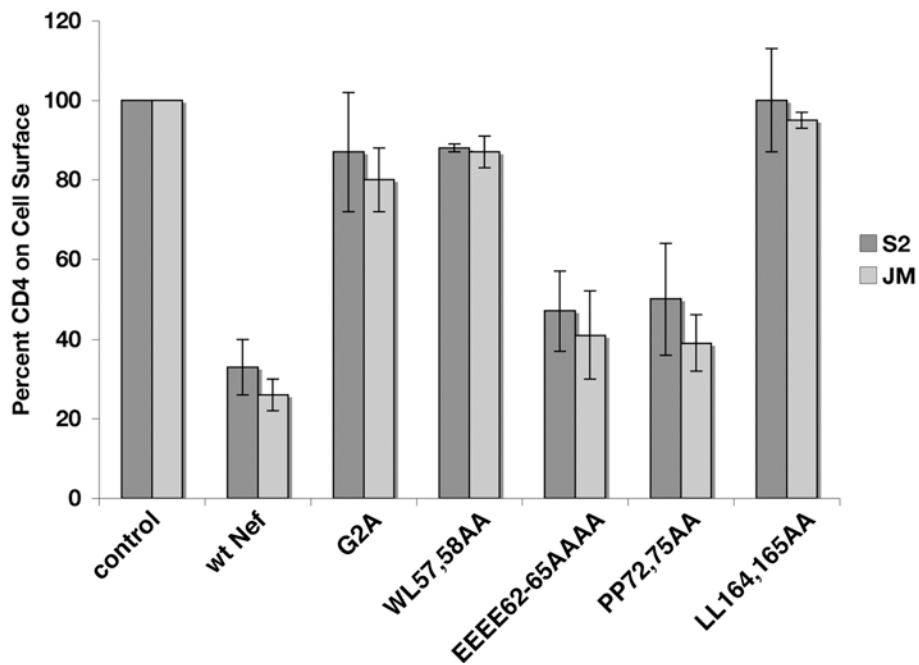
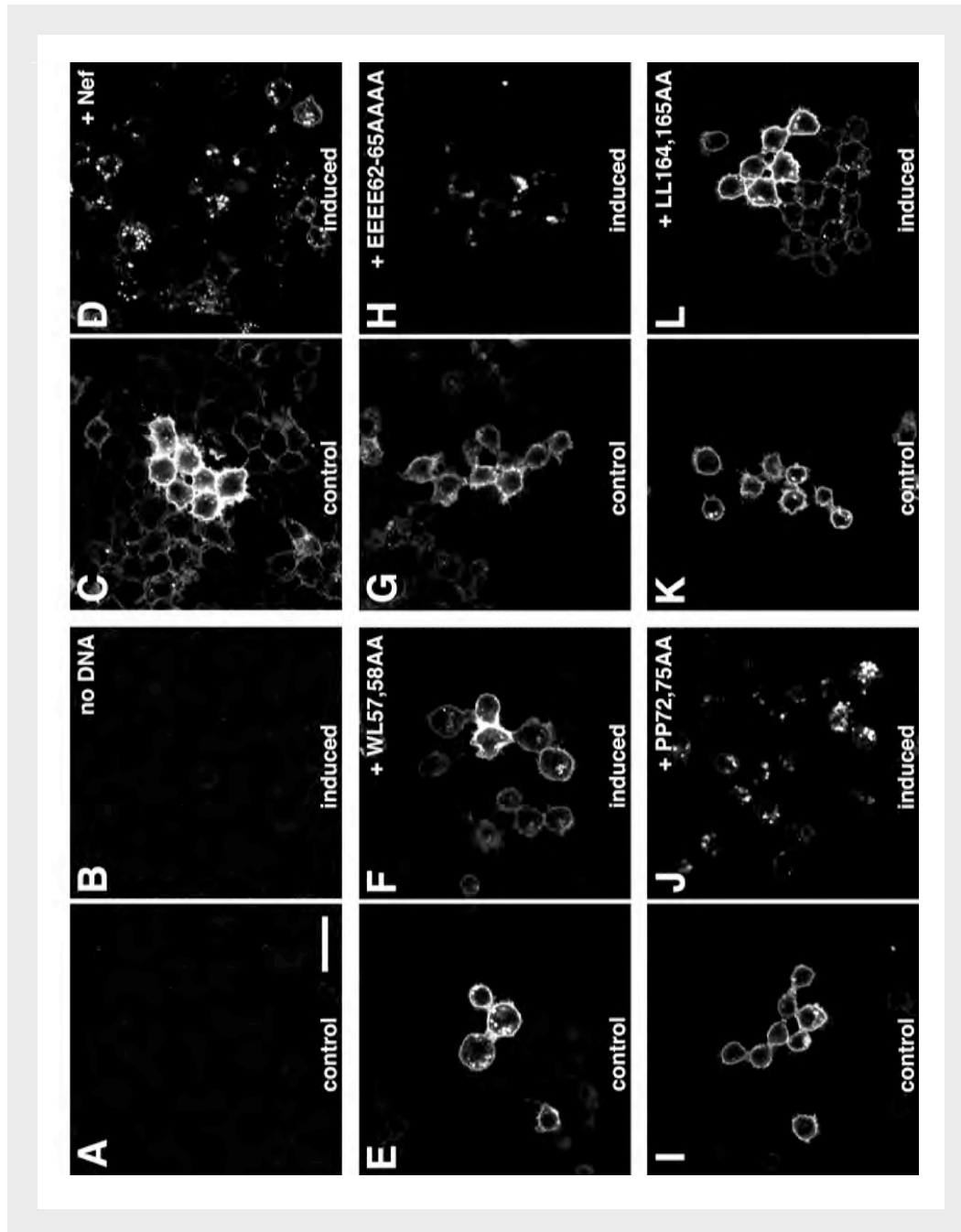


**FIG. 3.4: Immunofluorescence microscopy of CD4 in S2 cells**

S2 cells were transiently transfected with pAc.CD4 and pMt.Nef<sub>NL4-3</sub> (wild-type or the indicated mutant), incubated for 24 hours, and left uninduced (**C**, **E**, **G**, **I**, and **K**) or induced with CuSO<sub>4</sub> (**D**, **F**, **H**, **J**, and **L**) for another 24 hours. The cells were then fixed, permeabilized, and stained with mouse monoclonal antibody to human CD4 and AlexaFluor 594-conjugated donkey antibody to mouse IgG. Untransfected cells treated in a similar manner (**A** and **B**) were also stained as a control for antibody specificity. Stained cells were examined by confocal microscopy. Bar, 10  $\mu$ m.

FIG. 3.4



### 3.3.3 RNAi screen in S2 cells reveals a requirement for clathrin and AP-2 in the Nef-induced downregulation of CD4

Prior to conducting the RNAi screen, it was necessary to generate a stable CD4-Nef S2 cell line, and then to test the efficiency of RNAi-treatment on these cells. The wild-type pAc.CD4 and pMt.NL4-3 Nef plasmids were used to transfect S2 cells, from which a monoclonal cell line was chosen for its uniform surface expression of CD4 and consistent,  $\text{Cu}^{2+}$ -inducible downregulation of CD4 by Nef (see Materials and Methods, Section 2.5.2.3). The ability of RNAi to reduce protein expression levels in these cells was tested by the addition of dsRNAs targeted against CD4 and Nef (Fig. 3.5A). Compared to the negative control (a dsRNA targeting GFP, which is absent in these cells), the dsRNA directed against CD4 knocked down surface levels of this protein by approximately 85%, as measured by flow cytometry (Fig. 3.5A and Table 3.1). In addition, treatment of the stable cells with dsRNA targeted to Nef completely abolished the normal  $\text{Cu}^{2+}$ -induced downregulation of CD4 (Fig. 3.5A and Table 3.1), demonstrating that Nef expression had been effectively eliminated. The nearly complete elimination of surface CD4 expression and Nef function by dsRNA-treatment was taken as a general indicator of the effectiveness of RNAi in this system. To further assess the efficiency of RNAi in S2 cells, several epitope-tagged proteins were introduced into the cells by transient transfection, targeted for knockdown with dsRNAs, and then subjected to immunoblot analysis (Fig. 3.5C). Upon treatment with gene-specific dsRNAs, there was a significant reduction in the expression of these proteins relative to treatment with a non-specific dsRNA (Fig. 3.5C). Endogenous protein levels were not measured for this assay (or for the larger RNAi screen) due to a lack of available antibodies for most targets.

Given the effectiveness of RNAi knockdowns in S2 cells, it appeared reasonable to proceed with the larger RNAi screen. A total of 68 components of the *Drosophila* protein-trafficking machinery were screened for their potential contribution to the Nef-mediated downregulation of CD4. The targets included clathrin and clathrin-associated proteins, non-clathrin coat proteins, components of the multivesicular body (MVB) and endosomal recycling machineries, actin-associated proteins, components of the ubiquitin-modification machinery, phosphoinositide metabolism enzymes, and miscellaneous others (Table 3.1). For each protein tested in the screen, the stable

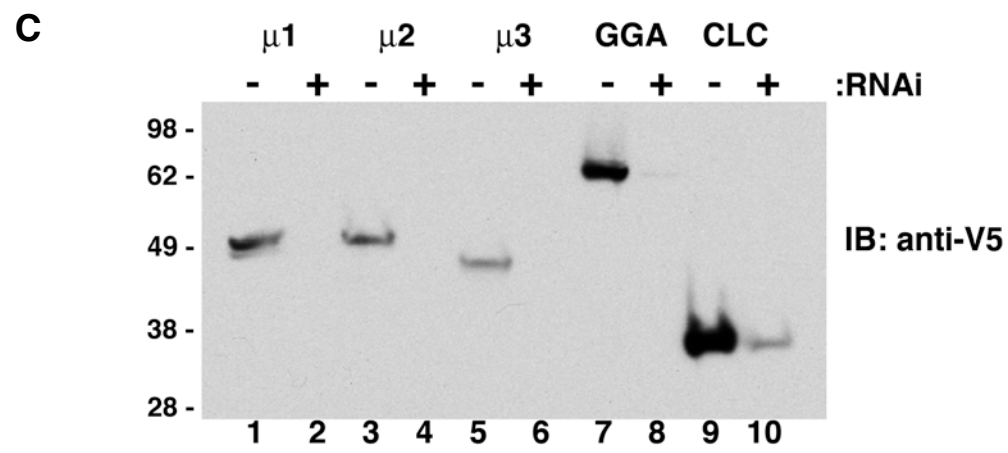
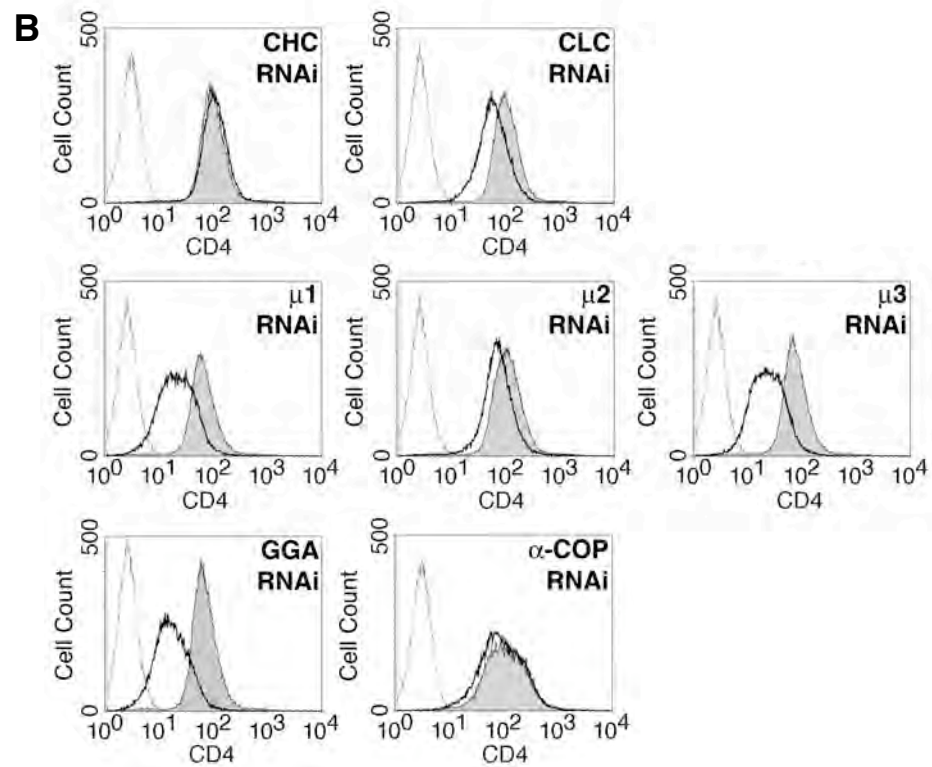
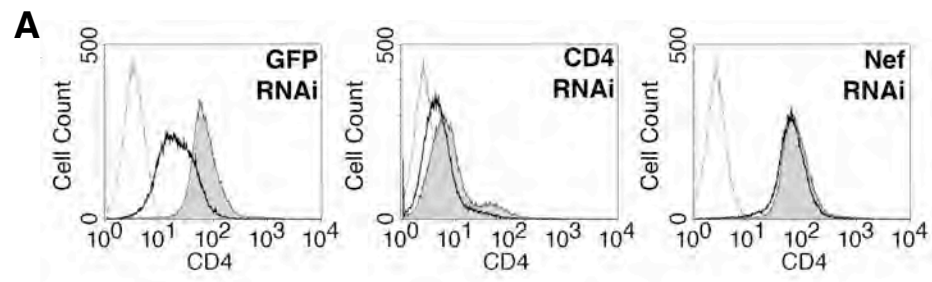
**FIG. 3.5: Effect of selected RNAi treatments on the Nef-induced downregulation of CD4 in stably transfected S2 cells**

(A) CD4 expression profiles of S2 cells stably expressing CD4 and Nef (the latter under the control of an inducible promoter), after treatment with dsRNAs targeting GFP (non-targeting control), CD4 (no CD4 expression control), and Nef (no down-regulation control). A portion of the dsRNA-treated cells were left uninduced (shaded gray), while the remainder were incubated with CuSO<sub>4</sub> to induce Nef expression (bold line). The cells were then stained with mouse monoclonal antibody to human CD4 and PE-conjugated goat antibody to mouse IgG. Cells stained with an isotype control and the PE-conjugated secondary antibody (light gray line) are also included as a measure of background fluorescence.

(B) CD4 expression profiles of S2 cells stably expressing CD4 and Nef (the latter under the control of an inducible promoter), after treatment with dsRNAs targeting the clathrin subunits CHC and CLC;  $\alpha$ -COP; AP-complex subunits  $\mu$ 1,  $\mu$ 2, and  $\mu$ 3; and GGA. Induction and staining of the dsRNA-treated cells was carried out as described above.

(C) Immunoblot (IB) analysis of lysates from S2 cells transiently transfected with V5-epitope-tagged *Drosophila* genes ( $\mu$ 1,  $\mu$ 2,  $\mu$ 3, GGA, and CLC). After transfection, each group of cells was seeded into two tissue culture wells and received dsRNA targeting either GFP (negative control; lanes 1, 3, 5, 7, and 9) or the specific transgene (lanes 2, 4, 6, 8, and 10). Lysates were subjected to SDS-PAGE and probed with anti-V5 monoclonal antibody. Positions of molecular mass markers (in kDa) are shown on the left.

**FIG. 3.5**



CD4-Nef S2 cells were treated with a specific dsRNA, incubated for 3 days, and then split into two parallel cultures. One culture was left uninduced, while Nef expression was induced in the other culture by the addition of CuSO<sub>4</sub>. After 24 hours, the CD4 surface levels of both uninduced and induced cells were measured by flow cytometry. The entire screen was conducted in duplicate, and most targets were tested additional times for purposes of confirmation.

The results for the RNAi screen are shown in Fig. 3.5B (histograms for selected targets), Fig. 3.6 (scatter plot of all the data), and Table 3.1 (numerical values for all data). Most of the RNAi treatments, including the non-targeting negative control, fall along a single regression line with a slope of 0.45 on the scatter plot (Fig. 3.6), indicating that these dsRNAs had no effect on the ability of Nef to downregulate CD4. This slope corresponds to an average downregulation of 2.2-fold for the entire data set, which is roughly equivalent to the observed value of approximately 2-fold in untreated cells. Because in most cases it is not known if the RNAi treatments caused effective elimination of the target proteins, it is not possible to rule out the involvement of the targets which tested negative in this screen. In addition, some targets that produced minor effects were difficult to replicate beyond the initial screen due to mild toxicity (see Table 3.1). A small number of dsRNAs, however, produced reliable outliers, evidence that they interfered with the ability of Nef to modulate CD4 expression. These included dsRNAs targeting the clathrin heavy chain (CHC), the clathrin light chain (CLC), the  $\mu$ 2 subunit of AP-2, and  $\alpha$ -COP (Fig. 3.5B and 3.6; Table 3.1). There also appeared to be a mild inhibition in cells treated with a dsRNA targeting Vps41, but the relatively large variation between experimental replicates precluded the assignment of this target as a true hit.

The CHC dsRNA displayed the strongest inhibition on Nef function, and was nearly as effective as the dsRNA that targeted Nef itself (Fig. 3.5B and 3.6; Table 3.1). A dsRNA targeting CLC had a weaker, but reproducible effect on Nef function (Fig. 3.5B and 3.6; Table 3.1). These findings are consistent with previously proposed models of Nef-induced CD4 downregulation that invoke a role for clathrin-dependent trafficking intermediaries. Nevertheless, these results are the first to directly demonstrate that clathrin is required for the Nef-mediated downregulation of CD4. A dsRNA targeting the  $\mu$ 2 subunit of AP-2 reduced Nef activity by roughly half in this

**FIG. 3.6: Results of the RNAi screen of 68 components of the protein trafficking machinery for their involvement in Nef-induced CD4 downregulation in S2 cells**

The mean CD4 surface levels ( $\pm$  the SEM;  $n = 2$  to 10) of cells treated with dsRNAs targeting 68 candidate and 3 control genes (see Table 3.1) are represented on an  $x$ - $y$  plot. Each datum point on the plot represents surface CD4 levels, as measured by flow cytometry, for cells treated with a particular dsRNA. The position on the  $x$  axis indicates the amount of CD4 on the cell surface without induction, while the position on the  $y$  axis indicates the amount of CD4 on the cell surface upon induction of Nef expression, in relative fluorescence units (rfu). According to this rubric, data points that have the same amount of CD4 expression in the absence and presence of Nef indicate dsRNA treatments that completely inhibited the ability of Nef to downregulate CD4. A least-squares fit regression line (solid black line) for the entire data set with 95% confidence intervals (dashed lines) is shown. The line  $y = x$  (gray line), indicating the position of no downregulation, has also been added to the plot. Data points for control targets are shown in **green**, while data points for selected targets from the screen are shown in **red**.

FIG. 3.6

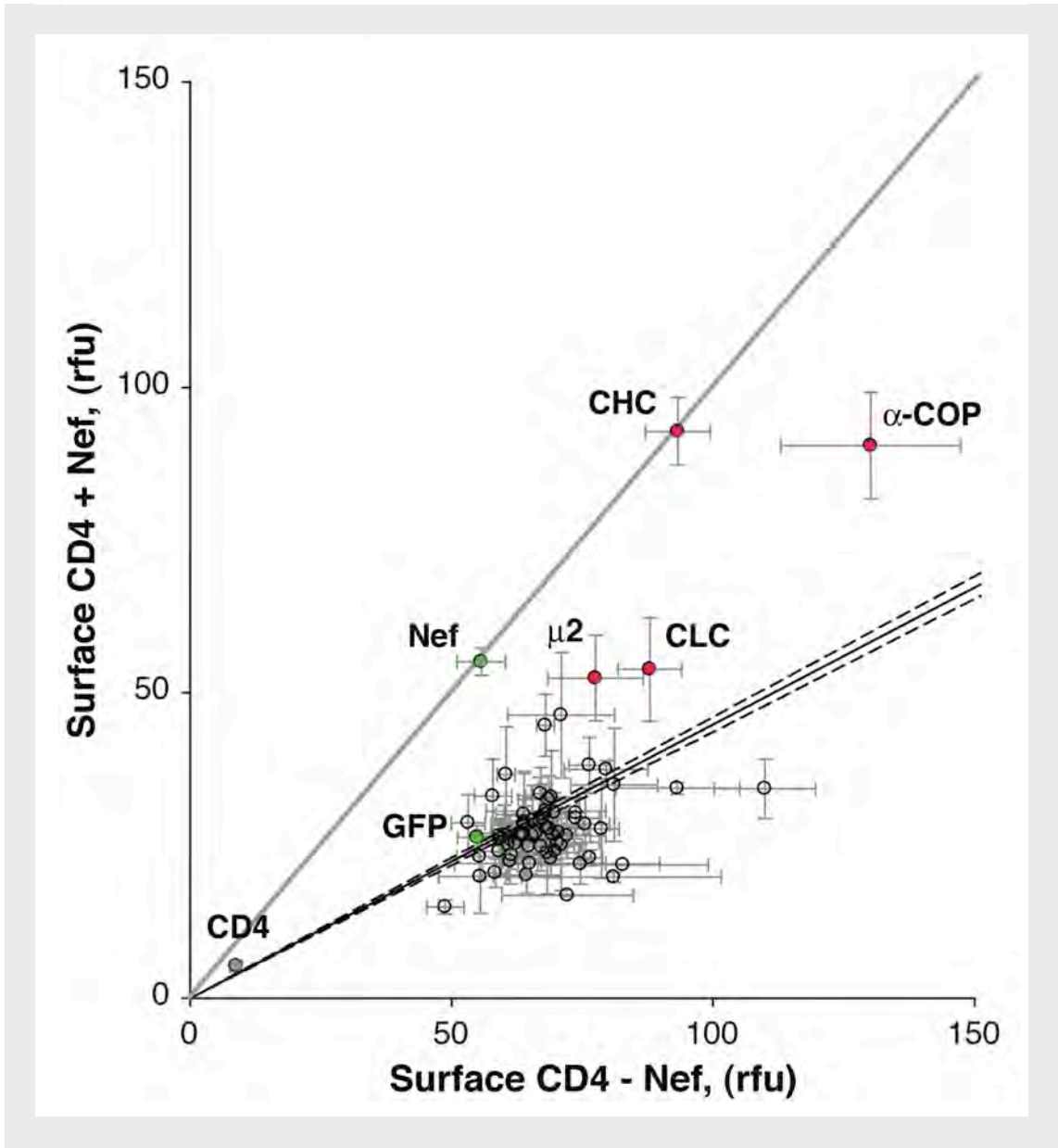


### **Table 3.1: Raw data from the RNAi screen of endogenous proteins involved in the Nef-mediated downregulation of CD4 in S2 cells**

Host-cell proteins were depleted by RNAi in S2 cells, and the effect of this depletion on Nef-induced CD4 downregulation was measured by flow cytometry. The raw data from this screen are presented below. RNAi targets are listed on the left-hand side, and are organized by ascending CG number (note that the first three genes targeted for depletion [GFP, CD4, and Nef] are heterologous controls and therefore do not have CG numbers). For all other RNAi targets, the human ortholog is also listed. Each target was depleted several times ( $n = 2$  to 10, see Number of Trials column), and the data shown represent the average CD4 fluorescence level in RNAi-treated cells in the absence or presence of Nef expression (in relative fluorescence units [rfu]). The standard error of the mean (SEM) is also given for each measurement; for those targets in which  $n = 2$ , the SEM is not considered statistically relevant, but it was used to judge the likelihood with which the data could be reproduced by future experiments. The fold downregulation (by definition, the CD4 fluorescence in the absence of Nef divided by the CD4 fluorescence in the presence of Nef) is also given. A fold downregulation of 1.00, therefore, is equal to no effect; i.e., the CD4 surface levels are not affected by Nef expression. RNAi targeting Nef provides a positive control for interference with Nef activity and approaches a total inhibition of downregulation (1.01-fold), as does RNAi against clathrin heavy chain (also 1.01-fold). Notes: RNAi targeting CG 4214 (Syx5) resulted in mildly toxic effects, and as such this result is not considered positive hit for the screen; the SEM for CG 18028 (Vps41) is large compared to the mean values and the data for this condition is not considered reproducible.

**Table 3.1: Raw data from the S2 RNAi screen.**

#	RNAi Target		Number of Trials	Mean surface rfu $\pm$ SEM		Fold Downregulation
	CG Number	Ortholog		CD4	CD4 plus Nef	
1	Control	GFP	10	54.8 $\pm$ 3.7	26.3 $\pm$ 1.9	2.1
2	Control	CD4	7	8.8 $\pm$ 1.1	5.3 $\pm$ 0.7	1.7
3	Control	Nef	5	55.6 $\pm$ 4.7	55.1 $\pm$ 2.2	1.0
4	1099	Intersectin	4	65.5 $\pm$ 4.3	29.1 $\pm$ 5.8	2.3
5	1107	Auxilin/GAK	4	63.1 $\pm$ 2.6	26.8 $\pm$ 3.4	2.4
6	1515	Ykt6	2	93.2 $\pm$ 11.9	34.4 $\pm$ 1.0	2.7
7	1951	CVAK104	3	59.1 $\pm$ 3.9	24.0 $\pm$ 4.2	2.5
8	2520	CALM/AP180	5	71.0 $\pm$ 4.0	25.2 $\pm$ 7.6	2.8
9	2929	PI4K II $\alpha$	4	58.4 $\pm$ 2.4	20.5 $\pm$ 2.4	2.9
10	3002	GGA	5	60.1 $\pm$ 1.9	26.6 $\pm$ 5.0	2.3
11	3035	AP-3 $\mu$ 3	3	61.1 $\pm$ 3.1	26.1 $\pm$ 3.7	2.3
12	3412	$\beta$ -TrCP	3	67.8 $\pm$ 7.3	28.1 $\pm$ 3.5	2.4
13	3529	TOM1	3	62.2 $\pm$ 2.1	25.3 $\pm$ 3.1	2.5
14	3637	Cortactin	4	53.2 $\pm$ 3.2	28.7 $\pm$ 4.6	1.9
15	3779	Numb	3	64.4 $\pm$ 6.5	20.2 $\pm$ 2.9	3.2
16	4214	Syx5	2	68.0 $\pm$ 1.7	44.87 $\pm$ 5.1	1.5
17	4260	AP-2 $\alpha$	4	70.2 $\pm$ 8.0	25.5 $\pm$ 1.9	2.8
18	5020	EEA1	2	68.3 $\pm$ 6.0	23.8 $\pm$ 6.8	2.9
19	5341	Sec6	5	73.8 $\pm$ 1.9	30.4 $\pm$ 2.4	2.4

**Table 3.1: Raw data from the S2 RNAi screen, continued.**

#	RNAi Target		Number of Trials	Mean surface rfu $\pm$ SEM		Fold Downregulation
	CG Number	Ortholog		CD4	CD4 plus Nef	
20	5373	PI3K Vps34	3	69.0 $\pm$ 7.6	22.9 $\pm$ 3.1	3.0
21	5915	Rab7	4	70.4 $\pm$ 3.2	27.2 $\pm$ 2.9	2.6
22	6148	EHD1	4	69.6 $\pm$ 4.2	30.4 $\pm$ 3.2	2.3
23	6359	Snx3	3	55.5 $\pm$ 8.0	19.9 $\pm$ 6.0	2.8
24	6488	Cog8	3	68.5 $\pm$ 3.0	27.8 $\pm$ 6.0	2.5
25	6521	STAM1	3	55.4 $\pm$ 4.4	23.2 $\pm$ 3.8	2.3
26	6562	Synaptojanin	4	67.0 $\pm$ 1.8	33.5 $\pm$ 4.2	2.0
27	6948	Clathrin light chain	4	87.9 $\pm$ 6.1	53.8 $\pm$ 8.5	1.6
28	7037	Cbl	3	65.0 $\pm$ 14.5	22.7 $\pm$ 1.7	3.0
29	7057	AP-2 $\mu$ 2	4	77.5 $\pm$ 9.1	52.4 $\pm$ 7.0	1.5
30	7085	GMX-33	3	81.1 $\pm$ 8.3	34.9 $\pm$ 9.3	2.3
31	7146	Vps39	3	59.2 $\pm$ 3.6	26.6 $\pm$ 2.7	2.2
32	7558	Arp3	3	57.9 $\pm$ 3.6	33.1 $\pm$ 6.1	1.8
33	7578	BIG	4	79.6 $\pm$ 8.0	37.5 $\pm$ 1.5	2.1
34	7961	$\alpha$ -COP	4	130.1 $\pm$ 17.2	90.5 $\pm$ 8.7	1.4
35	8156	Arf6	4	63.8 $\pm$ 6.3	28.5 $\pm$ 8.7	2.2
36	8282	Snx6	3	48.8 $\pm$ 3.6	14.9 $\pm$ 1.6	3.3
37	8287	Rab8	3	60.9 $\pm$ 5.3	25.2 $\pm$ 2.4	2.4
38	8385	Arf1	3	73.8 $\pm$ 4.4	29.5 $\pm$ 3.4	2.5

**Table 3.1: Raw data from the S2 RNAi screen, continued.**

#	RNAi Target		Number of Trials	Mean surface rfu $\pm$ SEM		Fold Downregulation
	CG Number	Ortholog		CD4	CD4 plus Nef	
39	8487	GBF1	2	60.4 $\pm$ 1.7	36.6 $\pm$ 7.9	1.7
40	8506	Rabenosyn-5	3	59.4 $\pm$ 3.9	26.1 $\pm$ 3.3	2.3
41	8532	Epsin	3	63.8 $\pm$ 4.2	26.7 $\pm$ 0.5	2.4
42	8604	Amphiphysin	3	63.8 $\pm$ 5.4	30.1 $\pm$ 6.6	2.1
43	8937	Hsc70	2	76.4 $\pm$ 2.5	23.0 $\pm$ 1.3	3.3
44	9012	Clathrin heavy chain	3	93.3 $\pm$ 6.2	92.8 $\pm$ 5.6	1.0
45	9113	AP-1 $\gamma$	2	75.6 $\pm$ 4.6	28.5 $\pm$ 5.9	2.7
46	9139	Rabex-5	4	67.1 $\pm$ 6.4	24.8 $\pm$ 4.0	2.7
47	9388	AP-1 $\mu$ 1	4	67.4 $\pm$ 2.4	29.5 $\pm$ 5.6	2.3
48	9575	Rab35	3	76.3 $\pm$ 3.4	38.2 $\pm$ 4.6	2.0
49	9695	Dab	3	68.7 $\pm$ 7.4	27.8 $\pm$ 4.4	2.5
50	9712	TSG101	4	109.9 $\pm$ 9.7	34.3 $\pm$ 4.9	3.2
51	9901	Arp2	3	63.9 $\pm$ 6.1	28.8 $\pm$ 2.7	2.2
52	9994	Rab9	3	61.5 $\pm$ 1.8	23.5 $\pm$ 2.3	2.6
53	10144	Vps8	3	68.5 $\pm$ 1.2	27.7 $\pm$ 2.4	2.5
54	10295	Pak1/2	3	64.8 $\pm$ 6.9	24.9 $\pm$ 2.2	2.6
55	10637	AAK1	3	61.3 $\pm$ 1.5	22.4 $\pm$ 3.8	2.7
56	10971	HIP1	2	65.5 $\pm$ 6.6	26.6 $\pm$ 0.8	2.5
57	10986	AP-3 $\delta$	3	69.8 $\pm$ 2.3	24.1 $\pm$ 1.3	2.9

**Table 3.1: Raw data from the S2 RNAi screen, continued.**

#	RNAi Target		Number of Trials	Mean surface rfu $\pm$ SEM		Fold Downregulation
	CG Number	Ortholog		CD4	CD4 plus Nef	
58	11804	ARH	2	72.08 $\pm$ 7.89	26.55 $\pm$ 3.64	2.7
59	11814	Lyst	3	66.18 $\pm$ 6.19	26.98 $\pm$ 3.42	2.5
60	12473	Stonin	2	72.11 $\pm$ 12.54	16.87 $\pm$ 16.87	4.3
61	12876	ALIX	3	68.57 $\pm$ 5.86	32.56 $\pm$ 3.79	2.1
62	14296	Endophilin	2	78.68 $\pm$ 3.29	27.76 $\pm$ 8.17	2.8
63	14619	USP2	3	63.62 $\pm$ 4.15	26.98 $\pm$ 6.20	2.4
64	14750	Vps25	2	80.96 $\pm$ 20.57	19.81 $\pm$ 0.82	4.1
65	14804	Vps26	3	68.03 $\pm$ 11.48	30.67 $\pm$ 4.35	2.2
66	16932	Eps15	2	82.77 $\pm$ 16.30	21.80 $\pm$ 0.07	3.8
67	17060	Rab10	4	69.12 $\pm$ 4.94	32.97 $\pm$ 7.53	2.1
68	17515	Rab21	2	74.66 $\pm$ 15.15	21.97 $\pm$ 3.29	3.4
69	18028	Vps41	3	70.99 $\pm$ 10.22	46.38 $\pm$ 10.27	1.5
70	18102	Dynammin	4	69.33 $\pm$ 7.19	26.81 $\pm$ 4.27	2.6
71	31064	Rabip4	5	66.84 $\pm$ 3.07	29.22 $\pm$ 6.91	2.3

system (Fig. 3.5B and 3.6; Table 3.1). Interestingly, dsRNAs targeting the  $\gamma$  and  $\mu 1$  subunits of AP-1 and the  $\delta$  and  $\mu 3$  subunits of AP-3, either alone (Fig. 3.5B; Table 3.1) or in combinations (data not shown), had no effect on CD4 downregulation. Because AP-1 and AP-3 have been proposed to act as mediators of CD4 downregulation (Bresnahan et al., 1998; Craig et al., 2000; Janvier et al., 2003b; Rose et al., 2005), the efficacy of the  $\mu 1$  and  $\mu 3$  dsRNAs on protein expression was tested directly. Immunoblot analysis clearly indicated a strong reduction of protein levels (Fig. 3.5C), supporting the conclusion that neither AP-1 nor AP-3 are required for Nef-mediated CD4 downregulation in S2 cells. *Drosophila* does not have orthologs for the subunits of a fourth, non-clathrin-associated AP complex in human cells called AP-4 (Boehm and Bonifacino, 2001), so this trafficking protein can be definitively ruled out as a required mediator of Nef effects on CD4.

The ability of Nef to downregulate CD4 was also inhibited by treatment of the S2 cells with dsRNA against  $\alpha$ -COP (Fig. 3.5B and 3.6). This effect was somewhat unusual in that higher levels of CD4 were found on the cell surface regardless of Nef induction.  $\alpha$ -COP is a subunit of the heteroheptameric COPI complex that appears to be primarily involved in endoplasmic reticulum and Golgi transport processes (for a review, see Kirchhausen, 2000), although a role for COPI in endosomal traffic has also been proposed (Gu and Gruenberg, 1999; Whitney et al., 1995). In this regard, Nef has been previously shown to interact with the  $\beta$ -COP subunit of COPI (Benichou et al., 1994; Schaefer et al., 2008), but the functional significance of this interaction remains a matter of debate (Janvier et al., 2001; Piguet et al., 1999; Schaefer et al., 2008).

### **3.3.4 Requirement of AP-2 for Nef-induced CD4 downregulation in human cells**

Next, the role of AP-1, AP-2, and AP-3 in the Nef-mediated downregulation of CD4 was assessed in the human cell line HeLa (experiments performed in collaboration with Wolf Lindwasser). Immunoblot assays indicated that the treatment of these cells with RNAi targeting the  $\mu$  subunits of the three AP complexes reduced the expression of  $\mu 1A$ ,  $\mu 2$ , and  $\mu 3A$  compared to treatment with non-targeting RNAi (Fig. 3.7A). The RNAi against  $\mu 2$  increased surface levels of the transferrin receptor (TfR) and RNAi against  $\mu 3A$  increased surface levels of lysosome associated membrane protein 1 (LAMP1) as measured by flow cytometry (Fig. 3.7B), indicators of impaired AP-2

**FIG. 3.7: Analysis of AP-2 knockdown in human cells**

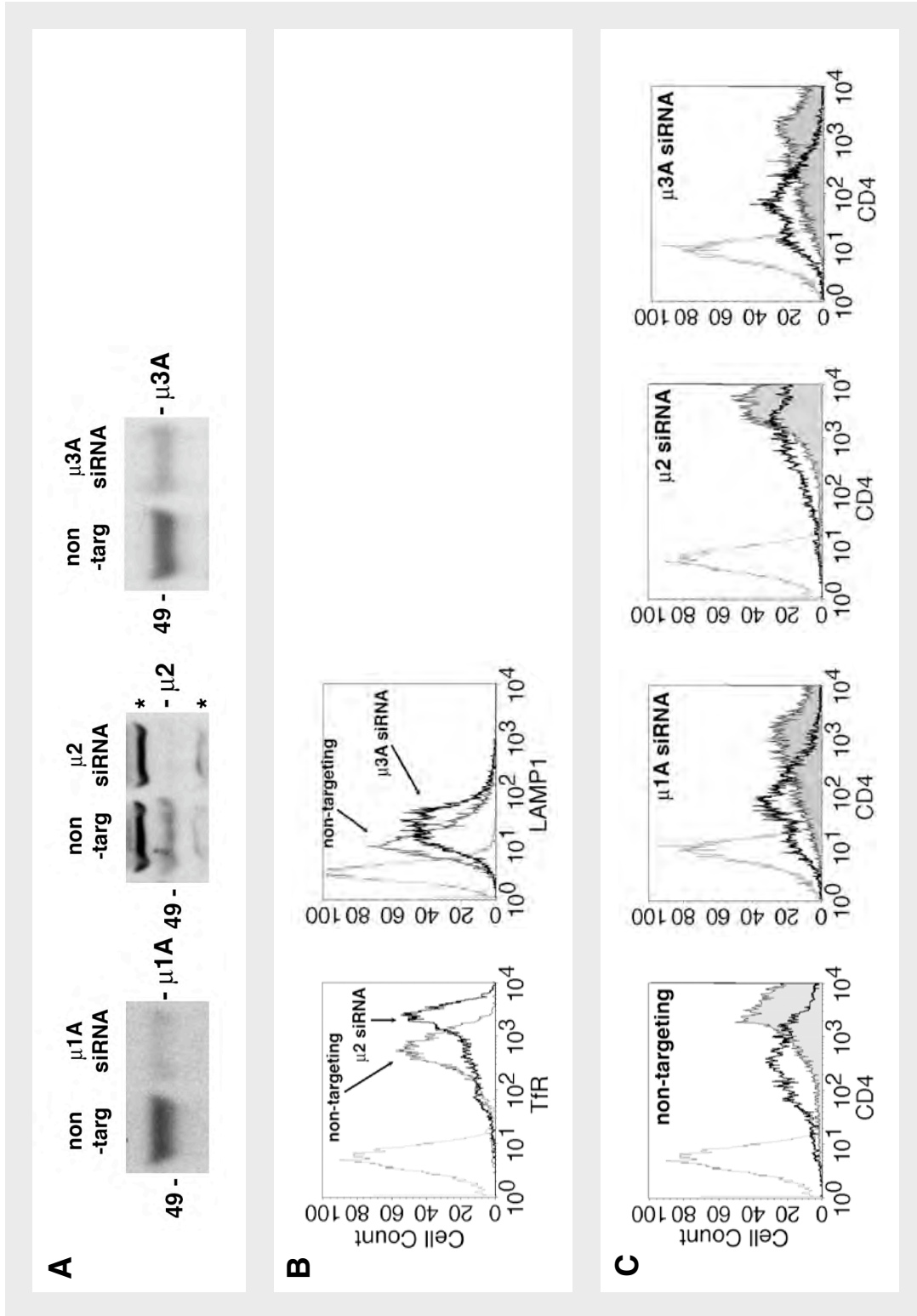
HeLa cells were treated with either non-targeting or specific siRNA targeting  $\mu$ 1A,  $\mu$ 2, or  $\mu$ 3A as described in the Materials and Methods (Section 2.6.3.4). After 5 days of treatment, the cells were transfected with expression vectors for CD4 and either wild-type Nef or the inactive mutant Nef LL164,165AA. The following day the cells were prepared for either immunoblotting or flow cytometric analysis.

**(A)** Immunoblotting of siRNA-treated HeLa cell lysates using rabbit antisera to human  $\mu$ 1A,  $\mu$ 2, or  $\mu$ 3A. Two non-specific bands on the  $\mu$ 2 blot are indicated by asterisks. The specific band migrates at approximately 50 kDa and is drastically reduced in the siRNA-treated cells. The positions of molecular mass markers (in kDa) are shown on the left.

**(B)** The level of TfR and LAMP1 on the cell surface was measured by flow cytometry as an indicator of impaired AP-2 and AP-3 function, respectively. The  $\mu$ 2 siRNA-treated cells exhibit a strong increase in surface TfR, a finding that is consistent with a decrease in AP-2-dependent endocytosis. The increase in surface LAMP1 in the  $\mu$ 3 siRNA-treated cells is indicative of improper AP-3-dependent intracellular sorting.

**(C)** Dependence of Nef-mediated CD4 downregulation on AP-2. Histograms for cells transfected with Nef LL164,165AA (shaded gray), wild-type Nef (bold line), and an isotype control (light gray line) are presented. Non-targeting,  $\mu$ 1A, and  $\mu$ 3A siRNA-treated cells exhibit a decrease in surface CD4 in the presence of wild-type Nef. In the  $\mu$ 2 siRNA-treated cells, this decrease is less marked.

**FIG. 3.7**



In collaboration with Wolf Lindwasser

and AP-3 function, respectively (Janvier and Bonifacino, 2005; Nesterov et al., 1999). The amount of plasma membrane-associated CD4 was then measured in RNAi-treated cells expressing either wild-type Nef or the Nef LL164,165AA null-mutant (Fig. 3.7C). Cells treated with a non-targeting RNAi displayed robust downregulation of CD4 by wild-type Nef (in comparison to the Nef LL164,165AA mutant), whereas cells depleted of  $\mu 2$  showed decreased downregulation. It should be noted that, in both S2 and HeLa cells, depletion of  $\mu 2$  was only partially effective in blocking the effect of Nef on CD4. This may be due to an incomplete knockdown of the AP-2 complex in RNA-treated cells or the activity of a partially redundant pathway. Given the data presented here, it is not possible to distinguish between these two possibilities (see Chapters 4 and 5 for additional work on this topic). In agreement with a previous study (Roeth et al., 2006), neither  $\mu 1A$  nor  $\mu 3A$  appeared to be required for the Nef-induced downregulation of CD4 (Fig. 3.7C). A similar experiment was attempted in cells depleted of CHC, but these cells proved refractory to transient DNA transfection after RNAi treatment, and reproducible results could not be obtained.

### 3.3.5 Physical interaction of Nef with AP-2 in a yeast three-hybrid system

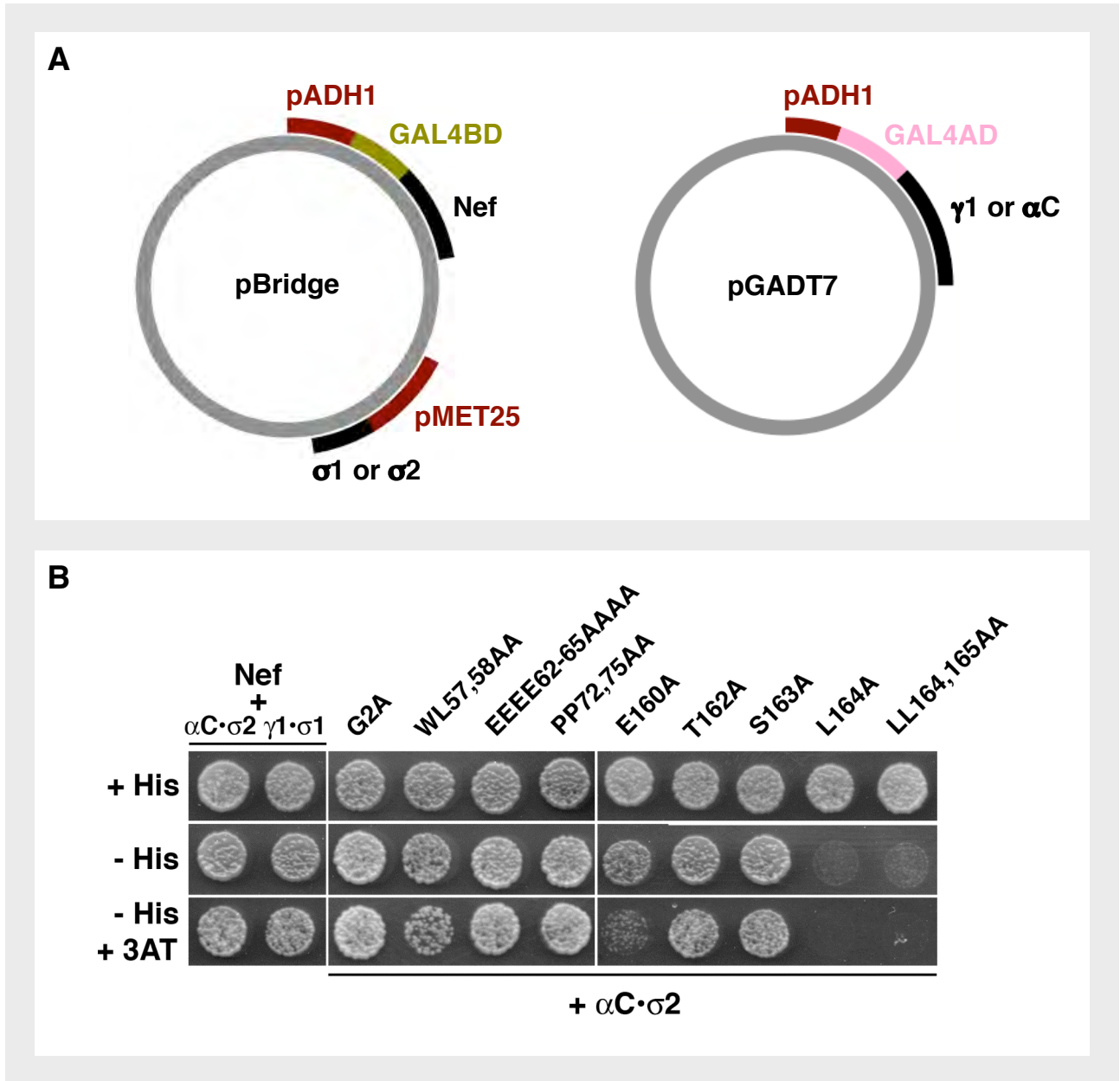
The RNAi experiments performed on *Drosophila* and human cells indicated that AP-2 was involved in the Nef-mediated downregulation of CD4. However, it was unclear if AP-2 was directly involved in this process, as there was little evidence in the literature of an interaction between Nef and AP-2. Others had previously reported interactions of Nef with the  $\gamma$ - $\sigma 1$  and  $\delta$ - $\sigma 3$  hemicomplexes of AP-1 and AP-3, respectively, using the yeast three-hybrid (Y3H) system (Janvier et al., 2003b). However, these authors had failed to detect an interaction between Nef and the analogous  $\alpha$ - $\sigma 2$  hemicomplex of AP-2. (Janvier et al., 2003b). Resequencing of the  $\alpha C$  clone used in the Y3H assays revealed the presence of a single base-pair mutation that resulted in the substitution of a threonine residue for alanine at codon 131. Based on the three-dimensional crystal structure of AP-2 (Collins et al., 2002), the A131T mutation placed a hydrophilic side chain within the normally hydrophobic core of the  $\alpha$  subunit. Such a mutation may be expected to have deleterious effects on the folding of the  $\alpha$  subunit and stability of the  $\alpha$ - $\sigma 2$  hemicomplex. The mutated  $\alpha$  residue was therefore changed back to alanine, and the Y3H assays were repeated. Nef was now observed to interact strongly with the  $\alpha$ - $\sigma 2$  hemicomplex (Fig. 3.8). Indeed, the interaction between Nef and  $\alpha$ - $\sigma 2$

**FIG. 3.8: Yeast three-hybrid analysis of Nef-AP-2 interactions**

**(A)** Wild-type and mutant versions of NL4-3 Nef were expressed as GAL4BD fusion proteins from pBridge, along with either  $\sigma 1$  or  $\sigma 2$ . The  $\gamma 1$  and  $\alpha C$  subunits were expressed as GAL4AD fusion proteins from pGADT7. See Materials and Methods (Sections 2.4.1.1 and 2.4.2.2 and Figs. 2.4 and 2.5) for more details.

**(B)** HF7c yeast cells co-transformed with pairs of pBridge and pGADT7 plasmids were inoculated on medium containing histidine (+His) or lacking histidine (–His) in the absence or presence of 3 mM 3-amino-1,2,4-triazole (3AT). Growth of yeast on the –His medium is indicative of an interaction between the fusion proteins, while growth on the –His +3AT medium is indicative of stronger interactions.

FIG. 3.8



appeared to be as robust as the previously reported interaction between Nef and  $\gamma$ - $\sigma$ 1 (Fig 3.8; Janvier et al., 2003b). The Nef dileucine motif (ENTSLL160-165 in NL4-3; ExxxLL consensus sequence in all HIV-1 Nef variants, where x is any amino acid) fits the canonical [D/E]xxxL[L/I] motif that has been shown to bind to AP complexes (Bonifacino and Traub, 2003). To determine whether the Nef dileucine motif also mediates binding to the  $\alpha$ - $\sigma$ 2 hemicomplex, several ENTSLL residues were mutated to alanine, either alone or in combination (Fig. 3.8). Mutation of the acidic residue (E160A) caused a partial loss of binding (apparent in the presence of 3-amino-1,2,4-triazole), while mutation of either the first leucine (L164A) or both leucines together (LL164,165AA) completely abrogated the interaction of Nef and  $\alpha$ - $\sigma$ 2. Mutation of two of the intervening residues (T162A and S163A) had no effect. Interestingly, mutation of four other Nef functional motifs (G2A, WL57,58AA, EEEE62-65AAAA, and PP72,75AA, initially described in Section 3.3.2) also had no effect on the binding of Nef and  $\alpha$ - $\sigma$ 2 (Fig. 3.8). These results indicated that the interaction of Nef with the  $\alpha$ - $\sigma$ 2 hemicomplex is specifically dependent on the conserved residues of the Nef dileucine motif. Importantly, these residues are also required for Nef downregulation of CD4 in cells (Fig. 3.3, Fig. 3.4; Bresnahan et al., 1998; Greenberg et al., 1998a). It is also worth noting that the interaction of Nef with  $\alpha$ - $\sigma$ 2 appears to be much stronger than a previously reported interaction of Nef and  $\mu$ 2 (Craig et al., 2000).

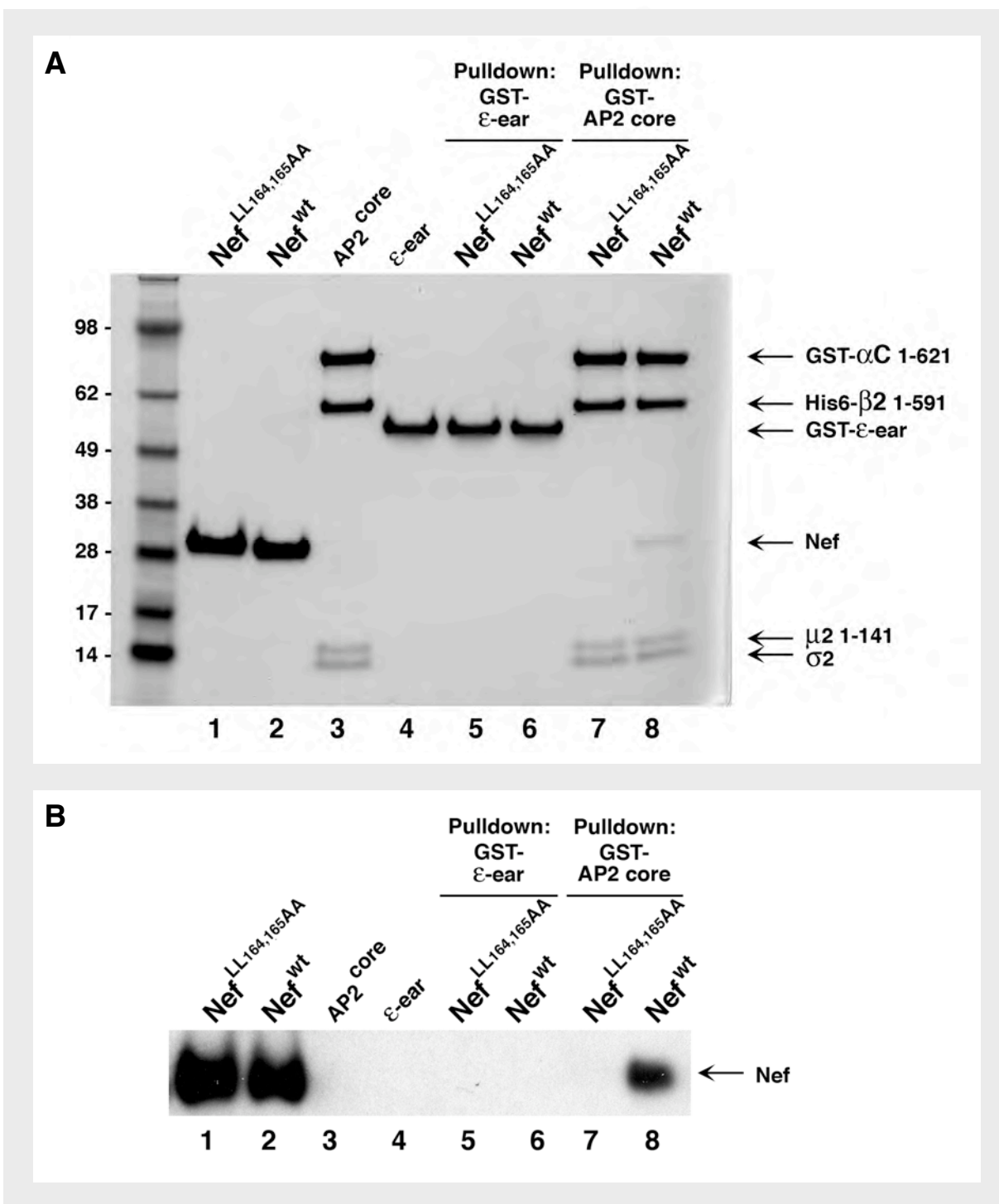
### 3.3.6 Direct interaction of Nef and AP-2 in vitro

Although Nef was shown to bind to  $\alpha$ - $\sigma$ 2 by Y3H, this association may not be direct, as other proteins in the yeast nucleus could potentially contribute to the interaction. It was therefore deemed necessary to test the ability of Nef to bind AP-2 in vitro (all assays described in this section were performed by William Smith; see the Materials and Methods, Section 2.3 for further information on the reagents and experiments mentioned below). Others had recently demonstrated that the dileucine motifs of several proteins bound in vitro to a recombinant AP-2 “core” complex consisting of the N-terminal trunk domains of  $\alpha$  and  $\beta$ 2, plus the full-length  $\mu$ 2 and  $\sigma$ 2 subunits (Höning et al., 2005). In addition, these authors showed that the dileucine binding site was not contained within the C-terminal domain of  $\mu$ 2 (Höning et al., 2005). Given these considerations, a similar AP-2 core construct (denoted AP-2<sup>CORE</sup>), lacking the C-terminal domain of  $\mu$ 2, was designed. The  $\alpha$  trunk was expressed as a GST fusion

**FIG. 3.9: Direct interaction of Nef and AP-2 detected in vitro**

Recombinant proteins were purified from bacteria, used in a GST pull-down assay, and then separated by SDS-PAGE (see Materials and Methods, Section 2.3). The separated proteins were then stained with Coomassie blue **(A)** and immunoblotted with an antibody targeting Nef **(B)**. Proteins were run individually in lane 1 (NL4-3 Nef LL164,165AA mutant), lane 2 (wild-type NL4-3 Nef), lane 3 (GST-AP-2<sup>CORE</sup>), and lane 4 (GST- $\epsilon$ -ear). Mutant and wild-type Nef proteins were incubated with GST- $\epsilon$ -ear (lanes 5 and 6; negative control) or with GST-AP-2<sup>CORE</sup> (lanes 7 and 8). Wild-type Nef is visible as an approximately 27-kDa band in lane 8 in both panels A and B. This experiment is representative of three trials with similar results. Molecular mass markers are visible on the left side of the Coomassie blue-stained gel. The masses (in kDa) are indicated.

**FIG. 3.9**



Performed by William Smith

protein, while the  $\beta 2$  trunk was expressed as a hexahistidine ( $\text{His}_6$ ) fusion protein. The presence of these epitope tags facilitated the purification of the  $\text{AP-2}^{\text{CORE}}$  complex from bacteria. Wild-type Nef and the dileucine mutant, Nef LL164,165AA, were also expressed as  $\text{His}_6$  fusion proteins and purified from bacteria. GST pull down assays using these recombinant proteins indicated that wild-type Nef, but not Nef LL164,165AA, bound to the  $\text{AP-2}^{\text{CORE}}$  complex, as determined by Coomassie blue staining (Fig. 3.9A) and immunoblot analysis (Fig. 3.9B). In contrast, neither Nef construct interacted with the GST- $\epsilon$  ear fusion protein, which was used as a negative control (Fig. 3.9). These observations thus demonstrated a direct and specific interaction of Nef, through its dileucine motif, with the fully assembled  $\text{AP-2}^{\text{CORE}}$  complex.

## 3.4 Discussion

### 3.4.1 Chapter overview

Recent studies have begun to exploit the ease and efficiency of RNAi screens in *Drosophila* S2 cells to identify host-cell factors that are required for infections by human pathogens such as bacteria and fungi (Agaisse et al., 2005; Derré et al., 2007; Elwell and Engel, 2005; Philips et al., 2005; Ramet et al., 2002; Stroschein-Stevenson et al., 2006). Here, the *Drosophila* S2 model system was used to investigate the molecular machinery involved in an aspect of viral pathogenesis: namely, the mechanism by which primate immunodeficiency viruses downregulate their own co-receptor, CD4. An RNAi screen of 68 components of the protein trafficking machinery in S2 cells revealed that CD4 downregulation by HIV-1 Nef requires clathrin and the heterotetrameric AP-2 complex, both of which are components of protein coats involved in endocytosis from the plasma membrane of host cells. The requirement for AP-2 in this process was confirmed in human HeLa cells. In contrast, other heterotetrameric (i.e., AP-1 and AP-3) and monomeric (i.e., GGA) clathrin adaptors appear to be dispensable for CD4 downregulation. In addition, Y3H assays were used to demonstrate an interaction of Nef with a combination of the  $\alpha$  and  $\sigma 2$  subunits of AP-2. Finally, a GST pull-down assay showed a direct and specific interaction of Nef with the heterotetrameric AP-2<sup>CORE</sup> complex in vitro. Importantly, both the function and interaction of Nef in these assays exhibited a dependence on a dileucine sequence in the viral protein that had previously been identified as critical for CD4 downregulation (Bresnahan et al., 1998; Greenberg et al., 1998a). These observations thus support a model in which Nef links the cytosolic tail of CD4 to clathrin-AP-2 coats at the plasma membrane, leading to the endocytic removal of the receptor from the cell surface.

### 3.4.2 Role of clathrin and AP-2 in Nef-mediated CD4 downregulation

As the major devices for sorting proteins at different stages of the endocytic and secretory pathways, clathrin-AP coats have long been suspected to play a role in the downregulation of CD4 by Nef (Blagoveshchenskaya et al., 2002; Bresnahan et al., 1998; Craig et al., 1998; Craig et al., 2000; Foti et al., 1997; Greenberg et al., 1997; Janvier et al., 2003a; Janvier et al., 2003b; Le Gall et al., 1998; Piguet et al., 1998). This hypothesis was affirmed by the discovery that downregulation is strictly depend-

ent on a Nef dileucine sequence (Bresnahan et al., 1998; Greenberg et al., 1998) that fits the [D/E]xxxL[L/I] consensus motif for signals that mediate clathrin-dependent sorting events and interaction with clathrin-associated AP complexes (Bonifacino and Traub, 2003). Much work has since been done to elucidate the exact role of clathrin and the various AP complexes in the downregulation of CD4. However, the evidence has thus far been largely indirect, and different studies have produced conflicting results.

Nef has previously been shown to localize to clathrin-AP-2 coated pits at the plasma membrane and to promote the recruitment of CD4 to such pits (Burtley et al., 2007; Foti et al., 1997; Greenberg et al., 1998a). This is consistent with the finding that Nef accelerates CD4 internalization from the cell-surface (Aiken et al., 1994; Rhee and Marsh, 1994). These observations led to the testing for an involvement of AP-2 in CD4 downregulation. Expression of an AP-2  $\mu$ 2 subunit construct rendered incapable of binding YxxØ-type signals by the mutation of aspartate-176 to alanine (Nesterov et al., 1999) was found to block the HIV-1 Nef-dependent redistribution of CD4 to endosomes in HeLa cells (Blagoveshchenskaya et al., 2002). This finding is puzzling, however, because neither HIV-1 Nef nor CD4 have YxxØ-type signals; instead, downregulation depends on dileucine-containing sequences in both Nef and CD4 (Aiken et al., 1994; Bresnahan et al., 1998; Coleman et al., 2005; Foti et al., 1997; Greenberg et al., 1998a). Since YxxØ and dileucine signals have different binding sites on AP-2 (Höning et al., 2005; Janvier et al., 2003b; Marks et al., 1996; Ohno et al., 1995; Rapoport et al., 1998; Kelly et al. 2008), it is unclear how such a mutant could have a “dominant-negative” effect on CD4 downregulation by Nef. Subsequent experiments showed that the depletion of  $\mu$ 2 by RNAi caused only a slight inhibition of Nef-mediated CD4 downregulation in HeLa cells and T cells (Jin et al., 2005; Rose et al., 2005). More complete inhibition required over-expression of a dominant-negative mutant of Eps15, a regulator of endocytosis, in conjunction with RNAi-mediated  $\mu$ 2 depletion in T cells (Jin et al., 2005). Attempts to demonstrate a clear physical connection between Nef and AP-2 have similarly yielded conflicting results. Yeast two-hybrid (Y2H) assays have been used to detect a very weak interaction of HIV-1 Nef with  $\mu$ 2 (Craig et al., 2000), whereas an interaction with the AP-2  $\beta$ 2 (Greenberg et al., 1998a) subunit was observed by using a chemical cross-linking approach. Thus, the role of AP-2 in downregulation remained unclear from all of this

work. The data presented here – in which RNAi-mediated depletion of either clathrin or AP-2 is shown to cause a profound inhibition of CD4 downregulation by Nef, and in which Nef is shown to interact robustly and specifically with AP-2 – now provide strong support to the AP-2-dependent, endocytic model of Nef action on CD4.

### **3.4.3 Recognition of dileucine signals by AP-2**

Upon correction of a point mutation in the AP-2  $\alpha$  construct used for previous Y3H assays (Janvier et al., 2003b), it was possible to detect a robust interaction between the  $\alpha$ - $\sigma$ 2 hemicomplex and Nef. This interaction requires the co-expression of both AP-2 subunits and is not observed with either  $\alpha$  or  $\sigma$ 2 alone (data not shown). This could indicate that Nef simultaneously binds to both the  $\alpha$  and  $\sigma$ 2 subunits, or that the subunits remain properly folded only in the context of the hemicomplex. In addition, the Y3H interaction is strictly dependent on the Nef dileucine (LL164,165) sequence and partially dependent on the upstream acidic residue (E160). It is not dependent, however, on neighboring residues or other functional motifs within the viral protein. These requirements exactly match those already defined for CD4 downregulation (Bresnahan et al., 1998; Coleman et al., 2006; Greenberg et al., 1998a), indicating that the interactions are likely to be functionally relevant. These interactions are analogous to those of Nef with the  $\gamma$ - $\sigma$ 1 subunits of AP-1 and  $\delta$ - $\sigma$ 3 subunits of AP-3 (Janvier et al., 2003b), suggesting that these three complexes bind to Nef in a similar manner. Moreover, like the corresponding AP-1 and AP-3 hemicomplexes, the AP-2  $\alpha$ - $\sigma$ 2 hemicomplex would be expected to bind to other [D/E]xxxL[L/I]-type dileucine signals involved in internalization from the cell surface. The easy detection of these interactions with the Y3H system now opens the way for further studies on the mechanism of dileucine signal recognition.

### **3.4.4 Do AP-1 and AP-3 participate in Nef-induced CD4 downregulation?**

In addition to the plasma membrane, HIV-1 Nef has been found to localize to an area of the cell that includes the Golgi complex (Janvier et al., 2003a; Mangasarian et al., 1997), and to induce the retention of CD4 in the Golgi region (Brady et al., 1993, Mangasarian et al., 1997). Together, these observations supported a model in which the intracellular retention of newly synthesized or recycling CD4 contributes to the downregulation of the receptor (Brady et al., 1993; Mangasarian et al., 1997; Rose et

al., 2005). The area of the Golgi which Nef has been localized to includes the TGN and a subset of endosomes, both of which have clathrin coats containing AP-1 and AP-3. Indeed, a variety of biochemical assays have shown interactions of Nef with AP-1 and AP-3. Specifically, HIV-1 Nef has been found to interact with AP-1 and AP-3 from cell extracts by GST pull-down assays (Bresnahan et al., 1998, Janvier et al., 2003a; Janvier et al., 2003b), with the  $\mu$ 1A subunit of AP-1 and the  $\mu$ 3A subunit of AP-3 by Y2H assays (Craig et al., 2000; Le Gall et al., 1998), and with the  $\gamma$ - $\sigma$ 1 and  $\delta$ - $\sigma$ 3 hemicomplexes of AP-1 and AP-3, respectively, by Y3H assays (Janvier et al., 2003b). All of these interactions are dependent on the dileucine sequence of Nef, indicating that they may be functionally relevant for CD4 downregulation. However, RNAi-mediated depletion of AP-1 and AP-3 subunits has been reported to have no effect on the downregulation of CD4 by Nef in human T cells and astrocytes (Roeth et al., 2006), a finding that has now been replicated in S2 and HeLa cells. Therefore, it is unclear what roles – if any – the interactions of Nef with AP-1 and AP-3 might play in CD4 downregulation. It is possible that these complexes participate in the post-endocytic routing of internalized CD4, but more work will be needed to either confirm or refute this hypothesis. Ideally, a Nef mutant capable of binding AP-1 and AP-3, but not AP-2, will be identified. Such a mutant would be useful in determining whether AP-1 and AP-3 contribute to the Nef-induced downregulation of CD4.

#### **3.4.5 Postendocytic fate of internalized CD4**

The downregulation of CD4 by Nef involves not only removal of the receptor from the cell surface, but also its targeting to lysosomes for eventual degradation (Piguet et al., 1999; Rhee and Marsh, 1994; Sanfridson et al., 1994). Thus, it is likely that Nef also functions to prevent the recycling of internalized CD4 to the plasma membrane and/or to promote its delivery to lysosomes, perhaps by following the MVB pathway. However, the depletion of various components of the endosomal recycling (e.g., EHD1, Rabenosyn-5, Arf6, Rab35, and Rabip4; Table 3.1) and MVB pathways (e.g., TSG101, STAM1, ALIX, and Vps25; Table 3.1) had no effect on the ability of Nef to decrease surface levels of CD4. This observation does not necessarily imply a lack of Nef involvement in these processes because of the following caveats: (i) the RNAi treatment may not have caused sufficient depletion of the target proteins to elicit an effect, (ii) the right target proteins may not have been picked for depletion, and (iii)

inhibition of recycling or lysosomal delivery may affect the intracellular distribution of the internalized proteins (as may also be the case for AP-1 and AP-3 depletion), without preventing the reduction in surface CD4 levels. To fully assess the role of these intracellular sorting events on CD4 downregulation, more components of the endosomal recycling and MVB pathways would have to be depleted; if possible, such depletions would also be verified by immunoblotting. In addition, the depleted cells should be subjected to confocal fluorescence microscopy, so that information on the intracellular localization of CD4 – and any changes therein – can be collected and analyzed.

### **3.4.6 Distinct mechanisms for CD4 and MHC-I downregulation**

CD4 is one of several plasma membrane-associated receptors downregulated by Nef. Among the other cell surface proteins that undergo Nef-induced downregulation are certain MHC-I haplotypes (Greenberg et al., 1998b; Mangasarian et al. 1999; Roeth et al., 2004; Schwartz et al., 1996; Swann et al., 2001). The redistribution of these MHC-I receptors from the plasma membrane to intracellular vesicles is thought to allow HIV-1 to evade immune surveillance (Cohen et al., 1999; Collins et al., 1998). Strikingly, Nef-induced MHC-I downregulation appears to occur by a mechanism that is quite distinct from that of CD4 downregulation. Indeed, downregulation of MHC-I by Nef primarily involves the misrouting of newly synthesized molecules from the TGN to lysosomes (Kasper et al., 2005), and requires AP-1 but not AP-3 (Roeth et al., 2004). This process is independent of the Nef dileucine sequence (Riggs et al., 1999) and instead depends on the acidic cluster (EEEE62-65) and the polyproline (PP72,75) motifs (Mangasarian et al., 1999; Piguet et al., 2000; Roeth et al., 2006). In addition, Nef promotes the association of MHC-I and AP-1 with sequence requirements that are identical to those required for downregulation (Mangasarian et al., 1999; Roeth et al., 2004; Williams et al., 2005). Thus, Nef is a multifunctional “connector” molecule capable of using distinct interfaces to link the cytosolic tails of different trans-membrane proteins to specific AP complexes. These alternative modes of interaction endow Nef with the ability to interfere with protein trafficking at different stages of the secretory and endocytic pathways.

#### **Chapter 4:**

**A diacidic motif in HIV-1 Nef is a novel determinant of binding to AP-2**

## 4.1 Abstract

Nef, an accessory protein of the primate immunodeficiency viruses, downregulates CD4 from the surface of infected cells. The ability of HIV-1 Nef to reduce the amount of CD4 at the cell surface is believed to increase the efficiency of viral replication, and contribute to progression of the disease. Current models suggest that Nef induces aberrant sorting of CD4 by binding to the cytoplasmic tail and physically linking it to specific components of the host-cell protein-trafficking machinery. This process is known to depend on the dileucine motif in the C-terminal flexible loop of Nef, which has been shown by others to mediate interactions between Nef and the AP-1 and AP-3 clathrin adaptor protein complexes. This has led to the proposal that Nef recruits AP-1 and AP-3 to intracellular membranes to redirect CD4 from the secretory pathway to lysosomes, where the receptor is degraded. In the previous chapter, Nef was found to interact with the plasma membrane-localized AP-2 complex in a dileucine-dependent manner. RNAi-mediated depletion of AP-2 inhibited the downregulation of CD4 by Nef, but similar knockdowns of AP-1 and AP-3 appeared to have no effect. Here, the identification of a second motif in the Nef flexible loop, required for the interaction with AP-2, is described. This motif is centered around an acidic pair that fits the consensus sequence [D/E]D. Mutation of either of these residues had no effect on the binding of Nef to AP-1 or AP-3; however, even minor modifications of the [D/E]D site disrupted the Nef-AP-2 interaction and prevented Nef from downregulating CD4. Interestingly, the dileucine motif of the endogenous protein tyrosinase was found to bind AP-2 independently of the diacidic motif, both in its native context and in the context of full-length Nef. Collectively, these results identify a novel type of AP-2 interaction determinant, support the notion that AP-2 is the key clathrin adaptor for the downregulation of CD4 by Nef, and reveal a previously unrecognized diversity among dileucine sorting signals.

## 4.2 Introduction

In the previous chapter, RNAi experiments in *Drosophila* and human cells confirmed the role of AP-2 in the Nef-mediated downregulation of CD4. Yeast three-hybrid and GST pull-down experiments were then used to demonstrate a direct, robust interaction between Nef and AP-2. This interaction was found to depend on the dileucine motif in the C-terminal flexible loop of Nef, which has been shown by others to be crucial for CD4 downregulation (Section 1.8; Bresnahan et al., 1998; Craig et al., 1998; Craig et al., 2000). In this chapter, the Nef flexible loop will be examined in greater detail to determine if it contains any other motifs that are required for AP-2 binding and CD4 downregulation.

The Nef flexible loop (which is comprised of residues 154 to 180 in the HIV-1 NL4-3 variant) sits between the final two strands of a  $\beta$ -sheet located in the Nef core, and is entirely exposed to the surrounding solvent (see Fig. 1.7). In addition to the dileucine sequence, three distinct motifs in the flexible loop have previously been implicated in the modulation of CD4 expression. All three of these motifs (EE154,155, DD174,175, and ERE177-179) are characterized by the presence of polar residues. Substitution of these residues with alanine, a non-polar amino acid, significantly decreases the ability of Nef to downregulate CD4 (Aiken et al., 1996; Piguet et al., 1999). Immunoblotting indicates that mutation of the charged residues does not affect stability of Nef, which is consistent with their position on a solvent-exposed loop (Aiken et al., 1996; Geyer et al., 1999; Grzesiek et al., 1996).

Instead, the alanine substitutions described above are believed to interfere with CD4 downregulation by disrupting electrostatic interactions between Nef and endogenous proteins (Aiken et al., 1996; Gibbs and Zoller, 1991). The EE154,155 motif has been suggested to bind COPI, which may promote the transport of CD4 from endosomes to lysosomes (for more information on this motif and the postendocytic fate of CD4, see Sections 3.4.5 and 6.4.2; also see Benichou et al., 1994; Piguet et al., 1999; Schaefer et al., 2008). The DD174,175 motif, on the other hand, has been implicated in binding to several host-cell proteins: the c-Raf1 kinase, the Eed Polycomb Group protein, and the V1H subunit of the vacuolar ATPase (Hodge et al., 1998; Lu et al., 1998; Witte et al., 2004). V1H has also been shown to interact with the  $\mu$ 2 subunit of AP-2, leading to the proposal that it acts as a bridge between Nef and AP-2 (Geyer et al., 2002). The

ERE177-179 motif, unlike the other two polar motifs in the Nef flexible loop, has not yet been linked to any protein interactions.

In the next section, each residue in the loop – including those that comprise the three polar motifs mentioned above – will be mutated to alanine to determine whether they contribute to the binding of Nef and AP-2. Special attention will be paid to D174 and D175, as these residues have been suggested by others to participate in AP-2 binding in an indirect fashion, via the V1H intermediary protein (Geyer et al., 2002; Lu et al., 1998). However, data presented in the previous chapter shows that Nef interacts with AP-2 directly; yeast three-hybrid and *in vitro* assays will therefore be used to evaluate whether the D174 and D175 residues are required for this direct binding. Results from these experiments will be correlated with functional data measuring the role of D174 and D175 in CD4 downregulation. Finally, yeast three-hybrid assays will also be used to ascertain whether D174 and D175 are involved in the interaction of Nef with AP-1 and AP-3, and whether diaspatic acid motifs mediate the binding of adaptins in other contexts, such as the cytoplasmic tail of tyrosinase. Collectively, the assays performed in this chapter should provide a clearer picture of the AP-2 binding surface on Nef, an improved understanding of the CD4 downregulation mechanism, and new insights on adaptin-cargo interactions.

## 4.3 Results

### 4.3.1 Identification of a diacidic motif required for the interaction of HIV-1 Nef with the AP-2 $\alpha$ - $\sigma$ 2 hemicomplex

The Nef dileucine motif (ENTSL160-165 in the HIV-1 NL4-3 strain) is contained within a 27-residue C-terminal flexible loop of the protein (residues 154-180 in NL4-3; see Fig. 1.7), and is highly conserved among all strains of HIV and SIV (Leitner et al., 2005; Munch et al., 2005; O'Neil et al., 2006). Such a high degree of conservation is consistent with the critical role the dileucine motif plays in CD4 downregulation and AP-2 binding (see Fig. 3.3, 3.4, 3.8, and 3.9; Bresnahan et al., 1998; Craig et al., 1998; Doray et al., 2007; Greenberg et al., 1998a; Janvier et al., 2003b; Rose et al., 2005). Analysis of 1,290 Nef sequences catalogued in the Los Alamos HIV sequence database revealed that this conservation extends beyond the dileucine motif, to include most of the residues within the C-terminal flexible loop (Fig. 4.1B). To determine whether these residues were also important for binding AP-2, 26 of the 27 loop residues were mutated to alanine in the context of full-length Nef (residue 156 is a naturally occurring alanine). These mutants were then tested for their ability to interact with AP-2 in the Y3H assay. Of the four subunits of AP-2, an assembly of two,  $\alpha$ - $\sigma$ 2, was shown in the previous chapter to be sufficient for the interaction with Nef (see Fig. 3.8), thus enabling the use of the Y3H system. As expected, mutation of either L164 or L165 of the Nef dileucine motif completely abrogated binding of  $\alpha$ - $\sigma$ 2 (Fig. 4.1C; see also Fig. 3.8). Mutation of the E160 residue, which is part of the consensus ExxxLL sequence, caused a partial loss of binding (Fig. 4.1C), as shown previously (see Fig. 3.8). Interestingly, mutation of several residues in the C-terminal half of the loop also caused defects in  $\alpha$ - $\sigma$ 2 binding, with varying degrees of severity (Fig. 4.1C). The strongest defects were observed for mutants with alterations of the acidic residues D174 and D175, which exhibited no binding to  $\alpha$ - $\sigma$ 2 (Fig. 4.1C). Mutation of several other residues in this region, including L170, H171, G172, M173, P176, R178, E179, and V180 caused partial binding defects (Fig. 4.1C). The charged residues in the C-terminal half of the loop have previously been implicated in CD4 downregulation (Aiken et al., 1996; Iafrate et al., 1997) and localization of Nef to clathrin-coated pits at the plasma membrane (Greenberg et al., 1997). In particular, the DD174,175AA and ERE177-179AAA mutants have been shown to be null for

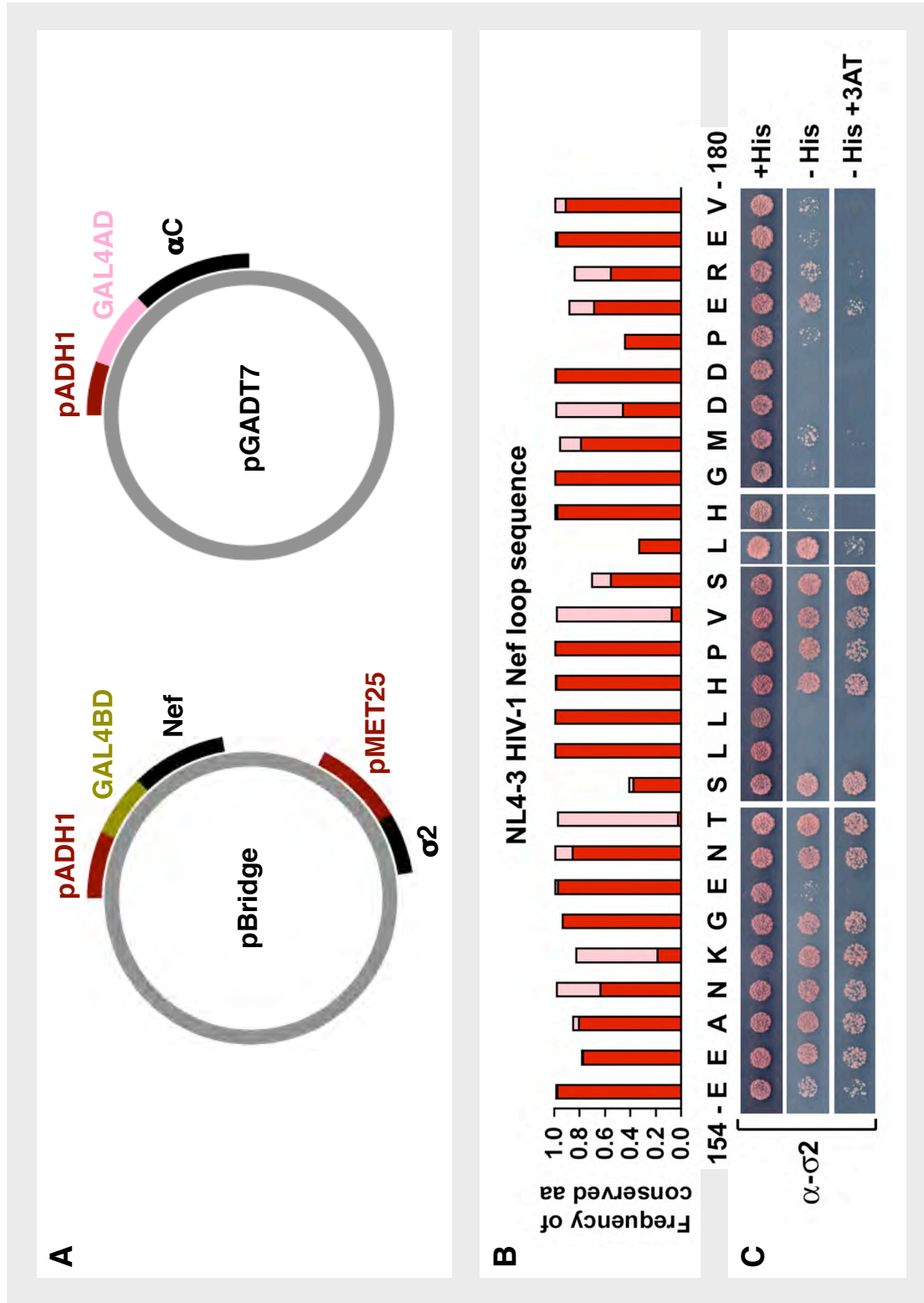
**FIG. 4.1: Identification of residues within the HIV-1 Nef C-terminal flexible loop that contribute to AP-2 binding**

**(A)** Plasmids used for the Y3H experiments. Nef was expressed as a GAL4BD fusion protein from the pBridge vector, along with the AP-2  $\sigma 2$  subunit. The AP-2  $\alpha$  subunit was expressed as a GAL4AD fusion protein from the pGADT7 vector.

**(B)** Comparison of the loop sequence (residues 154 to 180) of NL4-3 Nef to an alignment of 1,290 HIV-1 and SIV Nef sequences found on the Los Alamos HIV sequence database ([www.hiv.lanl.gov](http://www.hiv.lanl.gov)). The NL4-3 residues were scored for the frequency of identity and similarity at each position within the alignment. Similarity was defined by a log odds score of  $\geq 0$  on the BLOSUM62 substitution matrix (Henikoff and Henikoff, 1992). The bar graph indicates the frequency of occurrence of each NL4-3 residue in the aligned sequences (**red** bars) as well as the frequency of similar residues at each position (**pink** bars).

**(C)** Y3H analysis of the binding of NL4-3 Nef loop mutants to the AP-2  $\alpha$ - $\sigma 2$  hemicomplex. Each colony represents an alanine substitution mutant at the corresponding residue of the Nef loop, coexpressed with the AP-2 subunits by transformation of HF7c yeast with the plasmids shown in panel A. The third position (residue 156) is a naturally occurring alanine in the wild-type sequence, and was included for the sake of comparison. Growth in the absence of histidine (-His) or in the combined absence of histidine and presence of 3 mM 3-amino-1,2,4-triazole (+3AT) is indicative of interactions at two levels of stringency. Immunoblot analysis (performed in collaboration with Wolf Lindwasser) showed that all the Nef fusion proteins were expressed at similar levels in the transformed yeast cells (data not shown).

FIG. 4.1



CD4 downregulation (Aiken et al., 1996; Greenberg et al., 1997). The Y3H results presented here suggest that the requirement of these residues for Nef function may be due to their roles in mediating the interaction with AP-2. Because mutation of D174 and D175 caused the most severe defects in binding AP-2, subsequent experiments focused on these two residues (referred to below as the “diacidic motif”).

#### **4.3.2 The diacidic motif is required for direct binding of HIV-1 Nef to AP-2**

To determine if the diacidic motif was required for the direct interaction of Nef with AP-2, *in vitro* experiments were performed (by William Smith) using recombinant proteins produced in bacteria. These experiments were carried out using the AP-2<sup>CORE</sup> complex, which lacks the C-terminal domain of the  $\mu$ 2 subunit (see Section 2.3.1.3 for further information on this construct). In the previous chapter, pull-down assays demonstrated that the GST-tagged AP-2<sup>CORE</sup> complex interacted with Nef in a manner that was dependent on the Nef dileucine motif (see Fig. 3.9). Additional pull-down assays showed that the AP-2<sup>CORE</sup> complex was able to bind wild-type Nef, but not the Nef DD174,175AA mutant, as detected by SDS-PAGE followed by Coomassie blue staining (Fig. 4.2A, top) and immunoblot analysis (Fig. 4.2A, bottom). Under the same conditions, there was negligible binding of both wild-type and mutant Nef to GST- $\epsilon$ -ear (Fig. 4.2A), confirming the specificity of the Nef-AP-2 interaction. These results were corroborated by surface plasmon resonance (SPR) spectroscopy, which showed binding of untagged AP-2<sup>CORE</sup> to wild-type Nef but not to the DD174,175AA mutant (Fig. 4.2B). The affinity of AP-2<sup>CORE</sup> for wild-type Nef, as calculated from the SPR experiments, was  $6 \pm 1 \mu\text{M}$  ( $n = 3$ ). The GST pull-down and SPR assays thus demonstrated that the diacidic motif is required for the direct interaction of Nef with AP-2.

#### **4.3.3 Binding of HIV-1 Nef to AP-2 is dependent on electrostatic interactions**

The requirement of the diacidic motif, as well as other charged residues (such as E160 and ERE177-179), for Nef binding to AP-2 suggested that electrostatic interactions might be important contributors to the overall binding affinity. If so, binding of the two proteins should be sensitive to high salt concentrations. To test this prediction, GST pull-down assays were carried out (by William Smith) to examine the binding of Nef to AP-2<sup>CORE</sup> in the presence of increasing concentrations of NaCl (Fig. 4.2C).

**FIG. 4.2: In vitro analyses of Nef-AP-2 interaction determinants**

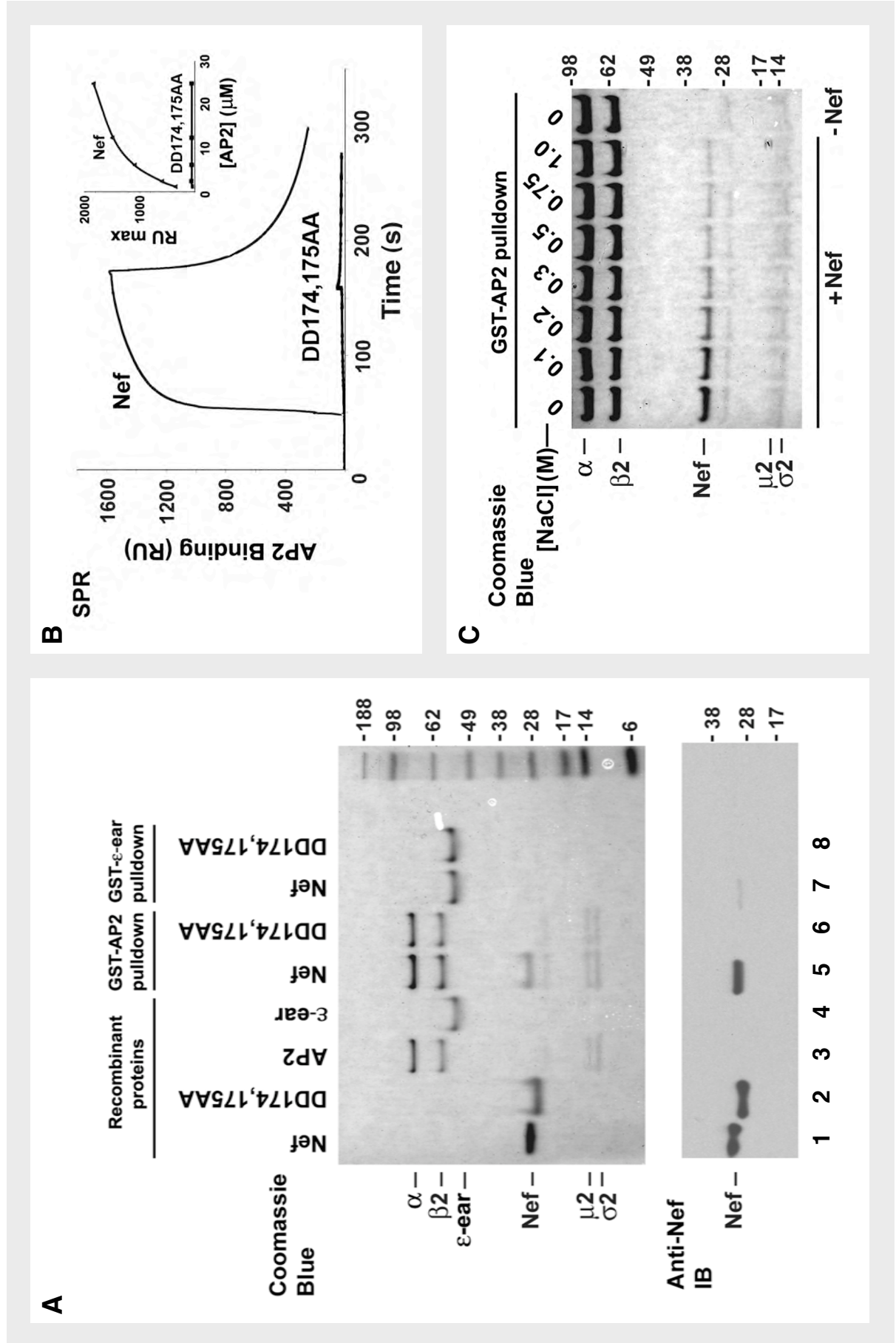
Purified recombinant proteins used in these experiments include His<sub>6</sub>-tagged wild-type and DD174,175AA mutant Nef, GST-tagged AP-2<sup>CORE</sup>, and GST-tagged AP-4  $\epsilon$  ear (included as a negative control for the experiments described in panels A and B).

**(A)** GST pull-down analysis indicates the Nef diacidic motif is required for direct binding to AP-2. His<sub>6</sub>-tagged wild-type and DD174,175AA mutant Nef were incubated with either GST-AP-2<sup>CORE</sup> or GST- $\epsilon$  ear in the presence of glutathione-Sepharose beads, after which the beads were washed and subjected to SDS-PAGE. The separated proteins were then stained with Coomassie blue (top) and immunoblotted (IB) with an anti-Nef antibody (bottom). The positions of the molecular weight markers (in kDa) are indicated on the right. For the sake of comparison, the input recombinant proteins (lanes 1-4) were run alongside the proteins used in the pull-down experiment (lanes 5-8). Wild-type Nef is visible as an approximately 27-kDa band in lane 5.

**(B)** SPR analysis indicates that wild-type Nef, but not DD174,175AA mutant Nef, is able to bind directly to AP-2. Equivalent amounts of GST- $\epsilon$  ear (included as a control), His<sub>6</sub>-Nef, and His<sub>6</sub>- Nef DD174,175AA were covalently attached to the surface of CM5 sensor chip. The ability of these proteins to bind AP-2 was then assayed by passing untagged AP-2<sup>CORE</sup> over the chip and measuring the response units (RU) for the three different conditions. Shown are control-subtracted sensograms of AP-2<sup>CORE</sup> at a concentration of 25  $\mu$ M. (Inset) Plot of the max RU for varying concentrations (0.05  $\mu$ M to 0.25  $\mu$ M) of untagged AP-2<sup>CORE</sup>.

**(C)** The interaction of Nef and AP-2 is sensitive to the ionic strength of the surrounding solution. GST-tagged AP-2<sup>CORE</sup> was incubated with His<sub>6</sub>-tagged wild-type Nef in the presence of increasing NaCl concentrations (0 M to 1.0 M) during the pull-down experiment. The positions of the molecular mass markers (in kDa) are shown on the right of the Coomassie blue-stained gel.

FIG. 4.2



Performed by William Smith

The interaction did, indeed, appear to be salt sensitive, as a dramatic loss of binding between Nef and AP-2<sup>CORE</sup> was observed at NaCl concentrations above physiological levels (150 mM). This indicated that electrostatic interactions are a driving factor in the formation of a Nef-AP-2 complex.

#### **4.3.4 The diacidic motif fits a [D/E]D consensus sequence and is not required for interaction with the AP-1 $\gamma$ - $\sigma$ 1 or AP-3 $\delta$ - $\sigma$ 3 hemicomplexes**

To further characterize the specific requirements for each residue of the Nef diacidic motif, the aspartate residues were mutated – either individually or in combination – to alanine, glutamate, and asparagine. The effect of these mutations on the ability of Nef to bind the AP-2  $\alpha$ - $\sigma$ 2 hemicomplex was then examined using the Y3H system (Fig. 4.3B, middle panel). The single or double mutation of Nef D174 and D175 to alanine completely abolished the interaction with  $\alpha$ - $\sigma$ 2. The isoelectric D174E mutation, on the other hand, had no effect on the ability of Nef to bind  $\alpha$ - $\sigma$ 2. This result correlates with the sequence conservation of Nef, as position 174 is nearly always occupied by either D or E (46.0% D, 52.2% E among all HIV-1 Nef variants; see Fig. 4.1B). In contrast, D175E displayed severely reduced binding to  $\alpha$ - $\sigma$ 2. This is in accordance with the almost exclusive occurrence of D at this position (98.9% D among all HIV-1 Nef variants; see Fig. 4.1B). The isosteric D174N and D175N substitutions resulted in elimination and reduction of Nef binding to  $\alpha$ - $\sigma$ 2, respectively. Thus, the Nef diacidic motif can be generally defined as [D/E]D, with N as a weak substitute for the second position. Remarkably, none of the mutations in the diacidic motif had any effect on the interaction of Nef with the homologous AP-1  $\gamma$ - $\sigma$ 1 (Fig. 4.3B, top panel) and AP-3  $\delta$ - $\sigma$ 3 (Fig. 4.3B bottom panel) hemicomplexes. Mutation of the Nef dileucine motif, however, disrupted binding to all three hemicomplexes (Fig 4.3; see also Fig. 3.8 and Janvier et al., 2003b). Therefore, the interaction of Nef with AP-2 depends on both the dileucine and diacidic motifs, whereas the interaction with AP-1 and AP-3 is exclusively dependent on the dileucine motif. This strongly suggests that the Nef diacidic motif is conserved for the purpose of binding AP-2.

#### **4.3.5 Correlation between the requirements of the Nef diacidic motif and CD4 downregulation**

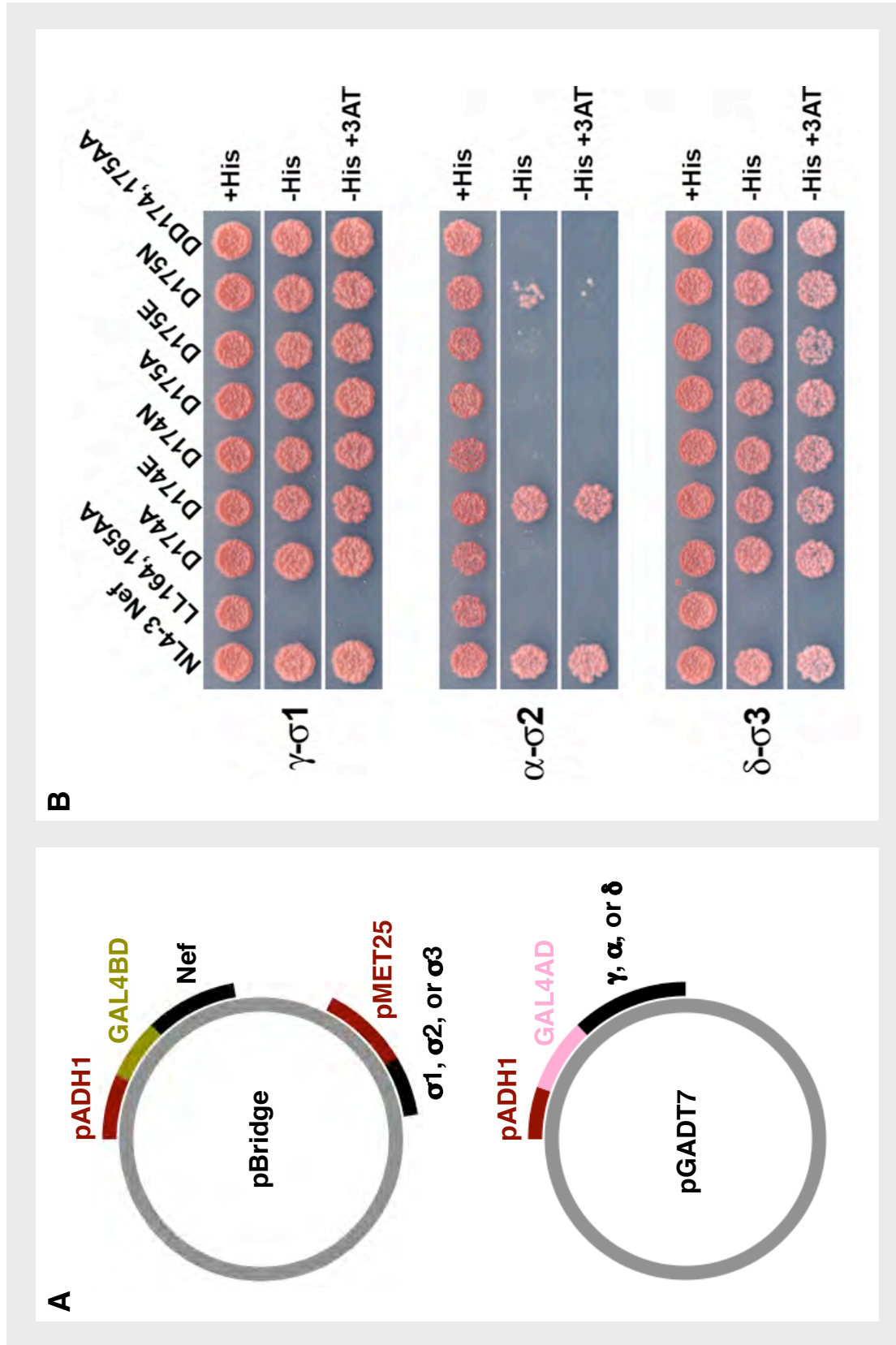
In order to assess whether – in addition to binding AP-2 – the Nef diacidic motif was

**FIG. 4.3: Mutational analysis of Nef binding to the AP-1  $\gamma$ - $\sigma$ 1, AP-2  $\alpha$ - $\sigma$ 2, and AP-3  $\delta$ - $\sigma$ 3 hemicomplexes**

**(A)** Wild-type and mutant versions of Nef were expressed as GAL4BD fusion proteins from the pBridge vector, along with either  $\sigma$ 1,  $\sigma$ 2, or  $\sigma$ 3. The large adaptin subunits,  $\gamma$ ,  $\alpha$ , and  $\delta$ , were expressed as GAL4AD fusion proteins from the pGADT7 plasmid.

**(B)** HF7c yeast were cotransformed with pairs of pBridge and pGADT7 plasmids, and then plated on selective media. Growth of the yeast on the  $-$ His media indicates an interaction between Nef and the AP hemicomplex. Growth on the  $-$ His +3AT media indicates a more robust interaction.

FIG. 4.3



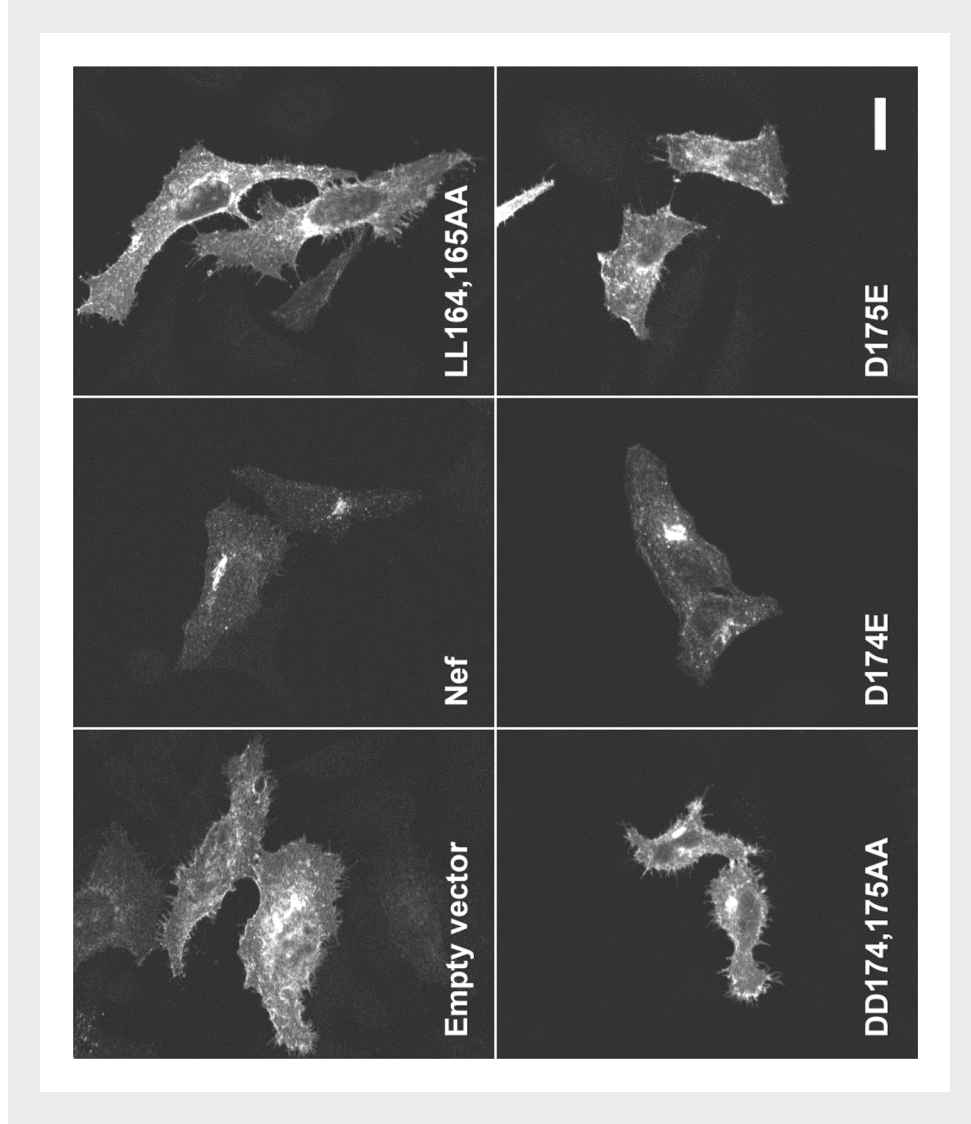
required for CD4 downregulation, the activity of several of the Nef mutants described above was observed in transfected HeLa cells by immunofluorescence (Fig. 4.4) and flow cytometry (Fig. 4.5). In agreement with previously published work (Aiken et al., 1996; Iafrate et al., 1997), the Nef DD174,175AA mutant, like the Nef LL164,165AA mutant, failed to downregulate CD4 in both assays (Fig. 4.4 and 4.5A and B). The individual mutation of D174 or D175 to alanine also significantly impaired the ability of Nef to downregulate CD4, as measured by flow cytometry (Fig 4.5A and B). Remarkably, mutation of D174 to glutamate had no effect on CD4 downregulation, while mutation of D175 to glutamate abolished downregulation in both assays (Fig. 4.4 and 4.5A and B). Immunoblot analysis showed that all constructs were expressed at similar levels (Fig. 4.5B), and consistent with a previous report (Stoddart et al., 2003), mutation of the diacidic motif did not affect the ability of Nef to downregulate the MHC-I receptor in HeLa cells, as observed by flow cytometry (assays performed by Wolf Lindwasser, data not shown). Therefore, the failure of some Nef mutants to downregulate CD4 was not due to either a lack of expression or misfolding of the viral protein. Rather, the ability of the Nef diacidic mutants to downregulate CD4 corresponded closely to their affinity for  $\alpha$ - $\sigma$ 2 in the Y3H experiments (see Fig. 4.3), which provides further evidence for a causal relationship between Nef-AP-2 binding and CD4 downregulation.

Although intracellular retention and enhanced endocytosis have both been proposed as potential mechanisms for the downregulation of CD4 by Nef (see Fig. 3.6 and 3.7; Aiken et al., 1994; Foti et al., 1997; Greenberg et al. 1998a; Greenberg et al., 1998b; Jin et al., 2005; Mangasarian et al., 1997; Rhee et al., 1994; Rose et al., 2005), only the latter pathway is consistent with a role for AP-2 in this process. To explore the correlation between Nef-AP-2 binding and CD4 downregulation in more detail, the rate at which CD4 was endocytosed from the plasma membrane was measured (in collaboration with Wolf Lindwasser) in the absence and presence of wild-type and mutant forms of Nef (Fig. 4.5C). Compared to an empty vector control, wild-type Nef increased the rate of CD4 internalization, but the Nef LL164,165AA dileucine mutant did not (Fig. 4.5C). Importantly, the Nef DD174,175AA diacidic mutant also failed to increase the rate of CD4 endocytosis above basal levels (Fig. 4.5C). Thus, both the dileucine and diacidic motifs of Nef are required for the enhanced endocytosis and downregulation of CD4.

**FIG. 4.4: Immunofluorescence microscopy analysis of CD4 downregulation by wild-type and mutant Nef proteins**

HeLa cells were cotransfected with two different plasmids: pCMV.CD4 and wild-type or mutant versions of pCI.Nef. The cells were then fixed, permeabilized, and stained with a mouse monoclonal antibody to human CD4 and AlexaFluor 594-conjugated donkey antibody to mouse IgG. The distribution of CD4 within the stained cells was imaged by confocal microscopy. Bar, 10  $\mu$ M.

**FIG. 4.4**



**In collaboration with Wolf Lindwasser**

**FIG. 4.5: Flow cytometric analysis of CD4 downregulation by wild-type and mutant Nef proteins**

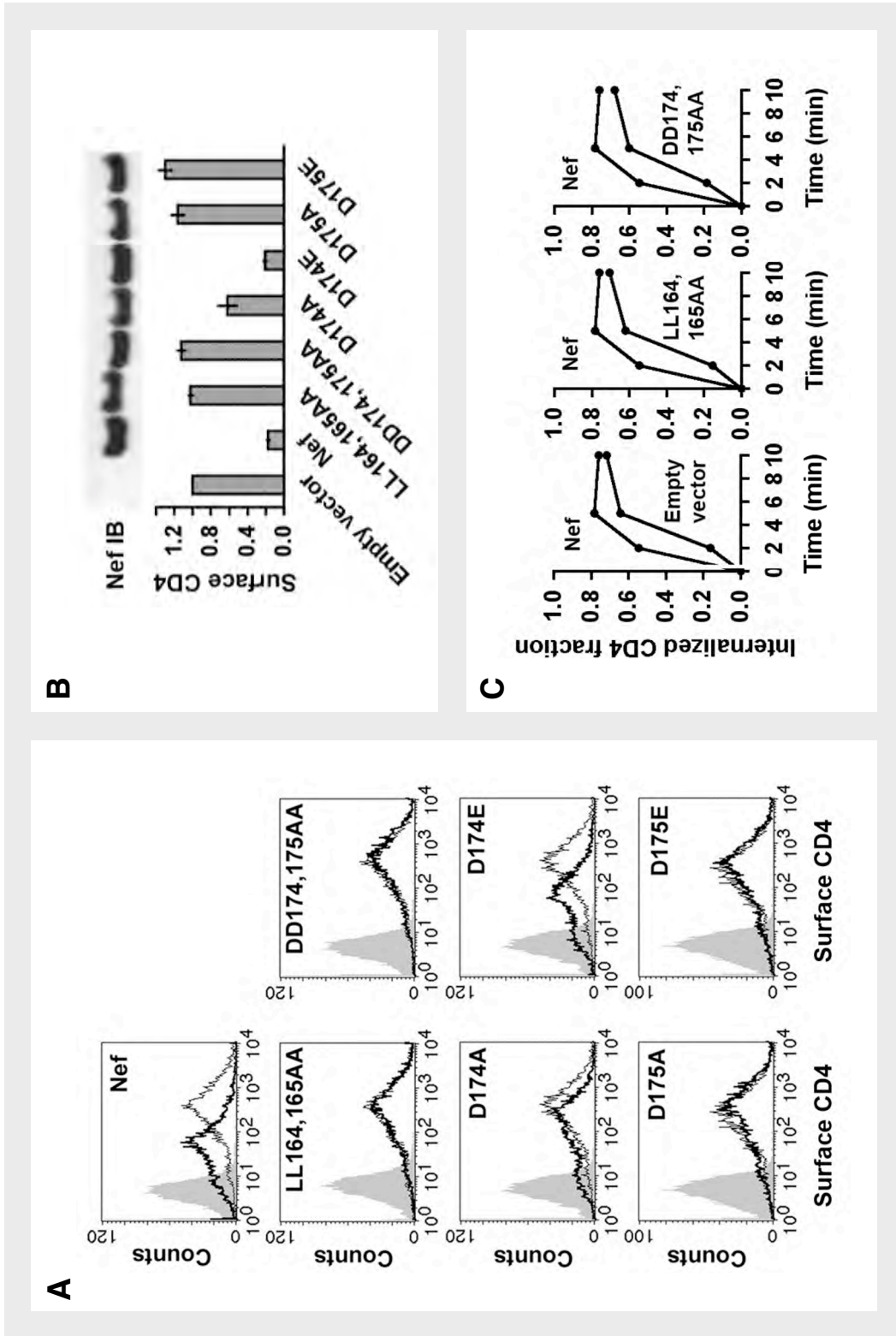
HeLa cells were cotransfected with pCMV.CD4 and either wild-type or mutant versions of pNef<sub>NL4.3</sub>.IRES.GFP, which is designed to express Nef and GFP as separate proteins from the same bicistronic transcript. For the flow cytometric analysis, GFP fluorescence was used as a marker to identify cells that had been transfected with a Nef expression plasmid.

**(A)** Representative histograms of CD4 surface levels in cells transfected with the plasmids described above. For each condition, the amount of CD4 at the plasma membrane is shown for cells transfected with the pIRES.GFP empty vector (i.e., no Nef expression; thin lines) and for cells transfected with wild-type or mutant Nef (bold lines). The profile of cells left untransfected (i.e., no CD4 expression; solid gray shading) is also shown to indicate the level of background fluorescence.

**(B)** (Top) Immunoblot analysis of the expression of wild-type and mutant versions of Nef in the transfected HeLa cells shown in panel A, using an antiserum to HIV-1 Nef. Cells transfected with the pIRES.GFP empty vector were included as a negative control. (Bottom) Quantification of the results from panel A. Bars represent the amount of CD4 on the cell surface (relative to the level of CD4 on cells transfected with the pIRES.GFP empty vector), in terms of the average geometric mean  $\pm$  SEM from three independent experiments.

**(C)** Endocytosis of CD4 in cells expressing wild-type or mutant versions of Nef. Data for cells that were transfected with the pIRES.GFP empty vector and do not express Nef are included as a control, and represent the basal rate of CD4 internalization.

FIG. 4.5



Part C in collaboration with Wolf Lindwasser

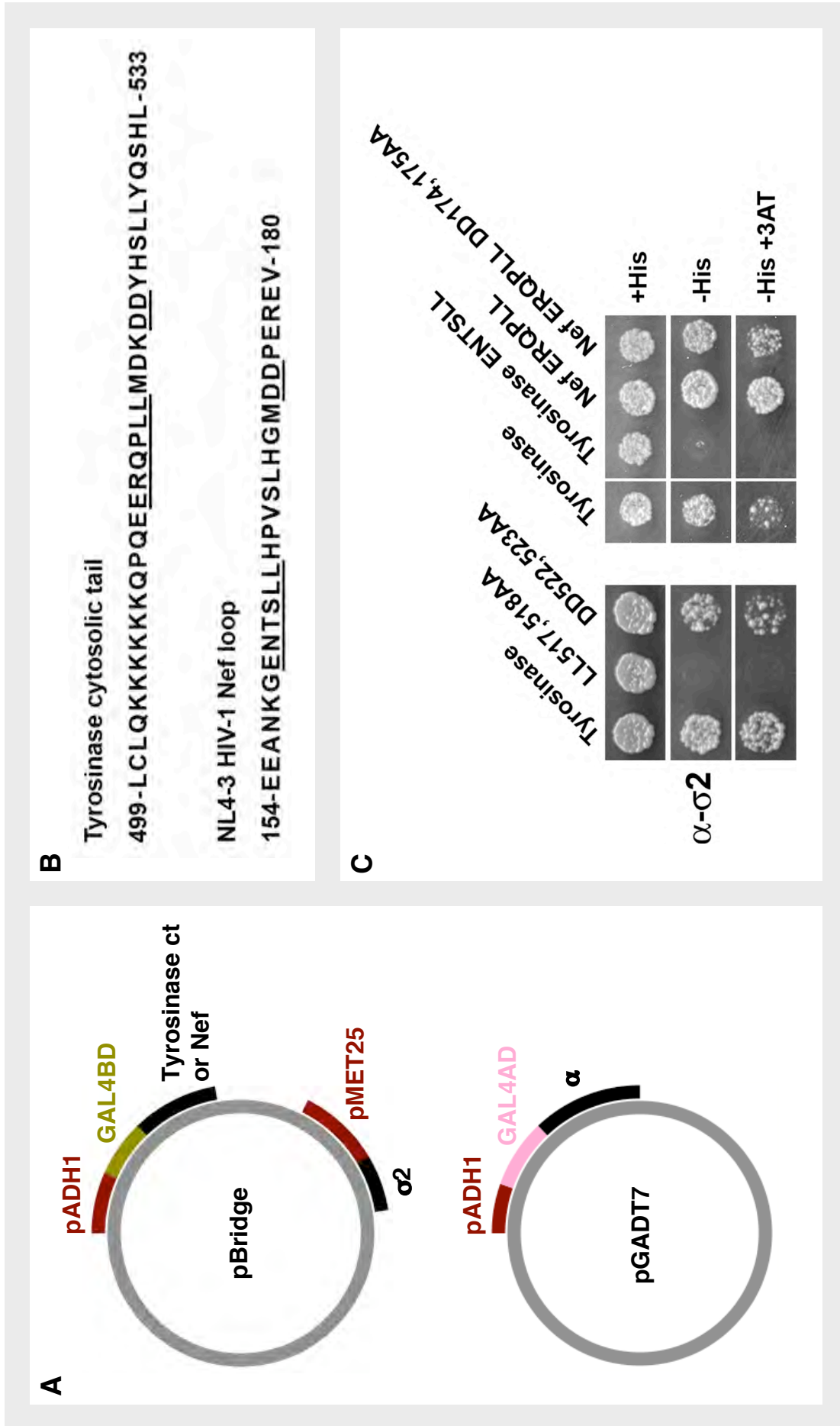
#### 4.3.6 Distinct requirements of different dileucine motifs for the contribution of diacidic motifs

Nef is one of several proteins that, in addition to a dileucine motif, contains a diacidic motif in its cytoplasmic domain. Another example is the enzyme tyrosinase, which is a type I transmembrane protein involved in the synthesis of melanin in melanosomes. Within the cytoplasmic tail of mouse tyrosinase (residues 499-533; Fig. 4.6B), the dileucine motif (ERQPLL; residues 513-518) is followed by a diacidic motif (DD; residues 522 and 523). The tyrosinase tail has previously been shown to bind to the AP-1  $\gamma$ - $\sigma$ 1 and AP-3  $\delta$ - $\sigma$ 3 hemicomplexes using the Y3H system (Theos et al. 2005). Here, the Y3H system was used to test the ability of the wild-type tyrosinase tail, as well as the LL517,518AA and DD522,523AA mutants, to bind to the AP-2  $\alpha$ - $\sigma$ 2 hemicomplex. These experiments revealed that the tyrosinase tail interacted with  $\alpha$ - $\sigma$ 2, and that this interaction was completely dependent on the dileucine motif, but only slightly dependent on the diacidic motif (Fig. 4.6C, left panel). This latter result is in contrast with the absolute requirement of the diacidic motif for the interaction of Nef and  $\alpha$ - $\sigma$ 2. However, it is possible that the dileucine motif of Nef might be weaker than that of tyrosinase, necessitating the additional contribution of the diacidic motif for detectable binding. To test this hypothesis, tyrosinase tail constructs were made in which the ERQPLL sequence was replaced by the Nef ENTSSL sequence, and vice versa. Unlike the wild-type tyrosinase tail, tyrosinase with the ENTSSL sequence was not able to bind  $\alpha$ - $\sigma$ 2 (Fig. 4.6C, right panel). Importantly, Nef ERQPLL interacted with  $\alpha$ - $\sigma$ 2 in a manner that was largely independent of the diacidic motif (Fig. 4.6C, right panel). Because swapping the dileucine signals involved replacement of only the intervening NTS and RQP residues (i.e., the X positions in the [D/E]xxxL[L/I] consensus sequence), the data shown here suggest that these residues are important contributors to the interaction between dileucine motifs and  $\alpha$ - $\sigma$ 2. These experiments thus highlight a previously unrecognized diversity among [D/E]xxxL[L/I] sorting signals, some of which require additional determinants for binding AP-2.

**FIG. 4.6: Y3H analysis reveals qualitative differences among dileucine motifs**

- (A)** Wild-type and mutant versions of the mouse tyrosinase cytosolic tail (ct) and mutant versions of NL4-3 Nef were expressed as GAL4BD fusion proteins from the pBridge vector, along with either  $\sigma 1$ ,  $\sigma 2$ , or  $\sigma 3$ . The large adaptin subunits,  $\gamma$ ,  $\alpha$ , and  $\delta$ , were expressed as GAL4AD fusion proteins from the pGADT7 plasmid.
- (B)** Amino acid sequences of the cytosolic tail of mouse tyrosinase and the NL4-3 Nef C-terminal flexible loop. The relevant dileucine and diacidic motifs are underlined. Residue numbers are given on the left and right of the sequences.
- (C)** Y3H analysis of the interaction of the AP-2  $\alpha$ - $\sigma 2$  hemicomplex with wild-type and mutant versions of the tyrosinase cytosolic tail and with mutant versions of full-length Nef. Growth of the yeast on media lacking histidine ( $-His$ ), or lacking histidine and supplemented with 3-amino-1,2,4-triazole (+3AT) is indicative of an interaction.

FIG. 4.6



## **4.4 Discussion**

### **4.4.1 Chapter overview**

The results shown in this chapter provide evidence for the existence of a novel, conserved diacidic motif within the C-terminal flexible loop of HIV-1 Nef. The diacidic motif (DD174,175 in the NL4-3 strain and [D/E]D in general) cooperates with the previously characterized dileucine motif (ENTSLL160-165 in NL4-3 and ExxxLL in general) to bind the AP-2 complex. Indeed, both the diacidic and dileucine motifs were required for the interaction of Nef and AP-2 in Y3H, GST pull-down, and SPR assays. Functional analysis of the diacidic motif revealed that it was essential for the downregulation of CD4 by Nef, as determined by confocal microscopy and flow cytometry. The diacidic motif, however, was not required for the interaction of Nef with the AP-1 and AP-3 complexes, nor was it required for the dileucine motif of tyrosinase to bind AP-2. Together, these results provide strong support for the proposed role of AP-2 in the Nef-mediated downregulation of CD4, and reveal qualitative differences among dileucine sorting signals and their binding sites on AP complexes.

### **4.4.2 The Nef diacidic motif is needed for AP-2 binding and CD4 downregulation**

The Nef DD174,175 residues were first ascribed a role in CD4 downregulation more than a decade ago (Aiken et al., 1996). In that study, the authors identified several clusters of conserved, charged residues within Nef. They then mutated those residues to alanine, and observed the effect of those substitutions on the stability and function of the viral protein. Mutation of the aspartate residues did not reduce the stability of the protein when compared to the expression of wild-type Nef; however, the DD174,175AA mutant was completely null for CD4 downregulation. Others subsequently demonstrated that the failure of Nef DD174,175AA to downregulate CD4 was not due to misfolding of the viral protein, as the mutant was capable of reducing the amount of MHC-I on the cell surface (Wolf Lindwasser, data not shown; Stoddart et al., 2003). Several years after the Nef DD174,175 residues were reported to be essential for the downregulation of CD4, a research group claimed that these residues were important for binding the V1H subunit of the vacuolar ATPase (Lu et al., 1998). The same group later suggested that, because V1H binds the  $\mu$ 2 subunit of AP-2, the Nef DD174,175 residues were important for linking the viral protein to the endocytic

machinery of the host cell (Geyer et al., 2002). This led to a model in which Nef was thought to bind to CD4 at the plasma membrane, and then promote the internalization of the receptor by interacting with V1H directly and AP-2 indirectly (Geyer et al., 2002; reviewed in Geyer et al., 2001).

In the previous chapter, Nef was found to bind directly to a combination of the  $\alpha$  and  $\sigma 2$  subunits of AP-2 (Fig. 3.7 and 3.8). In this chapter, several assays were used to show that this interaction depended on the Nef DD174,175 residues (Fig. 4.1, 4.2, and 4.3). Importantly, the ability of Nef to bind AP-2 was correlated with the amino acids most often found in that region of the viral protein (Fig. 4.1 and 4.3). This is best exemplified by the observation that glutamate – which is commonly found at position 174, but virtually never found at position 175 in HIV-1 Nef alleles – was only able to substitute for the first aspartate in Nef-AP-2 binding assays (Fig. 4.3). Two different functional assays also showed that the Nef D174E mutant, but not the D175E mutant, was able to downregulate CD4 (Fig. 4.4 and 4.5). Thus, it appears likely that the Nef diacidic motif is conserved for the purpose of directly binding AP-2, which the viral protein uses to accelerate the endocytosis of CD4 (Fig. 4.5C).

Compared to the V1H-dependent model of Nef function described earlier (Geyer et al., 2002), these results provide a simpler, more straightforward explanation for the strict conservation of the diacidic motif and its role in CD4 downregulation. However, a role for V1H in the Nef-mediated targeting of CD4 to lysosomes cannot be ruled out entirely. Indeed, it is possible that Nef binds to V1H after CD4 is internalized from the cell surface and the AP-2-clathrin coat is lost. An interaction between Nef and V1H at this stage could facilitate the assembly of functional vacuolar ATPases on CD4-positive endosomes, and promote acidification of these compartments prior to their eventual fusion with lysosomes (for reviews on vacuolar ATPases, see Nishi and Forgac, 2002; Marshansky and Futai, 2008). Additional experiments will have to be carried out to determine if Nef and V1H cooperate in this manner.

#### **4.4.3 The AP-1 and AP-3 complexes are largely dispensable for the Nef-mediated downregulation of CD4**

Although Nef has long been suspected to promote the downregulation of CD4 by an endocytic mechanism (Aiken et al., 1994; Rhee et al., 1994), more recent studies have

suggested that the AP-1 and AP-3 complexes, which mediate distinct protein sorting events, could be involved in the process (Bresnahan et al., 1998; Craig et al., 2000; Janvier et al., 2003b; Rose et al., 2005). The conclusions drawn from these studies were largely based on the observation that Nef binding to AP-1 and AP-3 depended on a dileucine motif in the viral protein, and that this motif was also required for CD4 downregulation (Bresnahan et al., 1998; Craig et al., 2000; Janvier et al., 2003b; Rose et al., 2005). One of the studies, however, did report the delayed transport of newly synthesized CD4 to the cell surface in the presence of Nef (Rose et al., 2005).

At least two major factors may have led those authors to include AP-1 and AP-3 in their models of Nef-induced CD4 downregulation. First, Nef was shown to interact with AP-1 and AP-3 (Bresnahan et al., 1998; Craig et al., 2000; Janvier et al., 2003b) several years before assays capable of detecting the robust binding of Nef to AP-2 were developed (Fig. 3.8 and 3.9). Second, prior to the identification of the diacidic motif (Fig. 4.1, 4.2, and 4.3), it was not possible to genetically separate the binding of Nef to the various AP complexes. Mutation of the previously mentioned Nef dileucine motif, for instance, not only inhibited CD4 downregulation, but also disrupted binding to AP-1, AP-2, and AP-3 (Fig. 3.3, 3.8, and 3.9; Bresnahan et al., 1998; Craig et al., 2000; Janvier et al., 2003b). Thus, it was difficult to ascribe the effect of this mutation on the ability of Nef to bind any one AP complex in particular. The RNAi-mediated depletion of adaptin subunits indicated that AP-2 was used by Nef to downregulate CD4 (Fig. 3.7; Jin et al., 2005), but the potential contribution of AP-1 and AP-3 to this process could not be ruled out, as residual amounts of these complexes may have been sufficient for Nef function (Fig. 3.7).

Experiments described in this chapter have identified, for the first time, mutants of Nef that are capable of interacting with AP-1 and AP-3, but not with AP-2 (Fig. 4.3). These mutants have substitutions in the conserved diacidic motif of the viral protein that profoundly inhibit the downregulation of CD4 (Fig. 4.3, 4.4, and 4.5). Therefore, the ability of Nef to downregulate CD4 appears to be dependent on its interaction with AP-2, and independent of its interactions with AP-1 and AP-3. From the data presented here, it is clear the Nef relies mainly on AP-2 to redistribute CD4 from the cell surface to intracellular vesicles (Fig. 4.4 and 4.5). However, it is still possible that Nef recruits AP-1 and/or AP-3 in support of this primary pathway. Nef could, for

example, use these other adaptors to either target CD4 from endosomes to lysosomes, delay the recycling of CD4 back to the cell surface, or route a small proportion of newly synthesized CD4 from the TGN to degradative compartments, as proposed earlier (Rose et al., 2005). To determine if this is the case, it will be important to measure how much CD4 is degraded in cells expressing a Nef diacidic mutant that is incapable of interacting with AP-2, such as DD174,175AA (Fig. 4.2 and 4.3). This experiment, and others like it, should provide an indication of whether AP-1 and AP-3 are involved in the downregulation of CD4, and could shed light on the mechanism Nef uses to target CD4 to lysosomes after the receptor is internalized from the plasma membrane.

#### **4.4.4 Analysis of the diacidic motif yields insights on the binding of dileucine signals to AP complexes**

As mentioned above, the Nef dileucine motif (ENTSLI) is able to mediate binding to AP-1 and AP-3 independently of the diacidic motif ([D/E]D), while both motifs are required for binding to the homologous AP-2 complex (Fig. 4.3). This immediately suggests that the dileucine binding sites on AP-1 and AP-3 differ, at least slightly, from that on AP-2, as these complexes have varying affinities for the same ligand. This also indicates that the binding site for the Nef diacidic motif is specific to AP-2 (a topic explored further in Chapter 5).

The Nef dileucine and diacidic motifs probably make direct, simultaneous contact with the surface of the AP-2  $\alpha$ - $\sigma$ 2 hemicomplex (Fig. 3.8, 3.9, 4.1, 4.2, and 4.3). The properties of the dileucine and diacidic binding sites on  $\alpha$ - $\sigma$ 2 are most likely quite distinct, as the key residues in these motifs have bulky hydrophobic and charged side chains, respectively. Consistent with an important contribution of electrostatic forces to the overall strength of the interaction, binding of Nef and AP-2 is inhibited *in vitro* by high salt concentrations (Fig. 4.2C). Interestingly, the observation that increasing the ionic strength of the solution disrupts the Nef-AP-2 interaction may indicate that charged residues (e.g., the diacidic motif) contribute more to the binding affinity than do hydrophobic residues (e.g., the dileucine motif).

Similar to Nef, the endogenous protein tyrosinase contains a dileucine sorting signal (ERQPLL) upstream of a pair of acidic residues (DD). These features make tyrosinase

an intriguing protein to study in parallel with Nef. Binding assays revealed that the diacidic motif was required for the interaction of Nef and AP-2, but was not required for the interaction of tyrosinase and AP-2 (Fig. 4.2, 4.3, and 4.6). One reason for this discrepancy may be that the tyrosinase dileucine motif is a stronger ligand than the Nef dileucine motif. In support of this idea, substitution of the Nef ENTSSL sequence for the ERQPLL sequence in the tyrosinase cytosolic tail abrogated binding to AP-2 (Fig. 4.6). Conversely, the replacement of ERQPLL with ENTSSL in the context of full-length Nef allowed the viral protein to bind AP-2 independently of the diacidic motif (Fig. 4.6). Thus, the tyrosinase dileucine motif does appear to have a greater affinity for AP-2 than the Nef dileucine motif. Since both motifs contain a glutamate and a pair of leucines, the differences in affinity must be due to the intervening residues (i.e., RQP and NTS). Consistent with this conclusion, a proline immediately upstream of the leucine pair has been found to induce more rapid endocytosis than an alanine at the same position (Patrycja Kozik and Margaret Robinson, personal communication).

Compared to the tyrosinase dileucine motif, the Nef dileucine motif does seem to be a weaker ligand for AP-2 binding. The diacidic motif may be required to compensate for this weakness and increase the avidity of Nef for AP-2. Given the reliance of Nef on AP-2 for CD4 downregulation, however, it is puzzling that the viral protein has not adopted a stronger dileucine motif. One possibility is that bivalent binding causes a conformational change in Nef that is required for its effect on CD4. Alternatively, the ENTSSL motif may be conserved because some residues are involved in functions other than AP-2 binding and CD4 downregulation. Some evidence for this already exists. Mutation of the NTS portion of the dileucine motif has recently been shown to have deleterious effects on the Nef-dependent upregulation of DC-SIGN and MHC class II-associated invariant chain (Coleman et al., 2006), despite the fact that these residues play little, if any, role in CD4 downregulation (Coleman et al., 2006; Janvier et al., 2003b).

#### **4.4.5: The diacidic motif: specific to Nef or broadly applicable?**

The diacidic motif, found in all HIV-1 Nef variants, represents a novel class of AP-2 cargo interaction determinant, in addition to the already well-characterized dileucine- and tyrosine-based sorting signals (reviewed in Bonifacino and Traub, 2003). In some

ways, this multiplicity of binding determinants is reminiscent of the endoplasmic reticulum-associated COPII complex, which can also interact with diverse signals through different interaction surfaces (reviewed in Barlowe, 2003). The Nef diacidic motif differs from most dileucine- and tyrosine-based signals, though, in that it does not appear capable of binding AP-2 on its own (Fig. 4.2 and 4.3). It remains to be seen whether acidic motifs from other proteins mediate interactions with AP-2. A pair of acidic residues in the cytosolic tail of tyrosinase, for instance, does not significantly contribute to AP-2 binding (Fig. 4.6). However, the cytosolic tails of many trans-membrane proteins have acidic clusters that are believed to function as sorting signals (Bonifacino and Traub, 2003). The acidic cluster of furin, in particular, has previously been found to mediate endocytosis as well as TGN localization (Vorhees et al., 1995), and is therefore a good candidate for interaction with AP-2. Alternatively, the binding of a diacidic motif with AP-2 might be particular to Nef. In that case, the interaction could be targeted for disruption by pharmacological agents in order to moderate the pathogenic effects of Nef.

**Chapter 5:**

**A basic patch on  $\alpha$ -adaptin is required for binding of HIV-1 Nef and cooperative assembly of a CD4-Nef-AP-2 complex**

## 5.1 Abstract

A critical function of the HIV-1 Nef protein is the downregulation of CD4 from the surfaces of infected cells. Nef is believed to act by linking the cytosolic tail of CD4 to the endocytic machinery of the host-cell, thereby increasing the rate at which CD4 is internalized. In support of this model, weak binary interactions between CD4, Nef, and the endocytic clathrin adaptor complex, AP-2, have been reported. In the previous two chapters, dileucine and diacidic motifs in the C-terminal flexible loop of Nef were shown to mediate binding to a combination of the  $\alpha$  and  $\sigma 2$  subunits of AP-2. In this chapter, the identification of a potential binding site for the Nef diacidic motif on  $\alpha$ -adaptin is described. This site is comprised of two basic residues, lysine-297 and arginine-340, on the  $\alpha$ -adaptin trunk domain. Mutation of these residues specifically inhibits the ability of Nef to bind AP-2 and downregulate CD4. In addition, evidence presented here indicates that the diacidic motif and the basic patch on  $\alpha$ -adaptin are both required for the cooperative assembly of a CD4-Nef-AP-2 tripartite complex. This cooperativity explains how Nef is able to efficiently downregulate CD4 despite weak binary interactions between components of the tripartite complex.

## 5.2 Introduction

In the previous chapter, the Nef diacidic motif (which is comprised of the DD174,175 residues in the HIV-1 NL4-3 variant) was found to be essential for AP-2 binding and CD4 downregulation (Fig. 4.1, 4.2, 4.4, and 4.5). Importantly, the diacidic motif was not required for the interaction of Nef with AP-1 and AP-3 (Fig. 4.3), which suggests that these clathrin adaptors contribute less to the modulation of CD4 expression than AP-2. Overall, these results are consistent with the RNAi data presented earlier (Fig. 3.5 and 3.7), and support the endocytic model of Nef-mediated CD4 downregulation (see Section 1.8.2). According to this model, Nef physically links the cytosolic tail of CD4 to AP-2, thereby increasing the rate at which the receptor is internalized from the plasma membrane.

The primary focus of this chapter will be to identify a binding site for the Nef diacidic motif on the surface of AP-2. Although a wide variety of motifs, belonging to a large number of proteins, have been found to interact with the appendage domains of  $\alpha$  and  $\beta$ 2 (reviewed by Schmid and McMahon, 2007), *in vitro* experiments indicate that the diacidic motif binds to the AP-2 core (Fig. 4.2; for a detailed description of the AP-2 core, see Fig. 1.10 and Section 1.6). Three other cargo motifs are known to bind to the AP-2 core: phosphatidylinositol phospholipid (PIP) headgroups, tyrosine signals, and dileucine signals. Negatively-charged PIP headgroups interact with basic patches on the  $\alpha$ -trunk and the C-terminus of  $\mu$ 2, and are probably responsible for targeting AP-2 to the plasma membrane (Chang et al., 1993; Collins et al., 2002; Gaidarov and Keen, 1999; Gaidarov et al., 1996). Tyrosine-based signals, which are found in the cytosolic domains of many transmembrane proteins, also bind to the C-terminus of  $\mu$ 2 (Ohno et al., 1995; Owen and Evans, 1995). Dileucine-based signals, another motif commonly found in transmembrane proteins, interact with the  $\alpha$ - $\sigma$ 2 region of the AP-2 core, but the specific binding site of these signals is still unknown (Fig. 3.8 and 3.9).

In the next section, a directed mutagenesis strategy will be used in concert with yeast three-hybrid assays to identify a candidate binding site for the Nef diacidic motif on the AP-2 core. Once this site is identified, it will be further evaluated using GST pull-downs, and its contribution to CD4 downregulation will be assessed using functional assays. Later, a novel yeast four-hybrid system will be used to test whether CD4, Nef,

and AP-2 interact simultaneously to form a tripartite complex. The formation of this complex – a critical component of the endocytic model of CD4 downregulation – has long been hypothesized, but never demonstrated experimentally. If a CD4-Nef-AP-2 tripartite complex is observed, then additional assays will be performed to determine whether assembly of the complex depends on key domains, such as the Nef diacidic motif and its prospective binding site on AP-2. When taken together, the results from these experiments should provide more information on the mechanism of Nef-induced CD4 downregulation, and may identify new targets for the pharmacological inhibition of this process.

## 5.3 Results

### 5.3.1 Identification of basic residues on $\alpha$ -adaplin required for the interaction of HIV-1 Nef

Data from the two previous chapters demonstrated that HIV-1 Nef binds to the  $\alpha$ - $\sigma$ 2 hemicomplex of AP-2 (Fig. 3.8), and that electrostatic interactions are an important component of the overall binding affinity (Fig. 4.2). In particular, a diacidic motif in the C-terminal flexible loop of Nef is essential for the interaction with AP-2 (Fig. 4.2 and 4.3). However, the Nef diacidic motif is not required for binding to the related AP-1 and AP-3 adaptor protein complexes (Fig. 4.3). These findings suggested that the Nef diacidic motif interacts with basic residues on AP-2 that are not conserved among the three AP complexes.

To test this hypothesis, 21 lysine and arginine residues on  $\alpha$ - $\sigma$ 2 that are not present on the corresponding  $\gamma$ - $\sigma$ 1 and  $\delta$ - $\sigma$ 3 hemicomplexes of AP-1 and AP-3 were identified (Fig. 5.1). These residues were then changed to either aspartate or glutamate, and the resulting  $\alpha$ - $\sigma$ 2 mutants were assayed for a loss of binding to wild-type Nef using the Y3H system (Fig. 5.2). Several alterations of the  $\alpha$ - $\sigma$ 2 hemicomplex, including the triple mutant  $\alpha$  KKK295,297,298EEE (initially mutated *en bloc* because the close proximity of these residues to each other), the single mutant  $\alpha$  R340E, and the double mutant  $\sigma$ 2 RK124,130EE, impaired the binding of Nef (Fig. 5.2).

In order to determine whether this loss of binding was due to the disruption of the Nef binding site, or to more global effects on the hemicomplex, the  $\alpha$ - $\sigma$ 2 mutants were also tested for their ability to bind to the cytoplasmic tail of mouse tyrosinase. Unlike Nef, the tyrosinase tail interacts with  $\alpha$ - $\sigma$ 2 in a manner that is not dependent on the presence of a diacidic motif (see Fig. 4.6). The  $\alpha$  KKK295,297,298EEE and  $\alpha$  R340E mutants, which were notable for their decreased affinity for Nef, bound to tyrosinase with relatively strong avidities (Fig. 5.2), suggesting that these mutations specifically interfered with the interaction between Nef and AP-2. The  $\sigma$ 2 RK124,130EE mutant, on the other hand, failed to bind either Nef or tyrosinase (Fig. 5.2), consistent with an adverse effect of these substitutions on either the folding of the  $\sigma$ 2 subunit or the stability of the  $\alpha$ - $\sigma$ 2 hemicomplex.

**FIG. 5.1: Identification of basic residues in the AP-2  $\alpha$ - $\sigma$ 2 hemicomplex that are not conserved in the homologous subunits of AP-1 and AP-3**

Sequence alignments of the AP-1  $\gamma$ - $\sigma$ 1, AP-2  $\alpha$ - $\sigma$ 2, and AP-3  $\delta$ - $\sigma$ 3 hemicomplexes were performed using the ClustalW2 program (available at <http://www.clustal.org/>). Amino acid numbers for the first residue in each row are indicated on the left, while amino acid numbers for the last residue in each row are indicated on the right. Lysine and arginine residues present in AP-2  $\alpha$ - $\sigma$ 2 but not on the corresponding AP-1 and AP-3 subunits are highlighted in **red**. These residues were mutated to either aspartate or glutamate (see Fig. 5.2). Asterisks indicate residues that were also mutated to alanine (see Fig. 5.3). **Red** asterisks denote AP-2  $\alpha$  residues K297 and R340, which were found to be required for the interaction with HIV-1 Nef (see Fig. 5.3).

**(A)** Protein sequence alignment of the trunk domains of human AP-1  $\gamma$  ( $\gamma$ 1 isoform; accession number AAH36283), AP-2  $\alpha$  ( $\alpha$ C isoform; accession number O94973), and AP-3  $\delta$  (accession number AAC51761).

**(B)** Protein sequence alignment of human AP-1  $\sigma$ 1 ( $\sigma$ 1A isoform; accession number AAA37243), AP-2  $\sigma$ 2 (accession number AAP36470), and AP-3  $\sigma$ 3 ( $\sigma$ 3A isoform; accession number EAW48952).

FIG. 5.1

A

$\gamma$ adaptin	1	----MPAPI	R-----LRE	LIRTIRTART	QAEEREMIQK	ECAAIRSSFR	39
$\alpha$ adaptin	1	----MPAVS	KGDGMRGLAV	FISDIRNCKS	KEAEIKRINK	ELANIRSKFK	45
$\delta$ adaptin	1	MALKMVKGSI	DRMPDKNLQD	LVRGIRNHK-	-EDEAKYISQ	CIDEIKQELK	48
$\gamma$ adaptin	40	EE---DNTYR	CRNVAKLLYM	HMLGYPAHFG	QLECLKLIAS	QKFTDKRIGY	86
$\alpha$ adaptin	46	GDKALDGYSK	KKYVCKLLFI	FLGHDDIDFG	HMEAVNLLSS	NRYTEKQIGY	95
$\delta$ adaptin	49	QD---NIAVK	ANAVCKLTYL	QMLGYDISWA	AFNIIIEVMSA	SKFTFKRIGY	95
$\gamma$ adaptin	87	LGAMLLDER	QDVHLLMTC	IKNDLNHSTQ	FVQGLALCTL	GCMGSSEMCR	137
$\alpha$ adaptin	96	LFISVLVNSN	SELI <sup>R</sup> LINNA	IKNDLAS <sup>R</sup> NP	TFMGLALHCI	ASVGS <sup>R</sup> EMAE	145
$\delta$ adaptin	96	LAASQSFHEG	TDVIMLTTNQ	IRKDLSSPSQ	YDTGVALTGL	SCFVTPDLAR	145
$\gamma$ adaptin	138	DLAGEVEKLL	KTSN--SYLR	KKAALCAVHV	IRKVPPELMM	--FLPATKNL	183
$\alpha$ adaptin	146	AFAGEIPKVL	VAGDTMDSVK	QSAALCLLRL	YRTSPDLVPM	GDWTSRVVHL	195
$\delta$ adaptin	146	DLANDIMTLM	SHTK--PYIR	KKAVLIMYKV	FLKYPESLRP	--AFPRLKEK	191
$\gamma$ adaptin	184	LNEKNHGV LH	TSVLLTEMC	ERSPDMLAHF	RKNEKLV PQ L	VRILKNLIMS	233
$\alpha$ adaptin	196	LNDQHLGVVT	AATSLITTLA	QKNPEEF <sup>K</sup> TS	VS--LAVS <sup>R</sup> L	SRIVTSASTD	243
$\delta$ adaptin	192	LEDDPDPGVQS	AAVNVICELA	RRPNKNYLS-	-----LAPLF	FKLMTSSTNN	235
$\gamma$ adaptin	234	GYSPEHDVSG	ISDPFLQVRI	LRLLRILGRN	DDDSSEAMND	ILAQVATNTE	283
$\alpha$ adaptin	244	--LQDYTYF	VPAPWLSVKL	LRLLCYPPP	DPAV <sup>R</sup> GRLTE	CLETILN <sup>K</sup> AQ	291
$\delta$ adaptin	236	-----	----WVLIKI	IKLFGALTPL	EPRLGKKLIE	PLTNLIHSTS	272
$\gamma$ adaptin	284	TS-----	KNVGNAILYE	TVLTIMDIKS	ESGLRVLAIN	ILGRFLLNND	325
$\alpha$ adaptin	292	EPP <sup>*</sup> K <sup>*</sup> K <sup>*</sup> VQH	SNAKNAVLFE	AISLIHHDS	EPNLLV <sup>R</sup> RACN	QLGQFLQH <sup>*</sup> RE	341
$\delta$ adaptin	273	AMS-----	LL YECVNTVIAV	LISLSSGMPN	HSASIQLCVQ	KLRILIEDSD	315
$\gamma$ adaptin	326	KNIRYVALT-	-SLLKTVQTD	HNAVQRHRST	IVDCLK-DLD	VSIKRRAMEL	372
$\alpha$ adaptin	342	TNLRYLALES	MCTLASSEFS	HEAV <sup>K</sup> THIET	VINALKTERD	VSVRQRAVDL	391
$\delta$ adaptin	316	QNLKYLGLL-	-AMSKILKTH	PKSVQSHKDL	ILQCLD-DKD	ESIRLRALDL	363
$\gamma$ adaptin	393	SFALVNGNNI	RGMMKELLYF	LDSCE-PEFK	ADCASGIFLA	AEK----YAP	417
$\alpha$ adaptin	392	LYAMCDRSNA	PQIVAEMLSY	LETAD-YSIR	EEIVLKVAIL	AEK----YAV	436
$\delta$ adaptin	364	LYGMVSKKNL	MEIVKKLMT H	VDKAEGTTYR	DELLTKIIDI	CSQSNYQYIT	413

B

$\sigma 1$ adaptin	1	MMRFMLLFSR	QGKRLRQKWY	LATSDKERKK	MVRELMQVVL	ARKPKMCSFL	50
$\sigma 2$ adaptin	1	MIRFILIQNR	AGKTRLAKWY	MQFDDDEKQK	LIEEVHAVVT	VRDAKHTNFV	50
$\sigma 3$ adaptin	1	MIKAILIFNN	HGKPRLSKPY	QPYSED <sup>T</sup> QQQ	IIRETFHLVS	KRDENVCNFL	50
$\sigma 1$ adaptin	51	EW-----	RD LKVVKRYAS	LYFCCAIEGQ	DNELITLLELI	HRYVELLDKY	94
$\sigma 2$ adaptin	51	EF-----	RN FKIIYRRYAG	LYFCICVDVN	DNNLAYLEAI	HNFVEVLNEY	94
$\sigma 3$ adaptin	51	EGGLLIGGSD	NKLIYRHYAT	LYFVFCVDSS	ESELGILDLI	QVFVETLDKC	100
$\sigma 1$ adaptin	95	FGSVCELDII	FNFEKAYFIL	DEFLMGGDVQ	DTSKKSVLKA	IEQADLLQEE	144
$\sigma 2$ adaptin	95	FHNVCELDLV	FNFYKVYTVV	DEMFLAGEIR	ETSQT <sup>K</sup> VLKQ	LLMLQSLE--	142
$\sigma 3$ adaptin	101	FENVCELDLI	FHVDKVHNIL	AEMVMGGMVL	ETNMNEIVTQ	IDAQNKLEKS	150
$\sigma 1$ adaptin	145	DE-----	S PRSVLEEMGL	A-----	-----	---	158
$\sigma 2$ adaptin	N/A	-----	-----	-----	-----	---	N/A
$\sigma 3$ adaptin	151	EAGLAGAPAR	AVSAVKMNML	PEIPRNINIG	DISIKVPNLP	SFK	193

**FIG. 5.2: Y3H analysis of the interaction between HIV-1 Nef and AP-2  $\alpha$ - $\sigma$ 2 hemicomplexes containing substitutions for nonconserved basic residues**

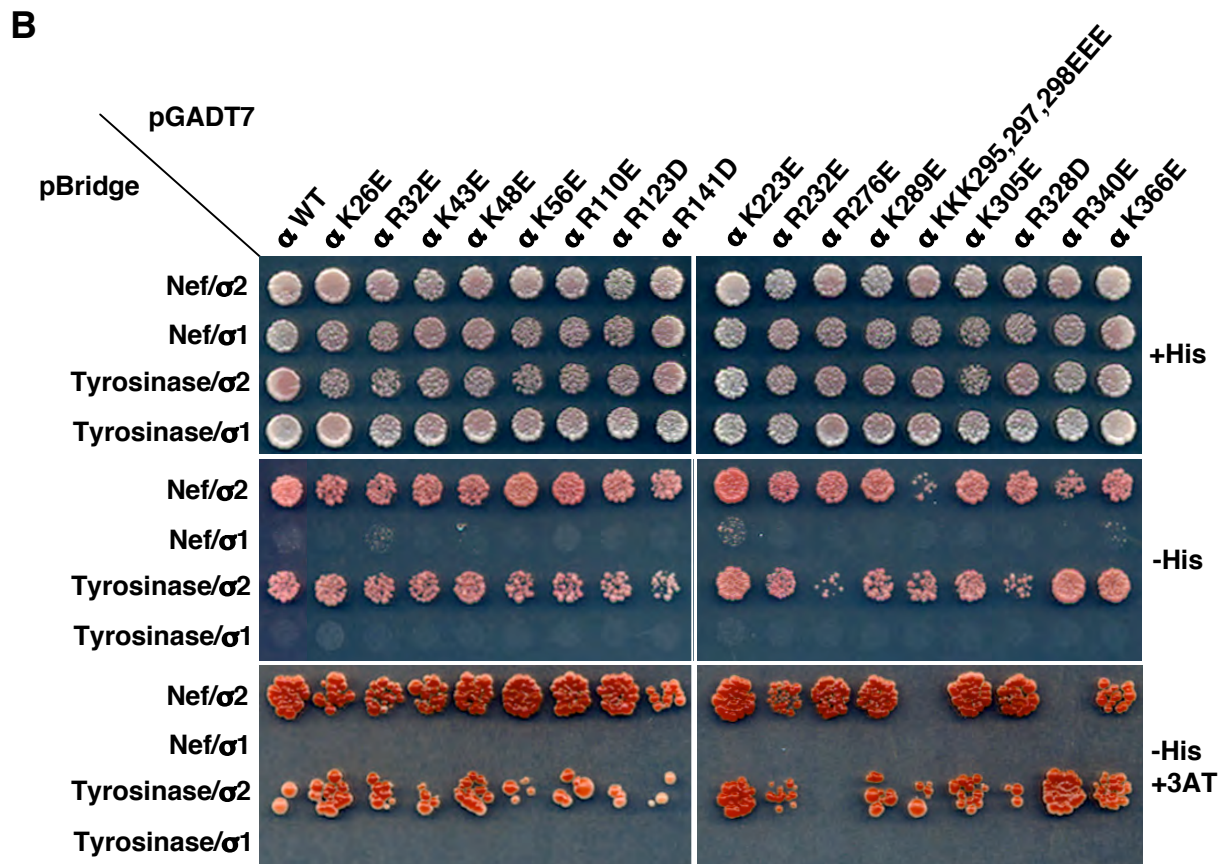
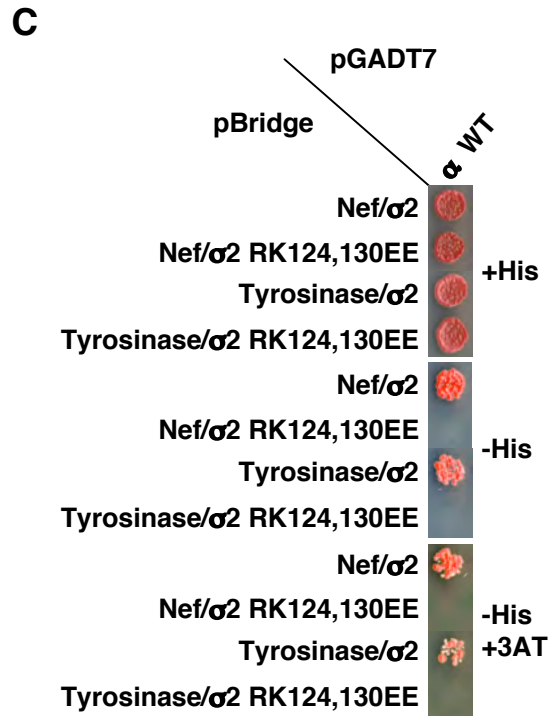
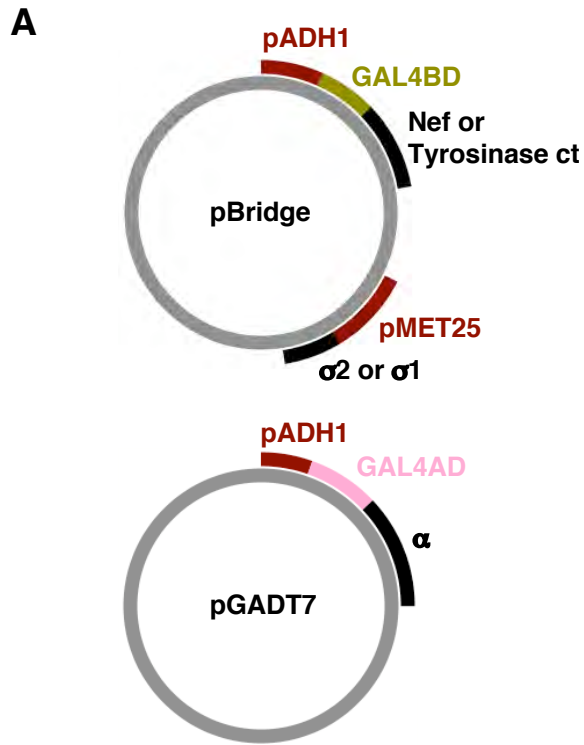
Lysine and arginine residues in AP-2  $\alpha$ - $\sigma$ 2 that are not conserved in the homologous AP-1  $\gamma$ - $\sigma$ 1 and AP-3  $\delta$ - $\sigma$ 3 hemicomplexes were mutated, either individually or in combination, to glutamate or aspartate (see Fig. 5.1). The resulting  $\alpha$ - $\sigma$ 2 constructs were then tested for their ability to interact with HIV-1 Nef and the cytosolic tail of mouse tyrosinase using the Y3H assay. To test whether mutation of the  $\alpha$  subunits resulted in self-activation, these constructs were also paired with  $\sigma$ 1, a combination that under normal circumstances would not bind to either Nef or tyrosinase.

**(A)** Plasmids used in the Y3H assays. Nef and the tyrosinase cytosolic tail (ct) were expressed as GAL4BD fusion proteins from pBridge, along with either  $\sigma$ 1 or  $\sigma$ 2;  $\alpha$  was expressed as a GAL4AD fusion protein from pGADT7.

**(B)** Y3H assay results for the seventeen  $\alpha$  mutants. Growth of yeast on media lacking histidine (-His), or lacking histidine and supplemented with 1 mM of 3-amino-1,2,4-triazole (+3AT), is indicative of an interaction with Nef or the tyrosinase cytosolic tail at two levels of stringency.

**(C)** Y3H assay result for the  $\sigma$ 2 RK124,130EE mutant. Interactions were analyzed as described above.

FIG. 5.2



The remaining mutants, all of which were generated by alteration of the  $\alpha$  subunit, interacted with both Nef and tyrosinase. To determine whether these were genuine interactions, each of the  $\alpha$  mutants was tested for self-activation by substituting  $\sigma 1$  for  $\sigma 2$  in the Y3H assay. Given that  $\alpha$  and  $\sigma 1$  do not form a functional hemicomplex (Page and Robinson, 1995), this adaptin subunit pair should not be able to bind either Nef or tyrosinase, and should not be able to stimulate yeast growth on selective media unless expression of the mutants results in self-activation. When combined with  $\sigma 1$ , none of the  $\alpha$  mutants induced yeast growth on the  $-His$  plates (Fig. 5.2), indicating that (i) the mutations do not cause self-activation, (ii) the observed interactions between mutant  $\alpha$ - $\sigma 2$  hemicomplexes and the ligands are genuine, and (iii) the only non-conserved arginine and lysine residues on the  $\alpha$ - $\sigma 2$  hemicomplex that potentially contribute to Nef binding are  $\alpha$  K295, K297, K298, and R340.

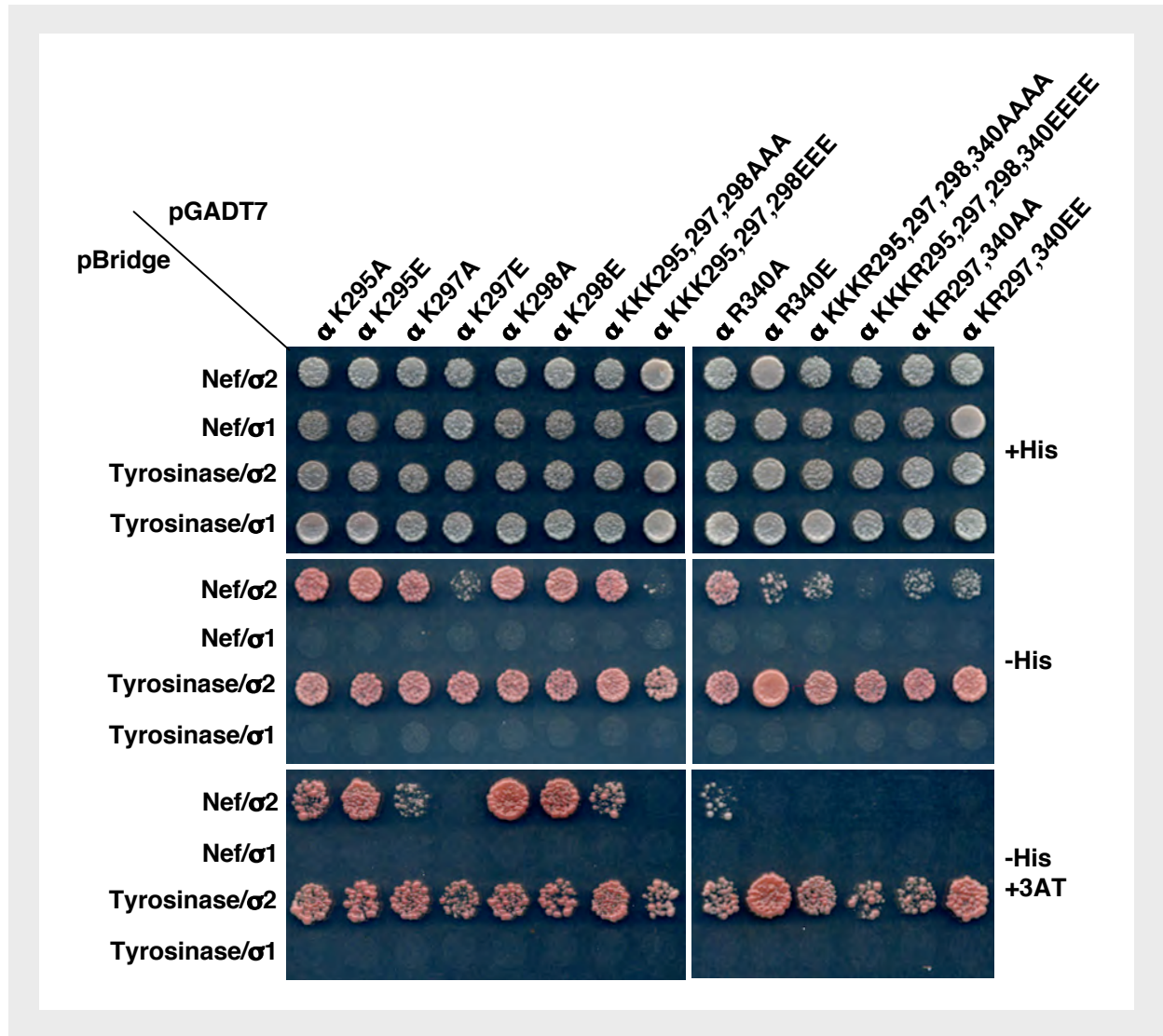
### **5.3.2 The $\alpha$ -adaptin K297 and R340 residues form a basic patch that is required for the binding of Nef**

In order to analyze the individual contributions of  $\alpha$  K295, K297, K298, and R340 on Nef binding, several additional constructs were made by mutating these residues to alanine or glutamate; the new constructs were then used in the Y3H assay described above (Fig. 5.3). As before, mutation of  $\alpha$  R340 alone, or the combined mutation of all three lysine residues impaired the ability of Nef to bind the  $\alpha$ - $\sigma 2$  hemicomplex (Fig. 5.3). The individual mutation of  $\alpha$  K295 and K298 revealed that these residues do not contribute to the interaction of Nef, while the alteration of  $\alpha$  K297 produced as significant a defect in Nef binding as the mutation of all three lysine residues at once (Fig. 5.3). Consistent with this finding, the double mutation of  $\alpha$  K297 and R340 caused approximately the same decrease in Nef binding as the quadruple mutation of  $\alpha$  K295, K297, K298, and R340 (Fig. 5.3). Thus,  $\alpha$  K297 and R340 were identified as key residues for the interaction of  $\alpha$ - $\sigma 2$  with Nef. Although the mutation of  $\alpha$  K297 and R340 to alanine decreased Nef binding (see the  $-His +3AT$  plates in Fig. 5.3), changing these residues to glutamate had a more dramatic effect (Fig. 5.3), providing further evidence that the coupling of Nef and AP-2 is at least partially dependent on electrostatic interactions. All of the mutants involving  $\alpha$  K297 and R340 bound to tyrosinase with wild-type affinity in the presence of  $\sigma 2$ , while none bound to either

**FIG. 5.3: AP-2  $\alpha$  residues K297 and R340 are required for the interaction of the  $\alpha$ - $\sigma$ 2 hemicomplex and HIV-1 Nef**

The AP-2  $\alpha$  residues K295, K297, K298, and R340 were mutated, individually and in combination, to alanine and glutamate (see Fig. 5.1). The effect of these mutations on the binding of  $\alpha$ - $\sigma$ 2 to HIV-1 Nef and the cytosolic tail of mouse tyrosinase were then analyzed using the Y3H system, as shown in the figure. The discordant  $\alpha$ - $\sigma$ 1 pair was also included as a negative control. Interactions were interpreted as described in the legend to Fig. 5.2B.

FIG. 5.3



Nef or tyrosinase in the presence of  $\sigma 1$  (Fig. 5.3). These controls demonstrate that the alteration of  $\alpha$  K297 and R340 specifically affects the ability of  $\alpha$ - $\sigma 2$  to interact with Nef in the Y3H system. Interestingly, mapping of  $\alpha$  K297 and R340 on the three-dimensional crystal structure of AP-2 (Collins et al., 2002) shows that these residues are brought into close proximity of each other by the folding of the  $\alpha$  subunit (Fig. 5.4). The  $\alpha$  K297 and R340 residues can therefore be described as a single basic patch, which likely coordinates the binding of a negatively charged, acidic region of Nef.

### **5.3.3 The AP-2 $\alpha$ K297 and R340 residues are required for direct binding of Nef**

To determine whether the  $\alpha$  K297 and R340 residues were required for the direct interaction of AP-2 and Nef, *in vitro* experiments were performed using recombinant proteins expressed in bacteria. In previous chapters, the AP-2<sup>CORE</sup> construct, which lacks the C-terminal domain of  $\mu 2$  and the hinge and ear domains of  $\alpha$  and  $\beta 2$ , was shown to bind Nef (Fig. 3.9 and 4.2). This construct (referred to in the accompanying figure as AP-2<sup>CORE</sup>  $\alpha$  wild-type [WT]) was mutated to generate AP-2<sup>CORE</sup>  $\alpha$  KR297, 340EE. SDS-PAGE analysis of the purified AP-2<sup>CORE</sup> constructs, which contain a GST-tag on the  $\alpha$ -trunk domain and a His<sub>6</sub>-tag on the  $\beta 2$ -trunk domain, indicated that the  $\alpha$  KR297,340EE mutation did not affect the assembly of the AP-2<sup>CORE</sup> complex (Fig. 5.5A). However, GST pull-down assays showed that the  $\alpha$  KR297,340EE mutation markedly impaired the binding of His<sub>6</sub>-Nef (Fig. 5.5B). Immunoblots using either anti-His<sub>6</sub> (Fig. 5.5B, top panel) or anti-Nef (Fig. 5.5B, bottom panel) antibodies revealed that AP-2<sup>CORE</sup>  $\alpha$  KR297,340EE had nearly the same affinity for the viral protein as several negative controls. Thus, the  $\alpha$  K297 and R340 residues are required for the direct interaction of AP-2 with Nef.

### **5.3.4 The $\alpha$ -adaptin K297 and R340 residues are required for Nef-induced CD4 downregulation**

Earlier, the downregulation of CD4 by Nef was shown to be dependent on AP-2 (Fig. 3.7, 4.4, and 4.5; Jin et al, 2005). Having already demonstrated that the  $\alpha$  K297 and R340 residues were required for the direct binding of AP-2 to Nef, the contribution of these residues to the Nef-mediated downregulation of CD4 was evaluated next, using

**FIG 5.4: Location of  $\alpha$  K297 and R340 on the three-dimensional structure of the AP-2 complex**

In both panels, the three-dimensional structure of AP-2 core (PDB ID numbers 1GW5 and 2VGL [Collins et al., 2002]) is shown, with the  $\alpha$ ,  $\beta$ 2,  $\mu$ 2, and  $\sigma$ 2 subunits drawn in **dark blue**, **green**, **magenta**, and **gold**, respectively. The polyphosphoinositide (**PIP**) binding site on the  $\alpha$  subunit is colored in **light blue**, while the  **$\alpha$  K297** and  **$\alpha$  R340** residues (including their side chains) are depicted in **red**. It should be noted that the  $\alpha$  K297 and  $\alpha$  R340 residues referred to throughout this work (and highlighted in this figure) correspond to  $\alpha$  K298 and  $\alpha$  R341 in the crystal structure of the AP-2 core, due to a one residue difference between the  $\alpha$  alleles used in the two studies. The images were drawn with PyMOL (Delano, 2002) and annotated using Microsoft PowerPoint.

**(A)** Surface representation of the AP-2 core complex.

**(B)** Magnified ribbon diagram of region surrounding  $\alpha$  K297 and  $\alpha$  R340.

FIG. 5.4

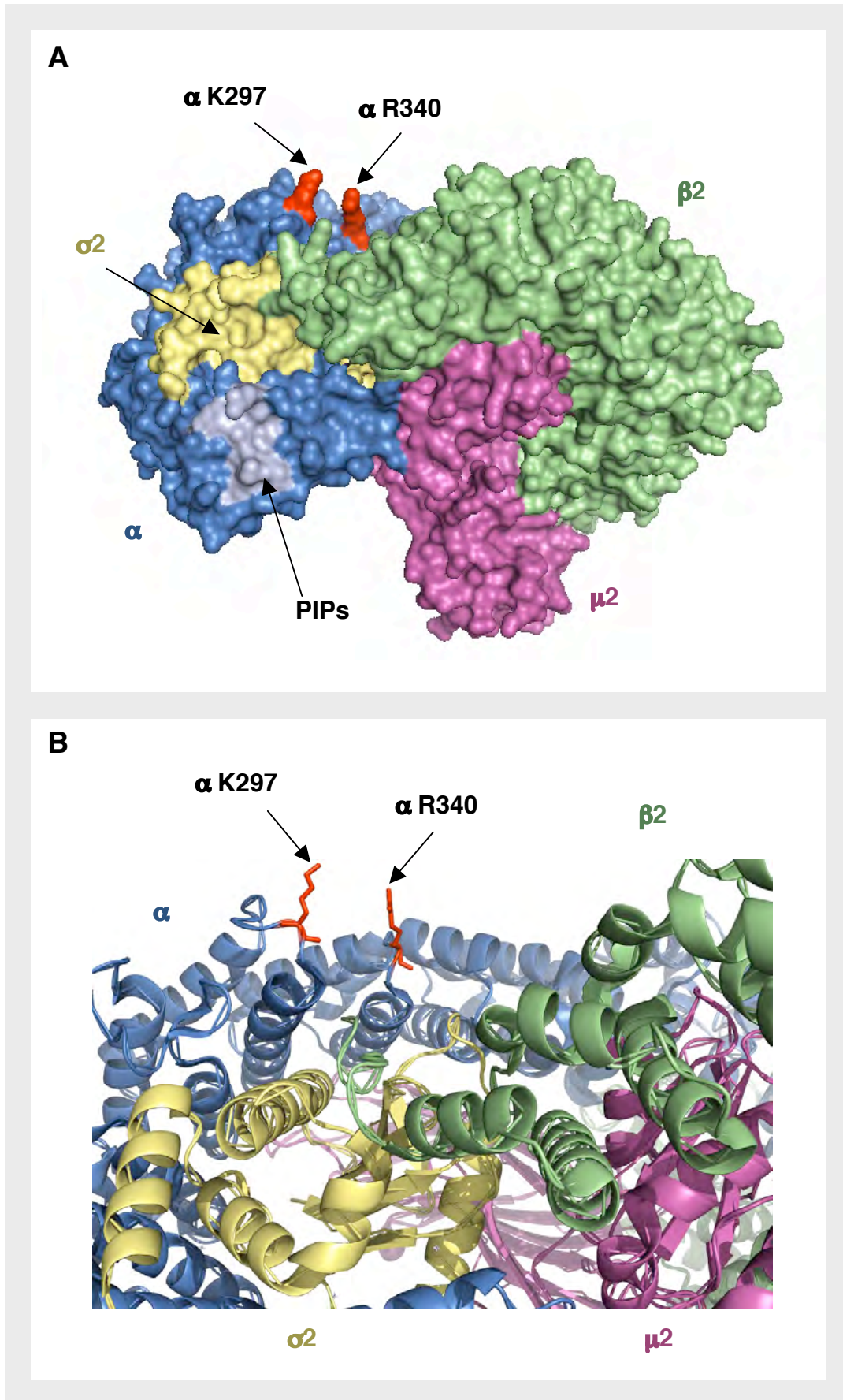
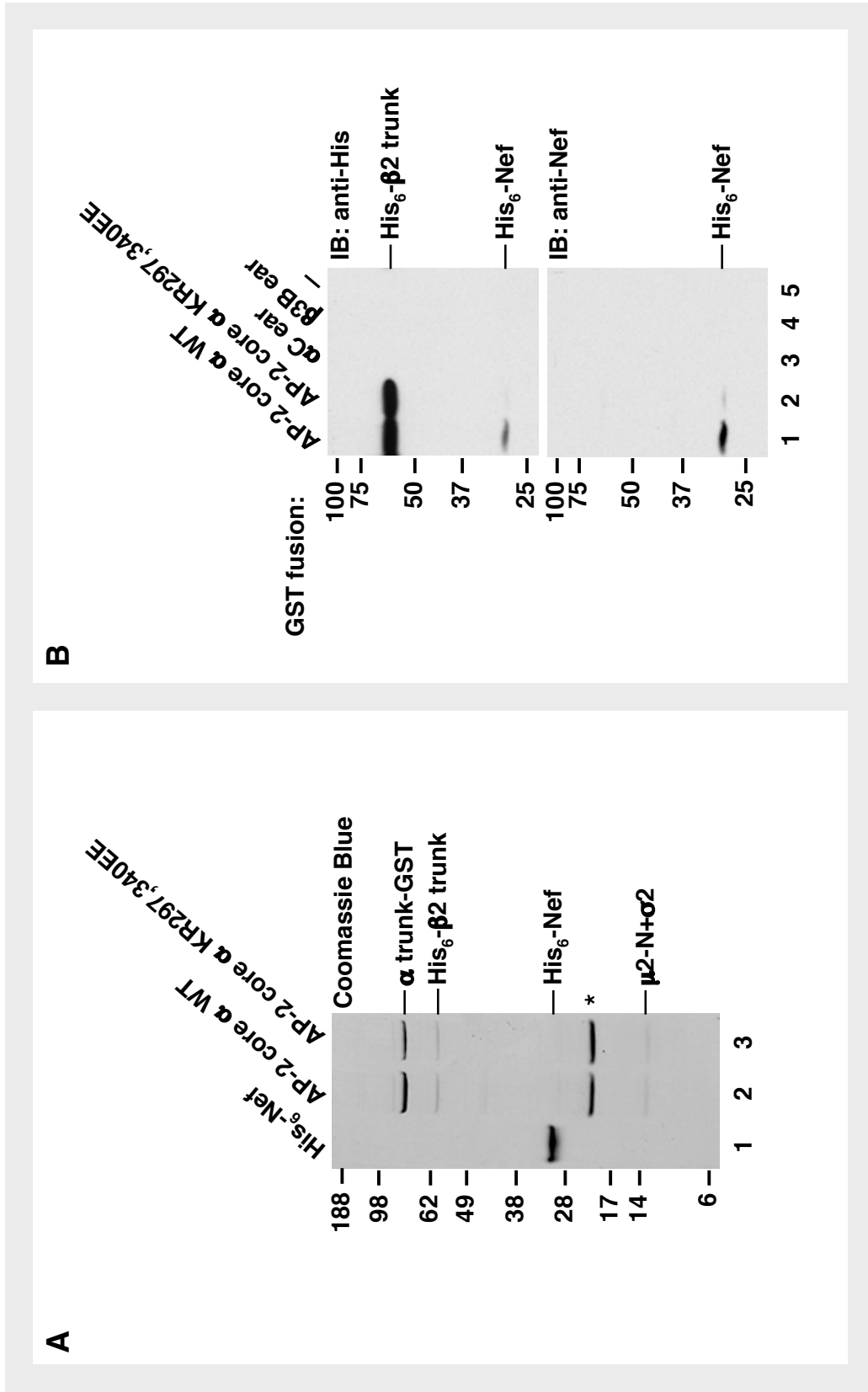


**FIG. 5.5: The  $\alpha$  K297 and R340 residues are required for direct binding of AP-2 to HIV-1 Nef**

**(A)** Recombinant His<sub>6</sub>-tagged Nef and AP-2<sup>CORE</sup> (containing a C-terminal GST tag on the  $\alpha$  trunk [ $\alpha$ -trunk-GST], a His<sub>6</sub> tag on the  $\beta$ 2 trunk [His<sub>6</sub>- $\beta$ 2-trunk], the N-terminal domain of  $\mu$ 2 [ $\mu$ 2-N], and full-length  $\sigma$ 2 [ $\sigma$ 2]) constructs were produced as described in the Materials and Methods (Section 2.3) and subjected to SDS-PAGE on a 4-12% gradient gel, followed by Coomassie blue staining. Lanes 2 and 3, which correspond to the AP-2<sup>CORE</sup> complexes with wild-type (WT) and KR297,340EE mutant  $\alpha$  chains, show the adaptin subunits in order of increasing mobility (in contrast to Fig. 3.9 and 4.2,  $\mu$ 2-N and  $\sigma$ 2 co-migrate in this gel system). Numbers on the left indicate the positions of molecular mass markers (in kDa). The band at approximately 20 kDa (marked by an asterisk) represents a GST degradation product.

**(B)** Equal amounts of GST-AP-2<sup>CORE</sup>  $\alpha$  WT, GST-AP-2<sup>CORE</sup>  $\alpha$  KR297,340EE, and the negative controls GST- $\alpha$ C-ear, GST- $\beta$ 3-ear, and unfused GST (represented as a dash) were immobilized onto glutathione-Sepharose beads, and then incubated with recombinant His<sub>6</sub>-Nef (see Materials and Methods, Section 2.3.3.1). Bound proteins were eluted and subjected to SDS-PAGE on a 10% gel, followed by immunoblotting (IB) with antibodies targeted against the His<sub>6</sub> tag (upper panel) and Nef (lower panel). Numbers on the left indicate the positions of molecular mass markers (in kDa). The approximately 60 kDa band in Lanes 1 and 2 of the upper blot correspond to the His<sub>6</sub>- $\beta$ 2-trunk in the recombinant AP-2<sup>CORE</sup> complex, and served as an internal loading control.

FIG. 5.5



In collaboration with Rafael Mattera

an RNAi and rescue approach. Others have shown that the depletion of AP-2 subunits destabilizes the complex and inhibits the internalization of a subset of transmembrane proteins from the plasma membrane, including the transferrin receptor (TfR) and CD4 (Huang et al., 2004; Janvier and Bonifacino, 2005; Jin et al., 2005; McCormick et al., 2005; Motley et al., 2003; Motley et al., 2006).

Consistent with these results, the siRNA-mediated depletion of endogenous  $\alpha$ -adaptin in HeLa cells increased the amount of TfR and CD4 on the cell surface, as determined by flow cytometry (Fig. 5.6A). The cytosolic tails of TfR and CD4 contain tyrosine- and dileucine-based sorting signals, respectively, that under normal circumstances are recognized by AP-2 for endocytosis from the plasma membrane (Motley et al., 2003; Pitcher et al., 1999). The accumulation of TfR and CD4 on the cell surface following the knockdown of  $\alpha$  expression, therefore, is indicative of impaired AP-2 function.

In an attempt to rescue the function of AP-2, cells depleted of endogenous  $\alpha$  were transfected with RNAi-resistant versions of wild-type and KR297,340EE mutant  $\alpha$ -adaptin (referred to below as  $\alpha$ R-WT and  $\alpha$ R-KR297,340EE, respectively). The two  $\alpha$ R constructs were able to reduce the amount of TfR and CD4 on the cell surface to approximately normal levels (Fig. 5.6B). This demonstrated that both the  $\alpha$ R-WT and the  $\alpha$ R-KR297,340EE constructs could rescue AP-2 function in regards to tyrosine- and dileucine-based sorting at the cell surface.

The RNAi and rescue assay was then applied to HeLa cells expressing Nef and CD4. Treatment of cells with RNAi against  $\alpha$ -adaptin completely eliminated the ability of Nef to downregulate CD4 from the plasma membrane (Fig. 5.6C). Importantly, the transfection of  $\alpha$ -depleted cells with the  $\alpha$ R-WT construct restored the ability of Nef to downregulate CD4, but expression of the  $\alpha$ R-KR297,340EE construct did not (Fig. 5.6D). Immunoblot analysis of the transfected cells indicated that this disparity in Nef function was not due to differences in the silencing of endogenous  $\alpha$ , the expression of the RNAi-resistant  $\alpha$  constructs, or the expression of Nef itself (Fig. 5.6F). This *in vivo* analysis thus demonstrates that the  $\alpha$  K297 and R340 residues are specifically required for the Nef-mediated downregulation of CD4.

**FIG. 5.6: The AP-2  $\alpha$  K297 and R340 residues are necessary for Nef-mediated downregulation of CD4**

HeLa cells were transfected with siRNA oligos and DNA constructs over a period of 7 days, as described in the Materials and Methods (see Sections 2.6.3.4 - 2.6.3.6 and Table 2.7). Control and  $\alpha$  siRNA-treated cells were cotransfected with three DNA plasmids: one expressing CD4, one lacking or expressing Nef, and one lacking or expressing either an siRNA-resistant version of wild-type  $\alpha$ -adaptin ( $\alpha$ R-WT) or an siRNA-resistant version of KR297,340EE mutant  $\alpha$ -adaptin ( $\alpha$ R-KR297,340EE). The cells were then prepared for flow cytometry and immunoblotting. Cells prepared for flow cytometry were either left unstained as a control for background fluorescence (shaded **gray** curves in all plots) or stained with PE-conjugated anti-human TfR and APC-conjugated anti-human CD4 antibodies.

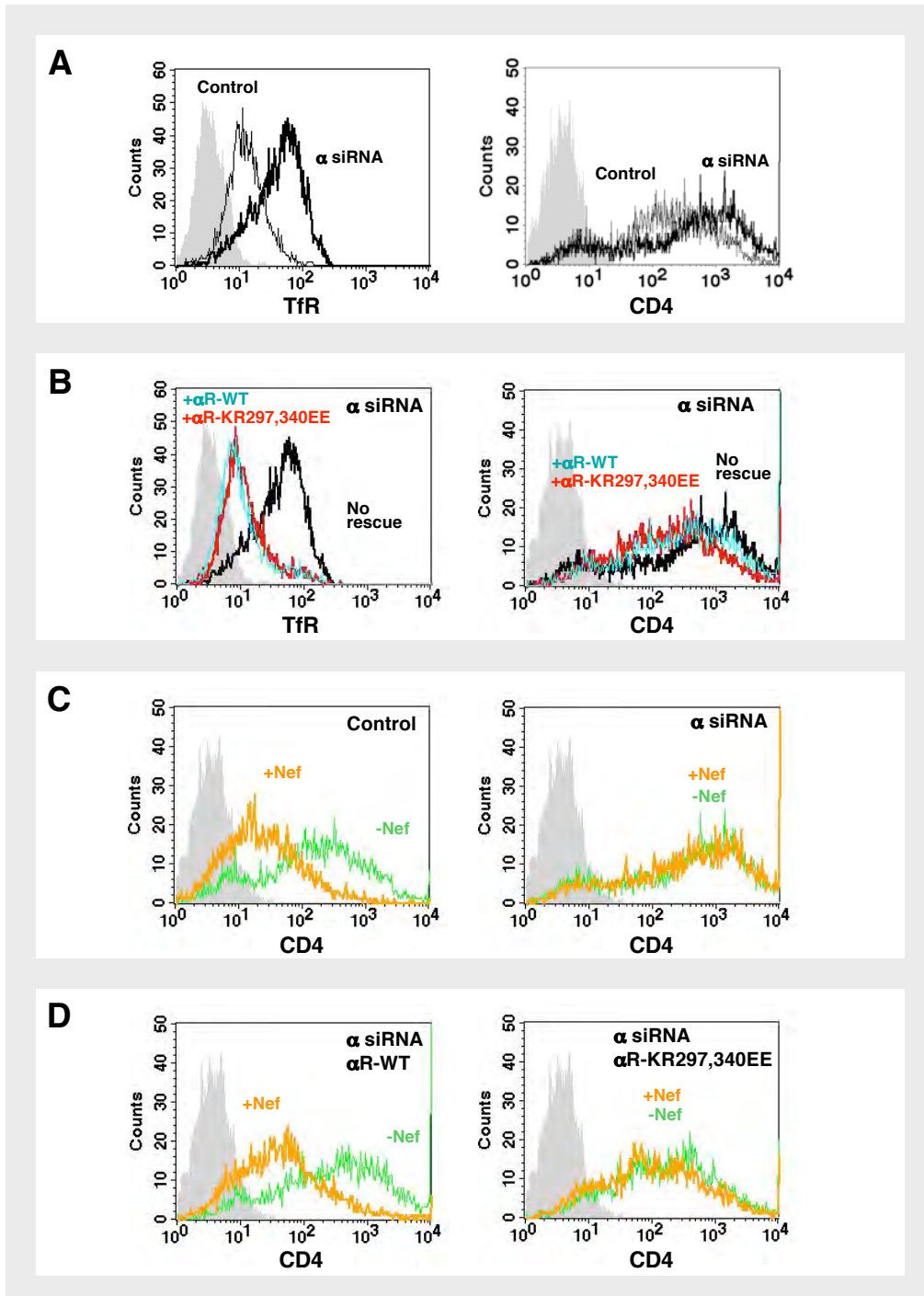
**(A)** Depletion of  $\alpha$ -adaptin increases the cell surface expression of TfR and CD4. The amount of TfR (left panel) and CD4 (right panel) on the plasma membrane of cells left untreated (thin black lines) or treated with siRNA targeting  $\alpha$ -adaptin (thick black lines) is shown.

**(B)** Both  $\alpha$ R-WT and  $\alpha$ R-KR297,340EE prevent the increase in cell surface TfR and CD4 expression caused by  $\alpha$  siRNA treatment. The amount of TfR (left panel) and CD4 (right panel) on the plasma membrane of cells treated with  $\alpha$  siRNA and then transfected with an empty vector (thick black lines), a vector containing  $\alpha$ R-WT (**blue** lines), or a vector containing  $\alpha$ R-KR297,340EE (**red** lines) is shown.

**(C)** The expression of Nef induces CD4 downregulation in control but not  $\alpha$  siRNA-treated cells. The amount of CD4 on the plasma membrane of cells that had not been treated with siRNA (left panel) or had been treated with  $\alpha$  siRNA (right panel), and that were either lacking Nef (**green** lines) or expressing Nef (**orange** lines), is shown.

**(D)** Nef-induced CD4 downregulation is rescued by  $\alpha$ R-WT but not by  $\alpha$ R-KR297,340EE in  $\alpha$  siRNA-treated cells. The amount of CD4 on the surface of  $\alpha$  siRNA-treated cells that had been transfected with either  $\alpha$ R-WT (left panel) or  $\alpha$ R-KR297,340EE (right panel), and were either lacking Nef (**green** lines) or expressing Nef (**orange** lines) is shown.

FIG. 5.6

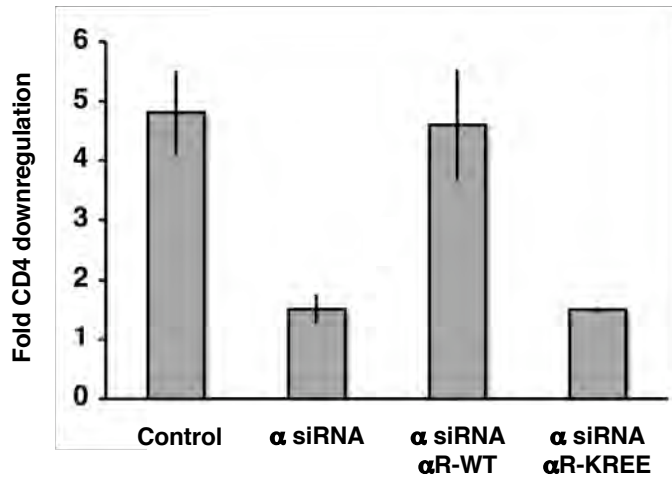


**(E)** Bar graph depicting the results of three independent experiments for the rescue of Nef-induced CD4 downregulation by  $\alpha$ R-WT but not by  $\alpha$ R-KR297,340EE [KREE]. Statistical analysis of the data from these experiments showed that Nef-mediated CD4 downregulation (expressed in terms of fold-downregulation [ratio of geometric means in the absence and presence of Nef]) was  $4.81 \pm 0.70$  for control cells,  $1.51 \pm 0.24^*$  for  $\alpha$  siRNA-treated cells,  $4.60 \pm 0.94$  for  $\alpha$  siRNA-treated cells expressing  $\alpha$ R-WT, and  $1.50 \pm 0.40^{*\dagger}$  for  $\alpha$  siRNA-treated cells expressing  $\alpha$ R-KREE (mean + standard error of the mean;  $n = 3$ ). The symbols \* and † indicate values that are significantly different ( $P < 0.05$ ) from those of control cells and  $\alpha$  siRNA-treated cells expressing  $\alpha$ R-WT, respectively, as calculated by an analysis of variance followed by a two-tail Dunnett's test.

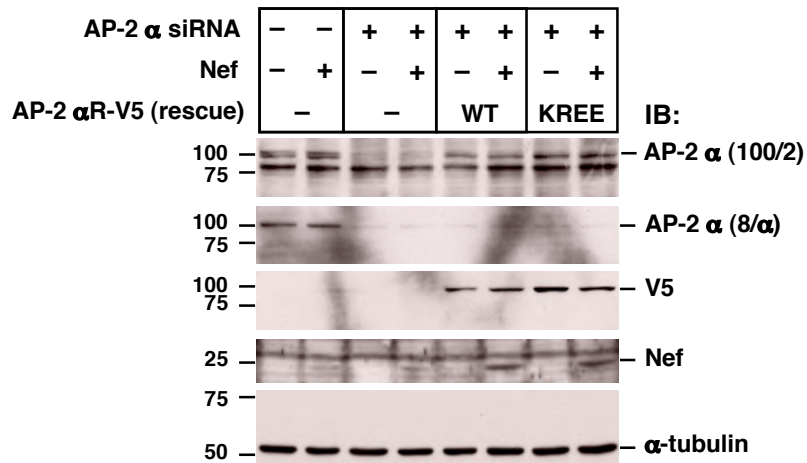
**(F)** Aliquots of transfected cells from all of the experimental groups were lysed and subjected to SDS-PAGE, followed by immunoblotting (IB) with the antibodies shown on the right. All of the cells were transfected with a plasmid encoding CD4, together with plasmids and siRNA oligos indicated in the grid above the blots (wild-type [WT] KR297,340EE [KREE]). Note that the anti-AP-2  $\alpha$  (100/2) antibody recognized both endogenous isoforms of  $\alpha$ -adaptin,  $\alpha$ A and  $\alpha$ C (apparent as an approximately 100 kDa doublet in which the upper band represents  $\alpha$ A, while the lower band represents  $\alpha$ C [Ball et al., 1995]), as well as a nonspecific band at approximately 85 kDa. The anti-AP-2  $\alpha$  (8/ $\alpha$ ) antibody, however, recognized only endogenous  $\alpha$ A-adaptin, since it was raised against a protein fragment unique to that isoform. The siRNA-resistant, V5-epitope-tagged  $\alpha$ C rescue constructs were detected by both the AP-2  $\alpha$  (100/2) and the anti-V5 antibodies. The anti- $\alpha$ -tubulin antibody was used as a loading control. Numbers on the left indicate the positions of molecular mass markers (in kDa).

FIG. 5.6, *continued*

**E**



**F**



In collaboration with Wolf Lindwasser and Rafael Mattera

### **5.3.5 The CD4 tail, Nef, and the AP-2 $\alpha$ - $\sigma$ 2 hemicomplex assemble cooperatively to form a CD4-Nef-AP-2 tripartite complex**

Nef is believed to downregulate CD4 by binding to the cytosolic tail of the receptor and linking it to the AP-2 complex, thereby accelerating the rate of CD4 endocytosis. Although previous work has provided evidence for weak binary interactions between Nef and CD4 (Rossi et al., 1996; Grzesiek et al., 1996; Presseur et al., 2001; Bentham et al., 2003), Nef and AP-2 (Fig. 3.8, 3.9, 4.1, 4.2, 4.3, 5.2, 5.3, and 5.6), and CD4 and AP-2 (Höning et al., 2005), a tripartite complex involving all three components has not yet been demonstrated. The possible formation of such a complex was analyzed using a combination of Y2H, Y3H, and Y4H assays. Yeast were transformed with the pBridge and pAD vectors, each of which contained two multiple cloning sites under the control of independent promoters (Fig. 5.7A). Thus, it was possible to express up to four proteins in the yeast system, each of which was targeted to the nucleus by the presence of nuclear localization signals.

Using this system, the ability of Nef (expressed as a GAL4BD fusion protein) to bind to the cytosolic tail of CD4 (expressed as a GAL4AD fusion protein) either alone or in the presence of the AP-2  $\alpha$  and  $\sigma$ 2 subunits was tested (Fig. 5.7B). In the absence of  $\alpha$  and  $\sigma$ 2, Nef did not appear to interact with CD4. This result likely differed from previous work due to the stringent requirements of the yeast system; only interactions of sufficient strength and stability to promote yeast growth could be observed in the assay. The individual expression of either  $\alpha$  or  $\sigma$ 2 also failed to yield a detectable interaction between Nef and CD4. However, when both  $\alpha$  and  $\sigma$ 2 were expressed, Nef bound to the CD4 cytosolic tail. The increased affinity of Nef for CD4, in the presence of the  $\alpha$ - $\sigma$ 2 hemicomplex, indicates that a CD4-Nef-AP-2 complex is formed by cooperative assembly.

In order to test whether the assembly of the CD4-Nef-AP-2 complex is dependent on binary interactions between its components, the Y4H assay was repeated with several mutants (Fig. 5.7C). Mutations that are known to prevent binding of Nef to either CD4 (Nef WL57,58AA) (Grzesiek et al., 1996) or AP-2 (Nef LL164,165AA and Nef DD174,175AA) (Fig. 3.8, 3.9, 4.2, and 4.3) inhibited formation of the larger complex. Expression of the  $\alpha$  KR297,340EE mutant, which earlier in the chapter was shown to

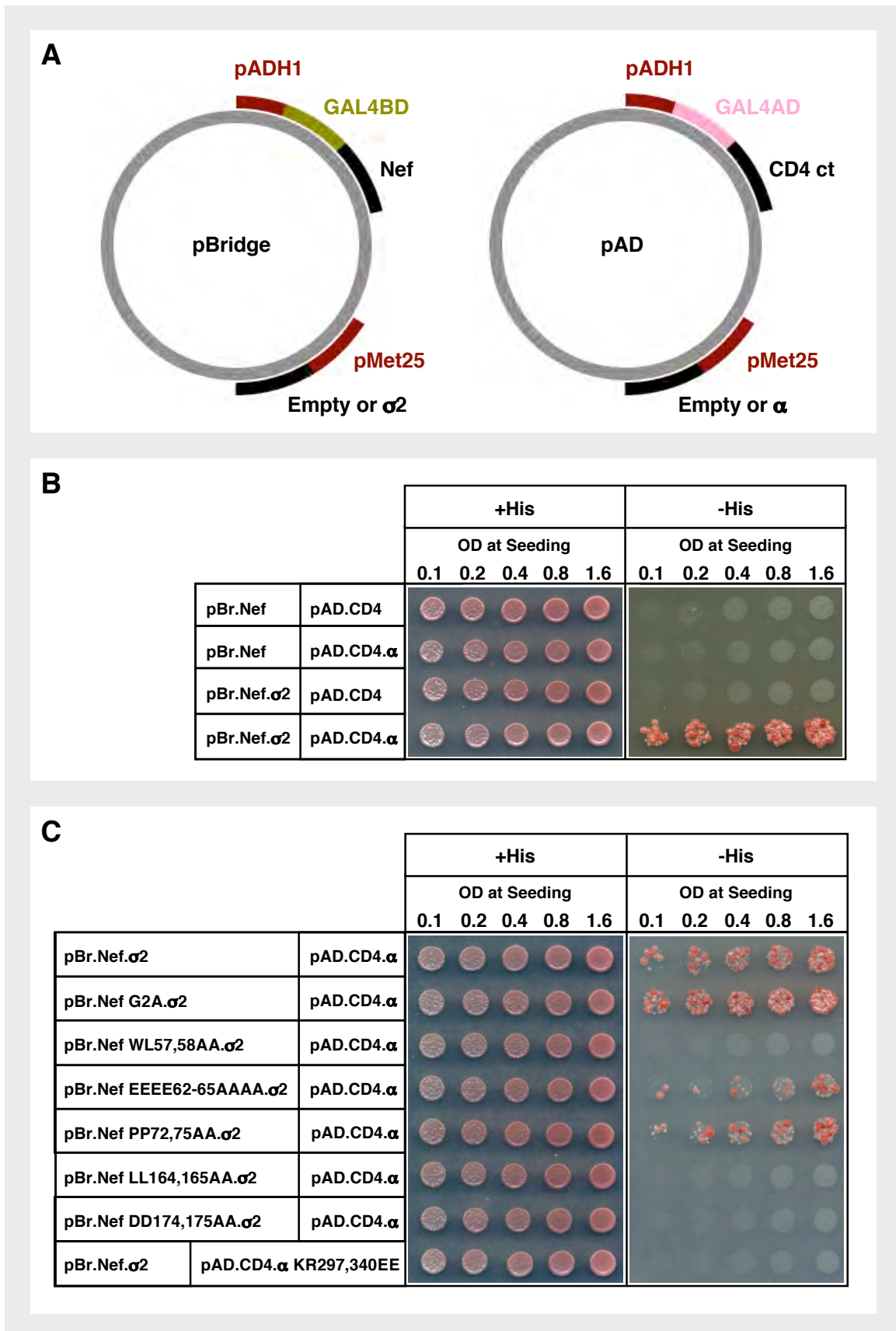
**FIG. 5.7: Cooperative assembly of a tripartite complex consisting of the CD4 cytosolic tail, full-length Nef, and the AP-2  $\alpha$ - $\sigma$ 2 hemicomplex, as demonstrated by yeast hybrid assays**

**(A)** Plasmids used in the Y2H, Y3H, and Y4H assays. In all assays, full-length HIV-1 Nef was expressed from pBridge as a GAL4BD fusion protein, while the cytosolic tail (ct) of human CD4 was expressed from pAD as a GAL4AD fusion protein. In the Y2H assay, no other proteins were expressed from these vectors; in the Y3H assay, either  $\sigma$ 2-adaptin or  $\alpha$ C-adaptin was expressed from pBridge or pAD, respectively; and in the Y4H assay, both  $\sigma$ 2-adaptin and  $\alpha$ C-adaptin were coexpressed.

**(B)** Y2H, Y3H, and Y4H analyses of the interaction between GAL4BD-Nef and GAL4AD-CD4 in the absence or presence of one or both components of the  $\alpha$ - $\sigma$ 2 hemicomplex. The plasmids used in the yeast hybrid experiments are noted in to the left of the panel, with the pBridge (pBr)-based vectors in the first column and the pAD-based vectors in the second column. Row 1 corresponds to the Y2H assay, rows 2 and 3 correspond to the Y3H assays, and row 4 corresponds to the Y4H assay. Yeast from all assays were seeded onto +His and -His plates at increasing levels of OD. Yeast grown on the -His plates indicates an interaction between GAL4BD-Nef and GAL4AD-CD4.

**(C)** Y4H analysis of the effect of several Nef and  $\alpha$  mutants on the interaction of GAL4BD-Nef and GAL4AD-CD4 in the presence of the  $\alpha$ - $\sigma$ 2 hemicomplex.

FIG. 5.7



be unable to interact with Nef (Fig. 5.3 and 5.5), yielded the same result. In contrast, mutation of three Nef motifs not required for binding either CD4 or AP-2 (Nef G2A, Nef EEEE62-65AAAA, and Nef PP72,75AA) (Grzesiek et al., 1996; Presseur et al., 2001) did not significantly affect formation of the complex. Thus, binary interactions between CD4, Nef, and AP-2 are required for the assembly of the CD4-Nef-AP-2 tripartite complex.

## 5.4 Discussion

### 5.4.1 Chapter overview

In the two previous chapters, Nef was shown to bind directly to AP-2 in a manner that depended on the well-conserved dileucine and diacidic motifs of the viral protein. In this chapter, a potential binding site for the Nef diacidic motif on AP-2 was identified. This site, which is comprised of two basic residues from  $\alpha$ -adaptin, K297 and R340, is required for the interaction of Nef and AP-2 and the Nef-mediated downregulation of CD4. The Nef diacidic motif and the  $\alpha$ -adaptin basic patch were also found to be essential for the cooperative assembly of a CD4-Nef-AP-2 tripartite complex. Taken together, these results begin to define a binding surface for Nef on AP-2, confirm the critical role of AP-2 in the Nef-mediated downregulation of CD4, and provide the first experimental evidence describing the formation of a CD4-Nef-AP-2 complex.

### 5.4.2 Characteristics of the $\alpha$ -adaptin basic patch

Y3H data presented earlier demonstrated that the Nef diacidic motif was required for the interaction between Nef and AP-2, but not for the interactions between Nef and the homologous AP-1 and AP-3 complexes (Fig. 4.3). Separately, GST pull-down assays showed that the binding of Nef and AP-2 was at least partially dependent on electrostatic interactions (Fig. 4.2). These results suggested that the Nef diacidic motif interacts with basic residues on the surface of AP-2 that are not present on either AP-1 or AP-3. A sequence alignment of the relevant portions of the AP-1, AP-2, and AP-3 complexes revealed 21 lysine and arginine residues that fit this description (Fig. 5.1). Of these, mutation of  $\alpha$  K297 and R340 inhibited Nef binding (Fig. 5.2, 5.3, and 5.5) and prevented the Nef-mediated downregulation of CD4 (Fig. 5.6C-F). In contrast, these residues were dispensable for AP-2 functions that do not depend on the presence of a diacidic motif in the ligand, such as the binding of tyrosinase (Fig. 5.3) and the maintenance of steady-state levels of TfR and CD4 on the plasma membrane (Fig. 5.6A and B). Thus,  $\alpha$  K297 and R340 define a previously uncharacterized feature on AP-2 that is required for the engagement of Nef, likely via the diacidic motif of the viral protein.

The K297 and R340 residues of  $\alpha$ -adaptin are part of a large, surface-exposed basic

patch that rivals in size the polyphosphoinositide binding site near the N-terminus of the protein (Fig. 5.8; Collins et al., 2002). K297 itself is contained within a flexible loop between helices 14 and 15 of the  $\alpha$  solenoid, while R340 is positioned nearby on a loop between helices 16 and 17 (Fig. 5.4 and 5.8; Collins et al., 2002). Interestingly, the basic patch that  $\alpha$  K297 and R340 contribute to is largely absent in the AP-1 and AP-3 complexes. Indeed, the AP-1  $\gamma$  and AP-3  $\delta$  subunits not only lack residues that are homologous to  $\alpha$  K297 and R340, but they are also devoid of several other amino acids that make up the  $\alpha$ -adaptin basic patch, such as K295 and K298 (Fig. 5.1A; Collins et al., 2002; Heldwein et al., 2004).

Although the basic patch appears to be a unique feature of AP-2, many of the residues in this region are conserved among  $\alpha$ -adaptins of the metazoan lineage (Fig. 5.9). The K295, K297, K298, and R340 residues, for instance, are found in both the  $\alpha$ A and  $\alpha$ C isoforms of human  $\alpha$ -adaptin, as well as in the  $\alpha$ -adaptins of a variety of other animal species, including mice, frogs, worms, and fruit flies (Fig. 5.9; see Chapter 3 for more information regarding the activity of Nef in *Drosophila* cells). Since Nef-encoding immunodeficiency viruses only infect primates, the phylogenetic conservation of the  $\alpha$ -adaptin basic patch suggests that it has a more general function.

One possibility is that the basic patch is involved in the recognition of acidic clusters, either alone or in combination with other sorting signals. As discussed in the previous chapter, furin is one of several transmembrane proteins that has such an acidic cluster in its cytosolic tail (reviewed in Bonifacino and Traub, 2003). In conjunction with sequences resembling tyrosine-based and dileucine-based sorting signals, the acidic cluster directs furin to the TGN (Jones et al., 1995; Schäfer et al., 1995; Voorhees et al., 1995) and to the basolateral membrane of polarized epithelial cells (Simmen et al., 1999). The intracellular movement of furin appears to be aided by the association of its acidic cluster with phosphofurin acidic cluster sorting protein-1 (PACS-1), which in turn interacts with the AP-1 and AP-3 complexes (Crump et al., 2001; Wan et al., 1998). Others have shown that, in the absence of all other sorting signals, the acidic cluster is also able to promote the clathrin-mediated endocytosis of furin (Lubben et al., 2007; Voorhees et al., 1995), even though PACS-1 does not bind to AP-2 (Crump et al., 2001). These results suggest that the acidic cluster engages AP-2 in a manner that is independent of PACS-1. Given that the  $\alpha$ -adaptin basic patch is present only in

**FIG. 5.8: The  $\alpha$  K297 and R340 residues are part of a large basic patch on the surface of AP-2**

(A) Surface representation of the three-dimensional structure of the AP-2 core (PDB ID numbers IGW5 and 2VGL [Collins et al., 2002]), with the same color conventions as described in the legend to Fig. 5.4. Relative to the image shown in Fig. 5.4A, this rendering of the AP-2 core has been rotated along the  $x$ -axis towards the reader by approximately  $60^\circ$ .

(B) Surface representation of the AP-2 core, in the same orientation as depicted in the previous panel, but colored according to electrostatic potential (contoured as **red** to **blue** from -74 kiloTesla [kT]/e to +74 kT/e). The images in panels A and B were both drawn using PyMOL (DeLano, 2002) and annotated with Microsoft Powerpoint.

FIG. 5.8

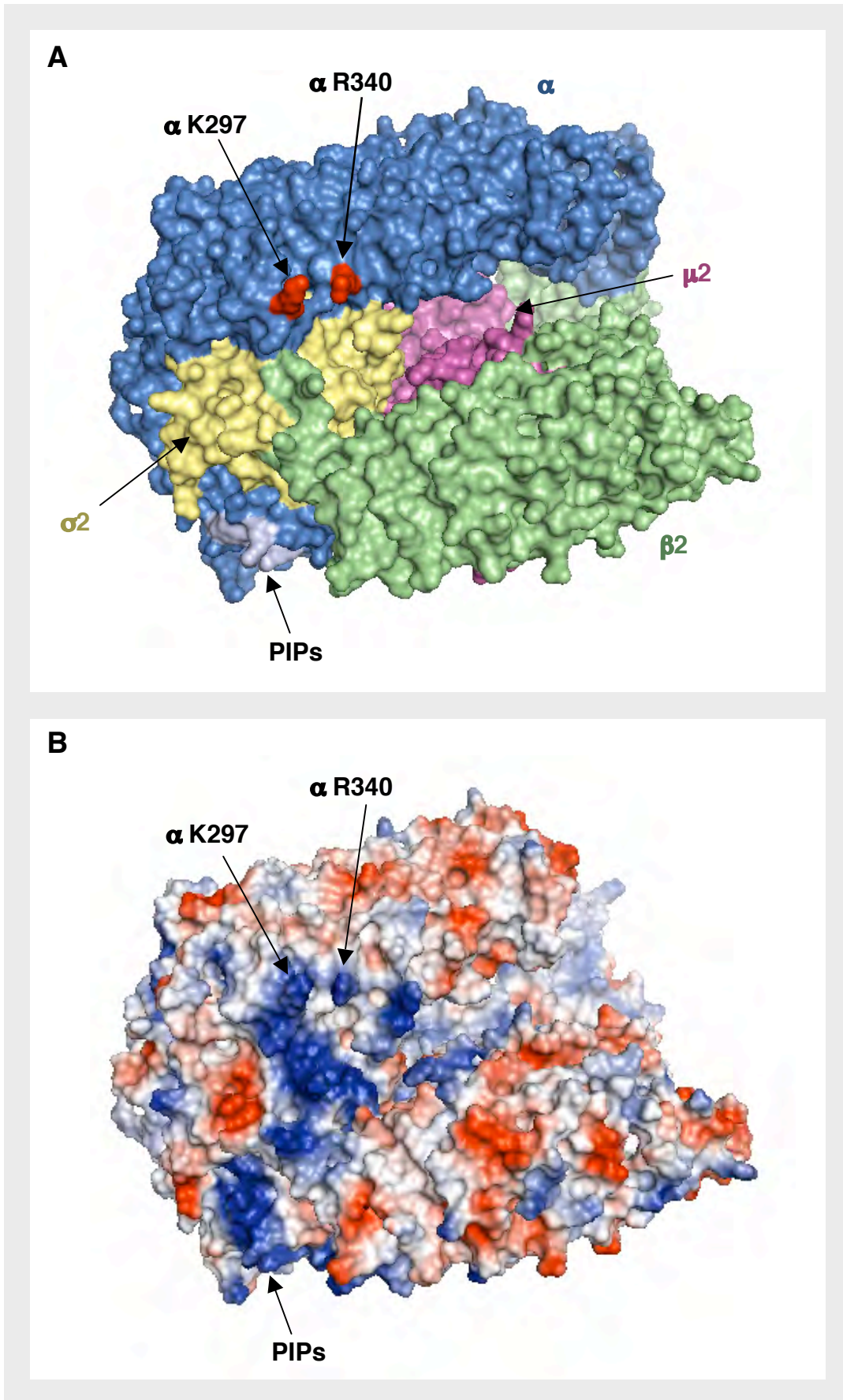


**FIG. 5.9: Phylogenetic conservation of  $\alpha$ -adaptin basic residues involved in the binding of HIV-1 Nef**

An amino acid sequence alignment of  $\alpha$ -adaptins from different metazoan species is shown. The alignment was carried out with the ClustalW2 program used to generate Fig. 5.1. The sequence shown on top corresponds to residues 292-341 of the human  $\alpha$ C isoform, and includes the basic residues identified in this chapter as critical for Nef binding. AP-2  $\alpha$ C residues analyzed in the experiments depicted in Fig. 5.3 are indicated in **red**. Asterisks above the sequence alignment denote the key  $\alpha$ C residues K297 and R340, and homologous residues in  $\alpha$ -adaptins from other species. Species abbreviations and accession numbers are as follows: *Hs* (*Homo sapiens*; O94973 for the  $\alpha$ C isoform and O95782 for the  $\alpha$ A isoform), *Bt* (*Bos taurus*; Q0VCK5), *Rn* (*Rattus norvegicus*; P18484), *Mm* (*Mus musculus*; P17427), *Gg* (*Gallus gallus*; NP\_001012941), *Xl* (*Xenopus laevis*; AAH91638), *Dr* (*Danio rerio*; XP\_001922436), *Ta* (*Trichoplax adhaerens*; EDV28677), *Aa* (*Aedes aegypti*; XP\_001649235), *Cq* (*Culex quinquefasciatus*; XP\_001868082), *Ag* (*Anopheles gambiae*; Q7QG73), *Dm* (*Drosophila melanogaster*; NP\_995607), *Tc* (*Tribolium castaneum*; XP\_971368), *Ci* (*Ciona intestinalis*; XP\_002119553), *Ce* (*Caenorhabditis elegans*; AAA68332), *Bm* (*Brugia malayi*; XP\_001892909), *Nv* (*Nematostella vectensis*; XP\_001641214).

FIG. 5.9

		*				*
<i>Hs</i> (C)	EPPKSKKVQH	SNAKNAVLFE	AISLIIHHDS	EPNLLVRACN	QLGQFLQHRE	
<i>Hs</i> (A)	EPPKSKKVQH	SNAKNAILFE	TISLIIHYDS	EPNLLVRACN	QLGQFLQHRE	
<i>Bt</i>	EPPKSKKVQH	SNAKNAVLFE	AISLVTHHDS	EPNLLVRACN	QLGQFLQHRE	
<i>Rn</i>	EPPKSKKVQH	SNAKNAVLFE	AISLIIHHDS	EPNLLVRACN	QLGQFLQHRE	
<i>Mm</i>	EPPKSKKVQH	SNAKNAVLFE	AISLIIHHDS	EPNLLVRACN	QLGQFLQHRE	
<i>Gg</i>	EPPKSKKVQH	SNAKNAVLFE	AISLIIHHDS	EPNLLVRACN	QLGQFLQHRE	
<i>Xl</i>	EPPKSKKVQH	SNAKNAVLFE	AISLIIYHDS	EPNLLVRACN	QLGQFLQHRE	
<i>Dr</i>	EPPKSKKVQH	SNAKNAILFE	AISLIIHYDS	EPNLLVRACN	QLGQFLQHRE	
<i>Ta</i>	EPPKSKKVQH	SNAKNAVIFE	AISLIIHYDN	DPDQMVRACN	QLGTFLSSRE	
<i>Aa</i>	EPPKSKKVQH	SNAKNAVLFE	AINLIIHNDS	EANLLVRACN	QLGQFLSNRE	
<i>Cg</i>	EPPKSKKVQH	SNAKNAVLFE	AINLIIHNDS	EANLLVRACN	QLGQFLSNRE	
<i>Ag</i>	EPPKSKKVQH	SNAKNAVLFE	AINLIIHNDS	EPSLLVRACN	QLGQFLSNRE	
<i>Dm</i>	EPPKSKKVQH	SNAKNAVLFE	AINLIIHSDS	EPNLLVRACN	QLGQFLSNRE	
<i>Tc</i>	EPPKSKKVQH	SNAKNAVLFE	AISLIIHNDS	EANLLVRACN	QLGQFLSNRE	
<i>Ci</i>	EPPKSKKVQH	SNSKNAVLFE	AINLIIHIDS	EPNLLVRACN	QLGQFLQHRE	
<i>Ce</i>	DAPKSKKVQH	SNAKNAVLFE	AIALIIHMDS	EPQLLVRACN	QLGTFLSHRE	
<i>Bm</i>	DAPKSKKVQH	SNAKNAVLFE	SIALIIHMDT	EPSLLVRACN	QLGTFLSHRE	
<i>Nv</i>	EPPKSKKVQH	SNARNAVLFE	AINLIIHMDS	DQSLLIRGCN	QLGQFLTHRE	

AP-2, it is tempting to speculate that the furin acidic cluster interacts directly with AP-2 via the basic patch and indirectly with AP-1 and AP-3 via PACS-1. Yeast hybrid and in vitro binding assays, similar to those described in this chapter, could be used to test whether the  $\alpha$ -adaptin basic patch does in fact interact with the acidic clusters found in furin and other transmembrane proteins.

If, however, these experiments reveal that the basic patch on  $\alpha$ -adaptin does not have any endogenous binding partners, then this site would be an appealing target for the pharmacologic inhibition of Nef function. The use of a rationally designed drug that binds to the  $\alpha$ -adaptin basic patch with high affinity ought to disrupt the interaction between Nef and AP-2 (Fig. 5.2, 5.3, and 5.5) and prevent the downregulation of CD4 (Fig. 5.6). Because Nef-induced CD4 downregulation has been identified as a critical determinant of viral pathogenesis and disease progression (reviewed in Foster and Garcia, 2008; Lama, 2003; Levesque et al., 2004), interfering with this pathway may be expected to have beneficial consequences for individuals infected with HIV-1. In addition, the binding of a small pharmacological agent to the  $\alpha$ -adaptin basic patch is unlikely to perturb the normal role of AP-2 in the cell, as this region of the complex is not involved in the endocytosis of cargo proteins with tyrosine- and dileucine-based sorting signals (Fig. 5.6).

#### **5.4.3 Cooperative assembly of a CD4-Nef-AP-2 tripartite complex**

The Y4H results shown earlier in the chapter describe, for the first time, the formation of a CD4-Nef-AP-2 tripartite complex (Fig. 5.7). This complex is comprised of the CD4 cytosolic tail, full-length Nef, and the  $\alpha$  and  $\sigma$ 2 subunits of AP-2 (Fig. 5.7). The detection of the CD4-Nef-AP-2 complex is dependent on the known determinants of bimolecular interactions between CD4 and Nef (i.e., the Nef WL57,58 hydrophobic pocket) and between Nef and AP-2 (i.e., the Nef LL164,165 dileucine and DD174,175 diacidic motifs and the  $\alpha$  KR297,340 basic patch) (Fig. 5.7). Furthermore, detection of the complex is independent of Nef residues that do not participate in binding to either CD4 or AP-2 (i.e., G2 myristoylation site, the EEEE62-65 acidic cluster, and the PP72,75 polyproline motif) (Fig. 5.7).

Importantly, these results correlate with the available functional data. Mutations that disrupt the formation of the CD4-Nef-AP-2 complex also prevent downregulation of

CD4 from the plasma membrane (Fig. 3.3, 3.4, 4.4, 4.5, and 5.6; Aiken et al., 1994; Aiken et al., 1996; Stove et al., 2005; Swigut et al., 2000), while mutations that do not affect assembly of the complex are not essential for CD4 downregulation (Fig. 3.3 and 3.4; Aiken et al., 1994; Aiken et al., 1996; Mangasarian et al., 1999; Swigut et al., 2000). The only exception to this correlation is the Nef G2A mutant, which fails to downregulate CD4 from the cell surface because it is not myristoylated, and therefore cannot associate with the inner leaflet of the plasma membrane (Fig. 3.3; Bentham et al., 2006; Kaminchick et al., 1991; Peng and Robert-Guroff, 2001; Stove et al., 2005; Yu and Felsted, 1992). However, myristoylation of Nef is not necessary for binding either CD4 or AP-2 *in vitro* (Fig. 3.9, 4.2, and 5.5; Grzesiek et al., 1996; Presseur et al., 2001). In a similar manner, the myristoylation of Nef should not be required for its incorporation into the CD4-Nef-AP-2 complex described here, as all the proteins in the Y4H experiments are targeted to the yeast nucleus by the presence of heterologous nuclear localization signals (see Materials and Methods, Section 2.4). The correlation between residues that are important for assembly of the CD4-Nef-AP-2 complex and the downregulation of CD4 underscores the biological significance of the tripartite complex.

In T cells, the majority of CD4 can be found at the plasma membrane in a complex with the protein tyrosine kinase Lck (Pelchen-Matthews et al., 1992; Veillete et al., 1988; reviewed in Oldridge and Marsh, 1998). In this complex, the CD4 cytosolic tail and the N-terminus of Lck form a folded zinc clasp structure, which obscures a region of CD4 that is bound by Nef and required for downregulation of the receptor (Bandres et al., 1995; Gratton et al., 1996; Grzesiek et al., 1996; Kim et al., 2003; Salghetti et al., 1995). Previous studies have suggested that Nef induces the dissociation of CD4 and Lck (Kim et al., 1999; Salghetti et al., 1995), although the mechanism by which Nef does so is poorly understood. Interestingly, a Nef mutant lacking the DD174,175 diacidic motif, which is now known to be critical for the binding of AP-2 (Fig. 4.1, 4.2 and 4.3) and assembly of the CD4-Nef-AP-2 complex (Fig. 5.7), was found to be defective in promoting the dissociation of CD4 and Lck (Kim et al., 1999). Thus, the establishment of the tripartite complex may either induce CD4 to separate from Lck, or prevent it from reassociating with the membrane-anchored kinase. This would then allow Nef to internalize CD4 from the cell surface and direct the receptor towards lysosomes for eventual degradation (Aiken et al., 1994; Rhee et al., 1994).

The assembly of the CD4-Nef-AP-2 complex is consistent with the previous proposal that Nef links the cytosolic tail of CD4 to AP-2 (Greenberg et al., 1997; Greenberg et al., 1998a; reviewed in Oldridge and Marsh, 1998). In addition, the data shown here indicates that the  $\alpha$ - $\sigma$ 2 hemicomplex promotes the interaction of Nef and the CD4 tail (Fig. 5.7B). Thus, the formation of the CD4-Nef-AP-2 complex involves cooperative interactions among its components. One possible explanation for this cooperativity is that the binding of AP-2 to Nef induces a conformational change in the viral protein that increases its affinity for CD4. In this model, AP-2 does not make direct contact with the CD4 tail. Instead, Nef serves as a physical link between the receptor and the clathrin adaptor. An alternative explanation is that each component of the CD4-Nef-AP-2 complex makes simultaneous contact with the other two, thereby enhancing the overall stability of the tripartite complex. This model requires that both Nef and AP-2 bind to the CD4 tail directly and at the same time. Detailed biochemical and structural studies will be needed to distinguish between these models, and to identify all the determinants of assembly for the CD4-Nef-AP-2 complex.

The observation of a CD4-Nef-AP-2 complex is not without precedent, as Nef has previously been shown to engage in cooperative interactions with other receptors and AP complexes. For example, the binding of HIV-1 Nef to the cytosolic tail of MHC-I increases the affinity of a tyrosine-like motif in this tail for the  $\mu$ 1 subunit of AP-1, thus stabilizing the assembly of a MHC-I-Nef-AP-1 complex (Noviello et al., 2008; Wonderlich et al., 2008). Similarly, the binding of SIV Nef to the TCR-associated CD3- $\zeta$  chain increases its affinity for AP-2, leading to the formation of a CD3- $\zeta$ -Nef-AP-2 complex (Swigut et al., 2003). These cooperative interactions enable Nef to reduce the expression of MHC-I and TCR-CD3 on the plasma membrane (Noviello et al., 2008; Swigut et al., 2003; Wonderlich et al., 2008). Together with the Y4H data shown here, these results indicate that the establishment of cooperative interactions with receptors and adaptors is a general feature of Nef that underlies its effect on host cell protein trafficking pathways.

**Chapter 6:**  
**Discussion**

## **6.1 Abstract**

This chapter is divided into four major sections (6.2 - 6.5). The first of these sections (6.2) summarizes the major findings of this thesis. The next two sections (6.3 and 6.4) describe ongoing and future work, respectively. Ongoing experiments are focused on the identification of the Nef dileucine binding site on AP-2, while future experiments could either explore how this interaction affects the surface-expression of endogenous receptors or the postendocytic fate of CD4. Some concluding remarks are provided in the final section of this thesis (6.5).

## 6.2 Summary of results

The primary goal of this thesis was to determine how HIV-1 Nef downregulates CD4 (see Section 1.9). Previous work on this topic had produced conflicting results; some studies favored an endocytic model of downregulation, while other studies favored an intracellular retention model (see Section 1.8). According to the endocytic model, Nef connects CD4 to AP-2 at the plasma membrane, thereby accelerating the rate at which the receptor is internalized from the cell-surface. In contrast, the intracellular retention model claimed that Nef uses either AP-1 or AP-3 to prevent newly synthesized CD4 from reaching the plasma membrane. Both models agree that Nef ultimately induces the transport of CD4 to lysosomes, where it is degraded (see Section 6.4).

A variety of cell and molecular biology assays were used to distinguish between these contrasting models. First, a novel CD4-Nef downregulation system was constructed in *Drosophila* S2 cells (Fig. 3.1, 3.2, 3.3, and 3.4). The RNAi-mediated depletion of host cell proteins in this heterologous system showed that clathrin and AP-2, but not AP-1 and AP-3, were required for CD4 downregulation (Fig. 3.5 and 3.6; Table 3.1). RNAi knockdowns in human HeLa cells later confirmed these results (Fig. 3.7). Yeast three-hybrid and GST pull-down experiments were then used to demonstrate a robust, direct interaction between Nef and the  $\alpha$ - $\sigma$ 2 hemicomplex of AP-2 (Fig. 3.8 and 3.9). This interaction was found to depend on the Nef dileucine motif, which is essential for the downregulation of CD4 (Fig. 3.3, 3.4, 3.8, and 3.9).

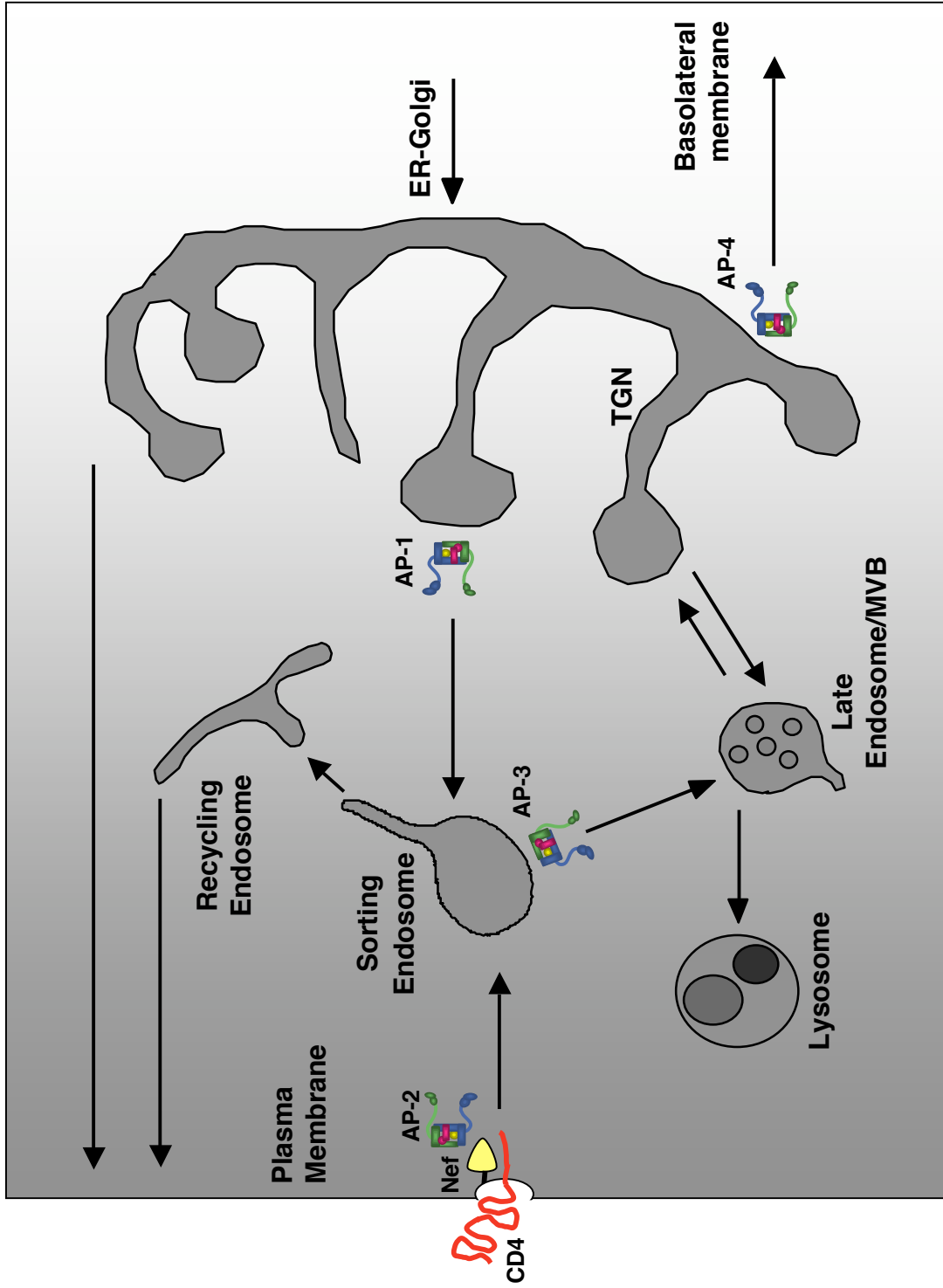
Subsequent experiments identified a second motif on Nef required for the interaction with AP-2. This motif, which conforms the [D/E]D consensus sequence, is strongly conserved among HIV-1 Nef alleles, and is necessary for both AP-2 binding and CD4 downregulation (Fig. 4.1, 4.2, 4.4, 4.5). Yeast three-hybrid assays showed that the Nef diacidic motif was dispensable for binding both AP-1 and AP-3, suggesting that these clathrin adaptors do not significantly contribute to the modulation of CD4 expression (Fig. 4.3). Yeast three-hybrid assays were also used to identify a prospective binding site for the Nef diacidic motif on the surface of AP-2 (Fig. 5.1, 5.2, 5.3, and 5.4). GST pull-downs confirmed that this site, a basic patch on the  $\alpha$ -adaptin trunk domain, was required for the interaction between Nef and AP-2 (Fig. 5.5). RNAi knockdown and rescue assays were then used to show that, like the Nef diacidic motif, the  $\alpha$ -adaptin

basic patch is critical for the downregulation of CD4 (Fig. 5.6). Finally, a novel yeast four-hybrid assay revealed that CD4, Nef, and AP-2 interact simultaneously to form a tripartite complex, the assembly of which depends on the Nef dileucine and diacidic motifs and the  $\alpha$ -adaptin basic patch (Fig. 5.7). The results from all these experiments uniformly support the endocytic model of downregulation, whereby Nef uses AP-2 to direct CD4 from the plasma membrane towards lysosomes (Fig. 6.1).

### **FIG 6.1: Revised model of Nef-mediated CD4 downregulation**

Based on the data presented in this thesis, the proximal stages of Nef-mediated CD4 downregulation occurs at the cell-surface. Nef increases the rate at which the receptor is internalized from the plasma membrane by physically linking the CD4 cytosolic tail to AP-2. The related clathrin adaptor proteins (AP-1, AP-3, and AP-4) do not appear to have significant roles in the downregulation of CD4. For reference, please compare this figure to Fig. 1.12, which was shown at the outset of this project.

FIG. 6.1



### 6.3 Ongoing work: identification of the Nef dileucine binding site on AP-2

As described in the last section, two new determinants of interaction between Nef and AP-2 were identified during the course of this work: the Nef diacidic motif and the  $\alpha$ -adaptin basic patch. However, these motifs are not sufficient to mediate the binding of Nef and AP-2. Another required element of this interaction is the Nef dileucine motif (Fig. 3.8 and 3.9). Previous attempts to identify the binding site of the Nef dileucine motif on the surface of AP-2 yielded ambiguous results; photoaffinity labeling assays indicated that leucine residues bound to  $\beta$ 2, while yeast two-hybrid assays suggested that  $\mu$ 2 was involved (Craig et al., 2000; Greenberg et al., 1998). Unfortunately, these interactions appeared to be of very low affinity, and may have been the result of non-specific binding. In contrast, the yeast three-hybrid and GST pull-down experiments shown here indicate that the Nef dileucine motif binds with relatively high affinity to the  $\alpha$ - $\sigma$ 2 region of the AP-2 core (Fig. 3.8, 3.9, 4.1, 4.2, and 4.3).

Based on these findings, an effort was made to locate the specific binding site of the Nef dileucine motif on AP-2. This motif (ENTSLI in the NL4-3 variant) conforms to the [D/E]xxxL[L/I] consensus sequence for dileucine motifs found in a large number of transmembrane proteins, including tyrosinase (ERQPLL). An important feature of these dileucine motifs is the presence of an acidic residue upstream of the leucine pair (reviewed by Bonifacino and Traub, 2003). In the case of HIV-1 Nef, this residue is almost always a glutamate (Fig. 4.1). Substitution of the glutamate with a basic amino acid, such as lysine, significantly impairs the ability of Nef to downregulate CD4 (see Coleman et al., 2006). This suggests that the acidic portion of the Nef dileucine motif binds to a basic patch on the surface of the  $\alpha$ - $\sigma$ 2 hemicomplex. Indeed, the binding of Nef to AP-2 probably involves the formation of salt bridges, as strong ionic solutions disrupt the interaction (Fig. 4.2). Furthermore, the region on AP-2 that binds the Nef dileucine motif is likely to be conserved among the AP complexes, because mutation of either the glutamate or the leucines inhibits the interaction of Nef with  $\gamma$ - $\sigma$ 1,  $\alpha$ - $\sigma$ 2, and  $\delta$ - $\sigma$ 3 (Fig. 3.8, 4.1, and 4.3; Janvier et al., 2003).

These considerations were taken into account while devising a strategy to identify the AP-2 residues that coordinate binding of the Nef dileucine motif. The first step of this strategy was to perform a sequence alignment of  $\gamma$ - $\sigma$ 1,  $\alpha$ - $\sigma$ 2, and  $\delta$ - $\sigma$ 3, and determine

which basic amino acids were conserved among all three adaptin hemicomplexes (see Fig. 6.2). Conserved arginine and lysine residues in the  $\alpha$  and  $\sigma 2$  subunits were then changed to aspartate or glutamate, and yeast three-hybrid assays were used to test the resulting mutants for a loss of binding to wild-type Nef (ENTSLL) (Fig. 6.3, 6.4, 6.5). The same  $\alpha$  and  $\sigma 2$  mutants were then tested for their ability to interact with a version of Nef that had its glutamate residue changed to lysine (KNTSLL) (Fig. 6.3, 6.4, 6.5). These assays were designed to show which AP-2 residues normally interact with the Nef glutamate; changing the relevant  $\alpha$ - $\sigma 2$  residues from bases to acids should inhibit their binding of Nef ENTSLL but promote the binding of Nef KNTSLL, as the latter condition would act as a charge-swap and reconstitute the necessary salt bridge. Only one AP-2 residue,  $\alpha$  R21, satisfied these requirements (Fig. 6.4). Indeed, the  $\alpha$  R21D mutant displayed decreased affinity for Nef ENTSLL but markedly increased affinity for Nef KNTSLL, when compared to wild-type  $\alpha$ -adaptin. This strongly suggests that  $\alpha$  R21 normally binds to the Nef glutamate. Similar assays were performed with wild-type and mutant tyrosinase, in place of Nef, to confirm that  $\alpha$  R21 binds to the acidic portion of dileucine motifs in general (Fig. 6.4 and 6.5).

Because the hydrophobic and acidic portions of dileucine motifs are separated by only three amino acids, the AP-2 residues that bind the leucine pair are probably located in the vicinity of  $\alpha$  R21. Mapping of  $\alpha$  R21 on the three-dimensional crystal structure of AP-2 indicates that it lies at the interface of the  $\alpha$  and  $\sigma 2$  subunits (Fig. 6.6; Collins et al., 2002). Thus, residues from either subunit might be responsible for the binding of the two leucines. With this in mind, several amino acids on  $\alpha$  and  $\sigma 2$  were selected as potential leucine-binding partners, based on their proximity to  $\alpha$  R21 and their strong conservation among the AP complexes (see Fig. 6.6 and 6.7). These amino acids were then changed to alanine or aspartate, and the resulting mutants were tested for a loss of binding to Nef ENTSLL using yeast three-hybrid assays (Fig. 6.8). The mutation of  $\sigma 2$  A63,  $\sigma 2$  V88, and  $\sigma 2$  L103 abolished the interaction between AP-2 and Nef, while the alteration of  $\sigma 2$  E89,  $\sigma 2$  E100, and  $\sigma 2$  D102 resulted in binding defects that were nearly as profound. Thus, these residues may interact with the leucines in Nef. Similar data were obtained when tyrosinase ERQPLL was substituted for Nef, suggesting that the  $\sigma 2$  residues mentioned above bind to the hydrophobic segment of other dileucine motifs. However, the AP-2 crystal structure indicates that this area of  $\sigma 2$  is normally

**FIG. 6.2: Identification of basic residues in the AP-2  $\alpha$ - $\sigma$ 2 hemicomplex that are conserved with the homologous subunits of AP-1 and AP-3**

Sequence alignments of the AP-1  $\gamma$ - $\sigma$ 1, AP-2  $\alpha$ - $\sigma$ 2, and AP-3  $\delta$ -s3 hemicomplexes were performed using the ClustalW2 program (available at <http://www.clustal.org/>), as previously described (Fig. 5.1). Amino acid numbers for the first residue in each row are indicated on the left, while amino acid numbers for the last residue in each row are indicated on the right. Lysine and arginine residues that are present in AP-2  $\alpha$ - $\sigma$ 2, and conserved among the corresponding AP-1  $\gamma$ - $\sigma$ 1 and AP-3  $\delta$ -s3 subunits, are highlighted in **red**. These residues were mutated to either aspartate or glutamate (see Fig. 6.4 and 6.5). The **red** asterisk denotes AP-2  $\alpha$  residue R21, which was found to bind the acidic portion of dileucine sorting signals (see Fig. 6.4).

**(A)** Protein sequence alignment of the trunk domains of human AP-1  $\gamma$  ( $\gamma$ 1 isoform; accession number AAH36283), AP-2  $\alpha$  ( $\alpha$ C isoform; accession number O94973), and AP-3  $\delta$  (accession number AAC51761).

**(B)** Protein sequence alignment of human AP-1  $\sigma$ 1 ( $\sigma$ 1A isoform; accession number AAA37243), AP-2  $\sigma$ 2 (accession number AAP36470), and AP-3  $\sigma$ 3 ( $\sigma$ 3A isoform; accession number EAW48952).

FIG. 6.2

A

$\gamma$ adaptin	1	-----MPAPI	R-----LRE	LIRTIRTART	QAEEREMIQK	ECAAIRSSFR	39
$\alpha$ adaptin	1	-----MPAVS	KGDGM <sup>R</sup> GLAV	FISDI <sup>R</sup> NC <sup>K</sup> S	KEAEIKRINK	ELANIRSKFK	45
$\delta$ adaptin	1	MALKMVKGSI	DRMFDKNLQD	LVRGIRNHK-	-EDEAKYISQ	CIDEIKQELK	48
$\gamma$ adaptin	40	EE---DNTYR	CRNVAKLLYM	HMLGYPAHFG	QLECLKLIAS	QKFTDKRIGY	86
$\alpha$ adaptin	46	GDKALDGYSK	KKYVCKLLFI	FLLGHDIDFG	HMEAVNLLSS	NRYTEKQIGY	95
$\delta$ adaptin	49	QD---NIAVK	ANAVCKLTYL	QMLGYDISWA	AFNIIIEVMSA	SKFTFKRIGY	95
$\gamma$ adaptin	87	LGAMLLLDER	QDVHLLMTNC	IKNDLNHSTQ	FVQGLALCTL	GCMGSSEMCR	137
$\alpha$ adaptin	96	LFISVLVNSN	SELIRLINNA	IKNDLASRNP	TFMGLALHCI	ASVGSREMAE	145
$\delta$ adaptin	96	LAASQSFHEG	TDVIMLTTNQ	IRKDLSSPSQ	YDTGVALTGL	SCFVTPDLAR	145
$\gamma$ adaptin	138	DLAGEVEKLL	KTSN--SYLR	KKAALCAVHV	IRKVPPELME	--FLPATKNL	183
$\alpha$ adaptin	146	AFAGEIPKVL	VAGDTMDSVK	QSAALCLLRL	YRTSPDLVPM	GDWTSRVVHL	195
$\delta$ adaptin	146	DLANDIMTLM	SHTK--PYIR	KKAVLIMYKV	FLKYPESLRP	--AFPRLKEK	191
$\gamma$ adaptin	184	LNEKNHGV LH	TSVLLTEMC	ERSPDMLAHF	RKNEKLV PQL	VRILKNLIMS	233
$\alpha$ adaptin	196	LNDQHLGVVT	AATSLITTLA	QKNPEEFKTS	VS--LAVSRL	SRIVTSASTD	243
$\delta$ adaptin	192	LEDPDPGVQS	AAVNVICELA	RRNPKNYLS-	-----LAPLF	FKLMTSSTNN	235
$\gamma$ adaptin	234	GYSPEHDVSG	ISDPFLQVRI	LRLLRILGRN	DDDSSEAMND	ILAQVATNTE	283
$\alpha$ adaptin	244	--LQDYTY YF	VPAPWLSVKL	LRL LQCYPPP	DPAVRCRLTE	CLETILNKAQ	291
$\delta$ adaptin	236	-----	----WVLIKI	IKLFGAL TPL	EPRLGKKLIE	PLTNLIHSTS	272
$\gamma$ adaptin	284	TS-----	KNVGNAILYE	TVLTIMDIKS	ESGLRVLAIN	ILGRFLNND	325
$\alpha$ adaptin	292	EPPKSKKQVH	SNAKNAVLFE	AISLIHHDS	EPNLLVRACN	QLGQFLQHRE	341
$\delta$ adaptin	273	AMS-----	LL YECVNTVIAV	LISLSSGMPN	HSASIQLCVQ	KLRILIEDSD	315
$\gamma$ adaptin	326	KNIRYVALT-	-SLKTVQTD	HNAVQRHRST	IVDCLK-DLD	VSIKRRAMEL	372
$\alpha$ adaptin	342	TNLRYLALES	MCTLASSEFS	HEAVKTHIET	VINALKTERD	VSVRQRAVDL	391
$\delta$ adaptin	316	QNLKYLGLL-	-AMSKILKTH	PKSVQSHKDL	ILQCLD-DKD	ESIRLRALDL	363
$\gamma$ adaptin	393	SFALVNGNNI	RGMKELLYF	LDSCE-PEFK	ADCASGIFLA	AEK----YAP	417
$\alpha$ adaptin	392	LYAMCDRSNA	PQIVAEMLSY	LETAD-YSIR	EEIVLKVAIL	AEK----YAV	436
$\delta$ adaptin	364	LYGMVSKKNL	MEIVKKLMT H	VDKAEGTTYR	DELLTKIIDI	CSQSNYQYIT	413

B

$\sigma 1$ adaptin	1	MMRFMLLFSR	QGKRLQKWY	LATSDKERKK	MVRELMQVVL	ARKPKMCSFL	50
$\sigma 2$ adaptin	1	MI <sup>R</sup> FILIQNR	AGK <sup>R</sup> RLAKWY	MQFDDDEKQK	LIEEVHAVVT	VRDAKHTNFV	50
$\sigma 3$ adaptin	1	MIKAILIFNN	HGKPRLSKFY	QPYSED TQQQ	IIRETFHLVS	KRDENVCNFL	50
$\sigma 1$ adaptin	51	EW-----	RD LKVVKRYAS	LYFCCAIEGQ	DNELITLELI	HRYVELLDKY	94
$\sigma 2$ adaptin	51	EF-----	RN FKIIYRRYAG	LYFCICVDVN	DNNLAYLEAI	HNFVEVLNEY	94
$\sigma 3$ adaptin	51	EGLLIGGSD	NKLIYRHYAT	LYFVFCVDSS	ESELGILDLI	QVFVETLDKC	100
$\sigma 1$ adaptin	95	FGSVCELDII	FNFEKAYFIL	DEFLMGDVQ	DTSKKSVLKA	IEQADLLQEE	144
$\sigma 2$ adaptin	95	FHNVCELDLV	FNFYKVYTVV	DEMFLAGEIR	ETSQTKVLKQ	LLMLQSLE---	142
$\sigma 3$ adaptin	101	FENVCELDLI	FHVDKVHNIL	AEMVMGGMVL	ETNMNEIVTQ	IDAQNKLEKS	150
$\sigma 1$ adaptin	145	DE-----	S PRSVLEEMGL	A-----	-----	---	158
$\sigma 2$ adaptin	N/A	-----	-----	-----	-----	---	N/A
$\sigma 3$ adaptin	151	EAGLAGAPAR	AVSAVKMNML	PEIPRNINIG	DISIKVPNLP	SFK	193

### **FIG. 6.3: Plasmids used for the Y3H assays shown in this chapter**

The pBridge and pGADT7 plasmids used in the yeast three-hybrid assays described in this chapter are shown here. The following constructs were expressed from pBridge as GAL4BD fusion proteins: wild-type HIV-1 Nef (ENTSLL), mutant Nef (KNTSLL), wild-type mouse tyrosinase (ERQPLL), and mutant tyrosinase (KRQPLL). Wild-type and mutant versions of  $\sigma$ 2-adaptin were also expressed from pBridge. The pGADT7 plasmid was used to express GAL4AD fusions of wild-type and mutant  $\alpha$ -adaptin. In some cases, the multiple cloning sites of one or both vectors were left empty for use as controls. Yeast were transformed with pairs of the pBridge and pGADT7 plasmids and plated on selective media as previously described (see Section 2.4). Growth of the yeast on media lacking histidine (–His), or lacking histidine and supplemented with 3 mM of 3-amino-1,2,4-triazole (+3AT) is indicative of an interaction between the  $\alpha$ - $\sigma$ 2 hemicomplex and either Nef or tyrosinase at two levels of stringency.

FIG. 6.3

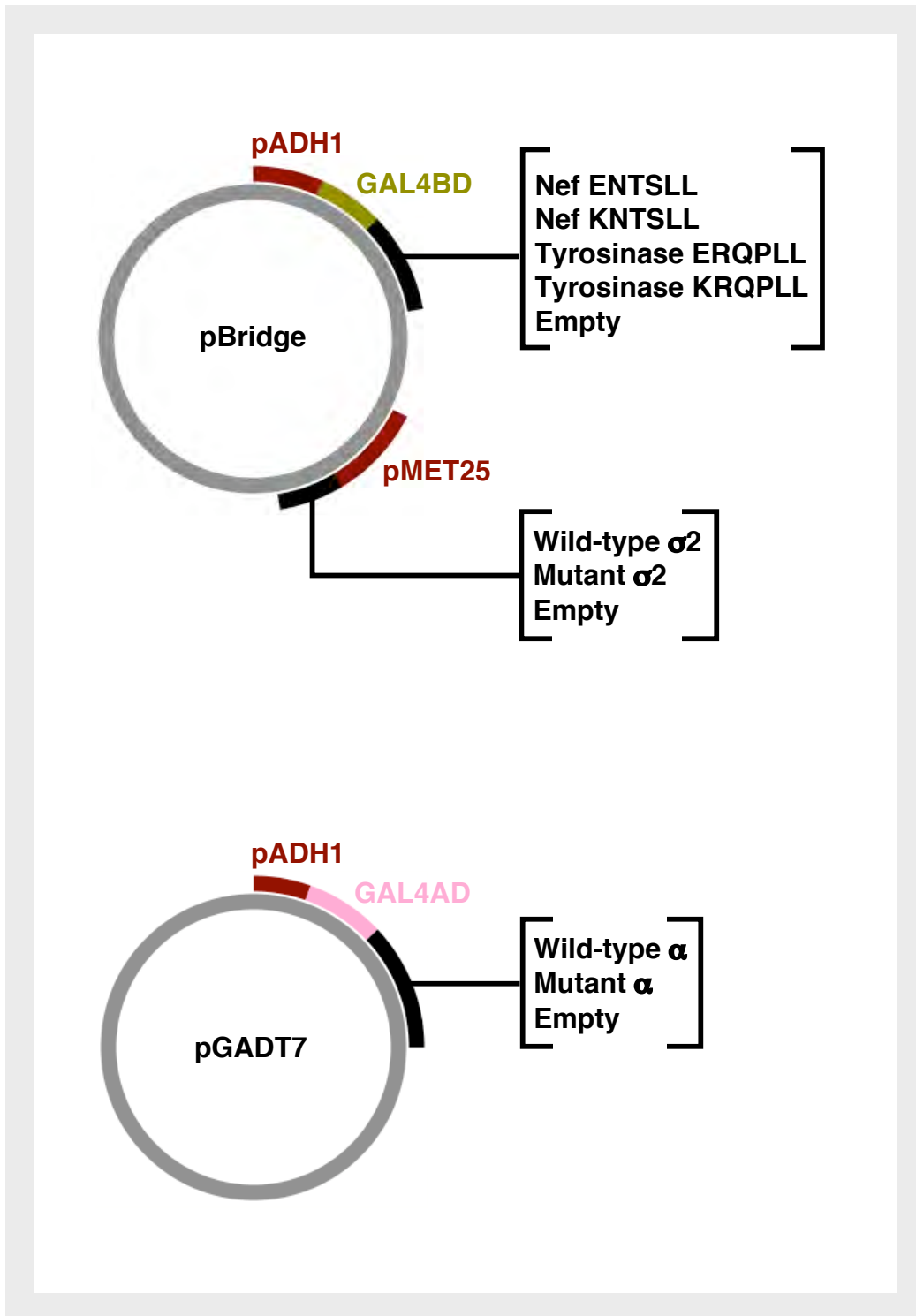


**FIG. 6.4: Y3H analysis of the  $\alpha$  mutants: role of the conserved, basic residues in binding the acidic portion of dileucine motifs**

Lysine and arginine residues in AP-2  $\alpha$  that are conserved in the homologous AP-1  $\gamma$  and AP-3  $\delta$  subunits were mutated to either aspartate or glutamate (see Fig. 6.2). The resulting  $\alpha$  constructs were then tested for loss of binding to wild-type Nef (ENTSLL) and gain of binding to mutant Nef (KNTSLL). If an  $\alpha$  residue is required for binding the acidic portion of dileucine signals, then its mutation to an acidic amino acid would be expected to disrupt the interaction between  $\alpha$ - $\sigma$ 2 and Nef ENTSLL. However, this  $\alpha$  mutant should be able to interact with Nef KNTSLL, because the critical salt bridge would be restored. Only one  $\alpha$  mutant, R21D, satisfied these conditions. Thus,  $\alpha$  R21 is most likely responsible for binding the acidic residue of the Nef dileucine motif. Similar assays were performed with wild-type (ERQPLL) and mutant (KRQPLL) versions of the tyrosinase cytosolic tail in place of Nef. Although somewhat less apparent in these assays,  $\alpha$  R21D showed lower affinity for tyrosinase ERQPLL and higher affinity for tyrosinase KRQPLL than the positive control. This result suggests that  $\alpha$  R21 might be important for binding the acidic regions of dileucine sorting signals in general. An empty vector condition, which lacks either Nef or the tyrosinase tail, was included to test whether any of the  $\alpha$  mutations caused self-activation. In the first two panels, the positive control represents the interaction between Nef ENTSLL and  $\alpha$ - $\sigma$ 2, while the negative control represents the interaction between Nef KNTSLL and  $\alpha$ - $\sigma$ 2. The same controls are used for the last (empty vector) panel. For the tyrosinase experiments, the positive control uses tyrosinase ERQPLL, while the negative control uses tyrosinase KRQPLL.

FIG. 6.4

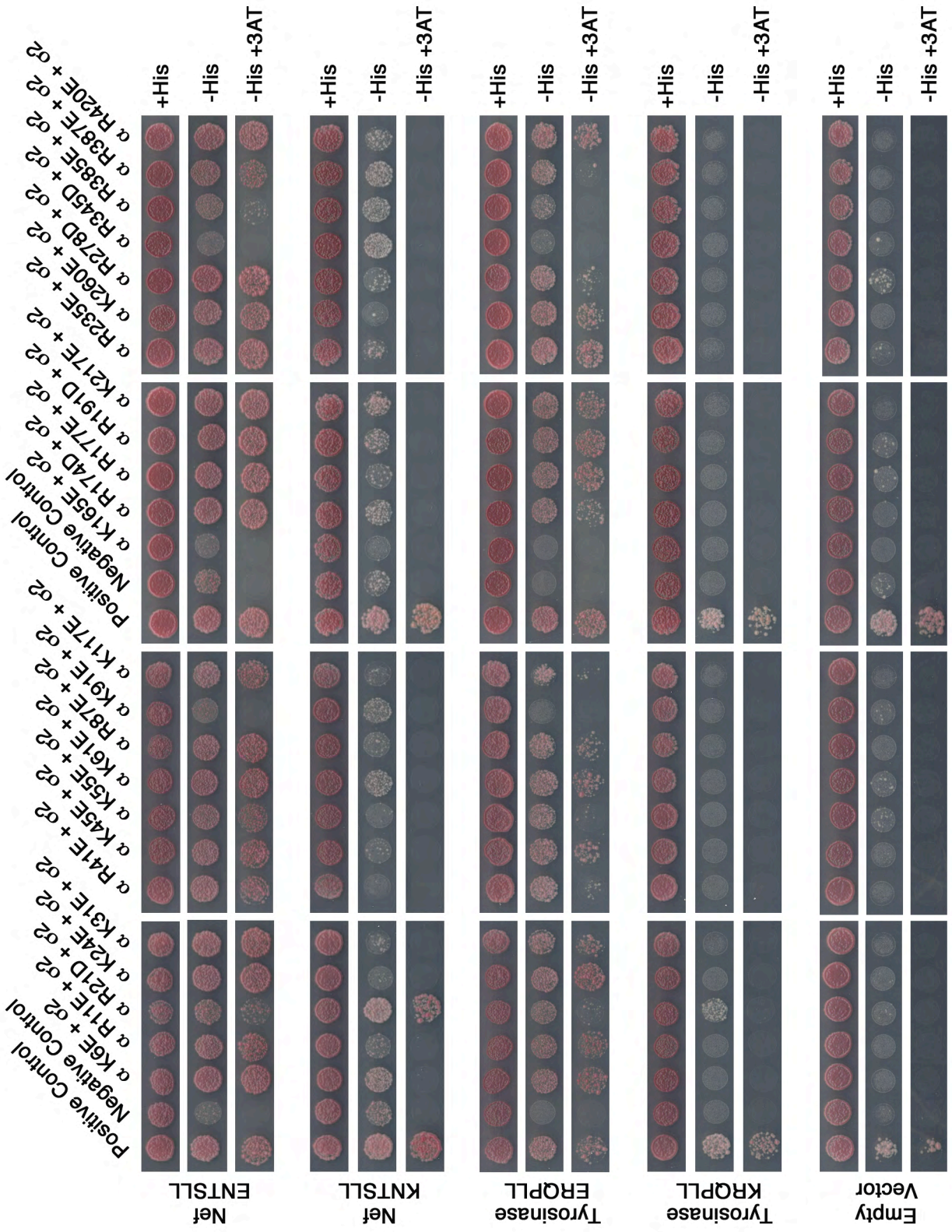


**FIG. 6.5: Y3H analysis of the  $\sigma$ 2 mutants: role of the conserved, basic residues in binding the acidic portion of dileucine motifs**

Lysine and arginine residues in AP-2  $\sigma$ 2 that are conserved in the homologous AP-1  $\sigma$ 1 and AP-3  $\sigma$ 3 subunits were mutated to aspartate or glutamate, combined with wild type  $\alpha$ -adaptin, and used in yeast three-hybrid assays to test for interactions with Nef ENTSSL, Nef KNTSSL, tyrosinase ERQPLL, tyrosinase KRQPLL, and empty vector (as described in the legend to Fig. 6.4). The mutation of several  $\sigma$ 2 residues, including R15, caused loss of binding to both Nef ENTSSL and tyrosinase ERQPLL. However, these mutants failed to bind either Nef KNTSSL or tyrosinase KRQPLL, precluding their assignment as ligands of dileucine sorting signals.

FIG. 6.5

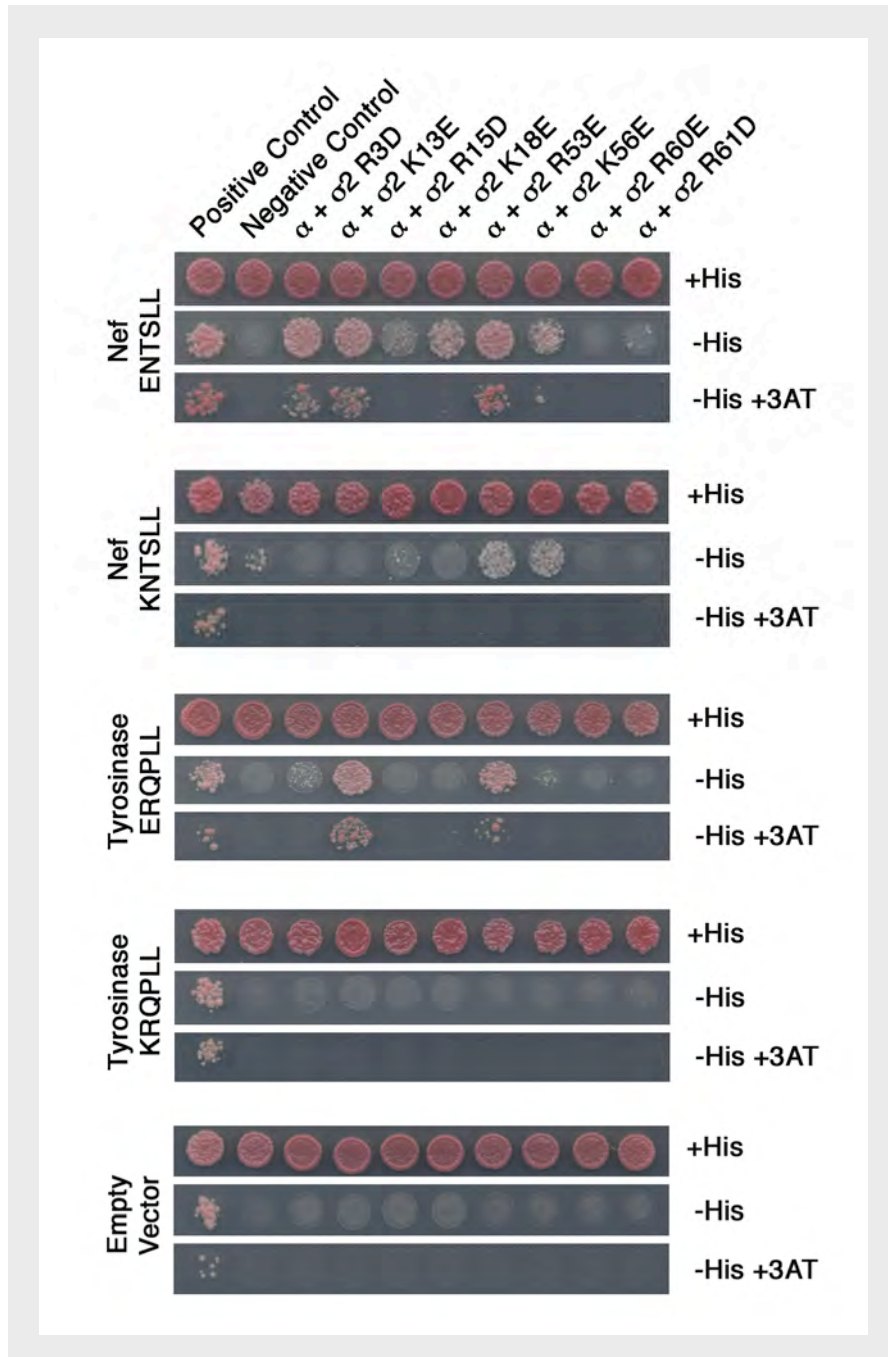


**FIG. 6.6: Location of  $\alpha$  R21 and adjacent residues on the crystal structure of the AP-2 complex**

(A) Ribbon diagram of the  $\alpha$ - $\sigma$ 2 hemicomplex (PDB ID numbers 1GW5 and 2VGL [Collins et al., 2002]) depicting the location of the  $\alpha$  R21 residue. For clarity, only the  $\alpha$  and  $\sigma$ 2 subunits of the AP-2 core are shown, with the  $\alpha$  subunit drawn in **dark blue** and the  $\sigma$ 2 subunit in **gold**. The  $\alpha$  R21 residue (including its side chain) is colored in **red**. The locations of  $\alpha$  K297 and  $\alpha$  R340, also colored in **red**, are provided as points of reference.

(B) Ribbon diagram of the  $\alpha$ - $\sigma$ 2 hemicomplex, with the locations of several candidate residues that might bind the hydrophobic portion of dileucine sorting signals. Only the portion of the  $\alpha$ - $\sigma$ 2 hemicomplex that lies within the dashed box of panel A is shown. As in panel A, the  $\alpha$  subunit is drawn in **dark blue**; the  $\sigma$ 2 subunit is colored in **gold**; and the  $\alpha$  R21,  $\alpha$  K297, and  $\alpha$  R340 residues are shaded **red**. The candidate leucine-binding residues (and their side chains) are depicted in **orange**.

FIG. 6.6

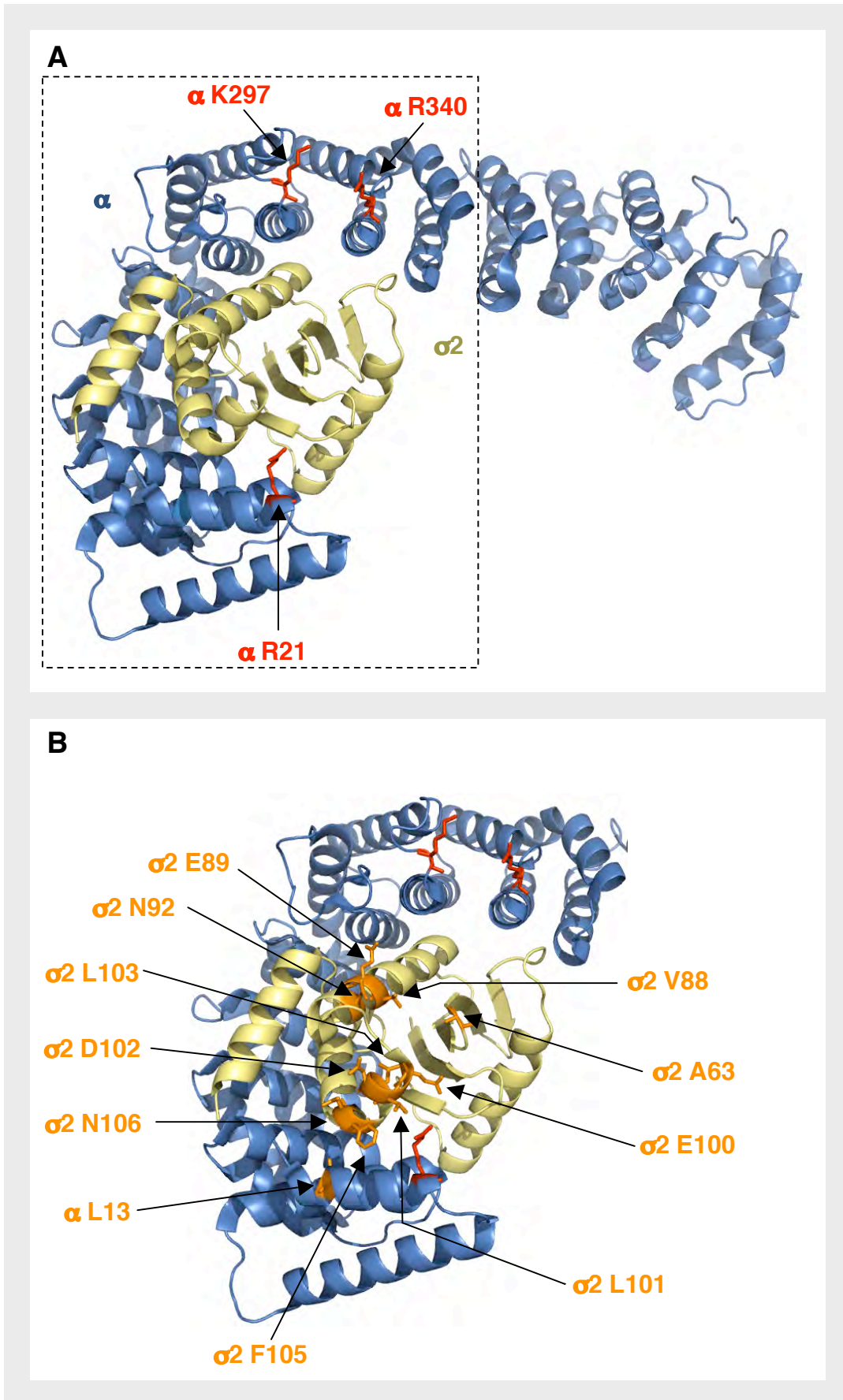


**FIG. 6.7: Sequence conservation of  $\alpha$ - $\sigma$ 2 residues potentially involved in binding the hydrophobic portion of dileucine sorting signals**

Sequence alignments of the AP-1  $\gamma$ - $\sigma$ 1, AP-2  $\alpha$ - $\sigma$ 2, and AP-3  $\delta$ - $\sigma$ 3 hemicomplexes were performed as described in the legend to Fig. 6.2. The position of the first amino acid in each row is indicated by the number on the left, while the position of the last amino acid in each row is indicated by the number on the right. Several  $\alpha$ - $\sigma$ 2 residues were identified as leucine-binding candidates, based on their physical proximity to  $\alpha$  R21 (see Fig. 6.6) and their conservation among the homologous  $\gamma$ - $\sigma$ 1 and  $\delta$ - $\sigma$ 3 hemicomplexes. These residues are highlighted in orange, and were mutated prior to their incorporation in a yeast three-hybrid assay (see Fig. 6.8). The orange asterisks denote  $\sigma$ 2 V88 and  $\sigma$ 2 L103, which were shown to be critical for binding the Nef, tyrosinase, and CD4 dileucine motifs (see Fig. 6.8 and Kelly et al., 2008).

**(A)** Protein sequence alignment of the trunk domains of human AP-1  $\gamma$  ( $\gamma$ 1 isoform; accession number AAH36283), AP-2  $\alpha$  ( $\alpha$ C isoform; accession number O94973), and AP-3  $\delta$  (accession number AAC51761).

**(B)** Protein sequence alignment of human AP-1  $\sigma$ 1 ( $\sigma$ 1A isoform; accession number AAA37243), AP-2  $\sigma$ 2 (accession number AAP36470), and AP-3  $\sigma$ 3 ( $\sigma$ 3A isoform; accession number EAW48952).

FIG. 6.7

A

$\gamma$ adaptin	1	-----MPAPI	R-----LRE	LIRTIRTART	QAEEREMIQK	ECAAIRSSFR	39
$\alpha$ adaptin	1	-----MPAVS	KGDGMRGLAV	FISDIRNCKS	KEAEIKRINK	ELANIRSKFK	45
$\delta$ adaptin	1	MALKMVKGSI	DRMFDKNLQD	LVRGIRNHK-	-EDEAKYISQ	CIDEIKQELK	48
$\gamma$ adaptin	40	EE---DNTYR	CRNVAKLLYM	HMLGYPAHFG	QLECLKLIAS	QKFTDKRIGY	86
$\alpha$ adaptin	46	GDKALDGYSK	KKYVCKLLFI	FLLGHDIDFG	HMEAVNLLSS	NRYTEKQIGY	95
$\delta$ adaptin	49	QD---NIAVK	ANAVCKLTYL	QMLGYDISWA	AFNIIIEVMSA	SKFTFKRIGY	95
$\gamma$ adaptin	87	LGAMLLLDER	QDVHLLMTNC	IKNDLNHSTQ	FVQGLALCTL	GCMGSSEMCR	137
$\alpha$ adaptin	96	LFISVLVNSN	SELIRLINNA	IKNDLASRNP	TFMGLALHCI	ASVGSREMAE	145
$\delta$ adaptin	96	LAASQSFHEG	TDVIMLTTNQ	IRKDLSSPSQ	YDTGVALTGL	SCFVTPDLAR	145
$\gamma$ adaptin	138	DLAGEVEKLL	KTSN--SYLR	KKAALCAVHV	IRKVPPELMM	--FLPATKNL	183
$\alpha$ adaptin	146	AFAGEIPKVL	VAGDTMDSVK	QSAALCLLRL	YRTSPDLVPM	GDWTSRVVHL	195
$\delta$ adaptin	146	DLANDIMTLM	SHTK--PYIR	KKAVLIMYKV	FLKYPESLRP	--AFPRLKEK	191
$\gamma$ adaptin	184	LNEKNHGVLH	TSVVLLTEMC	ERSPDMLAHF	RKNEKLVQPQ	VRILKNLIMS	233
$\alpha$ adaptin	196	LNDQHLGVVT	AATSLITTLA	QKNPEEFKTS	VS--LAVSRL	SRIVTSASTD	243
$\delta$ adaptin	192	LEDPDPGVQS	AAVNVICELA	RRNPKNYLS-	-----LAPLF	FKLMTSSTNN	235
$\gamma$ adaptin	234	GYSPEHDVSG	ISDPFLQVRI	LRLLRILGRN	DDDSSEAMND	ILAQVATNTE	283
$\alpha$ adaptin	244	--LQDYTYFY	VPAPWLSVKL	LRLLCQYPPP	DPAVRGRLTE	CLETILNKAQ	291
$\delta$ adaptin	236	-----	----WVLIKI	IKLFGALTPL	EPRLGKKLIE	PLTNLIHSTS	272
$\gamma$ adaptin	284	TS-----	KNVGNAILYE	TVLTIIMDIK	ESGLRVLAIN	ILGRFLLNND	325
$\alpha$ adaptin	292	EPPKSKKVQH	SNAKNAVLFE	AISLIHHDS	EPNLLVRACN	QLGQFLQHRE	341
$\delta$ adaptin	273	AMS-----	LL YECVNTVIAV	LISLSSGMPN	HSASIQLCVQ	KLRILIEDSD	315
$\gamma$ adaptin	326	KNIRYVALT-	-SLLKTVQTD	HNAVQRHRST	IVDCLK-DLD	VSIKRRAMEL	372
$\alpha$ adaptin	342	TNLRYLALAS	MCTLASSEFS	HEAVKTHIET	VINALKTERD	VSVRQRAVDL	391
$\delta$ adaptin	316	QNLKYLGLL-	-AMSKILKTH	PKSVQSHKDL	ILQCLD-DKD	ESIRLRALDL	363
$\gamma$ adaptin	393	SFALVNGNNI	RGMKELLYF	LDSCE-PEFK	ADCASGIFLA	AEK----YAP	417
$\alpha$ adaptin	392	LYAMCDRSNA	PQIVAEMLSY	LETAD-YSIR	EEIVLKVAIL	AEK----YAV	436
$\delta$ adaptin	364	LYGMVSKKNL	MEIVKKLMT	VDKAEGTYR	DELLTKIIDI	CSQSNYQYIT	413

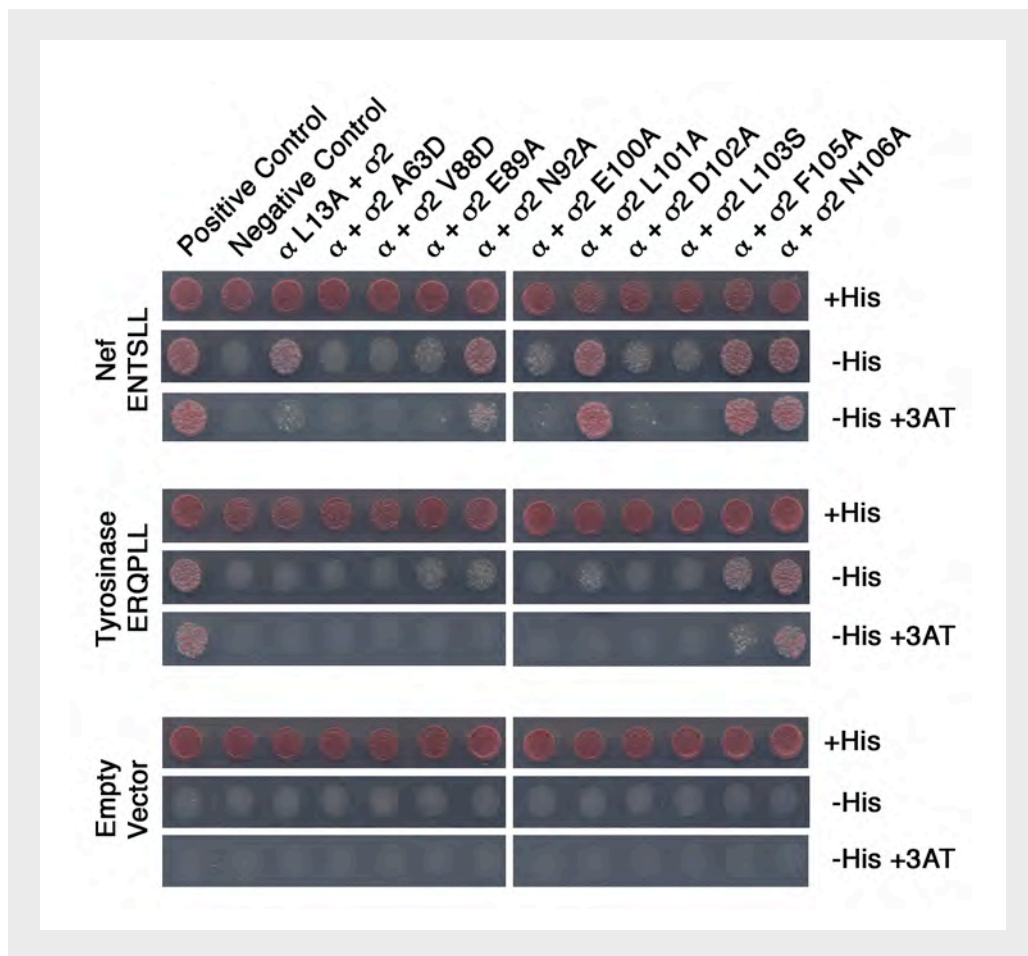
B

$\sigma 1$ adaptin	1	MMRFMLLFSR	QGKLRLOKWY	LATSDKERKK	MVRELMQVVL	ARKPKMCSFL	50
$\sigma 2$ adaptin	1	MIRFILIQRN	AGKTRLAKWY	MQFDDDEKQK	LIEEVHAVVT	VRDAKHTNFV	50
$\sigma 3$ adaptin	1	MIKAILIFNN	HGKPRLSKPY	QPYSEDTOQQ	IIRETFHLVS	KRDENVCNFL	50
$\sigma 1$ adaptin	51	EW-----	RD LKVVKRYAS	LYFCCAIEGQ	DNELITLELI	HRYVELLDKY	94
$\sigma 2$ adaptin	51	EF-----	RN FKIIYRRYAG	LYFCICVDVN	DNNLAYLEAI	HNF <sup>*</sup> EVV <sup>*</sup> NEY	94
$\sigma 3$ adaptin	51	EGLLIGGSD	NKLIYRHYAT	LYFVFCVDSS	ESELGILDLI	QVFVETLDKC	100
$\sigma 1$ adaptin	95	FGSVCELDII	FNFEKAYFIL	DEFLMGGDVQ	DTSKKSVLKA	IEQADLLQEE	144
$\sigma 2$ adaptin	95	FHNVC <sup>*</sup> ELDLV	F <sup>*</sup> WFYKVVTVV	DEMFLAGEIR	ETSQTKVLKQ	LLMLQSLE--	142
$\sigma 3$ adaptin	101	FENVCELDLI	FHVDKVHNIL	AEMVMGGMVL	ETNMNEIVTQ	IDAQNKLEKS	150
$\sigma 1$ adaptin	145	DE-----	S PRSVLEEMGL	A-----	-----	-----	158
$\sigma 2$ adaptin	N/A	-----	-----	-----	-----	-----	N/A
$\sigma 3$ adaptin	151	EAGLAGAPAR	AVSAVKMNL	PEIPRNINIG	DISIKVPLNP	SFK	193

**FIG. 6.8: Y3H analysis of the  $\alpha$ - $\sigma$ 2 residues potentially involved in binding the hydrophobic portion of dileucine motifs**

As described in the legend to Fig. 6.7, a small number of  $\alpha$ - $\sigma$ 2 residues were chosen, based on their physical proximity to  $\alpha$  R21 and their conservation among the related  $\gamma$ - $\sigma$ 1 and  $\delta$ - $\sigma$ 3 hemicomplexes, as candidates for binding the hydrophobic portion of dileucine-type sorting signals. These residues were then mutated to alanine, aspartate, or serine, and the resulting constructs were incorporated into the standard yeast three-hybrid assay. Each mutant was tested for loss of binding to wild-type Nef (ENTSLL) and wild-type tyrosinase (ERQPLL). An empty vector condition, in which neither Nef nor tyrosinase were expressed, was included as before (Fig. 6.4 and 6.5). Pairing the  $\alpha$ - $\sigma$ 2 mutants with empty vectors tests these constructs for self-activation, which may otherwise be interpreted as false-positives. In the top panel, the positive control shows the interaction between Nef ENTSLL and wild-type  $\alpha$ - $\sigma$ 2, while the negative control represents the interaction between Nef ENTSA A (i.e., Nef LL164,165AA) and wild-type  $\alpha$ - $\sigma$ 2. Similar positive and negative controls were used for the middle panel, but tyrosinase ERQPLL was substituted for Nef ETNSLL, and tyrosinase ERQPAA (i.e., tyrosinase LL517,518AA) was substituted for Nef ENTSA A. Unlike the Y3H assays shown earlier in this chapter, the positive control for the bottom (empty vector) panel was a combination of  $\alpha$ - $\sigma$ 2 with empty pBridge, while the negative control combined empty pGADT7 and empty pBridge (these controls were included to rule out spurious growth that might have been caused by the vector backbones). Mutation of several  $\sigma$ 2 residues (particularly A63, V88, and L103) inhibited binding with Nef and tyrosinase, suggesting that these amino acids either interact with the dileucine moiety directly, or are adjacent to the dileucine binding site. Mutation of several other  $\sigma$ 2 residues (such as E89, E100, and D102) also impair binding with Nef and tyrosinase, although to a somewhat lesser degree. In general, binding of tyrosinase to  $\alpha$ - $\sigma$ 2 was more sensitive to mutations of the hemicomplex than Nef. This might be due to subtle differences in their respective dileucine binding sites, or the greater overall affinity of Nef for AP-2 (as demonstrated in Fig. 5.2).

FIG. 6.8



occluded by the N-terminus of the  $\beta 2$  subunit (Fig. 6.9; Collins et al., 2002). Thus, in order for these  $\sigma 2$  residues to participate in the binding of dileucine signals, the AP-2 core would have to undergo a conformational change. Such a rearrangement might be triggered by phosphorylation of the  $\beta 2$  N-terminus, which has previously been shown to promote the internalization of proteins containing dileucine sorting signals from the cell-surface (see Huang et al., 2003). Additional experiments will be needed to verify that the  $\sigma 2$  residues identified here bind dileucine signals. These experiments could be variations of the GST pull-downs and RNAi rescue assays described earlier (Fig. 5.5 and 5.6). Much more information, though, would be provided by a crystal structure of the AP-2 core bound to a dileucine ligand.

Several months after completion of the yeast three-hybrid assays, the crystal structure of AP-2 in complex with a phosphorylated version of the CD4 dileucine sorting signal was solved and published (Kelly et al., 2009; see Section 1.3 for a brief description of CD4 phosphorylation and endocytosis). This crystal structure confirmed many of the observations made using the yeast three-hybrid system, including the role of  $\alpha$  R21 in binding the acidic portion of dileucine motifs, and the role of  $\sigma 2$  V88 and  $\sigma 2$  L103 in binding the hydrophobic portion (Fig. 6.10; Kelly et al., 2009). Four other  $\sigma 2$  residues were considered to be candidates for interacting with the leucine moiety, based on the results of the yeast experiments (Fig. 6.8). The crystal structure showed that most of these residues were adjacent to the dileucine binding site; their mutation in the yeast assay may have prevented the Nef and tyrosinase dileucine motifs from accessing the appropriate contact points on  $\sigma 2$  and caused loss of binding. The crystal structure also showed that the AP-2 core must undergo a significant conformational change in order to accommodate dileucine ligands, with the N-terminus of  $\beta 2$  shifting so as to expose the binding site on  $\sigma 2$  (Kelly et al., 2009). A comparison of the yeast three-hybrid and structural data indicates that there are subtle differences in the specific binding sites of each dileucine motif. In particular,  $\sigma 2$  L101 appears to be important for binding CD4 and tyrosinase, but is not required for binding Nef (Fig. 6.8; Kelly et al., 2009). Thus, the residues in dileucine motifs that separate the acidic and hydrophobic moieties (i.e., the xxx residues in the [D/E]xxxL[L/I] consensus sequence) most likely interact with slightly different regions of  $\sigma 2$ . This may explain why each dileucine signal binds to AP-2 with a unique affinity (Fig. 4.6). Despite these differences, the dileucine motifs

**FIG. 6.9: Location of the prospective Nef dileucine binding site on the structure of AP-2**

(A) Ribbon diagram of the  $\alpha$ - $\sigma$ 2 hemicomplex (PDB ID numbers 1GW5 and 2VGL [Collins et al., 2002]) with the locations of the  $\sigma$ 2 A63,  $\sigma$ 2 V88, and  $\sigma$ 2 L103 amino acids highlighted in orange. For the sake of clarity, only the  $\alpha$  and  $\sigma$ 2 subunits of the AP-2 core are shown in this panel; the  $\alpha$  subunit is colored in dark blue, while the  $\sigma$ 2 subunit is shaded in gold. The  $\alpha$  R21,  $\alpha$  K297, and  $\alpha$  R340 residues are highlighted in red, and included here as points of reference. Given the location of all these residues, Nef probably binds across the  $\alpha$ - $\sigma$ 2 hemicomplex, with Nef E160 binding  $\alpha$  R21; Nef LL 164,165 binding  $\sigma$ 2 L103,  $\sigma$ 2 V88, and  $\sigma$ 2 A63; and Nef DD174,175 binding  $\alpha$  K297 and  $\alpha$  R340. This arrangement may explain why the binding of Nef to AP-2 requires both the  $\alpha$  and  $\sigma$ 2 subunits (Janvier et al., 2003b).

(B) Surface representation of the unbound AP-2 core complex (PDB numbers 1GW5 and 2VGL [Collins et al., 2002]), with the  $\alpha$ ,  $\beta$ 2,  $\mu$ 2, and  $\sigma$ 2 subunits colored in dark blue, green, magenta, and gold, respectively. The positions of  $\alpha$  R21,  $\alpha$  K297, and  $\alpha$  R340 are colored in red. In this conformation, the Nef dileucine binding site on  $\alpha$ - $\sigma$ 2 is occluded by the N-terminus of  $\beta$ 2. Thus, for Nef to interact with AP-2, the adaptin core must undergo a conformational shift.

FIG. 6.9

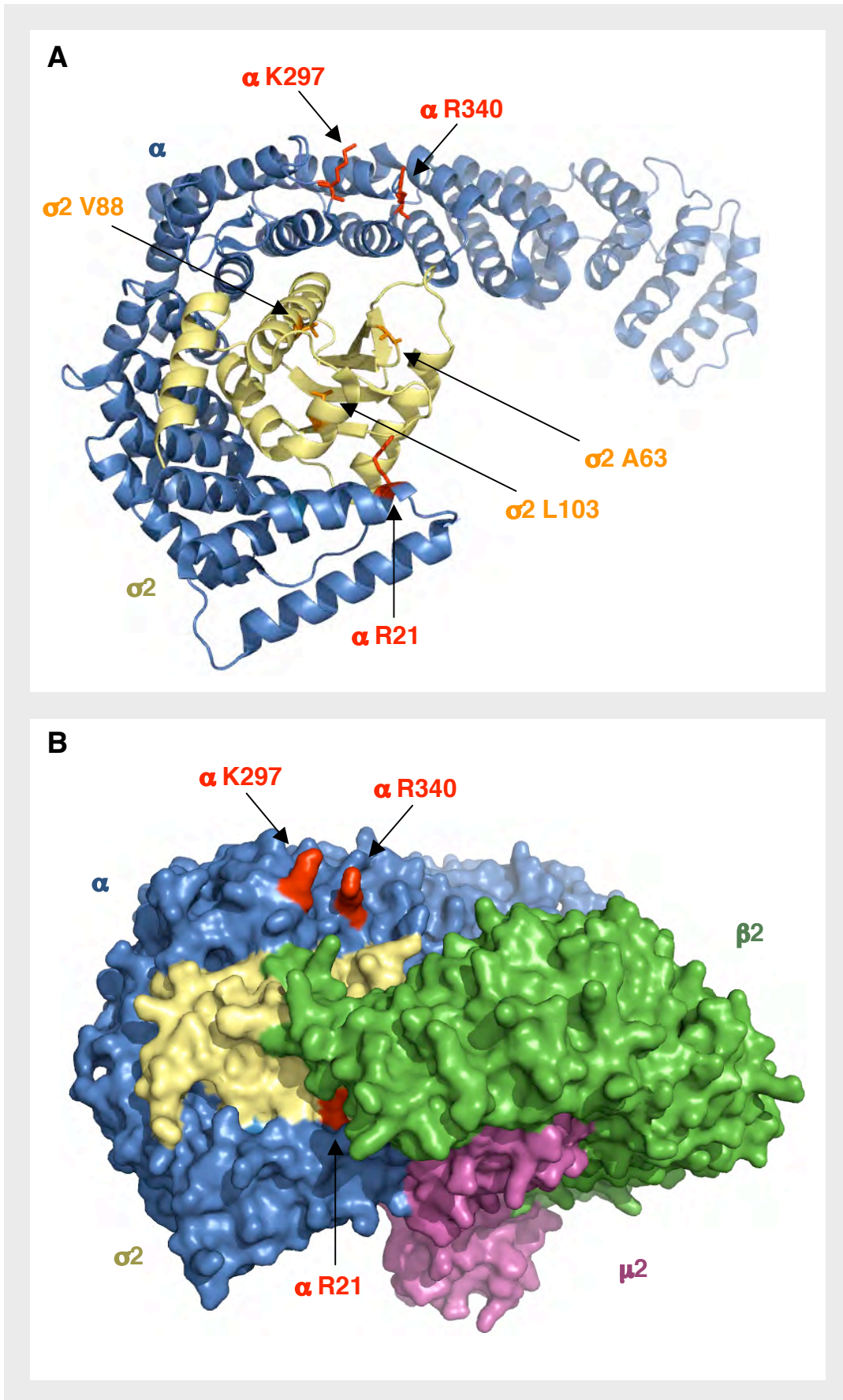


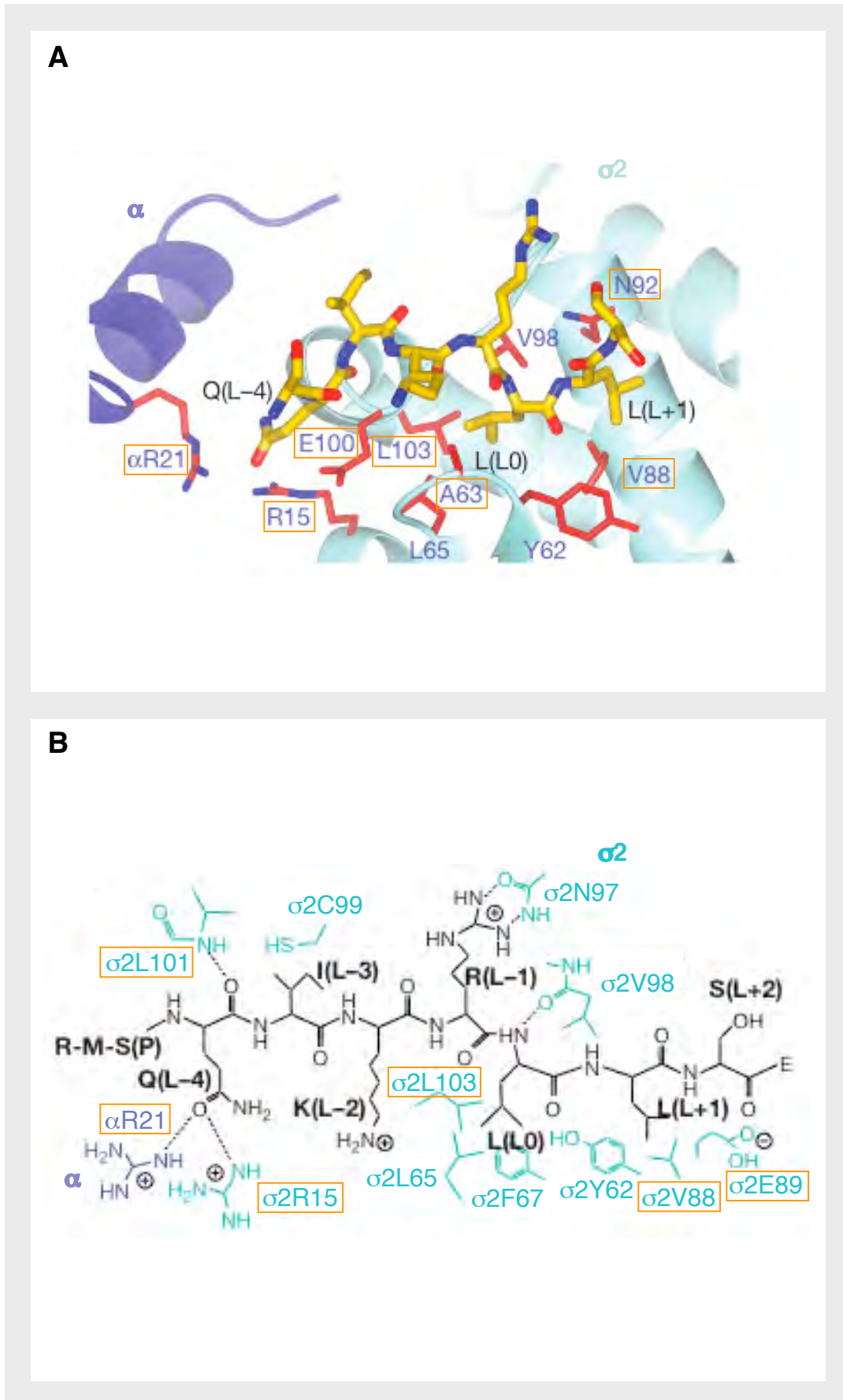
**FIG. 6.10: Location of the CD4 dileucine binding site on AP-2**

The three-dimensional crystal structure of the AP-2 core bound to the CD4 dileucine signal (pSQIKRLLS) was recently solved and published (PDB ID number 2JKR and 2JKT [Kelly et al., 2008]). The images shown here are taken from this publication. In both panels, the  $\alpha$  subunit is colored **dark blue**, while the  $\sigma 2$  subunit is shaded **light blue**. Residues that were mutated during the course of the yeast three-hybrid assays (see Fig. 6.4, 6.5, and 6.8) are surrounded by **orange** boxes.

**(A)** Ribbon diagram of the AP-2 core in complex with the CD4 dileucine peptide. For the sake of clarity, only the relevant portions of the  $\alpha$  and  $\sigma 2$  subunits are shown. The side chains of the CD4 residues are depicted in **yellow**, while the side chains of the  $\alpha$ - $\sigma 2$  residues are colored **red**.

**(B)** Schematic representation of the  $\alpha$ - $\sigma 2$  residues that participate in binding the CD4 dileucine peptide. In this diagram, the color conventions for the  $\alpha$  and  $\sigma 2$  subunits are maintained, but the CD4 residues are shown in **black**.

FIG. 6.10



Crystal structure from Kelly et al., 2008

of CD4 and Nef seem to interact with the same general region of  $\sigma_2$ , which suggests that only one of these sorting signals makes contact with AP-2 in the CD4-Nef-AP-2 tripartite complex. A tempting model that fits this description has the CD4 dileucine motif binding to the Nef hydrophobic pocket, and the Nef dileucine motif binding to  $\alpha$ - $\sigma_2$  (see Section 5.4). However, this is only one possibility, and careful biochemical and structural studies will be needed to determine the exact configuration of the CD4-Nef-AP-2 complex.

## **6.4 Future Work**

While the work presented in this thesis has firmly established the role of AP-2 in the Nef-mediated downregulation of CD4, several related topics remain to be explored. In light of the direct binding between Nef and AP-2 shown here, a natural extension of this thesis would be to investigate the effect of this interaction on other receptors. This line of study should focus on cell-surface proteins that contain dileucine-based sorting signals, as the binding of Nef to AP-2 might disrupt their endocytosis from the plasma membrane. Another subject that deserves greater attention is the postendocytic fate of CD4 itself. These topics will be discussed in more detail below.

### **6.4.1 The effect of Nef-AP-2 binding on surface receptor expression**

The robust binding of Nef to AP-2, via its dileucine and diacidic motifs (Fig. 3.8, 3.9, 4.1, and 4.2), allows the viral protein to downregulate CD4 (Fig. 3.3, 3.4, 4.4, 4.5, and 5.6). Interestingly, this interaction may also be responsible for the differential effects that Nef has several on other cell-surface receptors, including CD8, CD28, DC-SIGN, Ii, LIGHT, and TNF (see Section 1.4). Nef has been shown to downregulate CD8 and CD28 by increasing the rate at which these receptors are internalized from the plasma membrane (see Fig. 1.8; Stove et al., 2005; Swigut et al., 2001). Mutation of either the dileucine or diacidic motif prevents Nef from executing these functions (Stove et al., 2005), suggesting that like CD4, the downregulation of CD8 and CD28 depends on an interaction between Nef and AP-2.

Separately, Nef has also been shown to upregulate the expression of DC-SIGN, TNF, Ii, and LIGHT on the cell-surface by slowing their normal rate of endocytosis (Lama and Ware, 2000; Schindler et al., 2003; Sol-Foulon et al., 2002; Stumpner-Cuvelette et al., 2001). All four of these receptors contain dileucine-type sorting signals in their cytosolic domains, and in the absence of Nef, are internalized in an AP-2-dependent manner (Dugast et al., 2005; Engering et al., 2002; McCormick et al., 2005; Mitchell et al., 2008; Sol-Foulon et al., 2002). Upregulation of each receptor requires an intact Nef dileucine motif (see Coleman et al., 2006; Lama and Ware, 2000; Mitchell et al., 2008; Schindler et al., 2003; Sol-Foulon et al., 2002; Stumpner-Culvette et al., 2001), which also suggests that these processes depend on the interaction between Nef and AP-2.

The results described above have created an apparent contradiction: while the binding of Nef and AP-2 probably causes the downregulation of some surface receptors (such as CD4, CD8, and CD28), it may also cause the upregulation of other proteins located on the plasma membrane (like DC-SIGN, TNF, Ii, and LIGHT). In order to reconcile these findings, a new model of Nef activity at the cell-surface has been proposed (see Mitchell et al., 2008). According to this model, Nef binds AP-2 with a higher affinity than any of the aforementioned receptors, which effectively blocks their access to the dileucine binding site and disrupts their usual interaction with the cellular endocytic machinery. Downregulation would occur when Nef binds to a receptor and traps it in a clathrin-coated pit. On the other hand, upregulation would occur when Nef does not bind the receptor; because these proteins are unable to undergo either normal or Nef-induced endocytosis, they will accumulate on the plasma membrane. Support for this model is drawn from a variety of sources, including: the observation that all affected receptors have canonical dileucine sorting signals, or variations thereof; a requirement for the Nef dileucine motif, as described above; and the direct binding of Nef to AP-2, which was observed here for the first time (Fig. 3.8, 3.9, 4.2, and 5.5).

Before this model can be validated, at least two of its predictions must be tested. First, it will be necessary to show that Nef connects both CD8 and CD28 to AP-2. For this purpose, yeast four-hybrid assays could be used to determine whether Nef promotes the formation of CD8-Nef-AP-2 and CD28-Nef-AP-2 complexes. Downregulation of CD8 and CD28 requires the same motifs on Nef as the downregulation of CD4 (Stove et al., 2005; Swigut et al., 2001), suggesting that these processes are highly similar, if not identical. Second, it will be important to show that Nef only affects the expression of receptors which contain dileucine signals weaker than its own. Consistent with this prediction, Nef has been observed to alter the surface-expression of a limited number of receptors (Fig. 1.8). The AP-2 binding assays developed during the course of this work (Fig. 3.8, 3.9, and 4.2) should now make it possible to test whether Nef does, in fact, bind AP-2 with greater affinity than these receptors. The outcome of such assays will do much to explain the activity of Nef at the cell-surface.

#### **6.4.2 Postendocytic fate of CD4**

Nef uses AP-2 to transport CD4, and possibly a small number of other receptors, from the plasma membrane to endosomes (Fig. 3.7, 4.4, 4.5, 5.6, and 5.7). Nef then directs

CD4 to lysosomes, where the receptor is degraded (Rhee and Marsh, 1994). However, the intracellular pathway used by Nef to transfer CD4 from endosomes to lysosomes is poorly characterized, and remains controversial. Some groups have suggested that this process depends on an interaction between Nef and the COPI complex (Piguet et al., 1999; Schaefer et al., 2008), which has been reported to participate in endosomal sorting events (Aniento et al., 1996; Daro et al., 1997). The RNAi-mediated silencing of COPI expression appears to partially inhibit CD4 downregulation (Schaefer et al., 2008; Fig 3.5), but this treatment probably affects a wide variety of cellular functions, making it difficult to specifically attribute CD4 downregulation to COPI activity. In addition, mutation of the COPI binding site on Nef does not prevent CD4 degradation (Janvier et al., 2001; Schaefer et al., 2008), indicating that Nef likely uses a different pathway to target CD4 to lysosomes. Many receptors are directed towards lysosomes via the MVB pathway, which usually involves the attachment of ubiquitin to a transmembrane protein and its subsequent recognition by the ESCRT machinery (reviewed by Piper and Katzman, 2007). Both Nef and CD4 are ubiquitinated on multiple lysine residues (da Silva et al., 2009; Jin et al., 2008), but these modifications do not appear to be important for downregulation of the receptor (da Silva et al., 2009). Transport of CD4 from endosomes to lysosomes, however, was found to require components of the ESCRT machinery (da Silva et al., 2009). Thus, the Nef-mediated downregulation of CD4 might be a new example of the small number of cargo proteins which are sorted to the MVB pathway in an ESCRT-dependent, but ubiquitin-independent manner (see Hislop et al., 2004; Yamashita et al., 2008; Watson and Bonifacino, 2007). Given the uncertainty surrounding the final stages of CD4 downregulation, it will be necessary to perform additional experiments to determine the precise mechanism used by Nef to drive CD4 towards lysosomes.

## **6.5 Concluding remarks**

The primary goal of this thesis was to determine whether Nef downregulates CD4 via an accelerated endocytosis or intracellular retention pathway (please refer to Section 1.9). The data presented here uniformly supports the accelerated endocytosis model, whereby Nef increases the rate of CD4 internalization by linking the cytosolic tail of the receptor to AP-2. These findings (published in Chaudhuri et al., 2007; Chaudhuri et al., 2009; Lindwasser et al., 2008) have led to a general agreement within the field on the mechanism of Nef-mediated CD4 downregulation (da Silva et al., 2009; Foster and Garcia, 2008; Schaefer et al., 2008; Toussaint et al., 2008).

In the absence of an effective HIV-1 vaccine, some scientists have concluded that the inhibition of CD4 downregulation is the most promising strategy for combating AIDS (Foster and Garcia, 2008; Watkins et al., 2008). The discovery of AP-2 as an essential component of Nef-induced CD4 downregulation, and the subsequent identification of specific residues required for the interaction between Nef and AP-2, has created new opportunities for the development of antiviral agents. Indeed, the results of this thesis may now allow for the rational design of a drug that can block the binding of Nef and AP-2, prevent the downregulation of CD4, and – hopefully – moderate the pathogenic effects of Nef.

## References

- Agaisse, H., Burrack, L. S., Philips, J. A., Rubin, E. J., Perrimon, N., and Higgins, D. E. (2005). Genome-wide RNAi screen for host factors required for intracellular bacterial infection. *Science* 309, 1248-1251.
- Aguilar, R. C., Boehm, M., Gorshkova, I., Crouch, R. J., Tomita, K., Saito, T., Ohno, H., and Bonifacino, J. S. (2001). Signal-binding specificity of the mu4 subunit of the adaptor protein complex AP-4. *J Biol Chem* 276, 13145-13152.
- Ahle, S., Mann, A., Eichelsbacher, U., and Ungewickell, E. (1988). Structural relationships between clathrin assembly proteins from the Golgi and the plasma membrane. *Embo J* 7, 919-929.
- Ahmad, N., and Venkatesan, S. (1988). Nef protein of HIV-1 is a transcriptional repressor of HIV-1 LTR. *Science* 241, 1481-1485.
- Aiken, C., Konner, J., Landau, N. R., Lenburg, M. E., and Trono, D. (1994). Nef induces CD4 endocytosis: requirement for a critical dileucine motif in the membrane-proximal CD4 cytoplasmic domain. *Cell* 76, 853-864.
- Aiken, C., Krause, L., Chen, Y. L., and Trono, D. (1996). Mutational analysis of HIV-1 Nef: identification of two mutants that are temperature-sensitive for CD4 downregulation. *Virology* 217, 293-300.
- Aldrovandi, G. M., Feuer, G., Gao, L., Jamieson, B., Kristeva, M., Chen, I. S., and Zack, J. A. (1993). The SCID-hu mouse as a model for HIV-1 infection. *Nature* 363, 732-736.
- Aldrovandi, G. M., Gao, L., Bristol, G., and Zack, J. A. (1998). Regions of human immunodeficiency virus type 1 nef required for function in vivo. *J Virol* 72, 7032-7039.
- Alkhatib, G., Combadiere, C., Broder, C. C., Feng, Y., Kennedy, P. E., Murphy, P. M., and Berger, E. A. (1996). CC CKR5: a RANTES, MIP-1alpha, MIP-1beta receptor as a fusion cofactor for macrophage-tropic HIV-1. *Science* 272, 1955-1958.
- Allan, J. S., Coligan, J. E., Lee, T. H., McLane, M. F., Kanki, P. J., Groopman, J. E., and Essex, M. (1985). A new HTLV-III/LAV encoded antigen detected by antibodies from AIDS patients. *Science* 230, 810-813.
- Anderson, R. G., Brown, M. S., and Goldstein, J. L. (1977a). Role of the coated endocytic vesicle in the uptake of receptor-bound low density lipoprotein in human fibroblasts. *Cell* 10, 351-364.
- Anderson, R. G., Goldstein, J. L., and Brown, M. S. (1977b). A mutation that impairs the ability of lipoprotein receptors to localise in coated pits on the cell surface of human fibroblasts. *Nature* 270, 695-699.

Anderson, S. J., Lenburg, M., Landau, N. R., and Garcia, J. V. (1994). The cytoplasmic domain of CD4 is sufficient for its down-regulation from the cell surface by human immunodeficiency virus type 1 Nef. *J Virol* 68, 3092-3101.

Aniento, F., Gu, F., Parton, R. G., and Gruenberg, J. (1996). An endosomal beta COP is involved in the pH-dependent formation of transport vesicles destined for late endosomes. *J Cell Biol* 133, 29-41.

Arganaraz, E. R., Schindler, M., Kirchhoff, F., Cortes, M. J., and Lama, J. (2003). Enhanced CD4 down-modulation by late stage HIV-1 nef alleles is associated with increased Env incorporation and viral replication. *J Biol Chem* 278, 33912-33919.

Arold, S., Franken, P., Strub, M. P., Hoh, F., Benichou, S., Benarous, R., and Dumas, C. (1997). The crystal structure of HIV-1 Nef protein bound to the Fyn kinase SH3 domain suggests a role for this complex in altered T cell receptor signaling. *Structure* 5, 1361-1372.

Arora, V. K., Fredericksen, B. L., and Garcia, J. V. (2002). Nef: agent of cell subversion. *Microbes Infect* 4, 189-199.

Arya, S. K., and Gallo, R. C. (1986). Three novel genes of human T-lymphotropic virus type III: immune reactivity of their products with sera from acquired immune deficiency syndrome patients. *Proc Natl Acad Sci U S A* 83, 2209-2213.

Backer, J. M., Mendola, C. E., Fairhurst, J. L., and Kovesdi, I. (1991). The HIV-1 nef protein does not have guanine nucleotide binding, GTPase, or autophosphorylating activities. *AIDS Res Hum Retroviruses* 7, 1015-1020.

Ball, C. L., Hunt, S. P., and Robinson, M. S. (1995). Expression and localization of alpha-adaptin isoforms. *J Cell Sci* 108 ( Pt 8), 2865-2875.

Bandres, J. C., Shaw, A. S., and Ratner, L. (1995). HIV-1 Nef protein downregulation of CD4 surface expression: relevance of the lck binding domain of CD4. *Virology* 207, 338-341.

Barin, F., M'Boup, S., Denis, F., Kanki, P., Allan, J. S., Lee, T. H., and Essex, M. (1985). Serological evidence for virus related to simian T-lymphotropic retrovirus III in residents of west Africa. *Lancet* 2, 1387-1389.

Barlowe, C. (2003). Signals for COPII-dependent export from the ER: what's the ticket out? *Trends Cell Biol* 13, 295-300.

Barre-Sinoussi, F., Chermann, J. C., Rey, F., Nugeyre, M. T., Chamaret, S., Gruest, J., Dautet, C., Axler-Blin, C., Vezinet-Brun, F., Rouzioux, C., et al. (1983). Isolation of a T-lymphotropic retrovirus from a patient at risk for acquired immune deficiency syndrome (AIDS). *Science* 220, 868-871.

Benichou, S., Bomsel, M., Bodeus, M., Durand, H., Doute, M., Letourneur, F., Camonis, J., and Benarous, R. (1994). Physical interaction of the HIV-1 Nef protein

with beta-COP, a component of non-clathrin-coated vesicles essential for membrane traffic. *J Biol Chem* 269, 30073-30076.

Benson, R. E., Sanfridson, A., Ottinger, J. S., Doyle, C., and Cullen, B. R. (1993). Downregulation of cell-surface CD4 expression by simian immunodeficiency virus Nef prevents viral super infection. *J Exp Med* 177, 1561-1566.

Bentham, M., Mazaleyrat, S., and Harris, M. (2003). The di-leucine motif in the cytoplasmic tail of CD4 is not required for binding to human immunodeficiency virus type 1 Nef, but is critical for CD4 down-modulation. *J Gen Virol* 84, 2705-2713.

Bentham, M., Mazaleyrat, S., and Harris, M. (2006). Role of myristoylation and N-terminal basic residues in membrane association of the human immunodeficiency virus type 1 Nef protein. *J Gen Virol* 87, 563-571.

Bergeron, L., and Sodroski, J. (1992). Dissociation of unintegrated viral DNA accumulation from single-cell lysis induced by human immunodeficiency virus type 1. *J Virol* 66, 5777-5787.

Berkhout, B., Gatignol, A., Rabson, A. B., and Jeang, K. T. (1990). TAR-independent activation of the HIV-1 LTR: evidence that tat requires specific regions of the promoter. *Cell* 62, 757-767.

Bijlmakers, M. J., and Marsh, M. (1999). Trafficking of an acylated cytosolic protein: newly synthesized p56(lck) travels to the plasma membrane via the exocytic pathway. *J Cell Biol* 145, 457-468.

Birch, M. R., Learmont, J. C., Dyer, W. B., Deacon, N. J., Zaunders, J. J., Saksena, N., Cunningham, A. L., Mills, J., and Sullivan, J. S. (2001). An examination of signs of disease progression in survivors of the Sydney Blood Bank Cohort (SBBC). *J Clin Virol* 22, 263-270.

Blagoveshchenskaya, A. D., Thomas, L., Feliciangeli, S. F., Hung, C. H., and Thomas, G. (2002). HIV-1 Nef downregulates MHC-I by a PACS-1- and PI3K-regulated ARF6 endocytic pathway. *Cell* 111, 853-866.

Boehm, M., and Bonifacino, J. S. (2001). Adaptins: the final recount. *Mol Biol Cell* 12, 2907-2920.

Boll, W., Ohno, H., Songyang, Z., Rapoport, I., Cantley, L. C., Bonifacino, J. S., and Kirchhausen, T. (1996). Sequence requirements for the recognition of tyrosine-based endocytic signals by clathrin AP-2 complexes. *Embo J* 15, 5789-5795.

Bonavida, B., Katz, J., and Gottlieb, M. (1986). Mechanism of defective NK cell activity in patients with acquired immunodeficiency syndrome (AIDS) and AIDS-related complex. I. Defective trigger on NK cells for NKCF production by target cells, and partial restoration by IL 2. *J Immunol* 137, 1157-1163.

Bonifacino, J. S., and Lippincott-Schwartz, J. (2003). Coat proteins: shaping membrane transport. *Nat Rev Mol Cell Biol* 4, 409-414.

- Bonifacino, J. S., and Traub, L. M. (2003). Signals for sorting of transmembrane proteins to endosomes and lysosomes. *Annu Rev Biochem* 72, 395-447.
- Bonyhadi, M. L., Rabin, L., Salimi, S., Brown, D. A., Kosek, J., McCune, J. M., and Kaneshima, H. (1993). HIV induces thymus depletion in vivo. *Nature* 363, 728-732.
- Borner, G. H., Harbour, M., Hester, S., Lilley, K. S., and Robinson, M. S. (2006). Comparative proteomics of clathrin-coated vesicles. *J Cell Biol* 175, 571-578.
- Bour, S., Perrin, C., and Strebel, K. (1999). Cell surface CD4 inhibits HIV-1 particle release by interfering with Vpu activity. *J Biol Chem* 274, 33800-33806.
- Bowers, K., Pitcher, C., and Marsh, M. (1997). CD4: a co-receptor in the immune response and HIV infection. *Int J Biochem Cell Biol* 29, 871-875.
- Bradley, L. M., Croft, M., and Swain, S. L. (1993). T-cell memory: new perspectives. *Immunol Today* 14, 197-199.
- Brady, H. J., Pennington, D. J., Miles, C. G., and Dzierzak, E. A. (1993). CD4 cell surface downregulation in HIV-1 Nef transgenic mice is a consequence of intracellular sequestration. *Embo J* 12, 4923-4932.
- Bremnes, T., Lauvrak, V., Lindqvist, B., and Bakke, O. (1998). A region from the medium chain adaptor subunit ( $\mu$ ) recognizes leucine- and tyrosine-based sorting signals. *J Biol Chem* 273, 8638-8645.
- Bresnahan, P. A., Yonemoto, W., Ferrell, S., Williams-Herman, D., Geleziunas, R., and Greene, W. C. (1998). A dileucine motif in HIV-1 Nef acts as an internalization signal for CD4 downregulation and binds the AP-1 clathrin adaptor. *Curr Biol* 8, 1235-1238.
- Brett, T. J., Traub, L. M., and Fremont, D. H. (2002). Accessory protein recruitment motifs in clathrin-mediated endocytosis. *Structure* 10, 797-809.
- Brown, M. S., and Goldstein, J. L. (1979). Receptor-mediated endocytosis: insights from the lipoprotein receptor system. *Proc Natl Acad Sci U S A* 76, 3330-3337.
- Burtey, A., Rappoport, J. Z., Bouchet, J., Basmaciogullari, S., Guatelli, J., Simon, S. M., Benichou, S., and Benmerah, A. (2007). Dynamic interaction of HIV-1 Nef with the clathrin-mediated endocytic pathway at the plasma membrane. *Traffic* 8, 61-76.
- Bushman, F. D., Fujiwara, T., and Craigie, R. (1990). Retroviral DNA integration directed by HIV integration protein in vitro. *Science* 249, 1555-1558.
- Cammarota, G., Scheirle, A., Takacs, B., Doran, D. M., Knorr, R., Bannwarth, W., Guardiola, J., and Sinigaglia, F. (1992). Identification of a CD4 binding site on the beta 2 domain of HLA-DR molecules. *Nature* 356, 799-801.
- Canfield, W. M., Johnson, K. F., Ye, R. D., Gregory, W., and Kornfeld, S. (1991). Localization of the signal for rapid internalization of the bovine cation-independent

mannose 6-phosphate/insulin-like growth factor-II receptor to amino acids 24-29 of the cytoplasmic tail. *J Biol Chem* 266, 5682-5688.

Cao, Y., Qin, L., Zhang, L., Safrit, J., and Ho, D. D. (1995). Virologic and immunologic characterization of long-term survivors of human immunodeficiency virus type 1 infection. *N Engl J Med* 332, 201-208.

Carl, S., Daniels, R., Iafrate, A. J., Easterbrook, P., Greenough, T. C., Skowronski, J., and Kirchhoff, F. (2000). Partial "repair" of defective NEF genes in a long-term nonprogressor with human immunodeficiency virus type 1 infection. *J Infect Dis* 181, 132-140.

Chan, A. C., Iwashima, M., Turck, C. W., and Weiss, A. (1992). ZAP-70: a 70 kd protein-tyrosine kinase that associates with the TCR zeta chain. *Cell* 71, 649-662.

Chan, D. C., Fass, D., Berger, J. M., and Kim, P. S. (1997). Core structure of gp41 from the HIV envelope glycoprotein. *Cell* 89, 263-273.

Chang, M. P., Mallet, W. G., Mostov, K. E., and Brodsky, F. M. (1993). Adaptor self-aggregation, adaptor-receptor recognition and binding of alpha-adaptin subunits to the plasma membrane contribute to recruitment of adaptor (AP2) components of clathrin-coated pits. *Embo J* 12, 2169-2180.

Chaudhry, A., Das, S. R., Hussain, A., Mayor, S., George, A., Bal, V., Jameel, S., and Rath, S. (2005). The Nef protein of HIV-1 induces loss of cell surface costimulatory molecules CD80 and CD86 in APCs. *J Immunol* 175, 4566-4574.

Chaudhuri, R., Lindwasser, O. W., Smith, W. J., Hurley, J. H., and Bonifacino, J. S. (2007). Downregulation of CD4 by human immunodeficiency virus type 1 Nef is dependent on clathrin and involves direct interaction of Nef with the AP2 clathrin adaptor. *J Virol* 81, 3877-3890.

Chaudhuri, R., Mattera, R., Lindwasser, O. W., Robinson, M. S., and Bonifacino, J. S. (2009). A basic patch on alpha-adaptin is required for binding of human immunodeficiency virus type 1 Nef and cooperative assembly of a CD4-Nef-AP-2 complex. *J Virol* 83, 2518-2530.

Chen, B. K., Gandhi, R. T., and Baltimore, D. (1996). CD4 down-modulation during infection of human T cells with human immunodeficiency virus type 1 involves independent activities of vpu, env, and nef. *J Virol* 70, 6044-6053.

Cho, S., Knox, K. S., Kohli, L. M., He, J. J., Exley, M. A., Wilson, S. B., and Brutkiewicz, R. R. (2005). Impaired cell surface expression of human CD1d by the formation of an HIV-1 Nef/CD1d complex. *Virology* 337, 242-252.

Chun, T. W., Carruth, L., Finzi, D., Shen, X., DiGiuseppe, J. A., Taylor, H., Hermankova, M., Chadwick, K., Margolick, J., Quinn, T. C., et al. (1997). Quantification of latent tissue reservoirs and total body viral load in HIV-1 infection. *Nature* 387, 183-188.

Clavel, F., Hoggan, M. D., Willey, R. L., Strebel, K., Martin, M. A., and Repaske, R. (1989). Genetic recombination of human immunodeficiency virus. *J Virol* 63, 1455-1459.

Cluet, D., Bertsch, C., Beyer, C., Gloeckler, L., Erhardt, M., Gut, J. P., Galzi, J. L., and Aubertin, A. M. (2005). Detection of human immunodeficiency virus type 1 Nef and CD4 physical interaction in living human cells by using bioluminescence resonance energy transfer. *J Virol* 79, 8629-8636.

Coates, K., Cooke, S. J., Mann, D. A., and Harris, M. P. (1997). Protein kinase C-mediated phosphorylation of HIV-1 nef in human cell lines. *J Biol Chem* 272, 12289-12294.

Coates, K., and Harris, M. (1995). The human immunodeficiency virus type 1 Nef protein functions as a protein kinase C substrate in vitro. *J Gen Virol* 76 ( Pt 4), 837-844.

Cohen, G. B., Gandhi, R. T., Davis, D. M., Mandelboim, O., Chen, B. K., Strominger, J. L., and Baltimore, D. (1999). The selective downregulation of class I major histocompatibility complex proteins by HIV-1 protects HIV-infected cells from NK cells. *Immunity* 10, 661-671.

Coleman, S. H., Madrid, R., Van Damme, N., Mitchell, R. S., Bouchet, J., Servant, C., Pillai, S., Benichou, S., and Guatelli, J. C. (2006). Modulation of cellular protein trafficking by human immunodeficiency virus type 1 Nef: role of the acidic residue in the ExxxLL motif. *J Virol* 80, 1837-1849.

Coleman, S. H., Van Damme, N., Day, J. R., Noviello, C. M., Hitchin, D., Madrid, R., Benichou, S., and Guatelli, J. C. (2005). Leucine-specific, functional interactions between human immunodeficiency virus type 1 Nef and adaptor protein complexes. *J Virol* 79, 2066-2078.

Collins, B. M., McCoy, A. J., Kent, H. M., Evans, P. R., and Owen, D. J. (2002). Molecular architecture and functional model of the endocytic AP2 complex. *Cell* 109, 523-535.

Collins, K. L., Chen, B. K., Kalams, S. A., Walker, B. D., and Baltimore, D. (1998). HIV-1 Nef protein protects infected primary cells against killing by cytotoxic T lymphocytes. *Nature* 391, 397-401.

Cortes, M. J., Wong-Staal, F., and Lama, J. (2002). Cell surface CD4 interferes with the infectivity of HIV-1 particles released from T cells. *J Biol Chem* 277, 1770-1779.

Cowles, C. R., Odorizzi, G., Payne, G. S., and Emr, S. D. (1997). The AP-3 adaptor complex is essential for cargo-selective transport to the yeast vacuole. *Cell* 91, 109-118.

Craig, H. M., Pandori, M. W., and Guatelli, J. C. (1998). Interaction of HIV-1 Nef with the cellular dileucine-based sorting pathway is required for CD4 down-regulation and optimal viral infectivity. *Proc Natl Acad Sci U S A* 95, 11229-11234.

- Craig, H. M., Reddy, T. R., Riggs, N. L., Dao, P. P., and Guatelli, J. C. (2000). Interactions of HIV-1 nef with the mu subunits of adaptor protein complexes 1, 2, and 3: role of the dileucine-based sorting motif. *Virology* 271, 9-17.
- Crise, B., and Rose, J. K. (1992). Identification of palmitoylation sites on CD4, the human immunodeficiency virus receptor. *J Biol Chem* 267, 13593-13597.
- Crowther, R. A., and Pearse, B. M. (1981). Assembly and packing of clathrin into coats. *J Cell Biol* 91, 790-797.
- Crump, C. M., Xiang, Y., Thomas, L., Gu, F., Austin, C., Tooze, S. A., and Thomas, G. (2001). PACS-1 binding to adaptors is required for acidic cluster motif-mediated protein traffic. *Embo J* 20, 2191-2201.
- Dalgleish, A. G., Beverley, P. C., Clapham, P. R., Crawford, D. H., Greaves, M. F., and Weiss, R. A. (1984). The CD4 (T4) antigen is an essential component of the receptor for the AIDS retrovirus. *Nature* 312, 763-767.
- Daniel, R., Katz, R. A., and Skalka, A. M. (1999). A role for DNA-PK in retroviral DNA integration. *Science* 284, 644-647.
- Daro, E., Sheff, D., Gomez, M., Kreis, T., and Mellman, I. (1997). Inhibition of endosome function in CHO cells bearing a temperature-sensitive defect in the coatomer (COPI) component epsilon-COP. *J Cell Biol* 139, 1747-1759.
- daSilva, L. L., Sougrat, R., Burgos, P. V., Janvier, K., Mattera, R., and Bonifacino, J. S. (2009). Human immunodeficiency virus type 1 Nef protein targets CD4 to the multivesicular body pathway. *J Virol* 83, 6578-6590.
- de Ronde, A., de Rooij, E. R., Coutinho, R. A., and Goudsmit, J. (1996). [Zidovudine-resistant HIV strains in intravenous drug users and homosexual men in Amsterdam]. *Ned Tijdschr Geneesk* 140, 932-934.
- Deacon, N. J., Tsykin, A., Solomon, A., Smith, K., Ludford-Menting, M., Hooker, D. J., McPhee, D. A., Greenway, A. L., Ellett, A., Chatfield, C., et al. (1995). Genomic structure of an attenuated quasi species of HIV-1 from a blood transfusion donor and recipients. *Science* 270, 988-991.
- DeLano, W.L. (2002). *The PyMol User's Manual*. DeLano Scientific, San Carlos, CA.
- Dell'Angelica, E. C., Klumperman, J., Stoorvogel, W., and Bonifacino, J. S. (1998). Association of the AP-3 adaptor complex with clathrin. *Science* 280, 431-434.
- Dell'Angelica, E. C., Mullins, C., and Bonifacino, J. S. (1999). AP-4, a novel protein complex related to clathrin adaptors. *J Biol Chem* 274, 7278-7285.
- Dell'Angelica, E. C., Ohno, H., Ooi, C. E., Rabinovich, E., Roche, K. W., and Bonifacino, J. S. (1997). AP-3: an adaptor-like protein complex with ubiquitous expression. *Embo J* 16, 917-928.

- Dell'Angelica, E. C., Ooi, C. E., and Bonifacino, J. S. (1997). Beta3A-adaptin, a subunit of the adaptor-like complex AP-3. *J Biol Chem* 272, 15078-15084.
- Deng, H., Liu, R., Ellmeier, W., Choe, S., Unutmaz, D., Burkhart, M., Di Marzio, P., Marmon, S., Sutton, R. E., Hill, C. M., et al. (1996). Identification of a major co-receptor for primary isolates of HIV-1. *Nature* 381, 661-666.
- Dennis, C. A., Baron, A., Grossmann, J. G., Mazaleyrat, S., Harris, M., and Jaeger, J. (2005). Co-translational myristoylation alters the quaternary structure of HIV-1 Nef in solution. *Proteins* 60, 658-669.
- Derre, I., Pypaert, M., Dautry-Varsat, A., and Agaisse, H. (2007). RNAi screen in *Drosophila* cells reveals the involvement of the Tom complex in *Chlamydia* infection. *PLoS Pathog* 3, 1446-1458.
- Dong, X., Stothard, P., Forsythe, I. J., and Wishart, D. S. (2004). PlasMapper: a web server for drawing and auto-annotating plasmid maps. *Nucleic Acids Res* 32, W660-664.
- Doray, B., Ghosh, P., Griffith, J., Geuze, H. J., and Kornfeld, S. (2002). Cooperation of GGAs and AP-1 in packaging MPRs at the trans-Golgi network. *Science* 297, 1700-1703.
- Doray, B., Lee, I., Knisely, J., Bu, G., and Kornfeld, S. (2007). The gamma/sigma1 and alpha/sigma2 hemicomplexes of clathrin adaptors AP-1 and AP-2 harbor the dileucine recognition site. *Mol Biol Cell* 18, 1887-1896.
- Dragic, T., Litwin, V., Allaway, G. P., Martin, S. R., Huang, Y., Nagashima, K. A., Cayanan, C., Maddon, P. J., Koup, R. A., Moore, J. P., and Paxton, W. A. (1996). HIV-1 entry into CD4+ cells is mediated by the chemokine receptor CC-CKR-5. *Nature* 381, 667-673.
- Dugast, M., Toussaint, H., Dousset, C., and Benaroch, P. (2005). AP2 clathrin adaptor complex, but not AP1, controls the access of the major histocompatibility complex (MHC) class II to endosomes. *J Biol Chem* 280, 19656-19664.
- Dvorin, J. D., and Malim, M. H. (2003). Intracellular trafficking of HIV-1 cores: journey to the center of the cell. *Curr Top Microbiol Immunol* 281, 179-208.
- Elwell, C., and Engel, J. N. (2005). *Drosophila melanogaster* S2 cells: a model system to study *Chlamydia* interaction with host cells. *Cell Microbiol* 7, 725-739.
- Engering, A., Geijtenbeek, T. B., van Vliet, S. J., Wijers, M., van Liempt, E., Demaurex, N., Lanzavecchia, A., Fransen, J., Figdor, C. G., Piguet, V., and van Kooyk, Y. (2002). The dendritic cell-specific adhesion receptor DC-SIGN internalizes antigen for presentation to T cells. *J Immunol* 168, 2118-2126.
- Feilotter, H. E., Hannon, G. J., Ruddell, C. J., and Beach, D. (1994). Construction of an improved host strain for two hybrid screening. *Nucleic Acids Res* 22, 1502-1503.

- Fields, S., and Song, O. (1989). A novel genetic system to detect protein-protein interactions. *Nature* 340, 245-246.
- Fisher, A. G., Ratner, L., Mitsuya, H., Marselle, L. M., Harper, M. E., Broder, S., Gallo, R. C., and Wong-Staal, F. (1986). Infectious mutants of HTLV-III with changes in the 3' region and markedly reduced cytopathic effects. *Science* 233, 655-659.
- Fleis, R., Filzen, T., and Collins, K. L. (2002). Species-specific effects of HIV-1 Nef-mediated MHC-I downmodulation. *Virology* 303, 120-129.
- Foster, J. L., and Garcia, J. V. (2008). HIV-1 Nef: at the crossroads. *Retrovirology* 5, 84.
- Foster, J. L., and Garcia, J. V. (2008). HIV-1 Nef: at the crossroads. *Retrovirology* 5, 84.
- Foti, M., Mangasarian, A., Piguet, V., Lew, D. P., Krause, K. H., Trono, D., and Carpentier, J. L. (1997). Nef-mediated clathrin-coated pit formation. *J Cell Biol* 139, 37-47.
- Fotin, A., Cheng, Y., Sliz, P., Grigorieff, N., Harrison, S. C., Kirchhausen, T., and Walz, T. (2004). Molecular model for a complete clathrin lattice from electron cryomicroscopy. *Nature* 432, 573-579.
- Fowlkes, B. J., and Schweighoffer, E. (1995). Positive selection of T cells. *Curr Opin Immunol* 7, 188-195.
- Franchini, G., Robert-Guroff, M., Wong-Staal, F., Ghayeb, J., Kato, I., Chang, T. W., and Chang, N. T. (1986). Expression of the protein encoded by the 3' open reading frame of human T-cell lymphotropic virus type III in bacteria: demonstration of its immunoreactivity with human sera. *Proc Natl Acad Sci U S A* 83, 5282-5285.
- Frankel, A. D., and Young, J. A. (1998). HIV-1: fifteen proteins and an RNA. *Annu Rev Biochem* 67, 1-25.
- Fu, W., Sanders-Beer, B.E., Katz, K.S., Maglott, D.R., Pruitt, K.D., and Ptak, R.G. (2009) Human immunodeficiency virus type 1, human protein interaction database at NCBI. *Nuc Acids Res* 37 (Database Issue), D417-D4222.
- Gaidarov, I., Chen, Q., Falck, J. R., Reddy, K. K., and Keen, J. H. (1996). A functional phosphatidylinositol 3,4,5-trisphosphate/phosphoinositide binding domain in the clathrin adaptor AP-2 alpha subunit. Implications for the endocytic pathway. *J Biol Chem* 271, 20922-20929.
- Gaidarov, I., and Keen, J. H. (1999). Phosphoinositide-AP-2 interactions required for targeting to plasma membrane clathrin-coated pits. *J Cell Biol* 146, 755-764.
- Gallo, R., Wong-Staal, F., Montagnier, L., Haseltine, W. A., and Yoshida, M. (1988). HIV/HTLV gene nomenclature. *Nature* 333, 504.

- Gallo, R. C., Salahuddin, S. Z., Popovic, M., Shearer, G. M., Kaplan, M., Haynes, B. F., Palker, T. J., Redfield, R., Oleske, J., Safai, B., and et al. (1984). Frequent detection and isolation of cytopathic retroviruses (HTLV-III) from patients with AIDS and at risk for AIDS. *Science* 224, 500-503.
- Gallusser, A., and Kirchhausen, T. (1993). The beta 1 and beta 2 subunits of the AP complexes are the clathrin coat assembly components. *Embo J* 12, 5237-5244.
- Gao, F., Bailes, E., Robertson, D. L., Chen, Y., Rodenburg, C. M., Michael, S. F., Cummins, L. B., Arthur, L. O., Peeters, M., Shaw, G. M., et al. (1999). Origin of HIV-1 in the chimpanzee *Pan troglodytes*. *Nature* 397, 436-441.
- Garcia, J. V., and Miller, A. D. (1991). Serine phosphorylation-independent downregulation of cell-surface CD4 by nef. *Nature* 350, 508-511.
- Geyer, M., Fackler, O. T., and Peterlin, B. M. (2001). Structure--function relationships in HIV-1 Nef. *EMBO Rep* 2, 580-585.
- Geyer, M., Munte, C. E., Schorr, J., Kellner, R., and Kalbitzer, H. R. (1999). Structure of the anchor-domain of myristoylated and non-myristoylated HIV-1 Nef protein. *J Mol Biol* 289, 123-138.
- Geyer, M., and Peterlin, B. M. (2001). Domain assembly, surface accessibility and sequence conservation in full length HIV-1 Nef. *FEBS Lett* 496, 91-95.
- Geyer, M., Yu, H., Mandic, R., Linnemann, T., Zheng, Y. H., Fackler, O. T., and Peterlin, B. M. (2002). Subunit H of the V-ATPase binds to the medium chain of adaptor protein complex 2 and connects Nef to the endocytic machinery. *J Biol Chem* 277, 28521-28529.
- Gibbs, C. S., and Zoller, M. J. (1991). Identification of electrostatic interactions that determine the phosphorylation site specificity of the cAMP-dependent protein kinase. *Biochemistry* 30, 5329-5334.
- Gietz, R. D., and Schiestl, R. H. (1991). Applications of high efficiency lithium acetate transformation of intact yeast cells using single-stranded nucleic acids as carrier. *Yeast* 7, 253-263.
- Gietz, R. D., Schiestl, R. H., Willems, A. R., and Woods, R. A. (1995). Studies on the transformation of intact yeast cells by the LiAc/SS-DNA/PEG procedure. *Yeast* 11, 355-360.
- Glickman, J. N., Conibear, E., and Pearse, B. M. (1989). Specificity of binding of clathrin adaptors to signals on the mannose-6-phosphate/insulin-like growth factor II receptor. *Embo J* 8, 1041-1047.
- Glushakova, S., Munch, J., Carl, S., Greenough, T. C., Sullivan, J. L., Margolis, L., and Kirchhoff, F. (2001). CD4 down-modulation by human immunodeficiency virus type 1 Nef correlates with the efficiency of viral replication and with CD4(+) T-cell depletion in human lymphoid tissue ex vivo. *J Virol* 75, 10113-10117.

Gorry, P. R., Churchill, M., Learmont, J., Cherry, C., Dyer, W. B., Wesselingh, S. L., and Sullivan, J. S. (2007). Replication-dependent pathogenicity of attenuated nef-deleted HIV-1 in vivo. *J Acquir Immune Defic Syndr* 46, 390-394.

Gottlieb, M. S., Schroff, R., Schanker, H. M., Weisman, J. D., Fan, P. T., Wolf, R. A., and Saxon, A. (1981). Pneumocystis carinii pneumonia and mucosal candidiasis in previously healthy homosexual men: evidence of a new acquired cellular immunodeficiency. *N Engl J Med* 305, 1425-1431.

Gratton, S., Yao, X. J., Venkatesan, S., Cohen, E. A., and Sekaly, R. P. (1996). Molecular analysis of the cytoplasmic domain of CD4: overlapping but noncompetitive requirement for lck association and down-regulation by Nef. *J Immunol* 157, 3305-3311.

Greenberg, M., DeTulleo, L., Rapoport, I., Skowronski, J., and Kirchhausen, T. (1998). A dileucine motif in HIV-1 Nef is essential for sorting into clathrin-coated pits and for downregulation of CD4. *Curr Biol* 8, 1239-1242.

Greenberg, M. E., Bronson, S., Lock, M., Neumann, M., Pavlakis, G. N., and Skowronski, J. (1997). Co-localization of HIV-1 Nef with the AP-2 adaptor protein complex correlates with Nef-induced CD4 down-regulation. *Embo J* 16, 6964-6976.

Greenberg, M. E., Iafrate, A. J., and Skowronski, J. (1998). The SH3 domain-binding surface and an acidic motif in HIV-1 Nef regulate trafficking of class I MHC complexes. *Embo J* 17, 2777-2789.

Greenway, A. L., Holloway, G., and McPhee, D. A. (2000). HIV-1 Nef: a critical factor in viral-induced pathogenesis. *Adv Pharmacol* 48, 299-343.

Groot, F., Welsch, S., and Sattentau, Q. J. (2008). Efficient HIV-1 transmission from macrophages to T cells across transient virological synapses. *Blood* 111, 4660-4663.

Grzesiek, S., Bax, A., Clore, G. M., Gronenborn, A. M., Hu, J. S., Kaufman, J., Palmer, I., Stahl, S. J., and Wingfield, P. T. (1996). The solution structure of HIV-1 Nef reveals an unexpected fold and permits delineation of the binding surface for the SH3 domain of Hck tyrosine protein kinase. *Nat Struct Biol* 3, 340-345.

Grzesiek, S., Bax, A., Hu, J. S., Kaufman, J., Palmer, I., Stahl, S. J., Tjandra, N., and Wingfield, P. T. (1997). Refined solution structure and backbone dynamics of HIV-1 Nef. *Protein Sci* 6, 1248-1263.

Grzesiek, S., Stahl, S. J., Wingfield, P. T., and Bax, A. (1996). The CD4 determinant for downregulation by HIV-1 Nef directly binds to Nef. Mapping of the Nef binding surface by NMR. *Biochemistry* 35, 10256-10261.

Gu, F., and Gruenberg, J. (1999). Biogenesis of transport intermediates in the endocytic pathway. *FEBS Lett* 452, 61-66.

- Guermontprez, P., Valladeau, J., Zitvogel, L., Thery, C., and Amigorena, S. (2002). Antigen presentation and T cell stimulation by dendritic cells. *Annu Rev Immunol* 20, 621-667.
- Guy, B., Kieny, M. P., Riviere, Y., Le Peuch, C., Dott, K., Girard, M., Montagnier, L., and Lecocq, J. P. (1987). HIV F/3' orf encodes a phosphorylated GTP-binding protein resembling an oncogene product. *Nature* 330, 266-269.
- Hammes, S. R., Dixon, E. P., Malim, M. H., Cullen, B. R., and Greene, W. C. (1989). Nef protein of human immunodeficiency virus type 1: evidence against its role as a transcriptional inhibitor. *Proc Natl Acad Sci U S A* 86, 9549-9553.
- Hanna, Z., Priceputu, E., Kay, D. G., Poudrier, J., Chrobak, P., and Jolicoeur, P. (2004). In vivo mutational analysis of the N-terminal region of HIV-1 Nef reveals critical motifs for the development of an AIDS-like disease in CD4C/HIV transgenic mice. *Virology* 327, 273-286.
- Harding, C. V., and Unanue, E. R. (1990). Quantitation of antigen-presenting cell MHC class II/peptide complexes necessary for T-cell stimulation. *Nature* 346, 574-576.
- Harding, F. A., McArthur, J. G., Gross, J. A., Raulet, D. H., and Allison, J. P. (1992). CD28-mediated signalling co-stimulates murine T cells and prevents induction of anergy in T-cell clones. *Nature* 356, 607-609.
- Harrich, D., and Hooker, B. (2002). Mechanistic aspects of HIV-1 reverse transcription initiation. *Rev Med Virol* 12, 31-45.
- Harris, M., Hislop, S., Patsilinos, P., and Neil, J. C. (1992). In vivo derived HIV-1 nef gene products are heterogeneous and lack detectable nucleotide binding activity. *AIDS Res Hum Retroviruses* 8, 537-543.
- Harris, M. P., and Neil, J. C. (1994). Myristoylation-dependent binding of HIV-1 Nef to CD4. *J Mol Biol* 241, 136-142.
- Hehnly, H., and Stamnes, M. (2007). Regulating cytoskeleton-based vesicle motility. *FEBS Lett* 581, 2112-2118.
- Heldwein, E. E., Macia, E., Wang, J., Yin, H. L., Kirchhausen, T., and Harrison, S. C. (2004). Crystal structure of the clathrin adaptor protein 1 core. *Proc Natl Acad Sci U S A* 101, 14108-14113.
- Henikoff, S., and Henikoff, J. G. (1992). Amino acid substitution matrices from protein blocks. *Proc Natl Acad Sci U S A* 89, 10915-10919.
- Herz, A. V., Bonhoeffer, S., Anderson, R. M., May, R. M., and Nowak, M. A. (1996). Viral dynamics in vivo: limitations on estimates of intracellular delay and virus decay. *Proc Natl Acad Sci U S A* 93, 7247-7251.

- Heuser, J. (1980). Three-dimensional visualization of coated vesicle formation in fibroblasts. *J Cell Biol* 84, 560-583.
- Heuser, J. E., and Keen, J. (1988). Deep-etch visualization of proteins involved in clathrin assembly. *J Cell Biol* 107, 877-886.
- Hill, B. T., and Skowronski, J. (2005). Human N-myristoyltransferases form stable complexes with lentiviral nef and other viral and cellular substrate proteins. *J Virol* 79, 1133-1141.
- Hirst, J., Bright, N. A., Rous, B., and Robinson, M. S. (1999). Characterization of a fourth adaptor-related protein complex. *Mol Biol Cell* 10, 2787-2802.
- Hislop, J. N., Marley, A., and Von Zastrow, M. (2004). Role of mammalian vacuolar protein-sorting proteins in endocytic trafficking of a non-ubiquitinated G protein-coupled receptor to lysosomes. *J Biol Chem* 279, 22522-22531.
- Ho, D. D., Rota, T. R., and Hirsch, M. S. (1986). Infection of monocyte/macrophages by human T lymphotropic virus type III. *J Clin Invest* 77, 1712-1715.
- Hodge, D. R., Dunn, K. J., Pei, G. K., Chakrabarty, M. K., Heidecker, G., Lautenberger, J. A., and Samuel, K. P. (1998). Binding of c-Raf1 kinase to a conserved acidic sequence within the carboxyl-terminal region of the HIV-1 Nef protein. *J Biol Chem* 273, 15727-15733.
- Hogquist, K. A., Baldwin, T. A., and Jameson, S. C. (2005). Central tolerance: learning self-control in the thymus. *Nat Rev Immunol* 5, 772-782.
- Holmes, E. C. (2001). On the origin and evolution of the human immunodeficiency virus (HIV). *Biol Rev Camb Philos Soc* 76, 239-254.
- Honing, S., Ricotta, D., Krauss, M., Spate, K., Spolaore, B., Motley, A., Robinson, M., Robinson, C., Haucke, V., and Owen, D. J. (2005). Phosphatidylinositol-(4,5)-bisphosphate regulates sorting signal recognition by the clathrin-associated adaptor complex AP2. *Mol Cell* 18, 519-531.
- Hrecka, K., Swigut, T., Schindler, M., Kirchhoff, F., and Skowronski, J. (2005). Nef proteins from diverse groups of primate lentiviruses downmodulate CXCR4 to inhibit migration to the chemokine stromal derived factor 1. *J Virol* 79, 10650-10659.
- Hu, S. L., Kosowski, S. G., and Dalrymple, J. M. (1986). Expression of AIDS virus envelope gene in recombinant vaccinia viruses. *Nature* 320, 537-540.
- Hua, J., Blair, W., Truant, R., and Cullen, B. R. (1997). Identification of regions in HIV-1 Nef required for efficient downregulation of cell surface CD4. *Virology* 231, 231-238.
- Huang, F., Jiang, X., and Sorkin, A. (2003). Tyrosine phosphorylation of the beta2 subunit of clathrin adaptor complex AP-2 reveals the role of a di-leucine motif in the epidermal growth factor receptor trafficking. *J Biol Chem* 278, 43411-43417.

- Huang, F., Khvorova, A., Marshall, W., and Sorokin, A. (2004). Analysis of clathrin-mediated endocytosis of epidermal growth factor receptor by RNA interference. *J Biol Chem* 279, 16657-16661.
- Iafrate, A. J., Bronson, S., and Skowronski, J. (1997). Separable functions of Nef disrupt two aspects of T cell receptor machinery: CD4 expression and CD3 signaling. *Embo J* 16, 673-684.
- Iwashima, M., Irving, B. A., van Oers, N. S., Chan, A. C., and Weiss, A. (1994). Sequential interactions of the TCR with two distinct cytoplasmic tyrosine kinases. *Science* 263, 1136-1139.
- Jamieson, B. D., Aldrovandi, G. M., Planelles, V., Jowett, J. B., Gao, L., Bloch, L. M., Chen, I. S., and Zack, J. A. (1994). Requirement of human immunodeficiency virus type 1 nef for in vivo replication and pathogenicity. *J Virol* 68, 3478-3485.
- Janeway, C., Shlomchik, M.J., Walport, M., and Travers, P. (2005). *Immunobiology: The Immune System in Health and Disease*, 5th Edition. Garland Science Publishers.
- Janvier, K., and Bonifacino, J. S. (2005). Role of the endocytic machinery in the sorting of lysosome-associated membrane proteins. *Mol Biol Cell* 16, 4231-4242.
- Janvier, K., Craig, H., Hitchin, D., Madrid, R., Sol-Foulon, N., Renault, L., Cherfils, J., Cassel, D., Benichou, S., and Guatelli, J. (2003a). HIV-1 Nef stabilizes the association of adaptor protein complexes with membranes. *J Biol Chem* 278, 8725-8732.
- Janvier, K., Craig, H., Le Gall, S., Benarous, R., Guatelli, J., Schwartz, O., and Benichou, S. (2001). Nef-induced CD4 downregulation: a diacidic sequence in human immunodeficiency virus type 1 Nef does not function as a protein sorting motif through direct binding to beta-COP. *J Virol* 75, 3971-3976.
- Janvier, K., Kato, Y., Boehm, M., Rose, J. R., Martina, J. A., Kim, B. Y., Venkatesan, S., and Bonifacino, J. S. (2003b). Recognition of dileucine-based sorting signals from HIV-1 Nef and LIMP-II by the AP-1 gamma-sigma1 and AP-3 delta-sigma3 hemicomplexes. *J Cell Biol* 163, 1281-1290.
- Jin, Y. J., Cai, C. Y., Zhang, X., Zhang, H. T., Hirst, J. A., and Burakoff, S. J. (2005). HIV Nef-mediated CD4 down-regulation is adaptor protein complex 2 dependent. *J Immunol* 175, 3157-3164.
- Johnson, K. F., and Kornfeld, S. (1992). The cytoplasmic tail of the mannose 6-phosphate/insulin-like growth factor-II receptor has two signals for lysosomal enzyme sorting in the Golgi. *J Cell Biol* 119, 249-257.
- Johnson, K. F., and Kornfeld, S. (1992). A His-Leu-Leu sequence near the carboxyl terminus of the cytoplasmic domain of the cation-dependent mannose 6-phosphate receptor is necessary for the lysosomal enzyme sorting function. *J Biol Chem* 267, 17110-17115.

- Jones, B. G., Thomas, L., Molloy, S. S., Thulin, C. D., Fry, M. D., Walsh, K. A., and Thomas, G. (1995). Intracellular trafficking of furin is modulated by the phosphorylation state of a casein kinase II site in its cytoplasmic tail. *Embo J* 14, 5869-5883.
- Jordan, A., Defechereux, P., and Verdin, E. (2001). The site of HIV-1 integration in the human genome determines basal transcriptional activity and response to Tat transactivation. *Embo J* 20, 1726-1738.
- Jouvenet, N., Bieniasz, P. D., and Simon, S. M. (2008). Imaging the biogenesis of individual HIV-1 virions in live cells. *Nature* 454, 236-240.
- Kaminchik, J., Bashan, N., Itach, A., Sarver, N., Gorecki, M., and Panet, A. (1991). Genetic characterization of human immunodeficiency virus type 1 nef gene products translated in vitro and expressed in mammalian cells. *J Virol* 65, 583-588.
- Kanaseki, T., and Kadota, K. (1969). The "vesicle in a basket". A morphological study of the coated vesicle isolated from the nerve endings of the guinea pig brain, with special reference to the mechanism of membrane movements. *J Cell Biol* 42, 202-220.
- Kasper, M. R., and Collins, K. L. (2003). Nef-mediated disruption of HLA-A2 transport to the cell surface in T cells. *J Virol* 77, 3041-3049.
- Kasper, M. R., Roeth, J. F., Williams, M., Filzen, T. M., Fleis, R. I., and Collins, K. L. (2005). HIV-1 Nef disrupts antigen presentation early in the secretory pathway. *J Biol Chem* 280, 12840-12848.
- Keen, J. H. (1987). Clathrin assembly proteins: affinity purification and a model for coat assembly. *J Cell Biol* 105, 1989-1998.
- Keen, J. H., Willingham, M. C., and Pastan, I. H. (1979). Clathrin-coated vesicles: isolation, dissociation and factor-dependent reassociation of clathrin baskets. *Cell* 16, 303-312.
- Kelly, B. T., McCoy, A. J., Spate, K., Miller, S. E., Evans, P. R., Honing, S., and Owen, D. J. (2008). A structural explanation for the binding of endocytic dileucine motifs by the AP2 complex. *Nature* 456, 976-979.
- Kestler, H. W., 3rd, Ringler, D. J., Mori, K., Panicali, D. L., Sehgal, P. K., Daniel, M. D., and Desrosiers, R. C. (1991). Importance of the nef gene for maintenance of high virus loads and for development of AIDS. *Cell* 65, 651-662.
- Kienzle, N., Freund, J., Kalbitzer, H. R., and Mueller-Lantzsch, N. (1993). Oligomerization of the Nef protein from human immunodeficiency virus (HIV) type 1. *Eur J Biochem* 214, 451-457.
- Kim, P. W., Sun, Z. Y., Blacklow, S. C., Wagner, G., and Eck, M. J. (2003). A zinc clasp structure tethers Lck to T cell coreceptors CD4 and CD8. *Science* 301, 1725-1728.

Kim, S., Ikeuchi, K., Byrn, R., Groopman, J., and Baltimore, D. (1989). Lack of a negative influence on viral growth by the nef gene of human immunodeficiency virus type 1. *Proc Natl Acad Sci U S A* 86, 9544-9548.

Kim, S. Y., Byrn, R., Groopman, J., and Baltimore, D. (1989). Temporal aspects of DNA and RNA synthesis during human immunodeficiency virus infection: evidence for differential gene expression. *J Virol* 63, 3708-3713.

Kim, Y. H., Chang, S. H., Kwon, J. H., and Rhee, S. S. (1999). HIV-1 Nef plays an essential role in two independent processes in CD4 down-regulation: dissociation of the CD4-p56(lck) complex and targeting of CD4 to lysosomes. *Virology* 257, 208-219.

Kirchhausen, T. (1999). Adaptors for clathrin-mediated traffic. *Annu Rev Cell Dev Biol* 15, 705-732.

Kirchhausen, T. (2000). Three ways to make a vesicle. *Nat Rev Mol Cell Biol* 1, 187-198.

Kirchhoff, F., Greenough, T. C., Brettler, D. B., Sullivan, J. L., and Desrosiers, R. C. (1995). Brief report: absence of intact nef sequences in a long-term survivor with nonprogressive HIV-1 infection. *N Engl J Med* 332, 228-232.

Klatzmann, D., Champagne, E., Chamaret, S., Gruest, J., Guetard, D., Hercend, T., Gluckman, J. C., and Montagnier, L. (1984). T-lymphocyte T4 molecule behaves as the receptor for human retrovirus LAV. *Nature* 312, 767-768.

Klotman, M. E., Kim, S., Buchbinder, A., DeRossi, A., Baltimore, D., and Wong-Staal, F. (1991). Kinetics of expression of multiply spliced RNA in early human immunodeficiency virus type 1 infection of lymphocytes and monocytes. *Proc Natl Acad Sci U S A* 88, 5011-5015.

Konig, R., Ashwell, G., and Hanover, J. A. (1988). Glycosylation of CD4. Tunicamycin inhibits surface expression. *J Biol Chem* 263, 9502-9507.

Konig, R., Huang, L. Y., and Germain, R. N. (1992). MHC class II interaction with CD4 mediated by a region analogous to the MHC class I binding site for CD8. *Nature* 356, 796-798.

Korber, B., Muldoon, M., Theiler, J., Gao, F., Gupta, R., Lapedes, A., Hahn, B. H., Wolinsky, S., and Bhattacharya, T. (2000). Timing the ancestor of the HIV-1 pandemic strains. *Science* 288, 1789-1796.

Kowalski, M., Potz, J., Basiripour, L., Dorfman, T., Goh, W. C., Terwilliger, E., Dayton, A., Rosen, C., Haseltine, W., and Sodroski, J. (1987). Functional regions of the envelope glycoprotein of human immunodeficiency virus type 1. *Science* 237, 1351-1355.

Kwong, P. D., Ryu, S. E., Hendrickson, W. A., Axel, R., Sweet, R. M., Folena-Wasserman, G., Hensley, P., and Sweet, R. W. (1990). Molecular characteristics of

recombinant human CD4 as deduced from polymorphic crystals. *Proc Natl Acad Sci U S A* 87, 6423-6427.

Kwong, P. D., Wyatt, R., Robinson, J., Sweet, R. W., Sodroski, J., and Hendrickson, W. A. (1998). Structure of an HIV gp120 envelope glycoprotein in complex with the CD4 receptor and a neutralizing human antibody. *Nature* 393, 648-659.

Lama, J. (2003). The physiological relevance of CD4 receptor down-modulation during HIV infection. *Curr HIV Res* 1, 167-184.

Lama, J., and Ware, C. F. (2000). Human immunodeficiency virus type 1 Nef mediates sustained membrane expression of tumor necrosis factor and the related cytokine LIGHT on activated T cells. *J Virol* 74, 9396-9402.

Lanier, L. L. (1998). NK cell receptors. *Annu Rev Immunol* 16, 359-393.

Larder, B. A., Darby, G., and Richman, D. D. (1989). HIV with reduced sensitivity to zidovudine (AZT) isolated during prolonged therapy. *Science* 243, 1731-1734.

Larder, B. A., and Kemp, S. D. (1989). Multiple mutations in HIV-1 reverse transcriptase confer high-level resistance to zidovudine (AZT). *Science* 246, 1155-1158.

Lazarovits, J., and Roth, M. (1988). A single amino acid change in the cytoplasmic domain allows the influenza virus hemagglutinin to be endocytosed through coated pits. *Cell* 53, 743-752.

Le Borgne, R., Alconada, A., Bauer, U., and Hoflack, B. (1998). The mammalian AP-3 adaptor-like complex mediates the intracellular transport of lysosomal membrane glycoproteins. *J Biol Chem* 273, 29451-29461.

Le Gall, S., Erdtmann, L., Benichou, S., Berlioz-Torrent, C., Liu, L., Benarous, R., Heard, J. M., and Schwartz, O. (1998). Nef interacts with the mu subunit of clathrin adaptor complexes and reveals a cryptic sorting signal in MHC I molecules. *Immunity* 8, 483-495.

Learmont, J., Cook, L., Dunckley, H., and Sullivan, J. S. (1995). Update on long-term symptomless HIV type 1 infection in recipients of blood products from a single donor. *AIDS Res Hum Retroviruses* 11, 1.

Learmont, J., Tindall, B., Evans, L., Cunningham, A., Cunningham, P., Wells, J., Penny, R., Kaldor, J., and Cooper, D. A. (1992). Long-term symptomless HIV-1 infection in recipients of blood products from a single donor. *Lancet* 340, 863-867.

Learmont, J. C., Geczy, A. F., Mills, J., Ashton, L. J., Raynes-Greenow, C. H., Garsia, R. J., Dyer, W. B., McIntyre, L., Oelrichs, R. B., Rhodes, D. I., et al. (1999). Immunologic and virologic status after 14 to 18 years of infection with an attenuated strain of HIV-1. A report from the Sydney Blood Bank Cohort. *N Engl J Med* 340, 1715-1722.

- Ledergerber, B., Egger, M., Erard, V., Weber, R., Hirschel, B., Furrer, H., Battegay, M., Vernazza, P., Bernasconi, E., Opravil, M., et al. (1999). AIDS-related opportunistic illnesses occurring after initiation of potent antiretroviral therapy: the Swiss HIV Cohort Study. *Jama* 282, 2220-2226.
- Lee, T. H., Coligan, J. E., Allan, J. S., McLane, M. F., Groopman, J. E., and Essex, M. (1986). A new HTLV-III/LAV protein encoded by a gene found in cytopathic retroviruses. *Science* 231, 1546-1549.
- Letourneur, F., Gaynor, E. C., Hennecke, S., Demolliere, C., Duden, R., Emr, S. D., Riezman, H., and Cosson, P. (1994). Coatamer is essential for retrieval of dilysine-tagged proteins to the endoplasmic reticulum. *Cell* 79, 1199-1207.
- Levesque, K., Finzi, A., Binette, J., and Cohen, E. A. (2004). Role of CD4 receptor down-regulation during HIV-1 infection. *Curr HIV Res* 2, 51-59.
- Li, P. L., Wang, T., Buckley, K. A., Chenine, A. L., Popov, S., and Ruprecht, R. M. (2005). Phosphorylation of HIV Nef by cAMP-dependent protein kinase. *Virology* 331, 367-374.
- Li, Y., Hui, H., Burgess, C. J., Price, R. W., Sharp, P. M., Hahn, B. H., and Shaw, G. M. (1992). Complete nucleotide sequence, genome organization, and biological properties of human immunodeficiency virus type 1 in vivo: evidence for limited defectiveness and complementation. *J Virol* 66, 6587-6600.
- Lindemann, D., Wilhelm, R., Renard, P., Althage, A., Zinkernagel, R., and Mous, J. (1994). Severe immunodeficiency associated with a human immunodeficiency virus 1 NEF/3'-long terminal repeat transgene. *J Exp Med* 179, 797-807.
- Lindwasser, O. W., Smith, W. J., Chaudhuri, R., Yang, P., Hurley, J. H., and Bonifacino, J. S. (2008). A diacidic motif in human immunodeficiency virus type 1 Nef is a novel determinant of binding to AP-2. *J Virol* 82, 1166-1174.
- Linsley, P. S., Clark, E. A., and Ledbetter, J. A. (1990). T-cell antigen CD28 mediates adhesion with B cells by interacting with activation antigen B7/BB-1. *Proc Natl Acad Sci U S A* 87, 5031-5035.
- Littau, R. A., Oldstone, M. B., Takeda, A., Debouck, C., Wong, J. T., Tuazon, C. U., Moss, B., Kievits, F., and Ennis, F. A. (1991). An HLA-C-restricted CD8+ cytotoxic T-lymphocyte clone recognizes a highly conserved epitope on human immunodeficiency virus type 1 gag. *J Virol* 65, 4051-4056.
- Little, S. J., Riggs, N. L., Chowers, M. Y., Fitch, N. J., Richman, D. D., Spina, C. A., and Guatelli, J. C. (1994). Cell surface CD4 downregulation and resistance to superinfection induced by a defective provirus of HIV-1. *Virology* 205, 578-582.
- Liu, J., Perkins, N. D., Schmid, R. M., and Nabel, G. J. (1992). Specific NF-kappa B subunits act in concert with Tat to stimulate human immunodeficiency virus type 1 transcription. *J Virol* 66, 3883-3887.

- Liu, L. X., Heveker, N., Fackler, O. T., Arold, S., Le Gall, S., Janvier, K., Peterlin, B. M., Dumas, C., Schwartz, O., Benichou, S., and Benarous, R. (2000). Mutation of a conserved residue (D123) required for oligomerization of human immunodeficiency virus type 1 Nef protein abolishes interaction with human thioesterase and results in impairment of Nef biological functions. *J Virol* 74, 5310-5319.
- Lu, X., Yu, H., Liu, S. H., Brodsky, F. M., and Peterlin, B. M. (1998). Interactions between HIV1 Nef and vacuolar ATPase facilitate the internalization of CD4. *Immunity* 8, 647-656.
- Lubben, N. B., Sahlender, D. A., Motley, A. M., Lehner, P. J., Benaroch, P., and Robinson, M. S. (2007). HIV-1 Nef-induced down-regulation of MHC class I requires AP-1 and clathrin but not PACS-1 and is impeded by AP-2. *Mol Biol Cell* 18, 3351-3365.
- Luciw, P. A., Cheng-Mayer, C., and Levy, J. A. (1987). Mutational analysis of the human immunodeficiency virus: the orf-B region down-regulates virus replication. *Proc Natl Acad Sci U S A* 84, 1434-1438.
- Lundquist, C. A., Tobiume, M., Zhou, J., Unutmaz, D., and Aiken, C. (2002). Nef-mediated downregulation of CD4 enhances human immunodeficiency virus type 1 replication in primary T lymphocytes. *J Virol* 76, 4625-4633.
- Lundquist, C. A., Zhou, J., and Aiken, C. (2004). Nef stimulates human immunodeficiency virus type 1 replication in primary T cells by enhancing virion-associated gp120 levels: coreceptor-dependent requirement for Nef in viral replication. *J Virol* 78, 6287-6296.
- Luo, T., Downing, J. R., and Garcia, J. V. (1997). Induction of phosphorylation of human immunodeficiency virus type 1 Nef and enhancement of CD4 downregulation by phorbol myristate acetate. *J Virol* 71, 2535-2539.
- Madrid, R., Janvier, K., Hitchin, D., Day, J., Coleman, S., Noviello, C., Bouchet, J., Benmerah, A., Guatelli, J., and Benichou, S. (2005). Nef-induced alteration of the early/recycling endosomal compartment correlates with enhancement of HIV-1 infectivity. *J Biol Chem* 280, 5032-5044.
- Malim, M. H., Hauber, J., Le, S. Y., Maizel, J. V., and Cullen, B. R. (1989). The HIV-1 rev trans-activator acts through a structured target sequence to activate nuclear export of unspliced viral mRNA. *Nature* 338, 254-257.
- Mangasarian, A., Foti, M., Aiken, C., Chin, D., Carpentier, J. L., and Trono, D. (1997). The HIV-1 Nef protein acts as a connector with sorting pathways in the Golgi and at the plasma membrane. *Immunity* 6, 67-77.
- Mangasarian, A., Piguet, V., Wang, J. K., Chen, Y. L., and Trono, D. (1999). Nef-induced CD4 and major histocompatibility complex class I (MHC-I) down-regulation are governed by distinct determinants: N-terminal alpha helix and proline repeat of Nef selectively regulate MHC-I trafficking. *J Virol* 73, 1964-1973.

- Marchevsky, A., Rosen, M. J., Chrystal, G., and Kleinerman, J. (1985). Pulmonary complications of the acquired immunodeficiency syndrome: a clinicopathologic study of 70 cases. *Hum Pathol* 16, 659-670.
- Mariani, R., Kirchhoff, F., Greenough, T. C., Sullivan, J. L., Desrosiers, R. C., and Skowronski, J. (1996). High frequency of defective nef alleles in a long-term survivor with nonprogressive human immunodeficiency virus type 1 infection. *J Virol* 70, 7752-7764.
- Mariani, R., and Skowronski, J. (1993). CD4 down-regulation by nef alleles isolated from human immunodeficiency virus type 1-infected individuals. *Proc Natl Acad Sci U S A* 90, 5549-5553.
- Marks, M. S., Woodruff, L., Ohno, H., and Bonifacino, J. S. (1996). Protein targeting by tyrosine- and di-leucine-based signals: evidence for distinct saturable components. *J Cell Biol* 135, 341-354.
- Marshall, W. L., Diamond, D. C., Kowalski, M. M., and Finberg, R. W. (1992). High level of surface CD4 prevents stable human immunodeficiency virus infection of T-cell transfectants. *J Virol* 66, 5492-5499.
- Martin, J. C., and Bandres, J. C. (1999). Cells of the monocyte-macrophage lineage and pathogenesis of HIV-1 infection. *J Acquir Immune Defic Syndr* 22, 413-429.
- Masur, H., Michelis, M. A., Greene, J. B., Onorato, I., Stouwe, R. A., Holzman, R. S., Wormser, G., Brettman, L., Lange, M., Murray, H. W., and Cunningham-Rundles, S. (1981). An outbreak of community-acquired *Pneumocystis carinii* pneumonia: initial manifestation of cellular immune dysfunction. *N Engl J Med* 305, 1431-1438.
- McCormick, P. J., Martina, J. A., and Bonifacino, J. S. (2005). Involvement of clathrin and AP-2 in the trafficking of MHC class II molecules to antigen-processing compartments. *Proc Natl Acad Sci U S A* 102, 7910-7915.
- McCune, J. M., Namikawa, R., Kaneshima, H., Shultz, L. D., Lieberman, M., and Weissman, I. L. (1988). The SCID-hu mouse: murine model for the analysis of human hematolymphoid differentiation and function. *Science* 241, 1632-1639.
- McDonald, D., Wu, L., Bohks, S. M., KewalRamani, V. N., Unutmaz, D., and Hope, T. J. (2003). Recruitment of HIV and its receptors to dendritic cell-T cell junctions. *Science* 300, 1295-1297.
- McDougal, J. S., Kennedy, M. S., Sligh, J. M., Cort, S. P., Mawle, A., and Nicholson, J. K. (1986). Binding of HTLV-III/LAV to T4+ T cells by a complex of the 110K viral protein and the T4 molecule. *Science* 231, 382-385.
- Melikyan, G. B., Markosyan, R. M., Hemmati, H., Delmedico, M. K., Lambert, D. M., and Cohen, F. S. (2000). Evidence that the transition of HIV-1 gp41 into a six-helix bundle, not the bundle configuration, induces membrane fusion. *J Cell Biol* 151, 413-423.

- Mellman, I., and Warren, G. (2000). The road taken: past and future foundations of membrane traffic. *Cell* 100, 99-112.
- Meyer, C., Zizioli, D., Lausmann, S., Eskelinen, E. L., Hamann, J., Saftig, P., von Figura, K., and Schu, P. (2000). *mu1A*-adaptin-deficient mice: lethality, loss of AP-1 binding and rerouting of mannose 6-phosphate receptors. *Embo J* 19, 2193-2203.
- Michel, N., Allespach, I., Venzke, S., Fackler, O. T., and Keppler, O. T. (2005). The Nef protein of human immunodeficiency virus establishes superinfection immunity by a dual strategy to downregulate cell-surface CCR5 and CD4. *Curr Biol* 15, 714-723.
- Miller, M. D., Feinberg, M. B., and Greene, W. C. (1994). The HIV-1 nef gene acts as a positive viral infectivity factor. *Trends Microbiol* 2, 294-298.
- Miller, M. D., Warmerdam, M. T., Gaston, I., Greene, W. C., and Feinberg, M. B. (1994). The human immunodeficiency virus-1 nef gene product: a positive factor for viral infection and replication in primary lymphocytes and macrophages. *J Exp Med* 179, 101-113.
- Mitchell, R. S., Chaudhuri, R., Lindwasser, O. W., Tanaka, K. A., Lau, D., Murillo, R., Bonifacino, J. S., and Guatelli, J. C. (2008). Competition model for upregulation of the major histocompatibility complex class II-associated invariant chain by human immunodeficiency virus type 1 Nef. *J Virol* 82, 7758-7767.
- Mitsuya, H., Weinhold, K. J., Furman, P. A., St Clair, M. H., Lehrman, S. N., Gallo, R. C., Bolognesi, D., Barry, D. W., and Broder, S. (1985). 3'-Azido-3'-deoxythymidine (BW A509U): an antiviral agent that inhibits the infectivity and cytopathic effect of human T-lymphotropic virus type III/lymphadenopathy-associated virus in vitro. *Proc Natl Acad Sci U S A* 82, 7096-7100.
- Mosmann, T. R., and Coffman, R. L. (1989). TH1 and TH2 cells: different patterns of lymphokine secretion lead to different functional properties. *Annu Rev Immunol* 7, 145-173.
- Motley, A., Bright, N. A., Seaman, M. N., and Robinson, M. S. (2003). Clathrin-mediated endocytosis in AP-2-depleted cells. *J Cell Biol* 162, 909-918.
- Motley, A. M., Berg, N., Taylor, M. J., Sahlender, D. A., Hirst, J., Owen, D. J., and Robinson, M. S. (2006). Functional analysis of AP-2 alpha and mu2 subunits. *Mol Biol Cell* 17, 5298-5308.
- Muesing, M. A., Smith, D. H., Cabradilla, C. D., Benton, C. V., Lasky, L. A., and Capon, D. J. (1985). Nucleic acid structure and expression of the human AIDS/lymphadenopathy retrovirus. *Nature* 313, 450-458.
- Munch, J., Janardhan, A., Stolte, N., Stahl-Hennig, C., Ten Haaf, P., Heeney, J. L., Swigut, T., Kirchhoff, F., and Skowronski, J. (2002). T-cell receptor:CD3 down-regulation is a selected in vivo function of simian immunodeficiency virus Nef but is not sufficient for effective viral replication in rhesus macaques. *J Virol* 76, 12360-12364.

- Nabel, G., and Baltimore, D. (1987). An inducible transcription factor activates expression of human immunodeficiency virus in T cells. *Nature* 326, 711-713.
- Neil, S. J., Zang, T., and Bieniasz, P. D. (2008). Tetherin inhibits retrovirus release and is antagonized by HIV-1 Vpu. *Nature* 451, 425-430.
- Nesterov, A., Carter, R. E., Sorkina, T., Gill, G. N., and Sorkin, A. (1999). Inhibition of the receptor-binding function of clathrin adaptor protein AP-2 by dominant-negative mutant mu2 subunit and its effects on endocytosis. *Embo J* 18, 2489-2499.
- Newman, L. S., McKeever, M. O., Okano, H. J., and Darnell, R. B. (1995). Beta-NAP, a cerebellar degeneration antigen, is a neuron-specific vesicle coat protein. *Cell* 82, 773-783.
- Noviello, C. M., Benichou, S., and Guatelli, J. C. (2008). Cooperative binding of the class I major histocompatibility complex cytoplasmic domain and human immunodeficiency virus type 1 Nef to the endosomal AP-1 complex via its mu subunit. *J Virol* 82, 1249-1258.
- O'Neill, E., Kuo, L. S., Krisko, J. F., Tomchick, D. R., Garcia, J. V., and Foster, J. L. (2006). Dynamic evolution of the human immunodeficiency virus type 1 pathogenic factor, Nef. *J Virol* 80, 1311-1320.
- Oberlin, E., Amara, A., Bachelier, F., Bessia, C., Virelizier, J. L., Arenzana-Seisdedos, F., Schwartz, O., Heard, J. M., Clark-Lewis, I., Legler, D. F., et al. (1996). The CXC chemokine SDF-1 is the ligand for LESTR/fusin and prevents infection by T-cell-line-adapted HIV-1. *Nature* 382, 833-835.
- Odorizzi, G., Cowles, C. R., and Emr, S. D. (1998). The AP-3 complex: a coat of many colours. *Trends Cell Biol* 8, 282-288.
- Oelrichs, R., Tsykin, A., Rhodes, D., Solomon, A., Ellett, A., McPhee, D., and Deacon, N. (1998). Genomic sequence of HIV type 1 from four members of the Sydney Blood Bank Cohort of long-term nonprogressors. *AIDS Res Hum Retroviruses* 14, 811-814.
- Ohno, H., Aguilar, R. C., Yeh, D., Taura, D., Saito, T., and Bonifacino, J. S. (1998). The medium subunits of adaptor complexes recognize distinct but overlapping sets of tyrosine-based sorting signals. *J Biol Chem* 273, 25915-25921.
- Ohno, H., Fournier, M. C., Poy, G., and Bonifacino, J. S. (1996). Structural determinants of interaction of tyrosine-based sorting signals with the adaptor medium chains. *J Biol Chem* 271, 29009-29015.
- Ohno, H., Stewart, J., Fournier, M. C., Bosshart, H., Rhee, I., Miyatake, S., Saito, T., Gallusser, A., Kirchhausen, T., and Bonifacino, J. S. (1995). Interaction of tyrosine-based sorting signals with clathrin-associated proteins. *Science* 269, 1872-1875.
- Oldridge, J., and Marsh, M. (1998). Nef--an adaptor adaptor? *Trends Cell Biol* 8, 302-305.

Orci, L., Glick, B. S., and Rothman, J. E. (1986). A new type of coated vesicular carrier that appears not to contain clathrin: its possible role in protein transport within the Golgi stack. *Cell* 46, 171-184.

Owen, D. J., Collins, B. M., and Evans, P. R. (2004). Adaptors for clathrin coats: structure and function. *Annu Rev Cell Dev Biol* 20, 153-191.

Owen, D. J., and Evans, P. R. (1998). A structural explanation for the recognition of tyrosine-based endocytotic signals. *Science* 282, 1327-1332.

Owen, D. J., Vallis, Y., Noble, M. E., Hunter, J. B., Dafforn, T. R., Evans, P. R., and McMahon, H. T. (1999). A structural explanation for the binding of multiple ligands by the alpha-adaptin appendage domain. *Cell* 97, 805-815.

Owen, D. J., Vallis, Y., Pearse, B. M., McMahon, H. T., and Evans, P. R. (2000). The structure and function of the beta 2-adaptin appendage domain. *Embo J* 19, 4216-4227.

Page, L. J., and Robinson, M. S. (1995). Targeting signals and subunit interactions in coated vesicle adaptor complexes. *J Cell Biol* 131, 619-630.

Palade, G. (1975). Intracellular Aspects of the Process of Protein Synthesis. *Science* 189, 867.

Palella, F. J., Jr., Delaney, K. M., Moorman, A. C., Loveless, M. O., Fuhrer, J., Satten, G. A., Aschman, D. J., and Holmberg, S. D. (1998). Declining morbidity and mortality among patients with advanced human immunodeficiency virus infection. HIV Outpatient Study Investigators. *N Engl J Med* 338, 853-860.

Pantaleo, G., Menzo, S., Vaccarezza, M., Graziosi, C., Cohen, O. J., Demarest, J. F., Montefiori, D., Orenstein, J. M., Fox, C., Schrager, L. K., and et al. (1995). Studies in subjects with long-term nonprogressive human immunodeficiency virus infection. *N Engl J Med* 332, 209-216.

Pauza, C. D., Galindo, J. E., and Richman, D. D. (1990). Reinfection results in accumulation of unintegrated viral DNA in cytopathic and persistent human immunodeficiency virus type 1 infection of CEM cells. *J Exp Med* 172, 1035-1042.

Pearse, B. M., and Bretscher, M. S. (1981). Membrane recycling by coated vesicles. *Annu Rev Biochem* 50, 85-101.

Pearse, B. M., and Robinson, M. S. (1984). Purification and properties of 100-kd proteins from coated vesicles and their reconstitution with clathrin. *Embo J* 3, 1951-1957.

Peden, A. A., Rudge, R. E., Lui, W. W., and Robinson, M. S. (2002). Assembly and function of AP-3 complexes in cells expressing mutant subunits. *J Cell Biol* 156, 327-336.

- Pelchen-Matthews, A., Armes, J. E., Griffiths, G., and Marsh, M. (1991). Differential endocytosis of CD4 in lymphocytic and nonlymphocytic cells. *J Exp Med* 173, 575-587.
- Pelchen-Matthews, A., Boulet, I., Littman, D. R., Fagard, R., and Marsh, M. (1992). The protein tyrosine kinase p56lck inhibits CD4 endocytosis by preventing entry of CD4 into coated pits. *J Cell Biol* 117, 279-290.
- Pelchen-Matthews, A., Kramer, B., and Marsh, M. (2003). Infectious HIV-1 assembles in late endosomes in primary macrophages. *J Cell Biol* 162, 443-455.
- Pelchen-Matthews, A., Parsons, I. J., and Marsh, M. (1993). Phorbol ester-induced downregulation of CD4 is a multistep process involving dissociation from p56lck, increased association with clathrin-coated pits, and altered endosomal sorting. *J Exp Med* 178, 1209-1222.
- Peng, B., and Robert-Guroff, M. (2001). Deletion of N-terminal myristoylation site of HIV Nef abrogates both MHC-1 and CD4 down-regulation. *Immunol Lett* 78, 195-200.
- Perelson, A. S., Neumann, A. U., Markowitz, M., Leonard, J. M., and Ho, D. D. (1996). HIV-1 dynamics in vivo: virion clearance rate, infected cell life-span, and viral generation time. *Science* 271, 1582-1586.
- Pervez, N. K., Kleinerman, J., Kattan, M., Freed, J. A., Harris, M. B., Rosen, M. J., and Schwartz, I. S. (1985). Pseudomembranous necrotizing bronchial aspergillosis. A variant of invasive aspergillosis in a patient with hemophilia and acquired immune deficiency syndrome. *Am Rev Respir Dis* 131, 961-963.
- Philips, J. A., Rubin, E. J., and Perrimon, N. (2005). Drosophila RNAi screen reveals CD36 family member required for mycobacterial infection. *Science* 309, 1251-1253.
- Piguet, V., Chen, Y. L., Mangasarian, A., Foti, M., Carpentier, J. L., and Trono, D. (1998). Mechanism of Nef-induced CD4 endocytosis: Nef connects CD4 with the mu chain of adaptor complexes. *Embo J* 17, 2472-2481.
- Piguet, V., Gu, F., Foti, M., Demarex, N., Gruenberg, J., Carpentier, J. L., and Trono, D. (1999). Nef-induced CD4 degradation: a diacidic-based motif in Nef functions as a lysosomal targeting signal through the binding of beta-COP in endosomes. *Cell* 97, 63-73.
- Piguet, V., and Trono, D. (1999). The Nef protein of primate lentiviruses. *Rev Med Virol* 9, 111-120.
- Piguet, V., Wan, L., Borel, C., Mangasarian, A., Demarex, N., Thomas, G., and Trono, D. (2000). HIV-1 Nef protein binds to the cellular protein PACS-1 to downregulate class I major histocompatibility complexes. *Nat Cell Biol* 2, 163-167.

Pinching, A. J., McManus, T. J., Jeffries, D. J., Moshtael, O., Donaghy, M., Parkin, J. M., Munday, P. E., and Harris, J. R. (1983). Studies of cellular immunity in male homosexuals in London. *Lancet* 2, 126-130.

Piper, R. C., and Katzman, D. J. (2007). Biogenesis and function of multivesicular bodies. *Annu Rev Cell Dev Biol* 23, 519-547.

Pitcher, C., Honing, S., Fingerhut, A., Bowers, K., and Marsh, M. (1999). Cluster of differentiation antigen 4 (CD4) endocytosis and adaptor complex binding require activation of the CD4 endocytosis signal by serine phosphorylation. *Mol Biol Cell* 10, 677-691.

Plata, F., Autran, B., Martins, L. P., Wain-Hobson, S., Raphael, M., Mayaud, C., Denis, M., Guillon, J. M., and Debre, P. (1987). AIDS virus-specific cytotoxic T lymphocytes in lung disorders. *Nature* 328, 348-351.

Popov, S., Rexach, M., Zybarth, G., Reiling, N., Lee, M. A., Ratner, L., Lane, C. M., Moore, M. S., Blobel, G., and Bukrinsky, M. (1998). Viral protein R regulates nuclear import of the HIV-1 pre-integration complex. *Embo J* 17, 909-917.

Popovic, M., Read-Connole, E., and Gallo, R. C. (1984). T4 positive human neoplastic cell lines susceptible to and permissive for HTLV-III. *Lancet* 2, 1472-1473.

Popovic, M., Sarngadharan, M. G., Read, E., and Gallo, R. C. (1984). Detection, isolation, and continuous production of cytopathic retroviruses (HTLV-III) from patients with AIDS and pre-AIDS. *Science* 224, 497-500.

Preusser, A., Briese, L., Baur, A. S., and Willbold, D. (2001). Direct in vitro binding of full-length human immunodeficiency virus type 1 Nef protein to CD4 cytoplasmic domain. *J Virol* 75, 3960-3964.

Puertollano, R., van der Wel, N. N., Greene, L. E., Eisenberg, E., Peters, P. J., and Bonifacino, J. S. (2003). Morphology and dynamics of clathrin/GGA1-coated carriers budding from the trans-Golgi network. *Mol Biol Cell* 14, 1545-1557.

Purcell A.W., and Elliot T. (2008). Molecular machinations of the MHC-I peptide loading complex. *Curr Opin Immunol* 20: 75-81.

Purcell, D. F., and Martin, M. A. (1993). Alternative splicing of human immunodeficiency virus type 1 mRNA modulates viral protein expression, replication, and infectivity. *J Virol* 67, 6365-6378.

Rabson, A. B., Daugherty, D. F., Venkatesan, S., Boulukos, K. E., Benn, S. I., Folks, T. M., Feorino, P., and Martin, M. A. (1985). Transcription of novel open reading frames of AIDS retrovirus during infection of lymphocytes. *Science* 229, 1388-1390.

Ramet, M., Manfrulli, P., Pearson, A., Mathey-Prevot, B., and Ezekowitz, R. A. (2002). Functional genomic analysis of phagocytosis and identification of a *Drosophila* receptor for *E. coli*. *Nature* 416, 644-648.

Ranki, A., Lagerstedt, A., Ovod, V., Aavik, E., and Krohn, K. J. (1994). Expression kinetics and subcellular localization of HIV-1 regulatory proteins Nef, Tat and Rev in acutely and chronically infected lymphoid cell lines. *Arch Virol* 139, 365-378.

Rapoport, I., Chen, Y. C., Cupers, P., Shoelson, S. E., and Kirchhausen, T. (1998). Dileucine-based sorting signals bind to the beta chain of AP-1 at a site distinct and regulated differently from the tyrosine-based motif-binding site. *Embo J* 17, 2148-2155.

Ratner, L., Starcich, B., Josephs, S. F., Hahn, B. H., Reddy, E. P., Livak, K. J., Petteway, S. R., Jr., Pearson, M. L., Haseltine, W. A., Arya, S. K., and et al. (1985). Polymorphism of the 3' open reading frame of the virus associated with the acquired immune deficiency syndrome, human T-lymphotropic virus type III. *Nucleic Acids Res* 13, 8219-8229.

Reiner, S. L. (2007). Development in motion: helper T cells at work. *Cell* 129, 33-36.

Reusch, U., Bernhard, O., Koszinowski, U., and Schu, P. (2002). AP-1A and AP-3A lysosomal sorting functions. *Traffic* 3, 752-761.

Rhee, S. S., and Marsh, J. W. (1994). Human immunodeficiency virus type 1 Nef-induced down-modulation of CD4 is due to rapid internalization and degradation of surface CD4. *J Virol* 68, 5156-5163.

Rhodes, D., Solomon, A., Bolton, W., Wood, J., Sullivan, J., Learmont, J., and Deacon, N. (1999). Identification of a new recipient in the Sydney Blood Bank Cohort: a long-term HIV type 1-infected seroindeterminate individual. *AIDS Res Hum Retroviruses* 15, 1433-1439.

Riggs, N. L., Craig, H. M., Pandori, M. W., and Guatelli, J. C. (1999). The dileucine-based sorting motif in HIV-1 Nef is not required for down-regulation of class I MHC. *Virology* 258, 203-207.

Robert-Guroff, M., Popovic, M., Gartner, S., Markham, P., Gallo, R. C., and Reitz, M. S. (1990). Structure and expression of tat-, rev-, and nef-specific transcripts of human immunodeficiency virus type 1 in infected lymphocytes and macrophages. *J Virol* 64, 3391-3398.

Robey, W. G., Safai, B., Oroszlan, S., Arthur, L. O., Gonda, M. A., Gallo, R. C., and Fischinger, P. J. (1985). Characterization of envelope and core structural gene products of HTLV-III with sera from AIDS patients. *Science* 228, 593-595.

Robinson, H. L., and Zinkus, D. M. (1990). Accumulation of human immunodeficiency virus type 1 DNA in T cells: results of multiple infection events. *J Virol* 64, 4836-4841.

Robinson, M. S. (1987). 100-kD coated vesicle proteins: molecular heterogeneity and intracellular distribution studied with monoclonal antibodies. *J Cell Biol* 104, 887-895.

- Robinson, M. S. (2004). Adaptable adaptors for coated vesicles. *Trends Cell Biol* 14, 167-174.
- Rodionov, D. G., and Bakke, O. (1998). Medium chains of adaptor complexes AP-1 and AP-2 recognize leucine-based sorting signals from the invariant chain. *J Biol Chem* 273, 6005-6008.
- Roeth, J. F., and Collins, K. L. (2006). Human immunodeficiency virus type 1 Nef: adapting to intracellular trafficking pathways. *Microbiol Mol Biol Rev* 70, 548-563.
- Roeth, J. F., Williams, M., Kasper, M. R., Filzen, T. M., and Collins, K. L. (2004). HIV-1 Nef disrupts MHC-I trafficking by recruiting AP-1 to the MHC-I cytoplasmic tail. *J Cell Biol* 167, 903-913.
- Rose, J. J., Janvier, K., Chandrasekhar, S., Sekaly, R. P., Bonifacino, J. S., and Venkatesan, S. (2005). CD4 down-regulation by HIV-1 and simian immunodeficiency virus (SIV) Nef proteins involves both internalization and intracellular retention mechanisms. *J Biol Chem* 280, 7413-7426.
- Rosen, C. A., Sodroski, J. G., and Haseltine, W. A. (1985). Location of cis-acting regulatory sequences in the human T-cell leukemia virus type I long terminal repeat. *Proc Natl Acad Sci U S A* 82, 6502-6506.
- Rosen, F. S. (1985). The acquired immunodeficiency syndrome (AIDS). *J Clin Invest* 75, 1-3.
- Rosen, M. J., Tow, T. W., Teirstein, A. S., Chuang, M. T., Marchevsky, A., and Bottone, E. J. (1985). Diagnosis of pulmonary complications of the acquired immune deficiency syndrome. *Thorax* 40, 571-575.
- Ross, T. M., Oran, A. E., and Cullen, B. R. (1999). Inhibition of HIV-1 progeny virion release by cell-surface CD4 is relieved by expression of the viral Nef protein. *Curr Biol* 9, 613-621.
- Rossi, F., Gallina, A., and Milanesi, G. (1996). Nef-CD4 physical interaction sensed with the yeast two-hybrid system. *Virology* 217, 397-403.
- Roth, M. J., Schwartzberg, P. L., and Goff, S. P. (1989). Structure of the termini of DNA intermediates in the integration of retroviral DNA: dependence on IN function and terminal DNA sequence. *Cell* 58, 47-54.
- Roth, T. F., and Porter, K. R. (1964). Yolk Protein Uptake in the Oocyte of the Mosquito *Aedes Aegypti*. *J Cell Biol* 20, 313-332.
- Rous, B. A., Reaves, B. J., Ihrke, G., Briggs, J. A., Gray, S. R., Stephens, D. J., Banting, G., and Luzio, J. P. (2002). Role of adaptor complex AP-3 in targeting wild-type and mutated CD63 to lysosomes. *Mol Biol Cell* 13, 1071-1082.
- Rowland-Jones, S. L., and Whittle, H. C. (2007). Out of Africa: what can we learn from HIV-2 about protective immunity to HIV-1? *Nat Immunol* 8, 329-331.

- Rudd, C. E., Trevillyan, J. M., Dasgupta, J. D., Wong, L. L., and Schlossman, S. F. (1988). The CD4 receptor is complexed in detergent lysates to a protein-tyrosine kinase (pp58) from human T lymphocytes. *Proc Natl Acad Sci U S A* 85, 5190-5194.
- Russell, J. H., and Ley, T. J. (2002). Lymphocyte-mediated cytotoxicity. *Annu Rev Immunol* 20, 323-370.
- Rutherford, G. W., Lifson, A. R., Hessel, N. A., Darrow, W. W., O'Malley, P. M., Buchbinder, S. P., Barnhart, J. L., Bodecker, T. W., Cannon, L., Doll, L. S., and et al. (1990). Course of HIV-1 infection in a cohort of homosexual and bisexual men: an 11 year follow up study. *Bmj* 301, 1183-1188.
- Salghetti, S., Mariani, R., and Skowronski, J. (1995). Human immunodeficiency virus type 1 Nef and p56lck protein-tyrosine kinase interact with a common element in CD4 cytoplasmic tail. *Proc Natl Acad Sci U S A* 92, 349-353.
- Salmon, P., Olivier, R., Riviere, Y., Brisson, E., Gluckman, J. C., Kieny, M. P., Montagnier, L., and Klatzmann, D. (1988). Loss of CD4 membrane expression and CD4 mRNA during acute human immunodeficiency virus replication. *J Exp Med* 168, 1953-1969.
- Salmond, R. J., Filby, A., Qureshi, I., Caserta, S., and Zamojska, R. (2009). T-cell receptor proximal signaling via the Src-family kinases, Lck and Fyn, influences T-cell activation, differentiation, and tolerance. *Immunol Rev* 228, 9-22.
- Salvi, R., Garbuglia, A. R., Di Caro, A., Pulciani, S., Montella, F., and Benedetto, A. (1998). Grossly defective nef gene sequences in a human immunodeficiency virus type 1-seropositive long-term nonprogressor. *J Virol* 72, 3646-3657.
- Samuel, K. P., Seth, A., Konopka, A., Lautenberger, J. A., and Papas, T. S. (1987). The 3'-orf protein of human immunodeficiency virus shows structural homology with the phosphorylation domain of human interleukin-2 receptor and the ATP-binding site of the protein kinase family. *FEBS Lett* 218, 81-86.
- Sanchez-Pescador, R., Power, M. D., Barr, P. J., Steimer, K. S., Stempien, M. M., Brown-Shimer, S. L., Gee, W. W., Renard, A., Randolph, A., Levy, J. A., and et al. (1985). Nucleotide sequence and expression of an AIDS-associated retrovirus (ARV-2). *Science* 227, 484-492.
- Sanfridson, A., Cullen, B. R., and Doyle, C. (1994). The simian immunodeficiency virus Nef protein promotes degradation of CD4 in human T cells. *J Biol Chem* 269, 3917-3920.
- Sarngadharan, M. G., Popovic, M., Bruch, L., Schupbach, J., and Gallo, R. C. (1984). Antibodies reactive with human T-lymphotropic retroviruses (HTLV-III) in the serum of patients with AIDS. *Science* 224, 506-508.
- Schaefer, M. R., Wonderlich, E. R., Roeth, J. F., Leonard, J. A., and Collins, K. L. (2008). HIV-1 Nef targets MHC-I and CD4 for degradation via a final common beta-COP-dependent pathway in T cells. *PLoS Pathog* 4, e1000131.

- Schafer, W., Stroh, A., Berghofer, S., Seiler, J., Vey, M., Kruse, M. L., Kern, H. F., Klenk, H. D., and Garten, W. (1995). Two independent targeting signals in the cytoplasmic domain determine trans-Golgi network localization and endosomal trafficking of the proprotein convertase furin. *Embo J* 14, 2424-2435.
- Schekman, R., and Orci, L. (1996). Coat proteins and vesicle budding. *Science* 271, 1526-1533.
- Scheppler, J. A., Nicholson, J. K., Swan, D. C., Ahmed-Ansari, A., and McDougal, J. S. (1989). Down-modulation of MHC-I in a CD4+ T cell line, CEM-E5, after HIV-1 infection. *J Immunol* 143, 2858-2866.
- Schiestl, R. H., and Gietz, R. D. (1989). High efficiency transformation of intact yeast cells using single stranded nucleic acids as a carrier. *Curr Genet* 16, 339-346.
- Schindler, M., Wurfl, S., Benaroch, P., Greenough, T. C., Daniels, R., Easterbrook, P., Brenner, M., Munch, J., and Kirchhoff, F. (2003). Down-modulation of mature major histocompatibility complex class II and up-regulation of invariant chain cell surface expression are well-conserved functions of human and simian immunodeficiency virus nef alleles. *J Virol* 77, 10548-10556.
- Schneider, I. (1972). Cell lines derived from late embryonic stages of *Drosophila melanogaster*. *J Embryol Exp Morphol* 27, 353-365.
- Schneider, U., Schwenk, H. U., and Bornkamm, G. (1977). Characterization of EBV-genome negative "null" and "T" cell lines derived from children with acute lymphoblastic leukemia and leukemic transformed non-Hodgkin lymphoma. *Int J Cancer* 19, 621-626.
- Schroder, S., and Ungewickell, E. (1991). Subunit interaction and function of clathrin-coated vesicle adaptors from the Golgi and the plasma membrane. *J Biol Chem* 266, 7910-7918.
- Schupbach, J., Popovic, M., Gilden, R. V., Gonda, M. A., Sarngadharan, M. G., and Gallo, R. C. (1984). Serological analysis of a subgroup of human T-lymphotropic retroviruses (HTLV-III) associated with AIDS. *Science* 224, 503-505.
- Schwartz, O., Marechal, V., Le Gall, S., Lemonnier, F., and Heard, J. M. (1996). Endocytosis of major histocompatibility complex class I molecules is induced by the HIV-1 Nef protein. *Nat Med* 2, 338-342.
- Seligmann, M., Chess, L., Fahey, J. L., Fauci, A. S., Lachmann, P. J., L'Age-Stehr, J., Ngu, J., Pinching, A. J., Rosen, F. S., Spira, T. J., and et al. (1984). AIDS--an immunologic reevaluation. *N Engl J Med* 311, 1286-1292.
- Sen, R., and Baltimore, D. (1986). Multiple nuclear factors interact with the immunoglobulin enhancer sequences. *Cell* 46, 705-716.
- Sen, R., and Baltimore, D. (1986). Inducibility of kappa immunoglobulin enhancer-binding protein Nf-kappa B by a posttranslational mechanism. *Cell* 47, 921-928.

- Sheffield, P., Garrard, S., and Derewenda, Z. (1999). Overcoming expression and purification problems of RhoGDI using a family of "parallel" expression vectors. *Protein Expr Purif* 15, 34-39.
- Shih, W., Gallusser, A., and Kirchhausen, T. (1995). A clathrin-binding site in the hinge of the beta 2 chain of mammalian AP-2 complexes. *J Biol Chem* 270, 31083-31090.
- Shin, J., Doyle, C., Yang, Z., Kappes, D., and Strominger, J. L. (1990). Structural features of the cytoplasmic region of CD4 required for internalization. *Embo J* 9, 425-434.
- Shin, J., Dunbrack, R. L., Jr., Lee, S., and Strominger, J. L. (1991). Phosphorylation-dependent down-modulation of CD4 requires a specific structure within the cytoplasmic domain of CD4. *J Biol Chem* 266, 10658-10665.
- Shinya, E., Owaki, A., Shimizu, M., Takeuchi, J., Kawashima, T., Hidaka, C., Satomi, M., Watari, E., Sugita, M., and Takahashi, H. (2004). Endogenously expressed HIV-1 nef down-regulates antigen-presenting molecules, not only class I MHC but also CD1a, in immature dendritic cells. *Virology* 326, 79-89.
- Shugars, D. C., Smith, M. S., Glueck, D. H., Nantermet, P. V., Seillier-Moiseiwitsch, F., and Swanstrom, R. (1993). Analysis of human immunodeficiency virus type 1 nef gene sequences present in vivo. *J Virol* 67, 4639-4650.
- Siegal, F. P., Lopez, C., Hammer, G. S., Brown, A. E., Kornfeld, S. J., Gold, J., Hassett, J., Hirschman, S. Z., Cunningham-Rundles, C., Adelsberg, B. R., and et al. (1981). Severe acquired immunodeficiency in male homosexuals, manifested by chronic perianal ulcerative herpes simplex lesions. *N Engl J Med* 305, 1439-1444.
- Simmen, T., Honing, S., Icking, A., Tikkanen, R., and Hunziker, W. (2002). AP-4 binds basolateral signals and participates in basolateral sorting in epithelial MDCK cells. *Nat Cell Biol* 4, 154-159.
- Simmen, T., Nobile, M., Bonifacino, J. S., and Hunziker, W. (1999). Basolateral sorting of furin in MDCK cells requires a phenylalanine-isoleucine motif together with an acidic amino acid cluster. *Mol Cell Biol* 19, 3136-3144.
- Simpson, F., Bright, N. A., West, M. A., Newman, L. S., Darnell, R. B., and Robinson, M. S. (1996). A novel adaptor-related protein complex. *J Cell Biol* 133, 749-760.
- Simpson, F., Peden, A. A., Christopoulou, L., and Robinson, M. S. (1997). Characterization of the adaptor-related protein complex, AP-3. *J Cell Biol* 137, 835-845.
- Skowronski, J., Parks, D., and Mariani, R. (1993). Altered T cell activation and development in transgenic mice expressing the HIV-1 nef gene. *Embo J* 12, 703-713.

- Sol-Foulon, N., Moris, A., Nobile, C., Boccaccio, C., Engering, A., Abastado, J. P., Heard, J. M., van Kooyk, Y., and Schwartz, O. (2002). HIV-1 Nef-induced upregulation of DC-SIGN in dendritic cells promotes lymphocyte clustering and viral spread. *Immunity* 16, 145-155.
- Sorkin, A., and Carpenter, G. (1993). Interaction of activated EGF receptors with coated pit adaptins. *Science* 261, 612-615.
- Spina, C. A., Kwok, T. J., Chowes, M. Y., Guatelli, J. C., and Richman, D. D. (1994). The importance of nef in the induction of human immunodeficiency virus type 1 replication from primary quiescent CD4 lymphocytes. *J Exp Med* 179, 115-123.
- Stagg, S. M., LaPointe, P., and Balch, W. E. (2007). Structural design of cage and coat scaffolds that direct membrane traffic. *Curr Opin Struct Biol* 17, 221-228.
- Stevenson, M., Meier, C., Mann, A. M., Chapman, N., and Wasiak, A. (1988). Envelope glycoprotein of HIV induces interference and cytolysis resistance in CD4+ cells: mechanism for persistence in AIDS. *Cell* 53, 483-496.
- Stevenson, M., Stanwick, T. L., Dempsey, M. P., and Lamonica, C. A. (1990). HIV-1 replication is controlled at the level of T cell activation and proviral integration. *Embo J* 9, 1551-1560.
- Stoddart, C. A., Geleziunas, R., Ferrell, S., Linquist-Stepps, V., Moreno, M. E., Bare, C., Xu, W., Yonemoto, W., Bresnahan, P. A., McCune, J. M., and Greene, W. C. (2003). Human immunodeficiency virus type 1 Nef-mediated downregulation of CD4 correlates with Nef enhancement of viral pathogenesis. *J Virol* 77, 2124-2133.
- Stove, V., Van de Walle, I., Naessens, E., Coene, E., Stove, C., Plum, J., and Verhasselt, B. (2005). Human immunodeficiency virus Nef induces rapid internalization of the T-cell coreceptor CD8alpha. *J Virol* 79, 11422-11433.
- Stroschein-Stevenson, S. L., Foley, E., O'Farrell, P. H., and Johnson, A. D. (2006). Identification of Drosophila gene products required for phagocytosis of *Candida albicans*. *PLoS Biol* 4, e4.
- Stumptner-Cuvelette, P., Morchoisne, S., Dugast, M., Le Gall, S., Raposo, G., Schwartz, O., and Benaroch, P. (2001). HIV-1 Nef impairs MHC class II antigen presentation and surface expression. *Proc Natl Acad Sci U S A* 98, 12144-12149.
- Swann, S. A., Williams, M., Story, C. M., Bobbitt, K. R., Fleis, R., and Collins, K. L. (2001). HIV-1 Nef blocks transport of MHC class I molecules to the cell surface via a PI 3-kinase-dependent pathway. *Virology* 282, 267-277.
- Swanson, C. M., and Malim, M. H. (2008). SnapShot: HIV-1 proteins. *Cell* 133, 742, 742 e741.

- Swigut, T., Greenberg, M., and Skowronski, J. (2003). Cooperative interactions of simian immunodeficiency virus Nef, AP-2, and CD3-zeta mediate the selective induction of T-cell receptor-CD3 endocytosis. *J Virol* 77, 8116-8126.
- Swigut, T., Iafrate, A. J., Muench, J., Kirchhoff, F., and Skowronski, J. (2000). Simian and human immunodeficiency virus Nef proteins use different surfaces to downregulate class I major histocompatibility complex antigen expression. *J Virol* 74, 5691-5701.
- Swigut, T., Shohdy, N., and Skowronski, J. (2001). Mechanism for down-regulation of CD28 by Nef. *Embo J* 20, 1593-1604.
- Tan, S. (2001). A modular polycistronic expression system for overexpressing protein complexes in *Escherichia coli*. *Protein Expr Purif* 21, 224-234.
- ter Haar, E., Harrison, S. C., and Kirchhausen, T. (2000). Peptide-in-groove interactions link target proteins to the beta-propeller of clathrin. *Proc Natl Acad Sci U S A* 97, 1096-1100.
- Terwilliger, E., Sodroski, J. G., Rosen, C. A., and Haseltine, W. A. (1986). Effects of mutations within the 3' orf open reading frame region of human T-cell lymphotropic virus type III (HTLV-III/LAV) on replication and cytopathogenicity. *J Virol* 60, 754-760.
- Theos, A. C., Tenza, D., Martina, J. A., Hurbain, I., Peden, A. A., Sviderskaya, E. V., Stewart, A., Robinson, M. S., Bennett, D. C., Cutler, D. F., et al. (2005). Functions of adaptor protein (AP)-3 and AP-1 in tyrosinase sorting from endosomes to melanosomes. *Mol Biol Cell* 16, 5356-5372.
- Thompson, C. B., Lindsten, T., Ledbetter, J. A., Kunkel, S. L., Young, H. A., Emerson, S. G., Leiden, J. M., and June, C. H. (1989). CD28 activation pathway regulates the production of multiple T-cell-derived lymphokines/cytokines. *Proc Natl Acad Sci U S A* 86, 1333-1337.
- Tifft, C. J., Proia, R. L., and Camerini-Otero, R. D. (1992). The folding and cell surface expression of CD4 requires glycosylation. *J Biol Chem* 267, 3268-3273.
- Timonen, T., and Helander, T. S. (1997). Natural killer cell-target cell interactions. *Curr Opin Cell Biol* 9, 667-673.
- Tobiume, M., Takahoko, M., Yamada, T., Tatsumi, M., Iwamoto, A., and Matsuda, M. (2002). Inefficient enhancement of viral infectivity and CD4 downregulation by human immunodeficiency virus type 1 Nef from Japanese long-term nonprogressors. *J Virol* 76, 5959-5965.
- Toussaint, H., Gobert, F. X., Schindler, M., Banning, C., Kozik, P., Jouve, M., Kirchhoff, F., and Benaroch, P. (2008). Human immunodeficiency virus type 1 nef expression prevents AP-2-mediated internalization of the major histocompatibility complex class II-associated invariant chain. *J Virol* 82, 8373-8382.

Traub, L. M., Downs, M. A., Westrich, J. L., and Fremont, D. H. (1999). Crystal structure of the alpha appendage of AP-2 reveals a recruitment platform for clathrin-coat assembly. *Proc Natl Acad Sci U S A* 96, 8907-8912.

Trkola, A., Dragic, T., Arthos, J., Binley, J. M., Olson, W. C., Allaway, G. P., Cheng-Mayer, C., Robinson, J., Maddon, P. J., and Moore, J. P. (1996). CD4-dependent, antibody-sensitive interactions between HIV-1 and its co-receptor CCR-5. *Nature* 384, 184-187.

Tschachler, E., Groh, V., Popovic, M., Mann, D. L., Konrad, K., Safai, B., Eron, L., diMarzo Veronese, F., Wolff, K., and Stingl, G. (1987). Epidermal Langerhans cells--a target for HTLV-III/LAV infection. *J Invest Dermatol* 88, 233-237.

Turner, J. M., Brodsky, M. H., Irving, B. A., Levin, S. D., Perlmutter, R. M., and Littman, D. R. (1990). Interaction of the unique N-terminal region of tyrosine kinase p56lck with cytoplasmic domains of CD4 and CD8 is mediated by cysteine motifs. *Cell* 60, 755-765.

UN Program on HIV/AIDS. (2008). AIDS Epidemic Update: December 2007. Publication ID: UNAIDS/07.2.7E/JC1322E.

Unanue, E. R., Ungewickell, E., and Branton, D. (1981). The binding of clathrin triskelions to membranes from coated vesicles. *Cell* 26, 439-446.

Ungewickell, E., and Branton, D. (1981). Assembly units of clathrin coats. *Nature* 289, 420-422.

van Endert, P. M. (1999). Genes regulating MHC class I processing of antigen. *Curr Opin Immunol* 11, 82-88.

van Niel, G., Wubbolts, R., and Stoorvogel, W. (2008). Endosomal sorting of MHC class II determines antigen presentation by dendritic cells. *Curr Opin Cell Biol* 20, 437-444.

Veillette, A., Bookman, M. A., Horak, E. M., and Bolen, J. B. (1988). The CD4 and CD8 T cell surface antigens are associated with the internal membrane tyrosine-protein kinase p56lck. *Cell* 55, 301-308.

Veronese, F. D., DeVico, A. L., Copeland, T. D., Oroszlan, S., Gallo, R. C., and Sarngadharan, M. G. (1985). Characterization of gp41 as the transmembrane protein coded by the HTLV-III/LAV envelope gene. *Science* 229, 1402-1405.

Vigers, G. P., Crowther, R. A., and Pearse, B. M. (1986). Location of the 100 kd-50 kd accessory proteins in clathrin coats. *Embo J* 5, 2079-2085.

Vilmer, E., Rouzioux, C., Vezinet Brun, F., Fischer, A., Chermann, J.C., Barre-Sinoussi, F., Gazengel, C., Dauget, C., Manigne, P., Griscelli, C., and Montagnier, L. (1984). Isolation of new lymphotropic retrovirus from two siblings with haemophilia B, one with AIDS. *Lancet* 323, 753-757.

- Voorhees, P., Deignan, E., van Donselaar, E., Humphrey, J., Marks, M. S., Peters, P. J., and Bonifacino, J. S. (1995). An acidic sequence within the cytoplasmic domain of furin functions as a determinant of trans-Golgi network localization and internalization from the cell surface. *Embo J* 14, 4961-4975.
- Wain-Hobson, S., Sonigo, P., Danos, O., Cole, S., and Alizon, M. (1985). Nucleotide sequence of the AIDS virus, LAV. *Cell* 40, 9-17.
- Walker, B. D., Chakrabarti, S., Moss, B., Paradis, T. J., Flynn, T., Durno, A. G., Blumberg, R. S., Kaplan, J. C., Hirsch, M. S., and Schooley, R. T. (1987). HIV-specific cytotoxic T lymphocytes in seropositive individuals. *Nature* 328, 345-348.
- Wan, L., Molloy, S. S., Thomas, L., Liu, G., Xiang, Y., Rybak, S. L., and Thomas, G. (1998). PACS-1 defines a novel gene family of cytosolic sorting proteins required for trans-Golgi network localization. *Cell* 94, 205-216.
- Wang, J. H., Meijers, R., Xiong, Y., Liu, J. H., Sakihama, T., Zhang, R., Joachimiak, A., and Reinherz, E. L. (2001). Crystal structure of the human CD4 N-terminal two-domain fragment complexed to a class II MHC molecule. *Proc Natl Acad Sci U S A* 98, 10799-10804.
- Wang, J. H., Yan, Y. W., Garrett, T. P., Liu, J. H., Rodgers, D. W., Garlick, R. L., Tarr, G. E., Husain, Y., Reinherz, E. L., and Harrison, S. C. (1990). Atomic structure of a fragment of human CD4 containing two immunoglobulin-like domains. *Nature* 348, 411-418.
- Ward, J. W., Bush, T. J., Perkins, H. A., Lieb, L. E., Allen, J. R., Goldfinger, D., Samson, S. M., Pepkowitz, S. H., Fernando, L. P., Holland, P. V., and et al. (1989). The natural history of transfusion-associated infection with human immunodeficiency virus. Factors influencing the rate of progression to disease. *N Engl J Med* 321, 947-952.
- Waters, M. G., Griff, I. C., and Rothman, J. E. (1991). Proteins involved in vesicular transport and membrane fusion. *Curr Opin Cell Biol* 3, 615-620.
- Watkins, D. I., Burton, D. R., Kallas, E. G., Moore, J. P., and Koff, W. C. (2008). Nonhuman primate models and the failure of the Merck HIV-1 vaccine in humans. *Nat Med* 14, 617-621.
- Watson, H., and Bonifacino, J. S. (2007). Direct binding to Rsp5p regulates ubiquitination-independent vacuolar transport of Sna3p. *Mol Biol Cell* 18, 1781-1789.
- Whatmore, A. M., Cook, N., Hall, G. A., Sharpe, S., Rud, E. W., and Cranage, M. P. (1995). Repair and evolution of nef in vivo modulates simian immunodeficiency virus virulence. *J Virol* 69, 5117-5123.
- Whitney, J. A., Gomez, M., Sheff, D., Kreis, T. E., and Mellman, I. (1995). Cytoplasmic coat proteins involved in endosome function. *Cell* 83, 703-713.

- Wildum, S., Schindler, M., Munch, J., and Kirchhoff, F. (2006). Contribution of Vpu, Env, and Nef to CD4 down-modulation and resistance of human immunodeficiency virus type 1-infected T cells to superinfection. *J Virol* 80, 8047-8059.
- Willbold, D., and Rosch, P. (1996). Solution Structure of the Human CD4 (403-419) Receptor Peptide. *J Biomed Sci* 3, 435-441.
- Willey, R. L., Maldarelli, F., Martin, M. A., and Strebel, K. (1992). Human immunodeficiency virus type 1 Vpu protein induces rapid degradation of CD4. *J Virol* 66, 7193-7200.
- Williams, M., Roeth, J. F., Kasper, M. R., Filzen, T. M., and Collins, K. L. (2005). Human immunodeficiency virus type 1 Nef domains required for disruption of major histocompatibility complex class I trafficking are also necessary for coprecipitation of Nef with HLA-A2. *J Virol* 79, 632-636.
- Williams, M., Roeth, J. F., Kasper, M. R., Fleis, R. I., Przybycin, C. G., and Collins, K. L. (2002). Direct binding of human immunodeficiency virus type 1 Nef to the major histocompatibility complex class I (MHC-I) cytoplasmic tail disrupts MHC-I trafficking. *J Virol* 76, 12173-12184.
- Witte, V., Laffert, B., Rosorius, O., Lischka, P., Blume, K., Galler, G., Stilper, A., Willbold, D., D'Aloja, P., Sixt, M., et al. (2004). HIV-1 Nef mimics an integrin receptor signal that recruits the polycomb group protein Eed to the plasma membrane. *Mol Cell* 13, 179-190.
- Wolf, D., Giese, S. I., Witte, V., Krautkramer, E., Trapp, S., Sass, G., Haller, C., Blume, K., Fackler, O. T., and Baur, A. S. (2008). Novel (n)PKC kinases phosphorylate Nef for increased HIV transcription, replication and perinuclear targeting. *Virology* 370, 45-54.
- Wonderlich, E. R., Williams, M., and Collins, K. L. (2008). The tyrosine binding pocket in the adaptor protein 1 (AP-1)  $\mu$ 1 subunit is necessary for Nef to recruit AP-1 to the major histocompatibility complex class I cytoplasmic tail. *J Biol Chem* 283, 3011-3022.
- Wray, V., Mertins, D., Kiess, M., Henklein, P., Trowitzsch-Kienast, W., and Schubert, U. (1998). Solution structure of the cytoplasmic domain of the human CD4 glycoprotein by CD and  $^1\text{H}$  NMR spectroscopy: implications for biological functions. *Biochemistry* 37, 8527-8538.
- Wu, H., Kwong, P. D., and Hendrickson, W. A. (1997). Dimeric association and segmental variability in the structure of human CD4. *Nature* 387, 527-530.
- Wu, Y., and Marsh, J. W. (2003). Early transcription from nonintegrated DNA in human immunodeficiency virus infection. *J Virol* 77, 10376-10382.
- Xiong, Y., Kern, P., Chang, H., and Reinherz, E. (2001). T Cell Receptor Binding to a pMHCII Ligand Is Kinetically Distinct from and Independent of CD4. *J Biol Chem* 276, 5659-5667.

Yamasaki, S., Takamatsu, M., and Iwashima, M. (1996). The kinase, SH3, and SH2 domains of Lck play critical roles in T-cell activation after ZAP-70 membrane localization. *Mol Cell Biol* 16, 7151-7160.

Yamashita, Y., Kojima, K., Tsukahara, T., Agawa, H., Yamada, K., Amano, Y., Kurotori, N., Tanaka, N., Sugamura, K., and Takeshita, T. (2008). Ubiquitin-independent binding of Hrs mediates endosomal sorting of the interleukin-2 receptor beta-chain. *J Cell Sci* 121, 1727-1738.

Ybe, J. A., Greene, B., Liu, S. H., Pley, U., Parham, P., and Brodsky, F. M. (1998). Clathrin self-assembly is regulated by three light-chain residues controlling the formation of critical salt bridges. *Embo J* 17, 1297-1303.

Yewdell, J. W., and Bennink, J. R. (1999). Mechanisms of viral interference with MHC class I antigen processing and presentation. *Annu Rev Cell Dev Biol* 15, 579-606.

Yokoyama, W. M. (1998). Natural killer cell receptors. *Curr Opin Immunol* 10, 298-305.

Yu, G., and Felsted, R. L. (1992). Effect of myristoylation on p27 nef subcellular distribution and suppression of HIV-LTR transcription. *Virology* 187, 46-55.

Zaremba, S., and Keen, J. H. (1985). Limited proteolytic digestion of coated vesicle assembly polypeptides abolishes reassembly activity. *J Cell Biochem* 28, 47-58.

Zhang, W., Sloan-Lancaster, J., Kitchen, J., Tribble, R. P., and Samelson, L. E. (1998). LAT: the ZAP-70 tyrosine kinase substrate that links T cell receptor to cellular activation. *Cell* 92, 83-92.

### **Publications arising from this work**

Chaudhuri, R., Lindwasser, O. W., Smith, W. J., Hurley, J. H., and Bonifacino, J. S. (2007). Downregulation of CD4 by human immunodeficiency virus type 1 Nef is dependent on clathrin and involves direct interaction of Nef with the AP2 clathrin adaptor. *J Virol* 81, 3877-3890.

Chaudhuri, R., Mattera, R., Lindwasser, O. W., Robinson, M. S., and Bonifacino, J. S. (2009). A basic patch on alpha-adaptin is required for binding of human immunodeficiency virus type 1 Nef and cooperative assembly of a CD4-Nef-AP-2 complex. *J Virol* 83, 2518-2530.

Lindwasser, O.W., Chaudhuri, R., and Bonifacino, J.S. (2007) Mechanisms of CD4 downregulation by the Nef and Vpu proteins of primate immunodeficiency viruses. *Curr Mol Med* 7, 171-184.

Lindwasser, O. W., Smith, W. J., Chaudhuri, R., Yang, P., Hurley, J. H., and Bonifacino, J. S. (2008). A diacidic motif in human immunodeficiency virus type 1 Nef is a novel determinant of binding to AP-2. *J Virol* 82, 1166-1174.

Mitchell, R. S., Chaudhuri, R., Lindwasser, O. W., Tanaka, K. A., Lau, D., Murillo, R., Bonifacino, J. S., and Guatelli, J. C. (2008). Competition model for upregulation of the major histocompatibility complex class II-associated invariant chain by human immunodeficiency virus type 1 Nef. *J Virol* 82, 7758-7767.